Aus der Medizinischen Klinik und Poliklinik III

Klinik der Ludwig-Maximilians-Universität München

Volatile profiling above AML-derived cell culture supernatants and of AML patients' breath using an eNose as a refined diagnostic and biomonitoring strategy ex vivo and in vivo

Dissertation

zum Erwerb des Doktorgrades der Medizin

an der Medizinischen Fakultät der

Ludwig-Maximilians-Universität München

vorgelegt von

Baudrexler Tobias Georg

aus

München, Deutschland

Jahr

2024

Mit Genehmigung der Medizinischen Fakultät der

Ludwig-Maximilians-Universität zu München

Erster Gutachter:	*Prof. Dr. rer. nat. Helga Schmetzer, PhD*
Zweiter Gutachter:	Prof. Dr. Uwe Ködel
Dritter Gutachter:	Prof. Dr. Dennis Nowak
ggf. weitere Gutachter:	_____
	_____
Dekan:	Prof. Dr. med. Thomas Gudermann

Tag der mündlichen Prüfung: 16.12.2024

Affidavit

Eidesstattliche Versicherung

Baudrexler, Tobias Georg
Name, Vorname

Ich erkläre hiermit an Eides statt, dass ich die vorliegende Dissertation mit dem Titel:

Volatile profiling above AML-derived cell culture supernatants and of AML patients' breath using an eNose as a refined diagnostic and biomonitoring strategy ex vivo and in vivo

selbständig verfasst, mich außer der angegebenen keiner weiteren Hilfsmittel bedient und alle Erkenntnisse, die aus dem Schrifttum ganz oder annähernd übernommen sind, als solche kenntlich gemacht und nach ihrer Herkunft unter Bezeichnung der Fundstelle einzeln nachgewiesen habe.

Ich erkläre des Weiteren, dass die hier vorgelegte Dissertation nicht in gleicher oder in ähnlicher Form bei einer anderen Stelle zur Erlangung eines akademischen Grades eingereicht wurde.

München, 16.12.2024
Ort, Datum

Baudrexler, Tobias Georg
Unterschrift Doktorand

Inhaltsverzeichnis *Index of contents*

Abkürzungsverzeichnis *Index of abbreviations*

AML	Acute myeloid leukemia
APC	Antigen presenting cells
BM	Bone marrow
CD	Cluster of differentiation
CEBPA	CCAAT/enhancer-binding protein alpha
CIK	Cytokine-induced killer
CSA	Cytokine secretion assay
CTX	Cytotoxicity fluorolysis assay
DC	Dendritic cells
DC_{leu}	Leukemia-derived dendritic cells
DC_{mat}	Mature dendritic cells
DEG	Degranulation assay
ELN	EuropeanLeukemiaNet
eNose	Electronical Nose
FasL	Fas ligand
FLT3	Fms like tyrosine kinase
GM-CSF	Granulocyte-macrophage colony-stimulating factor
(H)SCT	(Hematopoietic) stem cell transplantation
InCyt	Intracellular cytokine assay
INFy	Interferon gamma
Kit M	Immune modulatory cocktail using response modifiers (GM-CSF and PGE_1
LAA	Leukemia associated antigen
LAMP	Lysosomal associated membrane protein
MHC	Major histocompatibility complex
MLC	Mixed lymphocyte culture
MNC	Mononuclear cells
NK	Natural killer
PB	Peripheral blood
PGE_1	Prostaglandin E1
TNFa	Tumor necrosis factor alpha
TRAIL	Tumor necrosis factor related apoptosis inducing ligand
VOC	Volatile organic compounds

WB	Whole blood
WHO	World Health Organization

Publikationsliste *Index of publications*

1. Publications included in this thesis (Original publications):

The following publications were summarized for this cumulative medical thesis in accordance with the examination rules of the medical faculty of the Ludwig-Maximilians-University Munich:

Publication I and II are used for the cumulative dissertation.

Publication I:

Unterfrauner, M.; Rejeski, H.A.; Hartz, A.; Bohlscheid, S.; Baudrexler, T.; Feng, X.; Rackl, E.; Li, L.; Rank, A.; Velázquez, G.F.; Schmid, C.; Schmohl, J.; Bojko, P.; Schmetzer H.M.: Granulocyte-Macrophage-Colony-Stimulating-Factor Combined with Prostaglandin E1 Create Dendritic Cells of Leukemic Origin from AML Patients' Whole Blood and Whole Bone Marrow That Mediate Antileukemic Processes after Mixed Lymphocyte Culture. International Journal of Molecular Sciences **2023**, 24,17436. https://doi.org/10.3390/ijms242417436. (Impact Factor: **4,9**, 2023)

Publication II:

Baudrexler, T.; Boeselt, T.; Li, L.; Bohlscheid, S.; Boas, U.; Schmid, C.; Rank, A.; Schmohl, J.; Koczulla, R.; Schmetzer, H.M.: Volatile Phases Derived from Serum, DC, or MLC Culture Supernatants to Deduce a VOC-Based Diagnostic Profiling Strategy for Leukemic Diseases. *Biomolecules* **2023**, *13*, 989. https://doi.org/10.3390/biom13060989. (Impact Factor: **6.06**, 2022)

Publication III (in addition/appendix of this thesis):

Baudrexler, T; Boeselt, T.; Atzler, M.; Hartz, A.; Boas, U.; Schmid, C.; Rank, A.; Schmohl, J.; Koczulla, R.; Schmetzer, H.M.: Volatile Profiling using an eNose – Exploiting Breath Volatile Organic Compounds for Disease Monitoring in Refractory Acute Myeloid Leukemia Patients. Annals of Case Reports **2024**, 9, 1836. https://doi.org/10.29011/2574-7754.101836. (Impact Factor: **4,99**, 2023)

Publication IV (not included in this thesis):

Schutti, O.; Klauer, L.; Baudrexler, T.; Burkert, F.; Schmohl, J.; Hentrich. M.; Bojko, P.; Kraemer, D.; Rank, A.; Schmid, C.; Schmetzer. H.M.: Effective and Successful Quantification of Leukemia-Specific Immune Cells in AML Patients' Blood or Culture, Focusing on Intracellular Cytokine and Degranulation Assay. International Journal of Molecular Sciences **2024**, 25, 6983. https://doi.org/10.3390/ijms25136983. (Impact Factor: **4,9**, 2023)

2. Manuscripts submitted for publication:

1) M. Atzler, T. Baudrexler, R. Wang, M. Rabe, Z. Stankova, C. Plett, J. Schmohl, D. Krämer, M. Inngjerdingen, H.M. Schmetzer: Treatment of AML-diseased rats and therapy-refractory AML-patients with blast modulating response modifiers increased (leukemia specific) adaptive and innate immune-reactive cells in vivo. (under review)

3. Manuscripts in preparation:

1) X. Feng, S. Bohlscheid, E. Pepeldjiyska, L. Li, J. Gao, C. Seidel, C. Blasi, T. Baudrexler, E. Özkaya, J. Schmohl, D. Kraemer, C. Schmid, A. Rank, H.M. Schmetzer: Kit-treatment of Antileukaemic T-cell responses can be predicted by compositions of regulatory T- cell subpopulations-under hypoxic and normoxic conditions. (in preparation)

2) S. Bohlscheid, G. Filippini Velazquez, T. Baudrexler, H. Aslan, M. Trepel, C. Schmid, H. Schmetzer: Aberrant expressions of Checkpoints on AML blasts and T-Cells result in downregulation of immune responses in patients relapsing after allogenic stem cell transplantation (in preparation)

3) L.Li, V. Mussack, T. Baudrexler, H.M. Schmetzer: Kit-treatment of leukemic blast- containing whole blood shifts release patterns of extracellular vesicle release after culture with kits as well as after MLC with patients' T-cells. (in preparation)

4) A.S. Hartz, L. Li, H. Aslan, E. Pepeldjiyska, E. Rackl, E. Özkaya, T. Baudrexler, P. Bojko, J. Schmohl, A. Rank, C. Schmid, H. M. Schmetzer: The role of tolerogenic dendritic cells and DC_{leu} in suppressing antileukemic cytotoxicity. (in preparation)

5) N. Schmieder, T. Baudrexler, H. M. Schmetzer: Monitoring of leukemia-specific cells in the clinical course allows an estimation of relapse free survival. (in preparation)

6) M. Unterfrauner, D. Amberger, Y. Vokac, A. Hirn-Lopez, D. Deen, T. Kroell, T. Baudrexler, C. Schmid, H. J. Kolb, J. Tischer, H. M. Schmetzer: Released soluble factors in serum or supernatants of leukemia-derived dendritic cell or mixed lymphocyte cultures are predictive for T-cells' antileukemic functionality or clinical response to immunotherapy. (in preparation)

4. Contributions to conferences:

1) H. Schmetzer; D. Amberger, L. Klauer, E. Rackl, M. Atzler, S. Ugur, C. Plett, A. Rabe, C. Kugler A. Rank, M. Inngjerdingen. T. Baudrexler, B. Eiz-Vesper, C. Schmid: CONTROL LEUKEMIA BY INDUCING ANTI-CANCER IMMUNE REACTIVITY IN VIVO: *POTENTIAL OF A DC-TRIGGERED MECHANISM (EBMT meeting 2021).*

2) S. Bohlscheid, G. Filippini Velazquez, T. Baudrexler, H. Aslan, M. Trepel, C. Schmid, H. Schmetzer: Aberrant expressions of Checkpoints on AML blasts and T-Cells result in downregulation of immune responses in patients relapsing after allogenic stem cell transplantation (EBMT meeting 2021, online*).*

3) H. Schmetzer; D. Amberger, L. Klauer, E. Rackl, M. Atzler, S. Ugur, C. Plett, A. Rabe, C. Kugler A. Rank, M. Inngjerdingen. T. Baudrexler, B. Eiz-Vesper, C. Schmid: CONTROL LEUKEMIA BY INDUCING ANTI-CANCER IMMUNE REACTIVITY IN VIVO: *POTENTIAL OF A DC-TRIGGERED MECHANISM (ITOC meeting 2022, Munich).*

4) H. Schmetzer; D. Amberger, L. Klauer, E. Rackl, M. Atzler, S. Ugur, C. Plett, A. Rabe, C. Kugler A. Rank, M. Inngjerdingen. T. Baudrexler, B. Eiz-Vesper, C. Schmid CONTROL LEUKEMIA BY INDUCING ANTI-CANCER IMMUNE REACTIVITY IN VIVO: *POTENTIAL OF A DC-TRIGGERED MECHANISM (EBMT 2022, online).*

5) G. F. Velazquez, D. Amberger, L. Klauer, E. Rackl, M. Atzler, S. Ugur, C. Plett, A. Rabe, C. Kugler A. Rank, M. Inngjerdingen. T. Baudrexler, B. Eiz-Vesper, C. Schmid, H. Schmetzer; P475: CONTROL LEUKEMIA BY INDUCING ANTI-CANCER IMMUNE REACTIVITY IN VIVO? POTENTIAL OF A DC-TRIGGERED MECHANISM. HemaSphere. 2022; 6:374-5.

6) S. Bohlscheid, G. Filippini Velazquez, T. Baudrexler, H. Aslan, M. Trepel, C. Schmid, H. Schmetzer: DYSREGULATED EXPRESSIONS OF INHIBITORY CHECKPOINT MOLECULES AND THEIR LIGANDS ON T-CELLS AND BLASTS IN AML RELAPSES AFTER STEM CELL TRANSPLANTATION (SCT). HemaSphere. 2022; 6:1194-5.

7) Bohlscheid S, Velazquez G, Aslan H, Baudrexler T, Schmetzer H, Schmid C. P1309: DYSREGULATED EXPRESSIONS OF INHIBITORY CHECKPOINT MOLECULES AND THEIR LIGANDS ON T-CELLS AND BLASTS IN AML RELAPSES AFTER STEM CELL TRANSPLANTATION (SCT). J. Immunotherapy of cancer 10(supp1),10.1136/jitc-2022-ITOC9.66.

8) Baudrexler T., Boeselt T., Bohlscheid S, Li L., Schmid C., Rank A., Schmohl J., Schmetzer HM: Volatile profiling using an eNose allows differentiation of volatile phases derived from serum, DC, or MLC culture supernatants from healthy or leukemic samples: J. Immunotherapy of cancer 10(supp1),10.1136/jitc-2022- ITOC9.37.

9) H. Schmetzer; D. Amberger, L. Klauer, E. Rackl, M. Atzler, S. Ugur, C. Plett, A. Rabe, C. Kugler A. Rank, M. Inngjerdingen. T. Baudrexler, B. Eiz-Vesper, C. Schmid, CONTROL LEUKEMIA BY INDUCING ANTI-CANCER IMMUNE REACTIVITY IN VIVO: *POTENTIAL OF A DC-TRIGGERED MECHANISM* J. Immunotherapy of cancer 10(supp1),10.1136/jitc-2022-ITOC9.46.

10) M. Unterfrauner, H. Aslan, A. Hartz, E. Rackl, L. Li, S. Bohlscheid, T. Baudrexler, X. Feng, A. Rank, G. F. Velazquez, C. Schmid, J. Schmohl, P. Bojko, H. Schmetzer: Impact of (leukaemia-derived) dendritic cells generated from AML-patients' whole blood- versus whole bone marrow cells on the mediation of antileukaemic processes after mixed lymphocyte culture. *(EBMT 2023).*

11) T. Baudrexler, T. Boeselt, M. Atzler, A. Hartz, U. Boas, C. Schmid, A. Rank, J. Schmohl, R. Koczulla, H. Schmetzer: VOLATILE PROFILING USING AN ENOSE ALLOWS DIFFERENTIATION OF HEALTHY AND LEUKEMIC BREATH SAMPLES (*EBMT 2023*).

12) T. Baudrexler, T. Boeselt, M. Atzler, A. Hartz, U. Boas, C. Schmid, A. Rank, J. Schmohl, R. Koczulla, H. Schmetzer: VOLATILE PROFILING USING AN ENOSE ALLOWS DIFFERENTIATION OF HEALTHY AND LEUKEMIC BREATH SAMPLES (*Med 3 Congress, Herrsching, 2023).*

13) M. Unterfrauner, H. Aslan, A. Hartz, E. Rackl, L. Li, S. Bohlscheid, T. Baudrexler, X. Feng, A. Rank, G. Velazquez, C. Schmid, J. Schmohl, P. Bojko, H. Schmetzer: Impact of (leukaemia-derived) dendritic cells generated from AML-patients' whole blood- versus whole bone marrow cells on the mediation of antileukaemic processes after mixed lymphocyte culture (*Med 3 Congress, Herrsching, 2023*).

14) A.S. Hartz, L. Li, H. Aslan, E. Pepeldjiyska, E. Rackl, E. Özkaya, T. Baudrexler, P. Bojko, J. Schmohl, A. Rank, C. Schmid, H.M. Schmetzer: The role of tolerogenic dendritic cells and DC_{leu} in suppressing antileukemic cytotoxicity *(EBMT 2024).*

1. Beitrag zu den Veröffentlichungen *Contributions to publications*

1.1 Contribution to Publication I:

Title: Granulocyte-Macrophage-Colony-Stimulating-Factor Combined with Prostaglandin E1 Create Dendritic Cells of Leukemic Origin from AML Patients' Whole Blood and Whole Bone Marrow That Mediate Antileukemic Processes after Mixed Lymphocyte Culture.

Authors: Unterfrauner, Marianne; Rejeski, Hazal Aslan; Hartz, Anne; Bohlscheid, Sophia; Baudrexler, Tobias; Feng, Xiaojia; Rackl, Elias.; Li, Lin; Rank, Andreas; Velázquez, Giuliano Filippini; Schmid, Christoph; Schmohl, Jörg; Bojko, Peter; Schmetzer Helga Maria.

Journal: Int. Journal of Molecular Sciences 2023: https://doi.org/10.3390/ijms242417436.

Contributions: Baudrexler Tobias performed and analyzed (together with Unterfrauner Marianne) DC-, MLC-, CTX-experiments and provided data for the DEG and InCyt. Therefore, Baudrexler Tobias was responsible for flowcytometric and statistical analyzes of a part of experiments. Baudrexler Tobias provided a template of figures listed in the manuscript. Baudrexler Tobias was responsible in part for the proofreading of the final article.

1.2 Contribution to Publication II:

Title: Volatile Phases Derived from Serum, DC, or MLC Culture Supernatants to Deduce a VOC-Based Diagnostic Profiling Strategy for Leukemic Diseases.

Authors: Baudrexler, Tobias*; Boeselt, Tobias*; Li, Lin.; Bohlscheid, Sophia; Boas, Ursel; Schmid, Christoph; Rank, Andreas; Schmohl, Jörg; Koczulla, Rembert; Schmetzer, Helga Maria.
*equally contributed

Journal: Biomolecules (MDPI), 2023: https://doi.org/10.3390/biom13060989

Contributions: Baudrexler Tobias designed the study together with Schmetzer Helga Maria, Boeselt Tobias and Koczulla Rembert. Baudrexler Tobias conducted all cell biological experiments and conducted serum and cell culture samples for VOC analyzes in Marburg. Baudrexler Tobias was responsible for data acquisition, formal analyzes, project administration, validation and all statistical analyzes. Baudrexler Tobias prepared (supervised by Schmetzer Helga Maria) the manuscript (including title, introduction, materials/methods, results, discussion, conclusion and the abstract) and created all figures and tables. After finalizing the composition Baudrexler Tobias submitted the final version to the journal, changed it according to reviewers' suggestions and resubmitted it to the journal. Baudrexler Tobias presented the project on various conferences and was/is together with Schmetzer Helga the contact person for content-related questions.

Reasons for equal contribution of first authors: Boeselt Tobias was part of the workgroup of Prof. Dr. Rembert Koczulla and was responsible for the VOC measurements, evaluations and discussions. Boeselt Tobias designed the study (together with Baudrexler Tobias and Schmetzer Helga) and is an expert in the field of VOC analyses and VOC-specific statistical evaluations.

1.3 Contribution to Publication III (in addition)

Publication III is not part of the cumulative dissertation but was added to present the special knowledge in the field of VOC profiling and the VOC monitoring of AML patients' breath samples in vivo (manuscript in the appendix).

Title: Volatile Profiling using an eNose – Exploiting Breath Volatile Organic Compounds for Disease Monitoring in Refractory Acute Myeloid Leukemia Patients.

Authors: Baudrexler, Tobias; Boeselt, Tobias; Atzler, Michael; Hartz, Anne; Boas, Ursel; Schmid, Christoph; Rank, Aandreas; Schmohl, Jörg; Koczulla, Rembert; Schmetzer, Helga Maria.

Journal: Annals of Case Reports, 2024: https://doi.org/10.29011/2574-7754.101836

Contributions: Baudrexler Tobias designed the study together with Schmetzer Helga Maria, Boeselt Tobias and Koczulla Rembert. Baudrexler Tobias evaluated the clinical reports of the patients and healthy breath donors and assessed the disease progression of AML patients. Baudrexler Tobias conducted cell biological experiments for immunological results and coordinated the VOC measurements and evaluations in Marburg. Boeselt Tobias conducted VOC analyzes. Baudrexler Tobias was responsible for data acquisition, formal analyzes, project administration, validation and all statistical analyzes. Baudrexler Tobias prepared (supervised by Schmetzer Helga Maria) the manuscript (including title, introduction, materials/methods, results, discussion, conclusion and the abstract) and designed all figures and tables. Baudrexler Tobias submitted the final manuscript to the journal, changed it according to reviewers' suggestions and resubmitted it to the journal. Baudrexler Tobias was/is together with Schmetzer Helga the contact person for content-related questions.

1.4 Contribution to Publication IV (not included in this thesis)

Publication IV is not part of the cumulative dissertation but is important to emphasize the experimental experience and scientific knowledges. Moreover, this project was the basis of further studies in our working group.

Title: Effective and Successful Quantification of Leukemia-Specific Immune Cells in AML Patients' Blood or Culture, Focusing on Intracellular Cytokine and Degranulation Assay.

Authors: Schutti, Olga; Klauer, Lara; Baudrexler, Tobias; Burkert, Florian; Schmohl, Jörg; Hentrich. Marcus; Bojko, Peter; Kraemer, Doris; Rank, Andreas; Schmid, Christoph; Schmetzer, Helga Maria.

Journal: Int. Journal of Molecular Sciences 2024: https://doi.org/10.3390/ijms25136983.

Contributions: Baudrexler Tobias performed and analyzed some of the DC-, MLC-, CTX-experiments and provided data for the DEG and InCyt. Therefore, Baudrexler Tobias was responsible for flowcytometric and statistical analyzes of a part of experiments.

2. **Einleitung** *Introduction*

2.1. Acute myeloid leukemia (AML)

AML is a hematopoiesis illness caused by clonal stem cells that also causes unchecked proliferation of myeloid progenitor cells (blasts), which renders hematopoiesis ineffective. Typical symptoms are fatigue, frequent infections, hemorrhage and fever (Hou et al., 1997, Lowenberg et al., 1999). The most prevalent type of leukemia, AML, usually affects older patients and has a worse prognosis (Appelbaum et al., 2006). For diagnosis and staging of AML, a venous blood sample collection and an invasive bone marrow aspiration is necessary. A combination of morphological analyzes, cytochemistry, immunophenotyping, cytogenetics and molecular biological investigations enables the diagnosis of AML (Malcovati and Nimer, 2008). Prognostically most relevant are chromosomal aberrations, mutations, blast counts and age (Marcucci et al., 2011). High-dose chemotherapy, hypomethylating drugs, and hematopoietic stem cell transplantation (HSCT in patients under 65) are the mainstays of standard AML treatment. These treatments result in significant rates of remission (more than 65% of cases within the first 1-2 therapy cycles), but they also cause high rates of relapses in up to 80% of cases in the next two years (Röllig, 2019, Gardin and Dombret, 2017, Ansprenger et al., 2020). Examples for new treatment strategies are antileukemic protein-kinase-inhibitors (e.g., FLT3-inhibitors), epigenetic modulators, new cytotoxic agents, mitochondrial inhibitors which include apoptosis-based therapies and therapies that affect specific oncogenic proteins (Ansprenger et al., 2020). Additionally, new immunotherapeutic therapies are investigated.

2.2. DC-based immunotherapy

DCs are antigen-presenting cells (APCs), which use the major histocompatibility complex (MHC) to mediate immune responses (Al-Daccak et al., 2004). Tumor cells are eliminated until cells of the adaptive immune system, particularly T cells, are activated by activating cells of the (fast, first line) innate immune system, such as NK cells or invariant natural killer cells (iNKT). DCs create immunological synapses that lead to a powerful and clonally restricted T-cell activation against the antigens that are presented. As a result, DCs are essential for the interface and communication between the innate and adaptive immune systems (Amberger and Schmetzer, 2020). Hematopoietic stem cells and monocytes are the progenitor cells for in vivo DCs. Following danger signaling (e.g., by nucleic acids, infectious particles), they are activated and mature, leading to the upregulation of chemokine receptors (like CD197), MHC-antigens, and other costimulatory factors (Amberger et al., 2019, Amberger and Schmetzer, 2020, Sabado et al., 2017, Schutti et al., 2024). Through the application of various combinations of response modifiers (Kits), ex vivo DCs can be produced from CD14+ monocytes, loaded with tumor antigens (DC_{mon}, monocyte derived DC) or from myeloid blasts (DC_{leu}, leukemia derived DC; without the induction of blast proliferation) from whole blood (WB) from AML patients (Klauer et al., 2021, Amberger and Schmetzer, 2020, Unterfrauner et al., 2023): After T cell-enriched mixed lymphocyte culture (MLC), leukemic blasts acquire a characteristic DC morphology, express more costimulatory molecules, and have a far stronger capacity to deliver antigens to activate innate and adaptive immune system cells than blasts do. These concepts have been shown to qualify for a treatment of AML patients: Ex vivo generated DC or DC_{leu} might be an useful option for an adoptive transfer. However, these ex vivo preparations are time-consuming and elaborating and lead to limited frequencies of cells. Direct use of Kits to patients with AML DC_{leu} from blasts could be generated in vivo, activating the immune system and afterwards leading to an antileukemic immunoreaction

(Amberger and Schmetzer, 2020, Baudrexler, 2024). The composition of granulocyte macrophage colony stimulating factor (GM-CSF) and prostaglandin E_1 (PGE_1) (immunomodulatory Kit M) has been demonstrated to be one of the most effective combinations of immune response modifiers. It activates the immune system, particularly against blasts, and downregulates the immunosuppressive mechanism without causing blast growth (Amberger and Schmetzer, 2020, Plett et al., 2022, Schwepcke et al., 2022, Pepeldjiyska et al., 2022, Unterfrauner et al., 2023). In this thesis/these publications Kit M was used.

2.3. Methodological techniques to monitor AML disease

Understanding leukemia-related and antileukemic processes is essential. As a result, it's important to examine and monitor the various (inhibitory or activating) cells, soluble compounds, and even the smallest ones that are involved (Amberger et al., 2019, Boeck et al., 2017, Vogt et al., 2014, Schutti et al., 2024). In the last years impact of physical elements (e.g., physiological hypoxia (Doraneh Gard et al., 2024) or circulating vesicles (e.g., extracellular vesicles (EVs) (Tkach et al., 2017, Li et al., 2020)) were tested to potentially refine monitoring. Their involvement in immune system or tumor stimulation or in the observation of leukemia-related processes may help us comprehend AML illness better.

2.3.1. Cytomorphology, cytochemistry, immunophenotyping and cytogenetics

Diagnostic of AML is based on morphological classification, immunophenotyping (evaluation of individual patients' blast phenotype), cytochemical assays and cytogenetic/molecular classification.

Modern immunophenotyping of hematological malignancies by flow cytometry is conducted by monoclonal antibodies conjugated to various fluorochromes, enabling (with a reduced number of cells) the identification and quantification of malignant cells (e.g., CD34+ blasts) and different subtypes as well as the determination of the degree of immunophenotypic heterogeneity of the malignant cell population was simplified (Campana and Behm, 2000, Paulose and Fathima, 2023).

A very important diagnostic tool for determining prognosis in AML are cytogenetic analyzes. Some specific chromosomal abnormalities (e.g., CEBPA or FLT3 mutation) correlate with cytomorphologic features, immunophenotype and clinical outcome. The WHO-classification as well as the ELN (European LeukemiaNet) risk stratification uses the cytogenetic information as a major criterion (Schoch and Haferlach, 2002, Harada et al., 2018, Döhner et al., 2022).

For diagnosis and classification of AML stage all those options depend on both an invasive venous blood sample collection and an invasive bone marrow aspiration. Moreover, diagnosis of leukemia is technically demanding, needs experience of the performer and is time-consuming.

2.3.2. VOC analysis as a novel method for characterizing and monitoring (malignant) diseases

All living things, including humans and animals, release organic chemicals into the environment. Through chemicals in exhaled air, they can reflect the state of the body's metabolism in both healthy and diseased settings (Mazzatenta et al., 2015). 'Biomarkers in exhaled air might qualify as a systemic tool to classify and monitor disease' (Baudrexler, 2024). The benefit of volatile

profiling of exhaled volatile organic compounds (VOCs) is that VOCs may be easily and noninvasively collected. This can be achieved by either directly measuring VOCs in an electronic nose (eNose) or by analyzing collected VOCs coupled to carriers (such as fleeze or earloop masks) (Biehl et al., 2019). VOCs are hydrocarbon-containing organic molecules. Proof of principle has been brought, that VOC analysis can contribute to detect disease associated markers: e.g., Parkinson, Alzheimer, lung cancer (Bach et al., 2015, Dragonieri et al., 2009, Biehl et al., 2019). Another study concluded that VOC analyzes are a promising tool to detect bladder tumor by headspace measurements of urine samples (Heers et al., 2018). Moreover, it has been demonstrated, that the volatile compounds above cell culture supernatants can predict VOC patterns that correspond to the underlying disease subtypes (e.g., higher content of granzyme A in the serum and supernatant in active Bechet's disease (Accardo-Palumbo et al., 2004, Baudrexler et al., 2023)).

2.4. Detection of VOCs and experimental set-up of the eNose

VOC samples (taken from breath masks or cell culture supernatants) were collected in a sealed environment and quantified using the Cyranose 320® electronic nose (eNose) in Marburg (Koczulla et al., 2011, Greulich et al., 2013). The Cyranose 320® is a polymer sensor composed of 32 thin-film carbon polymer chemiresistors (NoseChip). The sensor response is based on the binding of volatile organic compounds (VOCs) based on their structure, size, polarity, and proton affinity. Chemical signals are converted to electronic signals by the sensors (Lewis, 2004). Smellprints with a distinctive pattern are produced for single substances or mixtures. These smell prints are made up of 32 separate signals. Here, eNose technology was applied using a consistent methodology (Biehl et al., 2019, Boeselt et al., 2022). The sensors were trained using the so-called training set before to each measurement series. Among them were aromatics, menthol, licorice, etc. The samples were compared with the standard values (Boeselt et al., 2022, Baudrexler et al., 2023). Each measurement was carried out in three stages: Medicinal air was used to determine a reference value (Aer medicinalis, Linde Gas Therapeutics GmbH, Unterschleißheim, Germany) *(1)*. The second phase took place in 60 seconds, during which the volatile surface of the cell supernatants was measured (2). Then, in another 60 seconds, the eNoses' sensors were cleaned using exposed ambient air (3) (Biehl et al., 2019). Principal component analysis was performed using arithmetic mean values derived from triple measurements of each sample. Subsequently, the results of linear discriminant analysis (LD) were utilized for additional analyses, particularly contingency table analyses. The Mahalanobis distance between groups was calculated (Greulich et al., 2013, Koczulla et al., 2011, Baudrexler et al., 2023).

2.5. Immune system

The immune system (mediating the innate and the adaptive immunity) is an interactive network of cells, humoral factors, and cytokines (Parkin and Cohen, 2001). The innate immune system, which includes natural killer (NK) cells, cytokine-induced killer (CIK), invariant natural killer T cells (iNKT cells), and APCs (monocytes, macrophages, DC) mediates the first interactions with pathogens and is in charge of tumor immunosurveillance (Shimizu et al., 2020, Klauer et al., 2021, Robertson et al., 2014). Cytokines and chemokines producing NK cell subtypes (CD56+CD3-) modulate the adaptive immunity. With characteristics of both T and NK cells, CIK cell (CD56+CD3+) and iNKT cell subtypes (6B11+; expressing a semi-invariant T cell receptor) can suppress the immune system or fight tumors. CIK cells identify target cells independent of T cell receptor or MHC molecules (Wongkajornsilp et al., 2019, Klauer et al., 2021, Boeck et al., 2017,

Schutti et al., 2024). Key players of the adaptive immunity are B cells (CD19+) and T cells (CD3+) and their subtypes (e.g., early proliferating T cells: $T_{prol\text{-}early}$; late proliferating T cells: $T_{prol\text{-}late}$, memory T cells: $T_{em/eff}$). The primary functions of the adaptive immune system include generating immunologic memory, controlling immunological homeostasis, and responding specifically to antigens (Liu et al., 2020, Laumont et al., 2022). T cells express a T cell receptor that identifies antigens on blasts, which need to be presented by APCs on their MHC I or MHC II molecules. Following activation, naive T cells (T_{naive}, CD3+CD45RO-) transform into non-naive T cells ($T_{non\text{-}naive}$, CD3+CD45RO+), which mediate different immunological responses (e.g., T helper cells: T_{CD4+}, CD3+CD4+ or cytotoxic T cells: T_{CD4-}, CD3+CD4-) or create long-living central memory cells (T_{cm}, CD3+CD45RO+CD197+) or effector memory cells ($T_{em/eff}$, CD3+CD45RO+CD197-) to speed up the immune system's reactivation against recurrent antigens (Bonilla and Oettgen, 2010, Amberger et al., 2019). All subtype analyzes quantify these cell subtypes to understand immunological processes. Cell subtype abbreviations are given in e.g. *Publication II+III (Table 1)*.

2.6. Leukemia specific cells and antileukemic processes

Induction of apoptosis or lysis of malignant target cells are achieved via granules (e.g., granzymes and perforins) (Smyth and Trapani, 1995, Keefe et al., 2005), or via death receptor ligands (e.g., FasL and TRAIL) (Pistritto et al., 2016). In ex vivo assays these antileukemic reactions can be quantified. Granules are important for the mediation of cell apoptosis and released by the granule-dependent-pathway. The degranulation assay (DEG) can be used to identify this pathway: Granzymes and perforin are stored in the cytoplasm of immune cells encircled by a membrane containing lysosome-associated membrane glycoproteins (LAMPs) such as LAMP-1 (CD107a) and are transported to the cell surface, where CD107a can be stained using antibodies. Interferon gamma (INF_y) and tumor necrosis factor alpha (TNF_a), which are immune response triggers and mediators of cell apoptosis, can be quantified intracellularly using the intracellular cytokine assay (InCyt) and cytokine secretion assay (CSA). The simultaneous phenotypic characterization of antigen specific immunoreactive T cells is possible (Klauer et al., 2021, Letsch and Scheibenbogen, 2003, Schutti et al., 2024). The DEG and InCyt assay indicate a leukemia specific activation. Cytotoxicity assays (CTX) allow the assessment of viable target cells (blasts) in Kit M pretreatment vs. not pretreated samples by assessing the antileukemia potential of stimulated and unstimulated effector cells (Klauer et al., 2021, Unterfrauner et al., 2023).

The DEG test, when combined with the InCyt assay and the CTX, offers a sophisticated and intricate examination of the functioning of cells, particularly their (leukemia-specific) activity and cytotoxicity of several immune reactive cells (Klauer et al., 2021).

2.7. Outline and aims of this thesis

The aims of this thesis were to:

I. Generate and quantify DC/DC_{leu}, (leukemia specific) immune cell (subpopulations) and antileukemic effects using Kit M treated (vs. not treated) WB (and BM) or MLC from healthy probands and refractory AML patients *ex vivo* (and *in vivo* (in the course of the disease));
II. Analyze VOCs of collected healthy and leukemic serum, cell culture supernatants (or breath samples in the course of the disease using an eNose);
III. Correlate cell biological-/immunological- with VOC results in order to potentially derive a VOC-based profile approach.

Publication I: Granulocyte-Macrophage-Colony-Stimulating-Factor Combined with Prostaglandin E1 Create Dendritic Cells of Leukemic Origin from AML Patients' Whole Blood and Whole Bone Marrow That Mediate Antileukemic Processes after Mixed Lymphocyte Culture

Within this publication, as a basis of our further studies, especially for publication II, we wanted to demonstrate the ex vivo immune modulatory capacity of Kit M (GM-CSF + PGE_1) in WB and BM.

We evaluated Kit-M's possible impacts on WB and BM in order to assess the antileukemic effects of Kit-M on the two compartments. To produce DC/DC_{leu}, WB and BM samples from AML patients were treated with Kit M. Following MLC enrichment with the patients' T cells, the degranulation, intracellular IFNγ production, and cytotoxicity fluorolysis assays were used to evaluate the leukemia-specific antileukemic effects. We were able to demonstrate that, in comparison to untreated WB and BM samples, Kit M significantly improved blast lysis and resulted to much higher frequencies of DC_{leu} or leukemia specific immune cells. We could show comparable Kit M-impacts on WB and BM samples concerning the DC_{leu}-production and antileukemic immune cell-activation regardless of cells conducted before or after SCT (Unterfrauner et al., 2023).

Since our research demonstrates that Kit M in WB produces DC/DC_{leu} most effectively, we used it for additional studies.

Publication II: Volatile Phases Derived from Serum, DC, or MLC Culture Supernatants to Deduce a VOC-Based Diagnostic Profiling Strategy for Leukemic Diseases

Within this publication we investigated the potential of VOC based profiling strategy ex vivo.

To yield proof of concept we quantified cells in DC cultures and innate and adaptive immune cell subsets after MLC by flow cytometry. Moreover, we characterized and quantified leukemia-specific cells by degranulation assay (Deg) and an intracellular cytokine assay (InCyt). Anti-leukemic cytotoxicity was explored with a cytotoxicity fluorolysis assay (CTX). The eNose was used to acquire VOC profiles from serum or DC- and MLC culture supernatants (before vs. after culture, and with vs. without Kit M pre-treatment) (Baudrexler et al., 2023). 'The eNose could significantly distinguish between healthy and leukemic patients' serum, DC and MLC culture supernatant-derived volatile phases and could significantly differentiate several supernatants (with vs. without Kit M treatment, cultured vs. uncultured)-derived VOCs within subgroups (healthy DC or leukemic DC, or healthy MLC or leukemic MLC supernatants). Interestingly, the eNose could indicate Kit M- and culture-associated effect' (Baudrexler et al., 2023).

In summary, our ex vivo investigation suggests that the eNose could be a viable choice for the derivation of a VOC-based profiling technique using serum or cell culture supernatants, and it might also be a helpful diagnostic tool to identify or qualify AML illness (Baudrexler et al., 2023).

Publication III (in addition): Volatile Profiling using an eNose – Exploiting Breath Volatile Organic Compounds for Disease Monitoring in Refractory Acute Myeloid Leukemia Patients

Within this publication we investigated the potential of VOC based profiling strategy in vivo.

We combined clinical and immunological data with the volatile organic compound (VOC) results of breath samples taken in the course of the disease in order to profile the immunological changes

in vivo in patients with acute myeloid leukemia (AML). Three patients with refractory acute myeloid leukemia were observed throughout their treatment, each receiving a different medication. P1511, the control patient, underwent chemotherapy. Kit M (GM-CSF and PGE_1) was used to treat P1482 and P1601. Throughout the course of the treatment, these patients were kept under close clinical, hematological, and immunological observation. During the observation blood samples were collected to monitor (leukemia specific) immune cells using flow cytometry, CSA, and InCyt. VOCs were measured by an eNose using earloop masks that contained exhaled air from healthy probands and from AML patients in the course of the disease. Treatment with Kit M in vivo was demonstrated to be safe, to increase clinical parameters (neutrophils, thrombocytes, and reduction of blast counts), and to stimulate (leukemia specific) immunological activation; however, the effects subsided when the Kit M treatment was stopped. It was possible to distinguish between leukemic and healthy VOC profiles from P1511, P1482, and P1601 over the whole observation period. Additionally, there were significant differences in the VOC profiles obtained from healthy vs. AML breath donors and the VOC prints obtained during chemotherapy vs. Kit M therapy (Baudrexler, 2024).

In summary, breath profiling (in vivo-profiling) with the use of an eNose helps determine a disease-related monitoring tool based on volatile organic compounds (VOCs) and offers a potential option for a diagnostic tool (healthy vs. leukemia) (Baudrexler, 2024).

2.8. Conclusion

We assume, that:

1) Kit M (GM-CSF+PGE_1) pretreated patients' WB leads to induced/improved antileukemic reactions ex vivo and in vivo
2) VOCs, as biomarkers in cell cultures' supernatants or in exhaled air reflect the metabolism under healthy or pathological conditions and may be considered a systemic tool to monitor (underlying) disease (e.g., AML). Therefore, an eNose is generally suitable for VOC detection from cell culture supernatants and exhaled patients' breath. These findings contribute to investigate -and potentially confirm- the correlation between patients' cell biological- and VOC status to improve the field of AML diagnostic and disease monitoring.

3. Zusammenfassung *Summary*

VOCs sind flüchtige organische Chemikalien, die Kohlenwasserstoffverbindungen enthalten, den Stoffwechsel und pathologische Zustände von Gesunden und Patienten widerspiegeln und mit einer eNose gemessen werden können. Die VOC-Analyse kann zum Nachweis krankheitsbezogener Marker verwendet werden. Ihre Rolle bei der Monitorierung von tumor- oder immunaktivierungs-assoziierten Prozessen könnte dazu beitragen, antileukämische Prozesse zu überwachen, und könnte ein verfeinertes Diagnose- und Biomonitoring-Instrument darstellen.

VOCs wurden über Serum, DC- und MLC-Kulturüberständen oder aus Atemmasken (direkt aus der Ausatemluft der Patienten) gewonnen. Um immunologische (tumorassoziierte) Veränderungen in VOC-Proben von AML-Patienten und gesunden Probanden zu erkennen, korrelierten wir zellbiologische Analysen mit den VOC-Ergebnissen. In einer Studie (Publikation I) konnten wir den zellulären, antileukämischen Effekt von Kit M (GM-CSF+PGE_1) vorbehandeltem Vollblut und Knochenmark zeigen. Schließlich konnten wir in einer Ex-vivo-Studie (Publikation II) VOCs über Zellkulturüberständen analysieren und anschließend in einer In-vivo-Studie (Publikation III) VOCs in Ausatemluft von gesunden Probanden und leukämie-erkrankten Patienten analysieren.

1) Wir kultivierten dendritische Zellen (DC) aus leukämischem und gesundem Vollblut (WB) ohne (Kontrolle) oder mit immunmodulatorischem Kit M (bestehend aus Granulozyten-Makrophagen-Kolonie-stimulierendem Faktor (GM-CSF) und Prostaglandin E1 (PGE1)), um DC/DC_{leu} zu erzeugen. Mit Kit M vorbehandeltes/nicht vorbehandeltes Vollblut, das DC/DC_{leu} enthielt, wurde zur Stimulierung von mit T-Zellen angereicherten immunreaktiven Zellen in gemischten Lymphozytenkulturen (MLC-Kultur) verwendet. Leukämiespezifische Zellen des erworbenen und angeborenen Immunsystems wurden mit einem Degranulationstest (Deg) und einem intrazellulären Zytokintest (InCyt) nachgewiesen. Die antileukämische Zytotoxizität wurde mit einem Zytotoxizitäts-Fluorolyse-Assay (CTX) bewertet.

2) VOCs aus Serum oder DC- und MLC-Kulturüberständen (mit vs. ohne Kit M-Vorbehandlung und vor vs. nach der Kultivierung) wurden mit einer eNose gemessen. Im Vergleich zur Kontrolle (ohne Zusatz von Kit M) bildete leukämisches und gesundes Blut nach MLC-Kultivierung höhere Werte von (Kit M vorbehandelten) DC-Subtypen und von aktivierten und (Gedächtnis-)T-Zellen. Darüber hinaus wurden antigen-(leukämie-)spezifische Zellen verschiedener Abstammungslinien (Zellen der angeborenen und erworbenen Immunität) induziert, die zu Blasten-lysierenden Zellen führten. Die eNose war in der Lage, signifikant zwischen den flüchtigen Phasen aus dem Überstand von Seren, DCs und MLCs von gesunden und leukämischen Patienten zu unterscheiden. Auch konnte sie mehrere Überstände (mit vs. ohne Kit M-Behandlung, kultiviert vs. unkultiviert) innerhalb von Untergruppen (gesunde DCs oder leukämische DCs oder gesunde MLCs oder leukämische MLC-Überstände) signifikant differenzieren.

3) Drei therapie-refraktäre AML-Patienten wurden unterschiedlich therapiert: P1511 erhielt eine Chemotherapie und diente als Kontrolle. P1482 und P1601 wurden mit Kit M (GM-CSF bzw. PGE1) behandelt. Diese Patienten wurden während des gesamten Behandlungszeitraums klinisch, hämatologisch und immunologisch überwacht. Während des Beobachtungszeitraums wurden Blutproben entnommen, um (leukämiespezifische) Immunzellen zu überwachen (Durchflusszytometrie, CSA, InCyt). Flüchtige organische Verbindungen (VOC) wurden in Atemmasken (Ausatemluft von AML-Patienten) im Krankheitsverlauf und von gesunden Probanden gesammelt und mit einer eNose gemessen. Die In-vivo-Behandlung von Patienten mit Kit M erwies sich als sicher, verbesserte klinische Parameter (Neutrophilen-, Thrombozyten- und Blastenzahl) und induzierte eine (leukämiespezifische) Immunaktivierung, wobei die Effekte nach Absetzen der Kit

M-Behandlung abnahmen. Die VOC-Ergebnisse der gesunden und leukämischen Patienten P1511, P1482 und P1601 konnten während des gesamten Beobachtungszeitraums voneinander unterschieden werden. Darüber hinaus unterschieden sich die VOC-Profile von gesunden und AML-Patienten sowie die VOC-Ergebnisse während der Chemotherapie und die unter Kit M-Therapie signifikant.

Diese Proof-of-Concept-Studie, die auf Ex-vivo- und In-vivo-Ergebnissen beruht, bestätigt, dass VOCs, die aus Zellkulturüberständen und Atemmasken unter Verwendung einer eNose gewonnen werden, eine zukünftige Option für ein verfeinertes Diagnoseinstrument (gesund vs. Leukämie) darstellen und eine VOC-basierte krankheitsbezogene Überwachungsstrategie ableiten können.

4. Abstract

Hydrocarbon molecules found in volatile organic compounds (VOCs) are indicative of pathological states and metabolism in both healthy individuals and patients and can be measured by an eNose. VOC analysis can be used to detect disease associated markers. Their role in tumor and immune activation could contribute to monitor antileukemic processes and might offer a refined diagnostic- and biomonitoring tool. VOCs were collected from serum, DC- and MLC culture supernatants or from breath masks (directly derived from patients' exhaled breath). To prove immunological (tumor associated) changes in AML patients' and healthy probands' VOC samples we correlated cell biological analyzes with the VOC results. After we demonstrated the antileukemic effect of Kit M on whole blood and bone marrow (publication I), we first conducted an ex vivo study (publication II) and then an in vivo study (publication III).

1) To create DC/DC_{leu}, we established dendritic cell cultures (DC cultures) from leukemic and healthy whole blood (WB) either without (Control) or with immunomodulatory Kit M (which consists of prostaglandin E1 (PGE_1) and granulocyte macrophage colony stimulating factor (GM-CSF). In mixed lymphocyte cultures (MLC cultures), T cell-enriched immunoreactive cells were stimulated using Kit M-pretreated/not pretreated WB including DC/DC_{leu}. Using an intracellular cytokine test (InCyt) and a degranulation assay (Deg), leukemia-specific adaptive and innate immune cells were identified. Using a cytotoxicity fluorescence test (CTX), anti-leukemic cytotoxicity was assessed.

2) An eNose was used to assess volatile organic compounds (VOCs) extracted from serum or DC- and MLC culture supernatants (with vs. without Kit M pretreatment and before vs. after culture). Kit M-pretreated leukemic and healthy WB resulted in increased frequencies of (leukemia-derived) DC subtypes of activated and (memory) T cells after MLC compared to the Control (without treatment). Additionally, blast-lysing cells were produced by inducing antigen (leukemia)-specific cells of several lines (innate and adaptive immune cells). Between healthy and leukemic patients' serum, DC and MLC culture supernatant-derived volatile phases, and several supernatants (with vs. without Kit M treatment, cultured vs. uncultured)-derived VOCs within subgroups (healthy DC or leukemic DC, or healthy MLC or leukemic MLC supernatants) could all be significantly distinguished by the eNose. Moreover, the eNose could indicate a culture-associated and Kit M-effect.

3) Throughout the course of the disease, we monitored three refractory AML patients receiving various treatments: P1511, who had chemotherapy, acted as a control. Kit M (GM-CSF and PGE_1) was used to treat P1482 and P1601. During treatment period these patients were kept under close clinical, hematological and immunological observation. In the course of the disease blood samples were collected and analyzed to monitor (leukemia specific) immune cells using flow cytometry, CSA, and InCyt. VOCs were measured using an eNose after being collected in earloop masks (containing exhaled air from healthy probands and AML patients) in the course of the disease. Treatment with Kit M in vivo was demonstrated to be safe, to increase clinical parameters (neutrophils, thrombocytes, and a reduction of blasts), and to stimulate (leukemia specific) immunological activation; The effects subsided when the Kit M treatment was stopped. It was possible to distinguish between leukemic and healthy VOC profiles from P1511, P1482, and P1601 over the whole observation period. Additionally, there were significant differences in the VOC profiles obtained from healthy vs. AML breath donors and the VOC prints obtained during chemotherapy vs. Kit M therapy.

This proof-of-concept-study, based on ex vivo and in vivo results, confirms, that VOCs derived from cell culture supernatants and breath masks using an eNose contribute to be a prospective option for a refined diagnostic tool (healthy vs. leukemia) and help determine a disease-related monitoring strategy.

5. Publication I

International Journal of *Molecular Sciences*

MDPI

Article

Granulocyte-Macrophage-Colony-Stimulating-Factor Combined with Prostaglandin E1 Create Dendritic Cells of Leukemic Origin from AML Patients' Whole Blood and Whole Bone Marrow That Mediate Antileukemic Processes after Mixed Lymphocyte Culture

Marianne Unterfrauner [1], Hazal Aslan Rejeski [1], Anne Hartz [1], Sophia Bohlscheid [1], Tobias Baudrexler [1], Xiaojia Feng [1], Elias Rackl [1], Lin Li [1], Andreas Rank [2], Giuliano Filippini Velázquez [2], Christoph Schmid [2], Jörg Schmohl [3], Peter Bojko [4] and Helga Schmetzer [1,*]

[1] Department of Medicine III, University Hospital of Munich, 81377 Munich, Germany
[2] Department of Hematology and Oncology, University Hospital of Augsburg, 86156 Augsburg, Germany
[3] Department of Hematology and Oncology, Diakonieklinikum Stuttgart, 70176 Stuttgart, Germany
[4] Department of Hematology and Oncology, Rotkreuzklinikum Munich, 80634 Munich, Germany
* Correspondence: helga.schmetzer@med.uni-muenchen.de; Tel.: +49-0-89-4400-73137; Fax: +49-0-89-4400-76137

Abstract: Although several (chemotherapeutic) protocols to treat acute myeloid leukemia (AML) are available, high rates of relapses in successfully treated patients occur. Strategies to stabilize remissions are greatly needed. The combination of the (clinically approved) immune-modulatory compounds Granulocyte-Macrophage-Colony-Stimulating-Factor (GM-CSF) and Prostaglandine E1 (PGE-1) (Kit-M) converts myeloid blasts into dendritic cells of leukemic origin (DC_{leu}). After stimulation with DC_{leu} ex vivo, leukemia-specific antileukemic immune cells are activated. Therefore, Kit-M treatment may be an attractive immunotherapeutic tool to treat patients with myeloid leukemia. Kit-M-mediated antileukemic effects on whole bone marrow (WBM) were evaluated and compared to whole blood (WB) to evaluate the potential effects of Kit-M on both compartments. WB and WBM samples from 17 AML patients at first diagnosis, in persisting disease and at relapse after allogeneic stem cell transplantation (SCT) were treated in parallel with Kit-M to generate DC/DC_{leu}. Untreated samples served as controls. After a mixed lymphocyte culture enriched with patients' T cells (MLC), the leukemia-specific antileukemic effects were assessed through the degranulation- ($CD107a^+$ T cells), the intracellular IFNγ production- and the cytotoxicity fluorolysis assay. Quantification of cell subtypes was performed via flow cytometry. In both WB and WBM significantly higher frequencies of (mature) DC_{leu} were generated without induction of blast proliferation in Kit-M-treated samples compared to control. After MLC with Kit-M-treated vs. not pretreated WB or WBM, frequencies of (leukemia-specific) immunoreactive cells (e.g., non-naive, effector-, memory-, $CD3^+\beta7^+$ T cells, NK- cells) were (significantly) increased, whereas leukemia-specific regulatory T cells (T_{reg}, $CD152^+$ T cells) were (significantly) decreased. The cytotoxicity fluorolysis assay showed a significantly improved blast lysis in Kit-M-treated WB and WBM compared to control. A parallel comparison of WB and WBM samples revealed no significant differences in frequencies of DC_{leu}, (leukemia-specific) immunoreactive cells and achieved antileukemic processes. Kit-M was shown to have comparable effects on WB and WBM samples regarding the generation of DC_{leu} and activation of (antileukemic) immune cells after MLC. This was true for samples before or after SCT. In summary, a potential Kit-M in vivo treatment could lead to antileukemic effects in WB as well as WBM in vivo and to stabilization of the disease or remission in patients before or after SCT. A clinical trial is currently being planned.

Keywords: AML; whole blood; whole bone marrow; immune escape; leukemia-derived dendritic cells; dendritic cell-based therapy

check for updates

Citation: Unterfrauner, M.; Rejeski, H.A.; Hartz, A.; Bohlscheid, S.; Baudrexler, T.; Feng, X.; Rackl, E.; Li, L.; Rank, A.; Filippini Velázquez, G.; et al. Granulocyte-Macrophage-Colony-Stimulating-Factor Combined with Prostaglandin E1 Create Dendritic Cells of Leukemic Origin from AML Patients' Whole Blood and Whole Bone Marrow That Mediate Antileukemic Processes after Mixed Lymphocyte Culture. *Int. J. Mol. Sci.* **2023**, *24*, 17436. https://doi.org/10.3390/ijms242417436

Academic Editor: Akiyoshi Takami

Received: 31 October 2023
Revised: 2 December 2023
Accepted: 4 December 2023
Published: 13 December 2023

1. Introduction

1.1. Acute Myeloid Leukemia

Acute myeloid leukemia (AML) is a hematological malignancy defined by uncontrolled expansion of myeloid blasts [1]. According to the hypothesis of the simplified "two-hit model of leukemogenesis", in many cases, two types of mutations are involved in AML pathogenesis: one resulting in uncontrolled proliferation (e.g., *FLT3*, *NRAS*) and the other leading to impairment of physiological myeloid differentiation (e.g., *TP53*, *CEBPA*) [2]. Clinical symptoms of AML patients are heterogeneous and include hemorrhages and severe infections due to bone marrow failure [3,4].

1.2. The Physiologic and Leukemic Bone Marrow Niche

The bone marrow (BM) represents the main site of hematopoiesis [5]. The endosteum with its vessels forms the niche responsible for maintaining a constant pool of hematopoietic stem cells (HSCs) [5,6]. In a dense network of vasculature and fenestrated sinusoids occupying most of the space of BM, HSCs differentiate into erythrocytes, progenitor, myeloid and lymphoid cells. The highly-regulated interplay of reticular cells, endothelial cells, HSCs, mesenchymal stromal cells (MSCs), osteoblasts, adipocytes, immune cells, chemokines, and growth and adhesion factors is instrumental for the controlled differentiation of all blood cell lineages in the steady-state and in response to stress [5,7,8].

In AML however, the physiological BM niche is disrupted and remodeled into an environment favorable for leukemic growth and progression [8,9]. MSCs seem to play an important role in this development since MSCs isolated from AML patients vs. those from healthy donors showed a higher immunosuppressive effect. A dysregulated cytokine production from MSCs and leukemic blasts (e.g., inhibited IFNγ and increased IL-10 production) was shown to lead to impaired T cell functions and further blast proliferation [10–12]. In consequence, it was shown that the number of regulatory T cells (T_{reg}) was increased, and dendritic cell (DC) and natural killer (NK) cell functions were inhibited [10]. Leukemic blasts were shown to adhere to stromal cells, leading to the persistence of minimal residual disease and chemoresistance [9]. Furthermore, AML cells can change adipocytes' function to promote their own metabolism. The transport of fatty acids from adipocytes was shown to be induced and thus benefits the proliferation of blasts [13]. Moreover, in leukemia, the number of osteoblasts, important for the physiological differentiation of HSCs, was shown to be decreased [8]. Furthermore, neoangiogenesis in BM might be induced by angiogenic growth factors secreted by blasts and could play a role in the progression of leukemia [9].

1.3. Standard Treatment and Advances in AML Therapy

For decades, the standard AML therapy has been the administration of a "7 + 3" chemotherapy regimen (7 days Cytarabine and 3 days Daunorubicin) [2]. Until today, allogeneic hematopoietic stem cell transplantation (HSCT) is the only curative treatment option for most patients [14]. Relapse rates after chemotherapy varying from 30% (younger patients with favorable risk) to 80% (elderly patients with adverse risk) [15], and relapse rates after HSCT of 40% demonstrate that therapies to stabilize remissions are highly needed [16]. Enhanced understanding of the molecular mechanisms behind AML and the potential of blasts to escape the immune system has led to the development of targeted therapies using specific antibodies and cells [17]: e.g., antibodies targeting CD33 (e.g., Gemtuzumab-Ozogamicin), CD123 [17–19] or checkpoint molecules (e.g., Nivolumab) [20]. Furthermore, Midostaurin, inhibiting *FLT3* mutations (being present in 30% of newly diagnosed adults) [21], Venetoclax, inhibiting the anti-apoptotic protein BCL2 [22], and Ivosidenib or Enasidenib, inhibiting *IDH1* or *IDH2* mutations (being present in 7–19% of AML patients) [3], have become crucial components in AML therapy. The only approved drug for maintenance therapy (for patients in first remission following chemotherapy) is an oral hypomethylating agent: Azacytidine [23].

Another very promising approach is the use of chimeric antigen receptor (CAR) T cells, genetically modified T cells binding leukemia-specific antigens and inducing antileukemic

effects [3,17,24]. Finally, even if the AML blasts might be effectively combated by treatment, leukemic stem cells (LSCs) often persist (in the bone marrow or in the body tissue) through immune escape mechanisms that are not entirely understood and are responsible for relapses [2].

1.4. DC/DCleu-Based Therapy

DCs are potent antigen-presenting cells (APCs) bridging the gap between the innate and adaptive immune system and have the potential to express a full spectrum of (infectious or tumor) antigens in a costimulatory manner to immune cells [19,25].

In blood, DC can be subdivided into two major DC subsets: conventional DC (cDC), further divided into cDC1 (main surface markers: $CD141^+$, $CLEC9A^+$, $XCR1^+$) and cDC2 (main surface markers: $CD1c^+$ and $CD172a^+$), found in blood, lymphoid and non-lymphoid tissue and recognized as the major antigen-presenting cells and plasmacytoid DC (pDC; main surface markers: $CD123^+$, $CD303^+$ and $CD304^+$) secreting type 1 interferon [26–28]. DCs have the ability to recognize pathogen- or damage-associated patterns (PAMP or DAMP), subsequently undergo maturation processes (through, e.g., CCR7 expression), migrate to secondary lymphoid organs, present antigen fragments via major histocompatibility complex (MHC) I or II to naive T cells, and activate them through costimulatory molecules (e.g., CD80) and cytokine release [29].

A specialty of (myeloid) leukemic blasts is that they can be directly converted to "leukemia-derived dendritic cells" (DC_{leu}) [30]. Their leukemic derivation can be proven by "FISH-IPA", combining FISH-analysis of chromosomal aberration with surface staining (for DC phenotype) on slides [31] or flow cytometry (codetecting DC and blast markers) [32]. This is the best method to prove leukemic derivation of DC in all patient samples and is regularly used by us [33,34].

These DC_{leu}, presenting both DC- and individual patients' blast antigens, can initiate (patient-specific) anti-leukemic immune responses [30,32]. The comparison of several DC/DC_{leu}-generating protocols showed that Kit-M, a combination of Granulocyte-Macrophage-Colony-Stimulating-Factor (GM-CSF) and Prostaglandin E1 (PGE1), had the highest potential to produce DC/DC_{leu} from blast-containing leukemic whole blood (WB) (thereby stimulating physiological conditions) without induction of blast proliferation [33] (thereby simulating physiological conditions in the blood) and to induce anti-leukemic activity in AML patients [35,36]. In contrast to peripheral blood mononuclear cells (PBMCs) previously used to generate DCs, WB contains the broad spectrum of individual patients' soluble and cellular components [36]. With regard to potential future applications of Kit-M to convert blasts (in the hematopoietic system) to DC_{leu} in vivo, its effect on whole-bone-marrow-(WBM)-blasts in their inhibitory microenvironment and the primary center of leukemic origin needs to be further evaluated.

1.5. Aim of the Study

The aim of this study was to explore whether Kit-M treatment could overcome WBM's inhibitory microenvironment and lead to similar antileukemic effects as already shown in WB. Therefore, experiments with leukemic WB and WBM were performed in parallel, and results were compared.

In detail, we assessed:

- Composition of immune cells in uncultured (as well as after mixed lymphocyte culture (MLC) with Kit-M-treated vs. untreated) WB and WBM
- DC (subsets) from Kit-M-treated vs. untreated leukemic WB and WBM
- Platelet counts in WB and WBM DC culture supernatants under the influence of Kit-M vs. GM-CSF
- (Leukemia-specific/antileukemic) immunoreactive cells (activating/inhibitory cells of the adaptive and innate immune system: NK-, CIK-, iNKT- and T-cell subtypes) were specified using degranulation (DEG), intracellular cytokine (INCYT) as well as

cytotoxicity (CTX) assays in uncultured WB and WBM and after MLC with Kit-M-treated vs. untreated WB and WBM
- Differences of results obtained in WB vs. WBM
- Correlation analyses of ex vivo generated data with patients' allocation to clinical risk groups

2. Results

2.1. Uncultured WB and WBM

2.1.1. Composition of T and Innate Immune Cells in Uncultured Leukemic WB and WBM

No significant differences in the composition of T and innate immune cells were found in uncultured WB as compared to WBM (Figure 1).

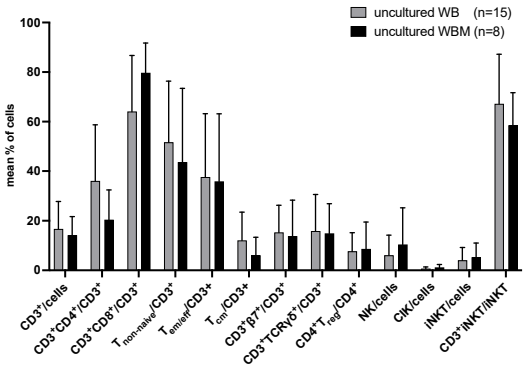

Figure 1. Composition of T and Innate Immune Cell Subtypes in Uncultured WB and WBM.

Flow cytometric analyses were performed to quantify T and innate immune cell subtypes in uncultured WB and WBM. Mean frequencies ± standard deviation (SD) of cell subtypes are given. Differences were considered as "highly significant" in cases with p-values ≤ 0.005, as "significant" with p-values ≤ 0.05, as "borderline significant" with p-values between 0.05 and 0.1, and as "not significant" (n.s.) with p-values ≥ 0.1. Abbreviations of cell subpopulations are given in table in Section 4.3.

2.1.2. Composition of (Leukemia-Specific) Degranulating or Intracellularly IFNγ- (and TNFα-) Producing Immunoreactive Cells in Uncultured WB and WBM

In WB (Figure 2A, left side), we found no significant differences in degranulating ($CD107a^+$) immunoreactive cells with LAA stimulation (WB^{+LAA}) vs. without (WB^{-LAA}). We found significantly higher frequencies of intracellularly IFNγ-producing ($IFN\gamma^+$) $CD3^+IFN\gamma^+$, $CD3^+CD4^+IFN\gamma^+$, and $CD3^+\beta7^+IFN\gamma^+$ cells in WB^{+LAA} as compared to WB^{-LAA} (Figure 2B, left side).

Similar results were obtained comparing degranulating WBM^{+LAA} vs. WBM^{-LAA} (Figure 2A, right side). In WBM, we found significantly higher frequencies of $CD3^+CD8^+IFN\gamma^+$, central memory (T_{cm}) $IFN\gamma^+$, and $CD3^+\beta7^+IFN\gamma^+$, and borderline significantly higher frequencies of $CD3^+IFN\gamma^+$ cells (Figure 2B, right side) in WBM^{+LAA} as compared to WBM^{-LAA}.

We detected significantly lower frequencies of $CD4^+T_{reg}CD107a^+$ in WB^{-LAA} as compared to WBM^{-LAA}. No significant differences in frequencies of $CD107a^+$ cells were found comparing WB^{+LAA} to WBM^{+LAA} (Figure 2A, left side vs. right side).

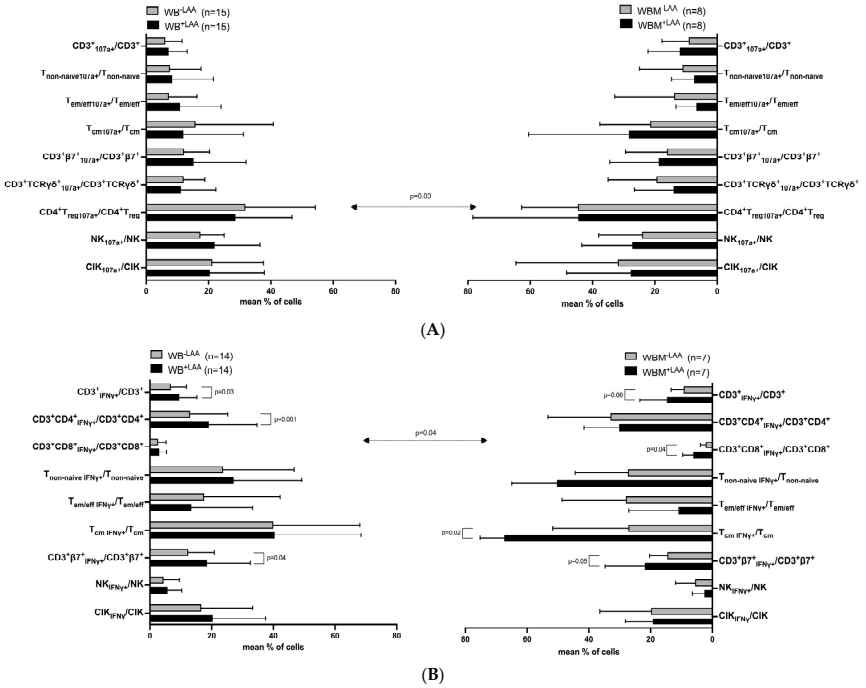

Figure 2. Composition of Leukemia-Specific Degranulating (**A**) or IFNγ-Secreting (**B**) Immunoreactive Cells in Uncultured WB and WBM.

Significantly higher frequencies of $CD3^+CD8^+IFN\gamma^+$ T cells were found comparing WB^{-LAA} with WBM^{-LAA}. We detected no significant differences in WB^{+LAA} vs. WBM^{+LAA} (Figure 2B, left side vs. right side).

Similar results were obtained studying intracellularly TNFα-producing immune cells [37].

The degranulation (Figure 2A) and the intracellular cytokine (Figure 2B) assay were performed to detect leukemia-specific cells in uncultured WB and WBM. Cells were stained with CD107a to detect degranulation activity and with IFNγ to examine intracellular cytokine production. Mean frequencies ± standard deviation (SD) of degranulating and IFNγ-secreting T and innate immune cells with or without previous LAA stimulation are given. Differences were considered as "highly significant" in cases with p-values ≤ 0.005, as "significant" with p-values ≤ 0.05, as "borderline significant" with p-values between 0.05 and 0.1, and as "not significant" (n.s.) with p-values ≥ 0.1. Double-sided arrows give (significant) differences between defined immunoreactive cell subtypes in WB and WBM. Abbreviations of cell subpopulations are given in table in Section 4.3.

2.2. Effects of Kit-M on the Generation of Mature DC/DC_{leu} from Leukemic WB and WBM

In WB, we generated significantly higher frequencies of DC, DC_{leu}, and mature DC (DC_{mat}) after treatment with Kit-M ($WB^{DC(M)}$) compared to control ($WB^{DC(Control)}$) (e.g., $\%DC_{leu}$/WB: $WB^{DC(M)}$: 9.59 ± 8.09; $WB^{DC(Control)}$: 5.99 ± 4.08, $p = 0.04$). Blasts' proliferation was not induced under the influence of Kit M (Figure 3A,B, left side).

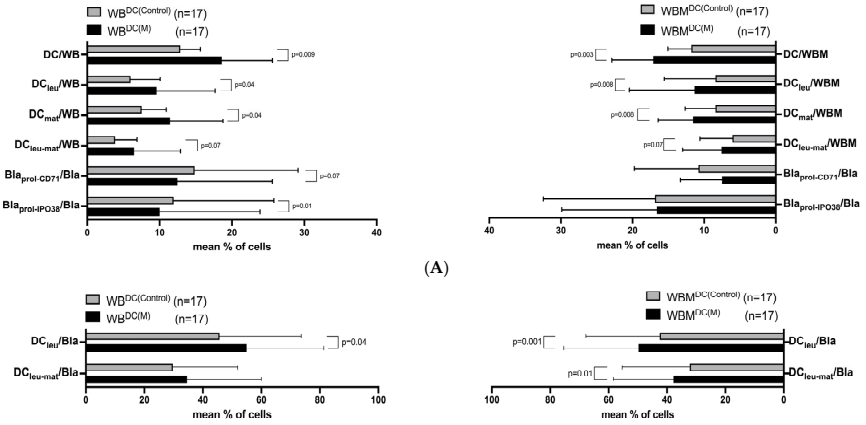

Figure 3. Effects of Kit-M on the Generation of (Mature) DC/DC_{leu} referred to WB (**A**) or Blasts (**B**) and on Blast Proliferation (**A**) in Leukemic WB and WBM.

In WBM, we found significantly higher frequencies of DC-subtypes comparing $WBM^{DC(M)}$ with $WBM^{DC(Control)}$ (e.g., $\%DC_{leu}$/WBM: $WBM^{DC(M)}$: 11.35 ± 9.11; $WBM^{DC(Control)}$: 8.42 ± 7.15, $p = 0.008$). Blasts' proliferation was not induced under the influence of Kit-M (Figure 3A,B, right side).

A parallel comparison of frequencies of DC-subtypes obtained with $WB^{DC(Control)}$ vs. $WBM^{DC(Control)}$ and $WB^{DC(M)}$ vs. $WBM^{DC(M)}$ (Figure 3A,B, left side vs. right side) revealed no significant differences.

WB and WBM samples were cultured in parallel for 7 days with Kit-M or without added Kit as control. Results with Kit-M ($WB^{DC(M)}$ and $WBM^{DC(M)}$) and without added Kit as control ($WB^{DC(Control)}$ and $WBM^{DC(Control)}$) are given. Mean frequencies ± SD of DC (subtypes) and proliferating blasts from leukemic WB (left side, Figure 3A,B) and leukemic WBM (right side, Figure 3A,B) samples are given. Differences were considered as "highly significant" in cases with p-values ≤ 0.005, as "significant" with p-values between 0.05 and 0.1, and as "not significant" (n.s.) with p-values ≥ 0.1. Abbreviations of cell subpopulations are given in table in Section 4.3.

2.3. Effects of Kit-M-Treated WB and WBM on Immunoreactive Cells before and after T Cell-Enriched Mixed Lymphocyte Culture (MLC)

We noticed a generally higher activation status of immune cells in WB after MLC ($WB^{DC\text{-}MLC}$) vs. WB^{DC} and in $WBM^{DC\text{-}MLC}$ vs. WBM^{DC} due to the stimulating effect of IL-2 [38].

After MLC, we found significantly higher frequencies of early proliferating ($T_{prol\text{-}early}$), non-naive ($T_{non\text{-}naive}$), effector memory ($T_{em/eff}$) and $CD3^+\beta7^+$ T cells comparing $WB^{DC\text{-}MLC(M)}$ with $WB^{DC\text{-}MLC(Control)}$ (e.g., $\%T_{non\text{-}naive}/CD3^+$: $WB^{DC\text{-}MLC(M)}$: 62.28 ± 22.74; $WB^{DC\text{-}MLC(Control)}$: 50.08 ± 25.37, $p = 0.001$). Furthermore, we found a significant decrease in frequencies of $CD152^+$ expressing T cells ($CD3^+CD152^+$) in $WB^{DC\text{-}MLC(M)}$ vs. $WB^{DC\text{-}MLC(Control)}$. Regarding cells of the innate immune system, we found significantly higher frequencies of NK and iNKT cells comparing $WB^{DC\text{-}MLC(M)}$ with $WB^{DC\text{-}MLC(Control)}$ (e.g., %NK/cells: $WB^{DC\text{-}MLC(M)}$: 10.42 ± 9.14; $WB^{DC\text{-}MLC(Control)}$: 5.57 ± 4.84, $p = 0.03$). Other cell subsets showed no significant differences in the groups compared (Figure 4, left side).

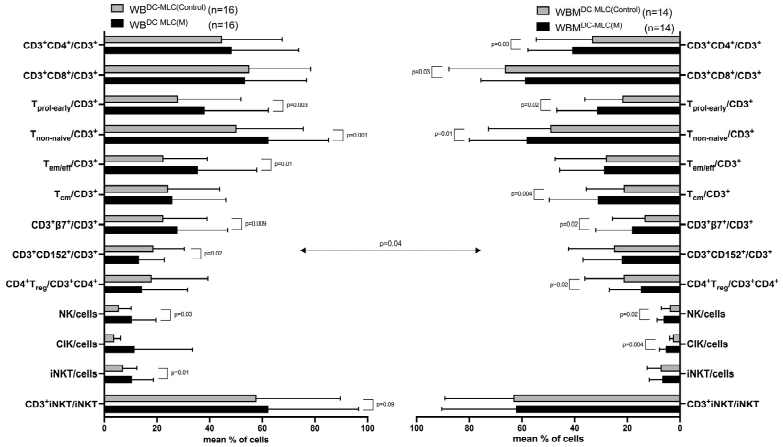

Figure 4. Effects of Kit-M-Treated WB and WBM on the Provision of Immunoreactive Cells After T cell-enriched Mixed Lymphocyte Culture (MLC).

In WBM, we found significantly higher frequencies of $CD3^+4^+$, $CD3^+CD8^+$, $T_{prol\text{-}early}$, $T_{non\text{-}naive}$, T_{cm}, and $CD3^+\beta7^+$ T cells comparing $WBM^{DC\text{-}MLC(M)}$ with $WBM^{DC\text{-}MLC(Control)}$ (e.g., $\%T_{non\text{-}naive}/CD3^+$: $WBM^{DC\text{-}MLC(M)}$: 58.32 ± 21.67; $WBM^{DC\text{-}MLC(Control)}$: 49.22 ± 23.43, $p = 0.01$). We detected significantly lower frequencies of $CD3^+CD8^+$ and $CD4^+T_{reg}$ in $WBM^{DC\text{-}MLC(M)}$ vs. $WBM^{DC\text{-}MLC(Control)}$. Significantly higher frequencies of NK and CIK cells were found comparing $WBM^{DC\text{-}MLC(M)}$ with $WBM^{DC\text{-}MLC(Control)}$ (e.g., %NK/cells: $WB^{DC\text{-}MLC(M)}$: 6.08 ± 2.67; $WB^{DC\text{-}MLC(Control)}$: 4.08 ± 3.11, $p = 0.02$). No other significant results were obtained from the groups compared (Figure 4, right side).

A parallel comparison of WB and WBM samples revealed significantly lower frequencies of $CD3^+CD152^+$ in $WB^{DC\text{-}MLC(M)}$ as compared to $WBM^{DC\text{-}MLC(M)}$ (Figure 4, left side vs. right side).

WB^{DC} and WBM^{DC} were enriched with autologous T cells, stimulated with IL-2, and cultured for 7 days in MLC. Given are the mean frequencies $\pm$ SD of T cell subsets and of cells of the innate immune system after MLC in $WB^{DC\text{-}MLC(Control)}$ and $WB^{DC\text{-}MLC(M)}$ (left side) and in $WBM^{DC\text{-}MLC(Control)}$ and $WBM^{DC\text{-}MLC(M)}$ (right side). Differences were considered as "highly significant" in cases with p-values ≤ 0.005, as "significant" with p-values ≤ 0.05, as "borderline significant" with p-values between 0.05 and 0.1, and as "not significant" (n.s.) with p-values ≥ 0.1. Double-sided arrows give (significant) differences between defined cell subtypes in WB and WBM. Abbreviations of cell subpopulations are given in table in Section 4.3.

2.4. Effects of Kit-M-Treated WB and WBM on the Degranulation Activity of Immunoreactive Cells after MLC

In WB, significantly higher frequencies of $CD3^+CD107a^+$, $T_{non\text{-}naive}CD107a^+$, $T_{em/eff}CD107a^+$, and $T_{cm}CD107a^+$ were found comparing $WB^{DC\text{-}MLC(M)}$ with $WB^{DC\text{-}MLC(Control)}$ (e.g., $\%T_{non\text{-}naive}CD107a^+/T_{non\text{-}naive}$: $WB^{DC\text{-}MLC(M)}$: 54.54 ± 24.65; $WB^{DC\text{-}MLC(Control)}$: 47.32 ± 22.55, $p = 0.002$). We showed a significant decrease in $CD4^+T_{reg}CD107a^+$ in $WB^{DC\text{-}MLC(M)}$ vs. $WB^{DC\text{-}MLC(Control)}$ (Figure 5, left side).

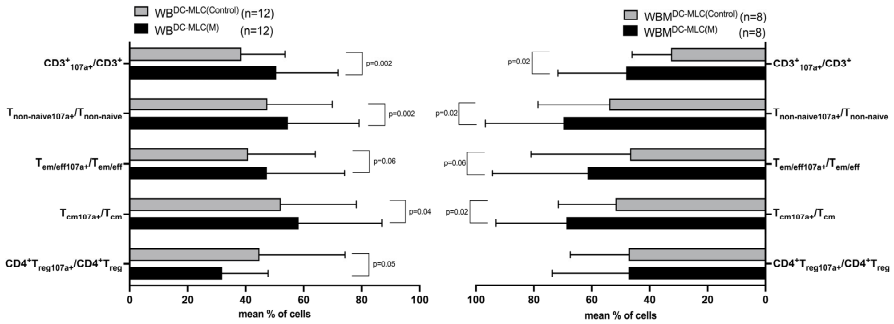

Figure 5. Effects of Kit-M-Treated WB and WBM on the Degranulation Activity of T cells After MLC.

In WBM, we obtained similar results to WB comparing $WBM^{DC\text{-}MLC(M)}$ to $WBM^{DC\text{-}MLC(Control)}$ (e.g., $\%T_{non\text{-}naive}CD107a^+/T_{non\text{-}naive}$: $WBM^{DC\text{-}MLC(M)}$: 69.70 ± 27.06; $WBM^{DC\text{-}MLC(Control)}$: 53.88 ± 24.68, $p = 0.02$). However, we could not detect significant differences of $CD4^+T_{reg}CD107a^+$ in the groups compared (Figure 5, right side).

A parallel comparison of frequencies obtained from $WB^{DC\text{-}MLC}$ vs. $WBM^{DC\text{-}MLC}$ showed no significant differences (Figure 5, left side vs. right side).

Kit-M-pretreated $WB^{DC\text{-}MLC(M)}$ and $WBM^{DC\text{-}MLC(M)}$ and untreated $WB^{DC\text{-}MLC(Control)}$ and $WBM^{DC\text{-}MLC(Control)}$ were stained with an antibody against CD107a to detect degranulating T cells as a marker for induced cell cytotoxicity. Given are the mean frequencies ± SD of T cell subsets expressing CD107a in leukemic WB (left side) and leukemic WBM (right side) without LAA stimulation. Differences were considered as "highly significant" in cases with p-values ≤ 0.005, as "significant" with p-values ≤ 0.05, as "borderline significant" with p-values between 0.05 and 0.1, and as "not significant" (n.s.) with p-values ≥ 0.1. Abbreviations of cell subpopulations are given in table in Section 4.3.

2.5. Effects of Kit-M-Treated WB and WBM on the Intracellular IFNγ (and TNFα) Production of Immunoreactive Cells after MLC

In WB, we found significantly higher frequencies of $CD3^+IFN\gamma^+$, $CD3^+CD8^+IFN\gamma^+$, $CD3^+\beta7^+IFN\gamma^+$, $T_{non\text{-}naive}IFN\gamma^+$, $T_{em/eff}IFN\gamma^+$ and $T_{cm}IFN\gamma^+$ comparing $WB^{DC\text{-}MLC(M)}$ with $WB^{DC\text{-}MLC(Control)}$ (e.g., $\%CD3^+IFN\gamma^+/CD3^+$: $WB^{DC\text{-}MLC(M)}$: 43.79 ± 18.77; $WB^{DC\text{-}MLC(Control)}$: 34.99 ± 18.05, $p = 0.00002$) (Figure 6, left side).

In WBM, higher frequencies of almost all previously mentioned cells were identified comparing $WBM^{DC\text{-}MLC(M)}$ with $WBM^{DC\text{-}MLC(Control)}$, though only $CD3^+IFN\gamma^+$ and $CD3^+\beta7^+IFN\gamma^+$ showed significant differences in the 7 parallelly studied cases (e.g., $\%CD3^+IFN\gamma^+/CD3^+$: $WBM^{DC\text{-}MLC(M)}$: 55.25 ± 18.90; $WBM^{DC\text{-}MLC(Control)}$: 38.98 ± 25.57, $p = 0.008$) (Figure 6, right side).

A parallel comparison of frequencies obtained from $WB^{DC\text{-}MLC}$ vs. $WBM^{DC\text{-}MLC}$ showed no significant differences (Figure 6, left side vs. right side).

The same applies to intracellularly TNFα-producing immune cells [37].

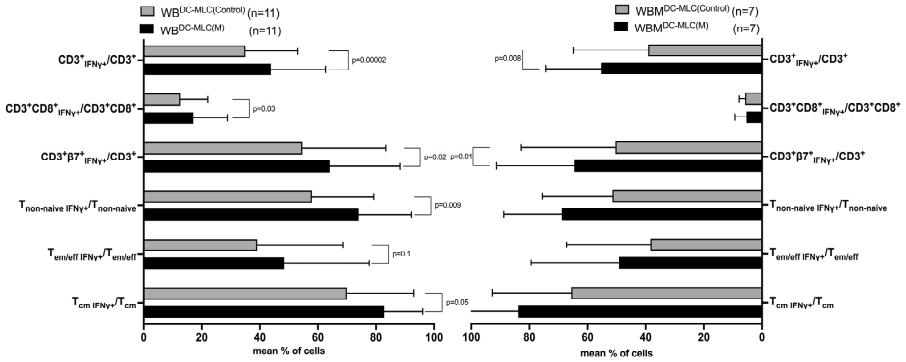

Figure 6. Effects of Kit-M-Treated WB and WBM on the Intracellular IFNγ Production of T cells After MLC.

Kit-M-pretreated WB$^{DC\text{-}MLC(M)}$ and WBM$^{DC\text{-}MLC(M)}$ and untreated WB$^{DC\text{-}MLC(Control)}$ and WBM$^{DC\text{-}MLC(Control)}$ were intracellularly stained with an antibody against IFNγ to detect cytokine-secreting T cells. Given are the mean frequencies ± SD of T cell subsets secreting IFNγ in cultured leukemic WB (left side) and leukemic WBM (right side) without LAA stimulation. Differences were considered as "highly significant" in cases with p-values ≤ 0.005, as "significant" with p-values ≤ 0.05, as "borderline significant" with p-values between 0.05 and 0.1, and as "not significant" (n.s.) with p-values ≥ 0.1. Abbreviations of cell subpopulations are given in table in Section 4.3.

2.6. Effects of Kit-M-Treated WB and WBM on the Anti-Leukemic, Blastolytic Functionality after MLC

In WB, after 3 h, we observed blast lysis in 69% of Kit-M-treated cases (WB$^{DC\text{-}MLC(M)}$) and in 62% of untreated cases (WB$^{DC\text{-}MLC(Control)}$). After 24 h, blast lysis was achieved in all cases of WB$^{DC\text{-}MLC(M)}$, whereas in WB$^{DC\text{-}MLC(Control)}$, in only 79% of cases (Figure 7A left side). After 3 h, average frequencies of blasts showed an increase in blasts in WB$^{DC\text{-}MLC(Control)}$ and blast lysis in WB$^{DC\text{-}MLC(M)}$. After 24 h, we found a highly significant decrease in frequencies of blasts in WB$^{DC\text{-}MLC(M)}$ vs. WB$^{DC\text{-}MLC(Control)}$ (Figure 7B left side). Concerning the lysis of blasts in WB$^{DC\text{-}MLC(M)}$ in relation to WB$^{DC\text{-}MLC(Control)}$, we could observe improved lysis in 85% of cases after 3 h and in 93% of cases after 24 h (Figure 7C left side). Frequencies of improved lysis were lower after 24 h as compared to after 3 h (Figure 7D). Overall, choosing the best lysis and the most-improved lysis after 3 h or 24 h showed the same results as after 24 h.

In WBM, after 3 h, we observed blast lysis in 58% of cases in WBM$^{DC\text{-}MLC(M)}$ and in 67% of cases in WBM$^{DC\text{-}MLC(Control)}$. After 24 h, blast lysis was achieved in 92% of cases in WBM$^{DC\text{-}MLC(M)}$ and in WBM$^{DC\text{-}MLC(Control)}$ in 69% of cases (Figure 7A right side). After 3 h, blasts increased and average frequencies of increased blasts were (n.s.) higher in WB$^{DC\text{-}MLC(M)}$ as compared to WB$^{DC\text{-}MLC(Control)}$. After 24 h, we found significantly lower frequencies of lysed blasts in WBM$^{DC\text{-}MLC(M)}$ vs. WBM$^{DC\text{-}MLC(Control)}$ (Figure 7B right side). Concerning the lysis of blasts in WBM$^{DC\text{-}MLC(M)}$ in relation to WBM$^{DC\text{-}MLC(Control)}$, we could observe improved lysis in 50% of cases after 3 h and in 92% of cases after 24 h (Figure 7C right side). After 3 h, the average frequencies did not show an improvement in blast lysis of WB$^{DC\text{-}MLC(M)}$ in relation to WB$^{DC\text{-}MLC(Control)}$. However, after 24 h, improved lysis could be seen. (Figure 7D). Analogous to WB, the best lysis and the most-improved lysis after 3 h or 24 h coincide with the results obtained after 24 h.

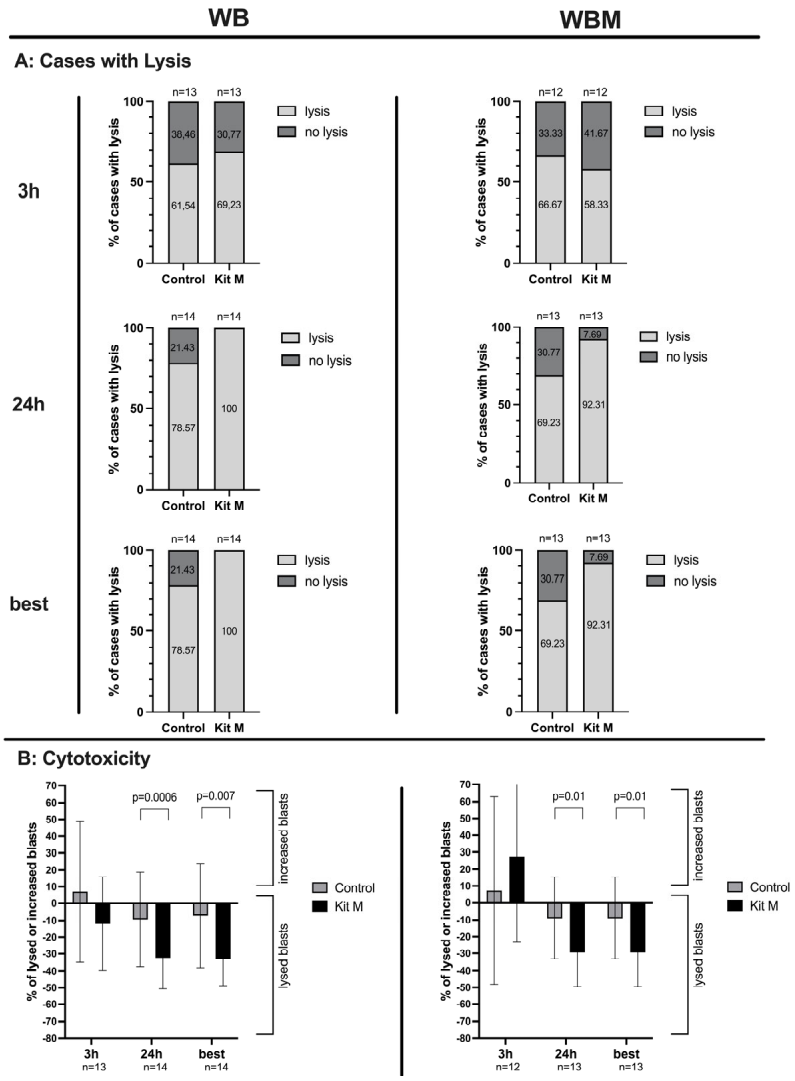

Figure 7. *Cont.*

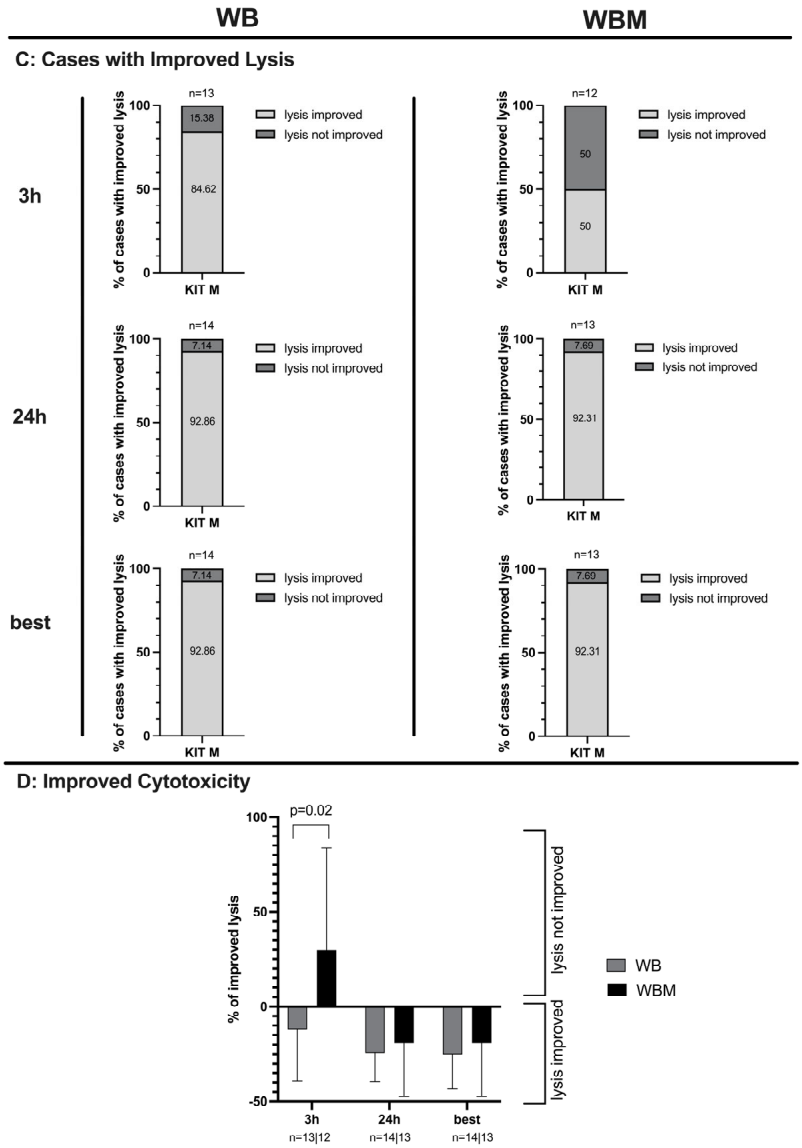

Figure 7. Effects of Kit-M-Treated WB and WBM on the Antileukemic Activity after MLC including Cases with Lysis (**A**), Cytotoxicity (**B**), Cases with Improved Lysis (**C**) and Improved Cytotoxicity (**D**).

Comparing the improved lysis in WB with WBM showed a significant difference ($p = 0.02$) in frequencies after 3 h, but not after 24 h (Figure 7D).

After MLC, $WB^{DC\text{-}MLC(M),(Control)}$ and $WBM^{DC\text{-}MLC(M),(Control)}$ served as "effector cells" and were cocultured with blasts ("target cells") for 3 h and 24 h to evaluate the lytic activity of Kit-M-Treated WB and WBM. Given are the proportions of cases with lysis (Figure 7A), the mean frequencies ± SD of increased or lysed blasts (Figure 7B), the proportion of cases with improved blast lysis (Figure 7C) and the mean frequencies ± SD of improved lysed blasts of Kit-M-Treated samples in relation to control (Figure 7D) after 3 h, 24 h and the best after 3 h or 24 h in WB (left side) and WBM (right side). Differences were considered as "highly significant" in cases with p-values ≤ 0.005, as "significant" with p-values ≤ 0.05, as "borderline significant" with p-values between 0.05 and 0.1 and as "not significant" (n.s.) with p-values ≥ 0.1. Abbreviations of cell subpopulations are given in table in Section 4.3.

2.7. Correlation of Results with Patients' Allocation to First Diagnosis and to Relapse after SCT

In patients at first diagnosis ($n = 10$) as well as at relapse after SCT ($n = 6$) higher frequencies of mature DC (subtypes) could be generated in Kit-M pretreated vs. control in WB as well as in WBM without induction of blast proliferation (e.g., at first diagnosis: $\%DC_{mat}$/WB: $WB^{DC(M)}$: 11.20 ± 5.17; $WB^{DC(Control)}$: 8.29 ± 3.20, $p = 0.14$; at relapse after SCT: $\%DC_{mat}$/WB: $WB^{DC(M)}$: 13.59 ± 9.77; $WB^{DC(Control)}$: 7.23 ± 3.14, $p = 0.15$; at first diagnosis: $\%DC_{mat}$/WBM: $WBM^{DC(M)}$: 11.49 ± 5.28; $WBM^{DC(Control)}$: 9.15 ± 4.36, $p = 0.08$; at relapse after SCT: $\%DC_{mat}$/WBM: $WBM^{DC(M)}$: 13.17 ± 2.47; $WBM^{DC(Control)}$: 8.26 ± 3.72, $p = 0.07$).

After MLC no significant differences in frequencies of ($CD107a^+$ and $IFN\gamma^+$) immunoreactive cells were found comparing samples at first diagnosis vs. at relapse after SCT in WB and WBM (e.g., $\%T_{non\text{-}naive}CD107a^+/T_{non\text{-}naive}$ (first diagnosis): $WB^{DC\text{-}MLC(M)}$: 55.00 ± 26.55; $WB^{DC\text{-}MLC(Control)}$: 45.71 ± 24.13, $p = 0.01$; $\%T_{non\text{-}naive}CD107a^+/T_{non\text{-}naive}$ (relapse after SCT): $WB^{DC\text{-}MLC(M)}$: 53.91 ± 24.76; $WB^{DC\text{-}MLC(Control)}$: 49.76 ± 22.4, $p = 0.04$).

Improved lysis was not different between cases at first diagnosis and relapse after SCT in WB as well as in WBM.

2.8. Correlation of Antileukemic Cytotoxicity with Patients' Allocation to Risk Groups

Cases with improved lysis after 3 h and 24 h and the best after 3 h or 24 h were allocated to patients' favorable ($n = 3$) vs. adverse ($n = 6$) cytogenetic risk allocation.

In WB, 100% of cases with favorable risk and 83.33% of cases of adverse risk achieved improved lysis after 3 h and 24 h (Figure 8A, left side).

In WBM, 100% of cases with favorable risk achieved improved lysis after 3 h and 24 h. In cases of adverse risk improved lysis was achieved in 16.67% of cases after 3 h and in 83.33% of cases after 24 h (Figure 8A, right side).

2.9. Correlation of Antileukemic Cytotoxicity with Patients' Allocation to Response to Induction Chemotherapy

Cases with improved lysis after 3 h, 24 h, and the best after 3 h or 24 h of coincubation were allocated to patients responding ("responders") ($n = 3$) and non-responding ("non-responders") ($n = 5$) to induction chemotherapy. In WB, 100% of responders and 80% of non-responders achieved improved lysis after 3 h and 24 h (Figure 8B, left side). In WBM, 100% of responders achieved improved lysis after 3 h and 24 h. Non-responders achieved improved lysis in 20% of cases after 3 h and in 80% of cases after 24 h (Figure 8B, right side).

WB (left side) and WBM (right side) samples were allocated to cytogenetic ELN risk groups (Figure 8A) and patients' response to induction chemotherapy (Figure 8B). Given the proportions of cases with improved blast lysis after 3 h, 24 h and the best after 3 h or 24 h.

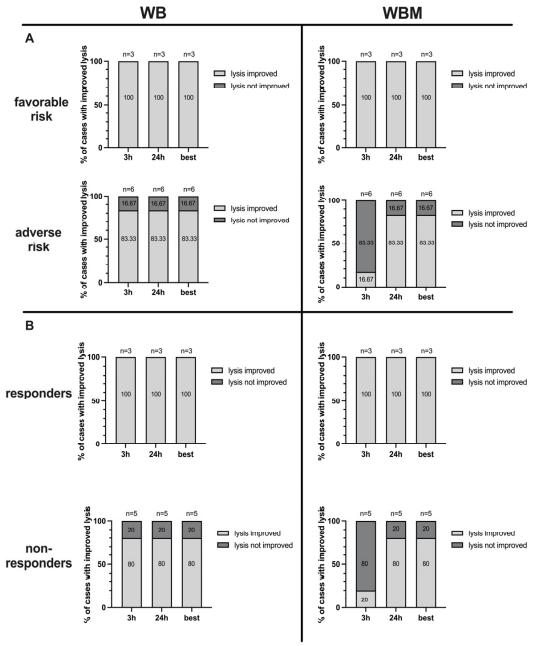

Figure 8. Cases with Improved Lysis in Patient Samples Subdivided into Risk Groups (**A**) and Response to Induction Chemotherapy (**B**) at First Diagnosis.

2.10. Effects of Kit-M-Treated WB and WBM on Platelet Counts

We found an average platelet count of 110.8 × 103/µL in WB (range: 59–215 × 103/µL) and of 82.8 × 103/µL in WBM (range: 35–225 × 103/µL). We studied the influence of Kit-M vs. GM-CSF alone on the provision of platelets in the course of culture in 5 cases: we found that in WB, on average platelet counts increased under the influence of GM-CSF alone as well as of GM-CSF+PGE-1 (Kit-M) (Figure 9). A detailed analysis showed that in two cases (1601, 1620) in WB results after GM-CSF vs. Kit-M treatment were comparable, leading to increased platelet counts, whereas in another case (1618), they decreased. In case 1621 platelets were more increased under the influence of GM-CSF vs. Kit-M, while in case 1624 Kit-M produced more platelets vs. GM-CSF.

In WBM, average platelet counts increased under the influence of GM-CSF alone as well as after Kit-M pretreatment. In two cases (1620, 1621), results of GM-CSF and Kit-M were comparable-leading to increased platelet counts, whereas in others (1624) they decreased. In cases 1601 and 1618 platelets decreased under GM-CSF treatment, whereas Kit-M treatment led to an increase.

Platelets were counted on day 0, 3, and 7 after culture of Kit-M-treated WB (Kit-M WB) and WBM (Kit-M WBM). GM-CSF-treated WB (GM-CSF WB) and WBM (GM-CSF WBM) served as a control. The average fold change values of platelets ± SD as well as single case fold changes are given in WB (Figure 9A) and WBM (Figure 9B).

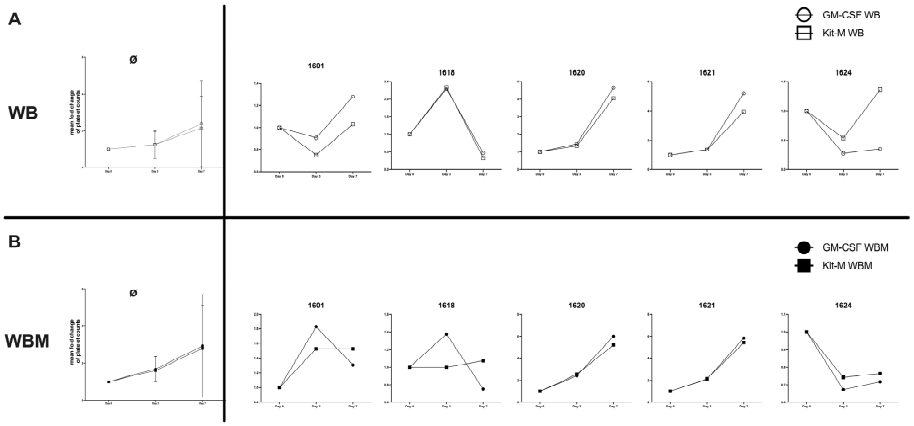

Figure 9. Effects of Kit-M or GM-CSF-Treated WB (**A**) and WBM (**B**) on Platelet Counts.

3. Discussion

3.1. WBM-the Immunosuppressive Leukemic Microenvironment

The physiological WBM-microenvironment (consisting of osteoblasts, MSC, HSC, adipocytes etc.) enables a strictly regulated hematopoiesis in the steady state as well as under stress [6,7]. However, the same microenvironment seems crucial in the transformation into a leukemic microenvironment through defective signaling pathways in specific cell types (e.g., β-catenin in osteoblasts, Notch signaling in endothelial cells) [39–41]. Leukemic cells and LSC express the chemokine receptor CXCR4 [42], which binds CXCL12, present on many WBM stromal cells [43]. With this binding, LSC replace HSC from their niche and remodel the microenvironment to their benefit in order to proliferate and migrate (e.g., adipocytes' fatty acids as a source for leukemic metabolism [13], neoangiogenesis in WBM induced by blasts secreting angiogenic growth factors [9]). The leukemic microenvironment is furthermore characterized by its ability to support (immune) cells to bypass the immune system through a wide variety of mechanisms (e.g., impairing T cell function by downregulation of MHC II, expression of inhibitory checkpoint receptors (e.g., PD-1), increasing frequencies of T_{reg}, inhibiting NK cell function, production of immunoinhibitory cytokines such as transforming growth factor beta (TGF β) and IL-10) [10,19]. These conditions and other mechanisms, which still need to be discovered in detail (e.g., LSC's niche protection, self-renewal capacity, phenotypic/epigenetic plasticity), favor the persistence of quiescent and therapy-resistant LSC and were found mainly responsible for relapse [2,44].

Although promising approaches targeting blasts of any kind (e.g., PD-1 Inhibitors, CAR T cells, . . .) are in the focus of research [17], the greatest challenge remains to find a targeted therapy that attacks specifically these quiescent LSCs, bypasses immune escape mechanisms, acts throughout the body and does not affect healthy tissue.

3.2. DC-Based Immunotherapy

We successfully showed in previous studies that blasts can be turned regularly into DC_{leu} treating leukemic PBMC or WB ex vivo with combinations of response modifiers like Kit-M (GM-CSF and PGE-1) [35]. DC/DC_{leu} are cells able to migrate to tissues in the whole body, present patient-specific blast antigens in a costimulatory manner to immune cells, and thus, induce potent patient-specific anti-leukemic activity [32,45]. To expand our understanding of the potential effects of Kit-M, in this study, we treated WBM with Kit-M and compared results to Kit-M-treated WB.

3.3. Composition of Uncultured WB and WBM

Since average blast counts were 20% in uncultured WB and 26% in uncultured WBM as detected by flow cytometry, achieved results in WB and WBM were comparable. Frequencies of uncultured and leukemia-specific (degranulating or IFNγ-producing) immunoreactive cells with or without LAA (WT-1 and PRAME) stimulation were comparable in WB vs. WBM (Figures 1 and 2). Interestingly, we found significantly higher frequencies of IFNγ-producing T_{cm} in WBM^{+LAA} compared to WBM^{-LAA} (Figure 2). This data confirm that LAA stimulation can increase the provision of leukemia-specific immunoreactive cells [46]. Here, we could confirm these findings in some subtypes. Comparing uncultured WB^{-LAA} vs. WBM^{-LAA} significantly lower frequencies of degranulating T_{reg} were found in WB. This was consistent with previous studies suggesting WBM being the preferential site of migration and function of T_{reg} going along with a higher activity of suppressive cells [11].

3.4. Generation of (Mature) DC/DC_{leu} in Kit-M-Treated WB and WBM

We could confirm preliminary data and generated significantly higher frequencies of DC/DC_{leu} in Kit-M-treated WB vs. control [32,35,46]. Comparable results were obtained in WBM. By generating higher frequencies of $DC_{mat/leu\text{-}mat}$ in both Kit-M-treated WB and Kit-M-treated WBM vs. control (Figure 3) we yield proof that in both compartments (WB and WBM) DC/DC_{leu} with migratory capacities (allowing their migration to lymph nodes and activating immune cells and allowing immunoreactive effects all over the body) were created [47]. Regarding safety considerations, we could confirm previous findings that blast proliferation was not induced in either WB or WBM [34].

3.5. Provision of Immunoreactive Cells after MLC in Kit-M-Treated WB and WBM

As previously shown, we could observe a generally higher activation status of immune cells comparing leukemic WB after a T cell-enriched MLC and before. Similar results were found in WBM. These results can probably be attributed to the effects of IL-2 stimulation [38,48,49]. In WB, Kit-M treatment led to significantly higher frequencies of (activated) T cell subsets (e.g., $T_{prol\text{-}early}$, $T_{non\text{-}naive}$) after MLC as compared to control (Figure 4). Here, we could confirm previous findings [48] and expand the potential effects of Kit-M to WBM, as comparable results were obtained. In the past, reduced β7-expressing T cells in leukemic compared to healthy samples were found, resembling an effect of leukemia-associated immunosuppression [50]. We showed increased β7-expressing T cells in Kit-M-treated leukemic WB and WBM as compared to control. This was previously correlated with a higher antileukemic potential in WB samples [46] and could now be confirmed also for WBM. High frequencies of regulatory cells (e.g., T_{reg} and CD152 expressing T cells) could already be correlated with immunosuppressive effects in leukemia [48,51,52]. In both Kit-M-treated WB and WBM, we were able to show decreased frequencies of these subtypes compared to control, suggesting a transformation into a less immunosuppressive environment. Comparing frequencies of WB's and WBM's control groups after MLC, we found significantly higher frequencies of $CD3^{+}CD152^{+}$ cells in WBM, confirming findings described in Section 3.3 about WBM being the preferential site of immunosuppression mediated by T_{reg} [11]. Innate immune cells, like NK, CIK, and iNKT cells, were shown to crosstalk with DC and lead to antitumor reactions [53,54]. We could already show a (significant) increase in NK, CIK, and iNKT cells in Kit-M-treated WB vs. control (e.g., [53]).

As already shown, we could demonstrate that in cultures with patients' cells at relapse after SCT (characterized by different chimerism), comparable antileukemic effects could be achieved, indicating a general blast modulatory/immune-activating mechanism in samples before or after SCT [55]. Here, we confirm these findings also for WBM, supporting the hypothesis that Kit-M treatment can contribute to overcome leukemic WBM's immunosuppressive environment, although these findings might not be true for iNKT cells in WBM (pointing to a more immunosuppressive environment in WBM vs. WB as shown before) [8,10].

3.6. Enhanced Degranulation Activity of T Cells after MLC in Kit-M-Treated WB and WBM

We could show an increased degranulation activity ($CD107a^+$) of T cell (e.g., $CD3^+CD107a^+$, $T_{non\text{-}naive}CD107a^+$, $T_{em/eff}CD107a^{+,}$ and $T_{cm}CD107a^+$) subtypes, proving the induction of leukemia-specific effector and memory cells, as demonstrated before [34,46]. Moreover, we found decreased frequencies of degranulating T_{reg} in Kit-M-treated WB vs. control (Figure 5). We thereby confirm previous studies indicating that Kit-M treatment leads to an enhanced anti-leukemic response in WB [46,56]. In WBM, similar results were obtained. However, Kit-M treatment seemed not to reduce frequencies of degranulating T_{reg} in WBM, which might confirm previous findings that WBM resident T_{reg} might be characterized by more immunosuppressive effects than T_{reg} detected in WB [10,57].

To evaluate potential proleukemic effects of T_{reg}' composition, blastolytic activities must be analyzed (Section 3.8).

3.7. Enhanced IFNγ Production of T Cells after MLC in Kit-M-Treated WB and WBM

We could confirm preliminary data by showing increased IFNγ production of antileukemically active β7-expressing, non-naive, as well as memory T cells (probably responsible for long-lasting immunity) in Kit-M-treated WB vs. control [34]. Results obtained in WBM were comparable, thereby proving the induction of leukemia-specific effects also in WBM (Figure 6). This means that the decrease of IFNγ production (being an immunoinhibitory effect in uncultured leukemic WB and WBM) could be overcome, as an increase in active anti-leukemic cells was detected in both compartments [10].

3.8. Improved Blastolytic Activity after MLC in Kit-M-treated WB and WBM

We could demonstrate a (significantly) improved lytic activity against leukemic blasts in WB and WBM through Kit-M-mediated pretreatment (Figure 7). In WB, more cases achieved lysis and improved lysis after 24 h compared to after 3 h. In WBM, only 50% of cases achieved improved lysis after 3 h. However, after 24 h, the results were comparable to WB. This occurrence might be explained by different cytotoxic mechanisms induced in immunoreactive cells in WB vs. WBM: the early and fast-acting perforin-granzyme pathway and the late and slow-acting Fas/FasL pathway, which can run separately or synergistically [35,58].

Interestingly, after collocating patients to adverse and favorable risks, as well as to responders (to induction chemotherapy) and non-responders, cases with no improved lysis after 3 h could be correlated in the majority to WBM of patients with adverse risk profiles and non-responders (Figure 8). In these cases, the immunoinhibitory mechanisms might be more pronounced, thus taking longer for the immune system to bypass them and elicit an anti-leukemic response [59].

3.9. Correlation of Results with Patients' Allocation to First Diagnosis and to Relapse after SCT

Comparison of results of Kit-M treatment (of WB and WBM) at first diagnosis vs. relapse after SCT showed no significant differences, suggesting potential effects of Kit-M treatment independent of patients' disease stages, before or after SCT, thereby confirming data of Ugur et al [55].

3.10. Influence of Kit-M or GM-CSF on Platelet Counts in WB and WBM

Studying the influence of Kit-M or GM-CSF (without added PGE-1) on the provision of platelets in WB or WBM in five cases in the course of the culture, we found an average increase in platelets in WB (twofold) and in WBM (twofold) compared to the start of culture. This was true in the presence of GM-CSF alone or Kit-M, thereby pointing to a potential of GM-CSF to stimulate thrombocytopoiesis as shown before [60,61]. Interestingly, these effects were seen without adding thrombopoietin or other thrombocytopoiesis-stimulating factors, which might point to the presence of these factors in WB or WBM [62]. However, the induction of platelets was not observed in every given case, which may have been due to insufficient thrombocytopoiesis-stimulating factors in these cases. Moreover, Kit-

M was shown to increase platelet counts compared to GM-CSF. This could point to an important potentially platelet-stimulating influence of Kit-M. These potential effects have to be explored in further (clinical) studies.

4. Materials and Methods

4.1. Sample Collection

Sample collection of heparinized WB and WBM was conducted after obtaining the written informed consent of the patients in accordance with the Declaration of Helsinki and the ethics committee of Ludwig-Maximilians-University-Hospital Munich (vote No. 339-05). Patient samples and clinical reports were provided by the University Hospital of Augsburg, the Diakonieklinikum Stuttgart, the Rotreuzklinikum Munich, and the St.-Josefs-Hospital Hagen.

4.2. Patients' Characteristics

WB and WBM samples were collected from 17 AML patients with an average age of 62 (range 22–78) years and a female-to-male ratio of 1.8:1. The average blast frequencies (as detected by flow cytometry) were 20% in WB and 26% in WBM. Patients were categorized based on the French American British (FAB) and World Health Organization (WHO) classification, the cytogenetic risk stratification (in favorable, intermediate, and adverse risks according to the European Leukemia Network (ELN) guideline 2017, molecular mutations and numeral and structural chromosomal aberrations are given), the stage of the disease (first diagnosis, persisting disease, relapse after SCT) and the etiology (primary, secondary, or therapy-related AML). Moreover, blast counts and phenotypes, as evaluated by flow cytometry, in WB and WBM are given. In patients at first diagnosis, the response to induction chemotherapy, and in patients after SCT, the leukocyte chimerism are given. An overview is given in Table 1.

4.3. Flow Cytometry

To assess and quantify phenotypes, frequencies, subgroups and functionality of leukemic blasts, DCs, T cells, NK cells, CIK cells, and iNKT cells flow cytometric analyses before and after culture were performed. Abbreviations of all cell types are given in Table 2.

Panels with various monoclonal antibodies (moAbs) labelled with Fluorescein isothiocyanate (FITC), Phycoerythrin (PE), Phycoerythrin Cyanin 7 (PC7) or Allophycocyanin (APC) were selected for cell staining. Antibodies were provided by Beckman Coulter[a] (Krefeld, Germany), Becton Dickinson[b] (Heidelberg, Germany), BioLegend[c] (Amsterdam, Netherlands), Miltenyi Biotec[d] (Bergisch Gladbach, Germany), and Santa Cruz Biotechnology[e] (Heidelberg, Germany).

Cells were stained with FITC-conjugated moAbs CD3[b], CD4[b], CD25[a], CD33[a], CD34[a], CD71[a], CD107[ac], CD117[c], CD154[b], CD45RO[a], IPO38[e]; PE-conjugated moAbs CD3[d], CD4[b], CD56[a], CD80[a], CD117[a], CD127[a], CD152[b], CD206[a], 6B11[b], IFNγ[c], TCR$\gamma\delta$[b]; PC7-conjugated moAbs CD3[a], CD4[a], CD25[b], CD33[a], CD34[a], CD56[a], CD117[a], CD197[b], TNFα[c]; and APC-conjugated moAbs CD3[a], CD33[a], CD34[a], CD56[a], CD80[c], CD117[a], CD137[b], CD206[b], CD45RO[c], Integrinβ7[b]. Death cells were detected using 7AADb. Isotype controls were conducted according to the manufacturer's instructions.

Prior to staining, erythrocytes in WB and WBM samples were lysed with lysing buffer (Becton Dickinson). Cells were then incubated with the corresponding moAbs for 15 min in the dark using a staining medium containing 95% PBS and 5% FCS (Biochrom, Berlin, Germany). Intracellular staining (IPO38, IFNγ, and TNFα) was conducted with the FIX&PERMTM Cell Fixation and Permeabilization Kit (ThermoFisher Scientific, Darmstadt, Germany).

Table 1. Patients' Characteristics.

Stage	Patient No.	Age at Sampling/Sex	FAB/WHO Classification	ELN (2017)-Risk-Stratification	Cyto-, Molecular Genetics	Blast Phenotype (CD)	IC in WB/WBM (%) *	Response to Induction Chemotherapy	Experiments Conducted with WB	Experiments Conducted with WBM
First Diagnosis	1615	78/F	sAML	Intermediate	*IDH1, ASXL1, JAK2, SRSF2*	**34**, **117**, 13	53/65	no	DC, MLC, Deg (UC, C), InCyt (UC, C), CTX	DC, MLC, CTX
	1618	63/M	pAML/M1	Favorable	*NPM1*	**117**, **33**, 13, 15	10/7	yes	DC, MLC, Deg (UC, C), InCyt (UC, C), CTX	DC, MLC, CTX
	1620	61/F	sAML	Adverse	t(2;3)(p23;q26), del (7)(q21), del(7)(q31), *MECOM* rearrangement, *ASXL1, RUNX1*	**34**, **117**, 33, 4	4/12	no	DC, MLC, Deg (UC), InCyt (UC), CTX	DC, MLC, CTX
	1621	71/M	sAML	Adverse	*TP53, ASXL1, SRSF2, SETPBP1, KRAS*	**34**, **117**, 5, 13	18/24	no	DC, MLC, Deg (UC, C), InCyt (UC, C), CTX	DC, MLC, CTX
	1624	77/F	sAML	Adverse	monosomy 7, der(7)t(1;7), der (2)t(2;3), del(7)(q31), ampl(3q26), *IDH2, STAG2, DNMT3A, MPL, NRAS, SRSF2*	**34**, **117**, 13	30/32	yes	DC, MLC, Deg (UC), InCyt (UC), CTX	DC, MLC, CTX
	1630	29/M	pAML	Favorable	*FLT3*-TKD, *NPM1, PTPN11*	**34**, **117**, 13, 33, 15, 64, 65	20/27	yes	DC, MLC, Deg (UC, C), InCyt (UC, C), CTX	DC, MLC, Deg (C), InCyt (C), CTX
	1638	68/M	sAML	Adverse	del(5)(q31), *TP53, RUNX1, RUNX1T1*	**34**, **117**, 33, 13, 56, 4	60/54	no	DC, MLC, Deg (UC, C), InCyt (UC, C), CTX	DC, MLC, Deg (UC, C), InCyt (UC, C), CTX
	1642	63/F	sAML	Adverse	*IDH2*, complex aberrant	**34**, **117**, 33, 13	1/19	yes	DC, MLC, Deg (UC, C), InCyt (UC, C), CTX	DC, MLC, Deg (UC, C), InCyt (UC, C), CTX
	1643	68/M	pAML	Favorable	*NPM1, IDH2*	**117**, **33**, 64, 13	23/39	no	DC, MLC, Deg (UC, C), InCyt (UC, C), CTX	DC, MLC, Deg (UC, C), InCyt (UC, C), CTX
	1645	58/F	pAML	Favorable	*IDH2, NPM1*	**117**, **33**, 56	36/47	yes	DC, MLC, Deg (UC), InCyt (UC)	DC, MLC, Deg (UC), InCyt (UC)

Table 1. *Cont.*

Stage	Patient No.	Age at Sampling/Sex	FAB/WHO Classification	ELN (2017)-Risk-Stratification	Cyto-, Molecular Genetics	Blast Phenotype (CD)	IC in WB/WBM (%) *	Response to Induction Chemotherapy	Experiments Conducted with WB	Experiments Conducted with WBM
Persisting Disease	1601	75/F	sAML	Adverse	none detected	**34**, **117**, 33, 13	61/49		DC, MLC, Deg (UC), InCyt (UC), CTX	DC, MLC, CTX
								Chimerism (%)		
Relapse After Stem Cell Transplantation	1628	22/F	tAML/M5		*RUNX1, WT1, FLT3-ITD, KMT2A-PTD*	**34**, **117**, 65, 33, 56, 64	3/31	77	DC, Deg (UC), InCyt (UC)	DC
	1640	73/F	pAML		del(9q), *NMP1, IDH2, WT1, DNMT3A*	**34**, **117**, 33, 13, 7	<1/<1	56	DC, MLC, Deg (UC, C), InCyt (UC, C), CTX	DC, MLC, Deg (UC, C), InCyt (UC, C), CTX
	1641	64/F	tAML		dup(13)(q12q33), *DLEU* signal, *FLT3-ITD, EZH2, WT1*	**34**, **117**, 33, 13, 64, 65, 15	6/16	62	DC, MLC, Deg (UC, C), InCyt (UC, C), CTX	DC, MLC, Deg (UC, C), InCyt (UC, C), CTX
	1650	64/F	AML-MRC		*RUNX1, BCOR, KMT2A-PTD, TP53*	**34**, **117**, 13	3/8	86	DC, MLC, Deg (UC, C), InCyt (UC, C), CTX	DC, Deg (UC), InCyt (UC)
	1654	71/M	pAML/M2		der(16)t(16;17), *NPM1*	**117**, **56**, 13, 34	3/3	97	DC, MLC, Deg (UC, C), InCyt (UC, C), CTX	DC, MLC, Deg (UC, C), InCyt (UC, C), CTX
	1656	42/F	pAML		*MECOM* rearrangement, complex aberrant, *PTPN11*	**34**, **117**, 33, 56, 13	7/14	86	DC, MLC, Deg (UC, C), InCyt (UC, C), CTX	DC, MLC, Deg (C), InCyt (C), CTX

Legend. F: female; M: male; AML: acute myeloid leukemia; FAB classification: French American British classification of AML; WHO classification: World Health Organization classification of AML; pAML: primary AML; sAML: secondary AML; tAML: therapy-related AML; AML-MRC: AML with myelodysplasia-related changes; ELN: European Leukemia Network; del: deletion; t: translocation; der: derivative; ampl: amplification; dup: duplication; CD: Cluster of differentiation; bold: antibody used for expression analyses; WB: whole blood; WBM: WBM; no rsp: no response DC: dendritic cell culture measurements; MLC: mixed lymphocyte culture measurement; Deg: degranulation assay; InCyt: intracellular cytokine assay; CTX: cytotoxicity measurements; UC: measurements in uncultured samples; C: measurements after mixed lymphocyte culture; * Immune cytologically evaluated blasts.

Table 2. Cells and cell subsets as evaluated by flow cytometry.

Cell Type	Name of Subgroups	Abbreviation of Subgroups	Surface Marker	Referred to	Abbreviation	Reference
Subtypes of blasts and DC						
Blast cells	Leukemic blasts	Bla	Bla^+ (e.g., $CD34^+$, $CD177^+$)	WB or WBM	Bla/WB or/WBM	[32]
	Proliferating blasts	$Bla_{prol\text{-}CD71}$	$Bla^+DC^-CD71^+$	Bla	$Bla_{prol\text{-}CD71}$/Bla	[33]
	Proliferating blasts	$Bla_{prol\text{-}Ipo38}$	$Bla^+DC^-Ipo38^+$	Bla	$Bla_{prol\text{-}Ipo38}$/Bla	[33]
Dendritic cells	Dendritic cells	DC	DC^+ ($CD80^+$, $CD206^+$)	WB or WBM	DC/WB or/WBM	[35]
	Leukemia derived DC	DC_{leu}	DC^+Bla^+	WB or WBM Bla	DC_{leu}/WB or/WBM DC_{leu}/Bla	[35]
	Mature DC	DC_{mat}	DC^+CD197^+	WB or WBM	DC_{mat}/WB or/WBM	[35]
	Mature DC_{leu}	$DC_{leu\text{-}mat}$	$DC^+CD197^+Bla^+$	WB or WBM	$DC_{leu\text{-}mat}$/WB or/WBM	[35]
				Bla	$DC_{leu\text{-}mat}$/Bla	[35]
Subtypes of Immune Reactive Cells						
T cells	$CD3^+$ pan T cells	$CD3^+$	$CD3^+$	cells	$CD3^+$/cells	[36]
	$CD4^+$coexpressing T cells	$CD3^+CD4^+$	$CD3^+CD4^+$	$CD3^+$	$CD3^+CD4^+/CD3^+$	[36]
	$CD8^+$coexpressing T cells	$CD3^+CD8^+$	$CD3^+CD8^+$	$CD3^+$	$CD3^+CD8^+/CD3^+$	[36]
	Proliferating T cells-early	$T_{prol\text{-}early}$	$CD3^+CD69+$	$CD3^+$	$T_{prol\text{-}early}/CD3^+$	[36]
	Non-naive T cells	$T_{non\text{-}naive}$	$CD3^+CD45RO^+$	$CD3^+$	$T_{non\text{-}naive}/CD3^+$	[34]
	Effector (memory) T cells	$T_{em/eff}$	$CD3^+CD45RO^+CD197^-$	$CD3^+$	$T_{em/eff}/CD3^+$	[34]
	Central (memory) T cells	T_{cm}	$CD3^+CD45RO^+CD197^+$	$CD3^+$	$T_{cm}/CD3^+$	[34]
	$CD137^+$ coexpressing T cells	$CD3^+CD137^+$	$CD3^+CD137^+$	$CD3^+$	$CD3^+CD137^+/CD3^+$	[63]
	Integrin$\beta7^+$ coexpressing T cells	$CD3^+\beta7^+$	$CD3^+$Integrin$\beta7^+$	$CD3^+$	$CD3^+\beta7^+/CD3^+$	[46]
	TCR$\gamma\delta^+$ coexpressing T cells	$CD3^+$TCR$\gamma\delta$	$CD3^+$TCR$\gamma\delta^+$	$CD3^+$	CD^{3+}TCR$\gamma\delta^+/CD3^+$	[46]
	$CD152^+$ coexpressing T cells	$CD3^+CD152^+$	$CD3^+CD152^+$	$CD3^+$	$CD3^+CD152^+/CD3^+$	[52]
	Regulatory T cells	$CD4^+T_{reg}$	$CD3^+CD4^+CD25^+CD127^{low}$	$CD3^+CD4^+$	$CD4^+T_{reg}/CD4^+$	[48]
Natural killer cells	$CD3^-CD56^+$NK cells	NK	$CD3^-CD56^+$	Cells	NK/cells	[53]

Table 2. *Cont.*

Cell Type	Name of Subgroups	Abbreviation of Subgroups	Surface Marker	Referred to	Abbreviation	Reference
Cytokine induced killer cells	$CD3^+CD56^+$ CIK cells	CIK	$CD3^+CD56^+$	Cells	CIK/cells	[53]
Invariant natural killer T cells	$6B11^+$ iNKT cells	iNKT	$6B11^+$	Cells	iNKT/cells	[53]
	$CD3^+$ coexpressing $6B11^+$ iNKT cells	$CD3^+$iNKT	$CD3^+6B11^+$	$6B11^+$	$CD3^+$iNKT/iNKT	[53]
Subtypes of different degranulating ($CD107a^+$) cells as evaluated by flow cytometry						
T cells	$CD3^+$ pan T cells	$CD3^+{}_{107a+}$	$CD107a^+CD3^+$	$CD3^+$	$CD3^+{}_{107a+}/CD3^+$	[64]
	Non-naive T cells	$T_{non\text{-}naive107a+}$	$CD107a^+CD3^+CD45RO+$	$T_{non\text{-}naive}$	$T_{non\text{-}naive107a+}/T_{non\text{-}naive}$	[64]
	Effector (memory) T cells	$T_{em/eff107a+}$	$CD107a^+CD3^+CD45RO^+CD197^-$	$T_{em/eff}$	$T_{em/eff107a+}/T_{em/eff}$	[64]
	Central (memory) T cells	$T_{cm107a+}$	$CD107a^+CD3^+CD45RO^+CD197^+$	T_{cm}	$T_{cm107a+}/T_{cm}$	[64]
	Integrin$\beta7^+$ coexpressing T cells	$CD3^+\beta7^+{}_{107a+}$	$CD107a^+CD3^+$Integrin$\beta7^+$	$CD3^+$	$CD3^+\beta7^+{}_{107a+}/CD3^+$	[46]
	TCR$\gamma\delta^+$ coexpressing T cells	$CD3^+TCR\gamma\delta^+{}_{107a+}$	$CD107a^+CD3^+TCR\gamma\delta^+$	$CD3^+TCR\gamma\delta^+$	$CD3^+TCR\gamma\delta^+{}_{107a+}/CD3^+$ TCR$\gamma\delta^+$	[65]
	Regulatory T cells	$CD4^+T_{reg107a+}$	$CD107a^+CD4^+CD25^+CD127^{low}$	$CD4^+T_{reg}$	$CD4^+T_{reg107a+}/CD4^+T_{reg}$	[48]
NK cells	$CD3^-CD56^+$NK cells	NK_{107a+}	$CD107a^+CD3^-CD56^+$	NKcell	NK_{107a+}/NK	[64]
CIK cells	$CD3^+CD56^+$ CIK cells	CIK_{107a+}	$CD107a^+CD3^+CD56^+$	CIKcell	CIK_{107a+}/CIK	[64]
Subtypes of different intracellularly IFNγ or TNFα-producing cells as evaluated by flow cytometry						
T cells	$CD3^+$ pan T cells	$CD3^+{}_{IFN\gamma/TNF\alpha}$	$IFN\gamma^+/TNF\alpha^+CD3^+$	$CD3^+$	$CD3^+{}_{IFN\gamma/TNF\alpha}/CD3^+$	[34]
	$CD4^+$-coexpressing T cells	$CD3^+CD4^+{}_{IFN\gamma/TNF\alpha}$	$IFN\gamma^+/TNF\alpha^+CD3^+CD4^+$	$CD3^+CD4^+$	$CD3^+CD4^+{}_{IFN\gamma/TNF\alpha}/CD3^+CD4^+$	[34]
	$CD8^+$-coexpressing T cells	$CD3^+CD8^+{}_{IFN\gamma/TNF\alpha}$	$IFN\gamma^+/TNF\alpha^+CD3^+CD8^+$	$CD3^+CD8^+$	$CD3^+CD4^-{}_{IFN\gamma/TNF\alpha}/CD3^+CD8^+$	[34]
	Non-naive T cells	$T_{non\text{-}naive\ IFN\gamma/TNF\alpha}$	$IFN\gamma^+/TNF\alpha^+CD3^+CD45RO^+$	$T_{non\text{-}naive}$	$T_{non\text{-}naive\ IFN\gamma/TNF\alpha}/T_{non\text{-}naive}$	[34]
	Effector (memory) T cells	$T_{em/eff\ IFN\gamma/TNF\alpha}/T_{em/eff}$	$IFN\gamma^+/TNF\alpha^+CD3^+CD45RO^+CD197^-$	$T_{em/eff}$	$T_{em/eff\ IFN\gamma/TNF\alpha}/T_{em/eff}$	[34]
	Central (memory) T cells	$T_{cm\ IFN\gamma/TNF\alpha}$	$IFN\gamma^+/TNF\alpha^+CD3^+CD45RO^+CD197^+$	T_{cm}	$T_{cm\ IFN\gamma/TNF\alpha}/T_{cm}$	[34]
	Integrin$\beta7^+$ coexpressing T cells	$CD3^+\beta7^+{}_{IFN\gamma/TNF\alpha}$	$IFN\gamma^+/TNF\alpha^+CD3^+\beta7^+$	$CD3^+\beta7^+$	$CD3^+\beta7^+{}_{IFN\gamma/TNF\alpha}/CD3^+\beta7^+$	[46]
NK cells	$CD3^-CD56^+$NK cells	$CD3^-CD56^+{}_{IFN\gamma/TNF\alpha}$	$IFN\gamma^+/TNF\alpha^+CD3^-CD56^+$	NK	$NK_{IFN\gamma/TNF\alpha}$/NK	[34]
CIK cells	$CD3^+CD56^+$ CIK cells	$CI_{IFN\gamma/TNF\alpha}$	$IFN\gamma^+/TNF\alpha^+CD3^+CD56^+$	CIK	$CIK_{IFN\gamma/TNF\alpha}$/CIK	[34]

All flow cytometric analyses were performed using the fluorescence-activated cell sorting flow cytometer FACSCalibur (Becton Dickinson) and the analysis software CellQuestPro 6.1 (Becton Dickinson) applying a refined gating strategy [34].

4.4. Sample Preparation

A fraction of WB and WBM was used directly to set up dendritic cell cultures and to perform the Degranulation Assay and the Intracellular Cytokine Assay. Peripheral blood mononuclear cells (PBMC) were isolated from WB using the Ficoll-Hypaque density gradient centrifugation (Biocoll separating solution, Biochrom, Berlin, Germany). Using the AML patients' PBMC T cell separation was carried out with the MACS® MicroBead Technology according to the manufacturer's protocol (Miltenyi Biotec).

PBMC and T cells were frozen in a freezing medium with 70% RPMI-1640 (Biochrom) containing 100 U/mL penicillin and 0.1 mg/mL streptomycin (PAN-Biotech, Aidenbach, Germany) (RPMI/PS), 20% human serum (PAN-Biotech), and 10% dimethyl sulfoxide (Sigma Aldrich Chemie GmbH, Steinheim, Germany) and stored at −80 °C until use.

4.5. Dendritic Cell Culture

Dendritic cells (DC) and leukemia-derived dendritic cells (DC_{leu}) were generated by treating WB and WBM in parallel with the DC/DC_{leu}-generating protocol "Kit-M", containing 800 U/mL Granulocyte-Macrophage-Colony-Stimulating-Factor (GM-CSF; Sanofi-Aventis, Frankfurt, Germany) and 1 µg/mL Prostaglandin-E1 (PGE1; Santa Cruz Biotechnology).

Therefore, WB and WBM were cultivated in sterile 24-well-plates (Cellstar®, Greiner Bio-One, Kremsmuenster, Austria) using 500 µL X-VivoTM 15 medium (Lonza, Verviers, Belgium) and 500µL WB and WBM. "Kit-M" was added on day 0 and after 2–3 days as described [35]. Untreated WB and WBM served as negative controls. DC cultures were incubated at 37 °C, 21% O_2, and 10% CO_2 for 7 days.

Flow cytometric analyses of DC-subtypes and proliferating blasts from both Kit-M-treated WB ($WB^{DC(M)}$) and WBM ($WBM^{DC(M)}$) and untreated WB ($WB^{DC(Control)}$) and WBM ($WBM^{DC(Control)}$) were performed before and after culture using a refined gating strategy [33,34]. In case of less than 1% blasts in the cell fractions, DC_{leu} and associated subgroups could not be evaluated.

4.6. T Cell-Enriched Mixed Lymphocyte Culture (MLC)

DC/DC_{leu} cultures were used as stimulators to activate T cell-enriched immune cells after MLC. Therefore, 2.5 × 105 cells from $WB^{DC(Control)/(M)}$ and $WBM^{DC(Control)/(M)}$ were cocultured in parallel with 1 × 106 previously thawed autologous T cells, diluted with RPMI/PS and incubated at 37 °C, 21% O_2 and 10% CO_2. 50 U/mL Interleukin-2 (IL-2, PeproTech, Berlin, Germany) was added to all cultures on day 0 and again after 2–3 and 5–6 days. Cells, later referred to as $WB^{DC\text{-}MLC(Control)/(M)}$ and $WBM^{DC\text{-}MLC(Control)/(M)}$, were harvested after 7 days.

Flow cytometric analyses of different immune cell subtypes were performed before and after culture [34].

4.7. Degranulation Assay (DEG)

As a marker for induced cell cytotoxicity, cell degranulation was quantified in uncultured WB and WBM and in $WB^{DC\text{-}MLC(Control)/(M)}$ and $WBM^{DC\text{-}MLC(Control)/(M)}$ using a FITC-conjugated antibody against CD107a. Uncultured WB and WBM were stimulated in parallel with leukemia-associated-antigens (LAA): 2 µg/mL "Wilms Tumor 1" (PepTivator®WT1, Miltenyi Biotec) and 2 µg/mL "Preferentially Expressed Antigen of Melanoma" (PepTivator®PRAME, Miltenyi Biotec). Unstimulated WB and WBM served as controls.

In previous studies, we showed that the addition of LAA after MLC had no further effect on immunoreactive cells [34]. Therefore, $WB^{DC\text{-}MLC(Control)/(M)}$ and $WBM^{DC\text{-}MLC(Control)/(M)}$ were not stimulated with WT1 and PRAME.

To avoid loss or weakening of CD107a antibodies' fluorescence, 2 µg/mL Monensin solution (BioLegend) was added to the cultures. After an incubation of 16 h at 37 °C, 21% O_2, and 10% CO_2 cells were harvested, stained, and analyzed by flow cytometry [48].

4.8. Intracellular Cytokine Assay (INTCYT)

To quantify the intracellular production of Interferon-γ (IFNγ) and Tumor Necrosis Factor-α (TNFα) of different immune cells in uncultured WB and WBM and in $WB^{DC\text{-}MLC(Control)/(M)}$ and $WBM^{DC\text{-}MLC(Control)/(M)}$, the Intracellular Cytokine Assay was performed. In analogy to the DEG, only uncultured WB and WBM were stimulated with LAA. To avoid spontaneous cytokine secretion, 5 µg/mL Brefeldin A solution (BioLegend) was added. All cultures were incubated for 16 h at 37 °C, 21% O_2, and 10% CO_2. After harvest, intracellularly produced IFNγ and TNFα were evaluated (as described in Section 4.3) [34].

4.9. Cytotoxicity Fluorolysis Assay (CTX)

The Cytotoxicity Fluorolysis Assay was conducted to assess the lytic activity of T cell-enriched immunoreactive cells in $WB^{DC\text{-}MLC(Control)/(M)}$ and $WBM^{DC\text{-}MLC(Control)/(M)}$ ("effector cells") against leukemic blasts ("target cells"). Therefore, effector and target cells (with a ratio of 1:1) were cocultured in a medium containing 85% RPMI/PS and 15% human serum and incubated for 3 and 24 h at 37 °C, 21% O_2, and 10% CO_2. Target cells were stained with respective antibodies before incubation. After harvest, 7AAD and a defined number of Fluorosphere beads (Beckman Coulter) were added. As a control, effector, and target cells were cultured separately and mixed shortly before measurements.

Flow cytometric analyses were performed after 3 and 24 h using a refined gating strategy [49]. The lytic activity against blasts ("blast lysis") is defined as the difference in frequencies of viable blasts in the effector-target-cell-cultures as compared to controls, and "improved blast lysis" is defined as the difference in proportions of "blast lysis" achieved in $WB^{DC\text{-}MLC(M)}$ as compared to $WB^{DC\text{-}MLC(Control)}$ and in $WBM^{DC\text{-}MLC(M)}$ as compared to $WBM^{DC\text{-}MLC(Control)}$.

4.10. Platelet Counts

To assess the influence of Kit-M on platelet counts, Kit-M-pretreated WB and WBM were analyzed on day 0 and after 3 and 7 days of DC cultures using the Automated Hematology Analyser XP-300 (Sysmex, Norderstedt, Germany). GM-CSF-treated WB and WBM served as control groups.

4.11. Statistical Methods

Statistical analyses and figures were implemented with Excel 2022 (Microsoft, Redmond, WA, USA) and Prism 9 (GraphPad Software, San Diego, CA, USA). Data are presented as mean ± standard deviation (SD). Statistical comparisons between the two groups were performed using the two-tailed *t*-test. Differences were considered as "highly significant" in cases with p-values ≤ 0.005, as "significant" with p-values ≤ 0.05, as "borderline significant" with p-values between 0.05 and 0.1, and as "not significant" (n.s.) with p-values ≥ 0.1.

5. Conclusions

In this ex vivo study, we showed that DC_{leu}-generation is possible in comparable frequencies in WB as well as in WBM with Kit-M (GM-CSF and PGE-1). Furthermore, we showed that Kit-M induces leukemia-specific/antileukemic innate immune cells and effector, as well as memory T cells in both WB and WBM. We showed increased antileukemic activity in WB and WBM. Studies are currently being planned to examine if these cells could qualify to overcome the inhibitory microenvironment in vivo, specifically eradicate leukemic cells and stabilize remissions in patients with leukemia before or after SCT.

Author Contributions: M.U. performed a great portion of the experiments and analyzed all flow cytometric and statistical data. H.A.R., A.H., E.R., L.L., S.B., T.B. and X.F. contributed data to the DC, MLC, CTX and DEG/INTCYT experiments, which were evaluated by M.U. and H.S. helped with manuscript preparation. A.R., G.F.V., C.S., J.S. and P.B. provided the patients' samples and reports. H.S. was responsible for the study design. M.U. and H.S. contributed to drafting of the manuscript. M.U. and H.S. contributed to editing the manuscript. All authors have read and agreed to the published version of the manuscript.

Funding: The project was supported by intramural funding from the working group of HS. Lin Li was funded by grants from the China Scholarship Council (CSC) (File No. 201808210307). Xiaojia Feng was funded by the Peking University International Hospital. The funders did not influence the study design, data collection or analysis; the publishing decision; or the manuscript preparation.

Institutional Review Board Statement: Samples were collected and patients' informed consent gathered according to the Helsinki guidelines and with the vote of the Ethics Committee of LMU in Munich (vote number: 33905).

Informed Consent Statement: Informed consent was obtained from all subjects involved in the study.

Data Availability Statement: The data presented in this study are available in this article.

Acknowledgments: The authors thank the patients, nurses and physicians for their work and support with the sample material and diagnostic reports and the technicians of the leukemia laboratory of the Medical Department III for platelet counting. The results presented in this article are part of the doctoral thesis of Marianne Unterfrauner at the Ludwig Maximilian University of Munich.

Conflicts of Interest: H.M.S. is involved with Modiblast Pharma GmbH (Oberhaching, Germany), which holds the European Patent 15 801 987.7-1118 and US Patent 15-517627, "Use of immunomodulatory effective compositions for the immunotherapeutic treatment of patients suffering from myeloid leukemias".

References

1. Estey, E.; Dohner, H. Acute myeloid leukaemia. *Lancet* **2006**, *368*, 1894–1907. [CrossRef] [PubMed]
2. Carter, J.L.; Hege, K.; Yang, J.; Kalpage, H.A.; Su, Y.; Edwards, H.; Huttemann, M.; Taub, J.W.; Ge, Y. Targeting multiple signaling pathways: The new approach to acute myeloid leukemia therapy. *Signal Transduct. Target. Ther.* **2020**, *5*, 288. [CrossRef] [PubMed]
3. Newell, L.F.; Cook, R.J. Advances in acute myeloid leukemia. *BMJ* **2021**, *375*, n2026. [CrossRef] [PubMed]
4. Pelcovits, A.; Niroula, R. Acute Myeloid Leukemia: A Review. *Rhode Isl. Med. J.* **2020**, *103*, 38–40.
5. Lucas, D. Structural organization of the bone marrow and its role in hematopoiesis. *Curr. Opin. Hematol.* **2021**, *28*, 36–42. [CrossRef]
6. Comazzetto, S.; Shen, B.; Morrison, S.J. Niches that regulate stem cells and hematopoiesis in adult bone marrow. *Dev. Cell* **2021**, *56*, 1848–1860. [CrossRef] [PubMed]
7. Horas, K.; Menale, C.; Maurizi, A. Editorial: The bone/bone marrow microenvironment: A hub for immune regulation of the tumor cells fate. *Front. Immunol.* **2022**, *13*, 1019489. [CrossRef] [PubMed]
8. Yamaguchi, T.; Kawamoto, E.; Gaowa, A.; Park, E.J.; Shimaoka, M. Remodeling of Bone Marrow Niches and Roles of Exosomes in Leukemia. *Int. J. Mol. Sci.* **2021**, *22*, 1881. [CrossRef]
9. Ayala, F.; Dewar, R.; Kieran, M.; Kalluri, R. Contribution of bone microenvironment to leukemogenesis and leukemia progression. *Leukemia* **2009**, *23*, 2233–2241. [CrossRef]
10. Tettamanti, S.; Pievani, A.; Biondi, A.; Dotti, G.; Serafini, M. Catch me if you can: How AML and its niche escape immunotherapy. *Leukemia* **2022**, *36*, 13–22. [CrossRef]
11. Zhao, E.; Xu, H.; Wang, L.; Kryczek, I.; Wu, K.; Hu, Y.; Wang, G.; Zou, W. Bone marrow and the control of immunity. *Cell Mol. Immunol.* **2012**, *9*, 11–19. [CrossRef]
12. Mohanty, A.; Polisetti, N.; Vemuganti, G.K. Immunomodulatory properties of bone marrow mesenchymal stem cells. *J. Biosci.* **2020**, *45*, 98. [CrossRef]
13. Shafat, M.S.; Oellerich, T.; Mohr, S.; Robinson, S.D.; Edwards, D.R.; Marlein, C.R.; Piddock, R.E.; Fenech, M.; Zaitseva, L.; Abdul-Aziz, A.; et al. Leukemic blasts program bone marrow adipocytes to generate a protumoral microenvironment. *Blood* **2017**, *129*, 1320–1332. [CrossRef]
14. Yang, X.; Wang, J. Precision therapy for acute myeloid leukemia. *J. Hematol. Oncol.* **2018**, *11*, 3. [CrossRef]
15. de Lima, M.; Roboz, G.J.; Platzbecker, U.; Craddock, C.; Ossenkoppele, G. AML and the art of remission maintenance. *Blood Rev.* **2021**, *49*, 100829. [CrossRef]
16. Nayak, R.K.; Chen, Y.B. Maintenance therapy for AML after allogeneic HCT. *Front. Oncol.* **2022**, *12*, 895771. [CrossRef]
17. Isidori, A.; Cerchione, C.; Daver, N.; DiNardo, C.; Garcia-Manero, G.; Konopleva, M.; Jabbour, E.; Ravandi, F.; Kadia, T.; Burguera, A.F.; et al. Immunotherapy in Acute Myeloid Leukemia: Where We Stand. *Front. Oncol.* **2021**, *11*, 656218. [CrossRef]

18. Albinger, N.; Pfeifer, R.; Nitsche, M.; Mertlitz, S.; Campe, J.; Stein, K.; Kreyenberg, H.; Schubert, R.; Quadflieg, M.; Schneider, D.; et al. Primary CD33-targeting CAR-NK cells for the treatment of acute myeloid leukemia. *Blood Cancer J.* **2022**, *12*, 61. [CrossRef]
19. Vago, L.; Gojo, I. Immune escape and immunotherapy of acute myeloid leukemia. *J. Clin. Investig.* **2020**, *130*, 1552–1564. [CrossRef] [PubMed]
20. Kohler, N.; Ruess, D.A.; Kesselring, R.; Zeiser, R. The Role of Immune Checkpoint Molecules for Relapse After Allogeneic Hematopoietic Cell Transplantation. *Front. Immunol.* **2021**, *12*, 634435. [CrossRef]
21. Stone, R.M.; Larson, R.A.; Dohner, H. Midostaurin in FLT3-Mutated Acute Myeloid Leukemia. *N. Engl. J. Med.* **2017**, *377*, 1903. [CrossRef]
22. Liu, H. Emerging agents and regimens for AML. *J. Hematol. Oncol.* **2021**, *14*, 49. [CrossRef]
23. Dohner, H.; Wei, A.H.; Appelbaum, F.R.; Craddock, C.; DiNardo, C.D.; Dombret, H.; Ebert, B.L.; Fenaux, P.; Godley, L.A.; Hasserjian, R.P.; et al. Diagnosis and management of AML in adults: 2022 recommendations from an international expert panel on behalf of the ELN. *Blood* **2022**, *140*, 1345–1377. [CrossRef]
24. Haslauer, T.; Greil, R.; Zaborsky, N.; Geisberger, R. CAR T-Cell Therapy in Hematological Malignancies. *Int. J. Mol. Sci.* **2021**, *22*, 8996. [CrossRef]
25. Gardner, A.; de Mingo Pulido, Á.; Ruffell, B. Dendritic Cells and Their Role in Immunotherapy. *Front. Immunol.* **2020**, *11*, 924. [CrossRef]
26. Yang, L.; Li, S.; Chen, L.; Zhang, Y. Emerging roles of plasmacytoid dendritic cell crosstalk in tumor immunity. *Cancer Biol. Med.* **2023**, *20*, 728–747. [CrossRef] [PubMed]
27. Patente, T.A.; Pinho, M.P.; Oliveira, A.A.; Evangelista, G.C.M.; Bergami-Santos, P.C.; Barbuto, J.A.M. Human Dendritic Cells: Their Heterogeneity and Clinical Application Potential in Cancer Immunotherapy. *Front. Immunol.* **2018**, *9*, 3176. [CrossRef] [PubMed]
28. Collin, M.; Bigley, V. Human dendritic cell subsets: An update. *Immunology* **2018**, *154*, 3–20. [CrossRef] [PubMed]
29. Chrisikos, T.T.; Zhou, Y.; Slone, N.; Babcock, R.; Watowich, S.S.; Li, H.S. Molecular regulation of dendritic cell development and function in homeostasis, inflammation, and cancer. *Mol. Immunol.* **2019**, *110*, 24–39. [CrossRef]
30. Yu, J.; Sun, H.; Cao, W.; Song, Y.; Jiang, Z. Research progress on dendritic cell vaccines in cancer immunotherapy. *Exp. Hematol. Oncol.* **2022**, *11*, 3. [CrossRef]
31. Kremser, A.; Kufner, S.; Konhaeuser, E.; Kroell, T.; Hausmann, A.; Tischer, J.; Kolb, H.J.; Zitzelsberger, H.; Schmetzer, H. Combined immunophenotyping and fluorescence in situ hybridization with chromosome-specific DNA probes allows quantification and differentiation of ex vivo generated dendritic cells, leukemia-derived dendritic cells and clonal leukemic cells in patients with acute myeloid leukemia. *Leuk. Lymphoma* **2013**, *54*, 1297–1308. [CrossRef]
32. Schmetzer, H.M.; Kremser, A.; Loibl, J.; Kroell, T.; Kolb, H.J. Quantification of ex vivo generated dendritic cells (DC) and leukemia-derived DC contributes to estimate the quality of DC, to detect optimal DC-generating methods or to optimize DC-mediated T-cell-activation-procedures ex vivo or in vivo. *Leukemia* **2007**, *21*, 1338–1341. [CrossRef] [PubMed]
33. Plett, C.; Klauer, L.K.; Amberger, D.C.; Ugur, S.; Rabe, A.; Fischer, Z.; Deen, D.; Hirn-Lopez, A.; Gunsilius, C.; Werner, J.O.; et al. Immunomodulatory kits generating leukaemia derived dendritic cells do not induce blast proliferation ex vivo: IPO-38 as a novel marker to quantify proliferating blasts in acute myeloid leukaemia. *Clin. Immunol.* **2022**, *242*, 109083. [CrossRef] [PubMed]
34. Klauer, L.K.; Schutti, O.; Ugur, S.; Doraneh-Gard, F.; Amberger, D.C.; Rogers, N.; Kramer, D.; Rank, A.; Schmid, C.; Eiz-Vesper, B.; et al. Interferon Gamma Secretion of Adaptive and Innate Immune Cells as a Parameter to Describe Leukaemia-Derived Dendritic-Cell-Mediated Immune Responses in Acute Myeloid Leukaemia in vitro. *Transfus. Med. Hemother* **2021**, *49*, 44–61. [CrossRef] [PubMed]
35. Schwepcke, C.; Klauer, L.K.; Deen, D.; Amberger, D.C.; Fischer, Z.; Doraneh-Gard, F.; Gunsilius, C.; Hirn-Lopez, A.; Kroell, T.; Tischer, J.; et al. Generation of Leukaemia-Derived Dendritic Cells (DCleu) to Improve Anti-Leukaemic Activity in AML: Selection of the Most Efficient Response Modifier Combinations. *Int. J. Mol. Sci.* **2022**, *23*, 8333. [CrossRef]
36. Amberger, D.C.; Doraneh-Gard, F.; Gunsilius, C.; Weinmann, M.; Mobius, S.; Kugler, C.; Rogers, N.; Bock, C.; Kodel, U.; Werner, J.O.; et al. PGE1-Containing Protocols Generate Mature (Leukemia-Derived) Dendritic Cells Directly from Leukemic Whole Blood. *Int. J. Mol. Sci.* **2019**, *20*, 4590. [CrossRef]
37. Schutti, O.; Schmetzer, H. *Intracellular Cytokine (IFNγ, TNFα) Assays in Combination with a Degranulation Assay Contribute Significantly to Detect and Quantify Potentially Leukemia-Specific Cells of Several Lines in Leukemia Patients' Blood or Culture Settings*; Department of Medicine III, University Hospital of Munich: Munich, Germany, 2023; *in preparation*.
38. Boyman, O.; Sprent, J. The role of interleukin-2 during homeostasis and activation of the immune system. *Nat. Rev. Immunol.* **2012**, *12*, 180–190. [CrossRef]
39. Duarte, D.; Hawkins, E.D.; Lo Celso, C. The interplay of leukemia cells and the bone marrow microenvironment. *Blood* **2018**, *131*, 1507–1511. [CrossRef]
40. Kim, Y.W.; Koo, B.K.; Jeong, H.W.; Yoon, M.J.; Song, R.; Shin, J.; Jeong, D.C.; Kim, S.H.; Kong, Y.Y. Defective Notch activation in microenvironment leads to myeloproliferative disease. *Blood* **2008**, *112*, 4628–4638. [CrossRef]
41. Kode, A.; Manavalan, J.S.; Mosialou, I.; Bhagat, G.; Rathinam, C.V.; Luo, N.; Khiabanian, H.; Lee, A.; Murty, V.V.; Friedman, R.; et al. Leukaemogenesis induced by an activating beta-catenin mutation in osteoblasts. *Nature* **2014**, *506*, 240–244. [CrossRef]
42. Pozzobon, T.; Goldoni, G.; Viola, A.; Molon, B. CXCR4 signaling in health and disease. *Immunol. Lett.* **2016**, *177*, 6–15. [CrossRef]

43. Zhou, W.; Guo, S.; Liu, M.; Burow, M.E.; Wang, G. Targeting CXCL12/CXCR4 Axis in Tumor Immunotherapy. *Curr. Med. Chem.* **2019**, *26*, 3026–3041. [CrossRef]
44. Stelmach, P.; Trumpp, A. Leukemic stem cells and therapy resistance in acute myeloid leukemia. *Haematologica* **2023**, *108*, 353–366. [CrossRef]
45. Van Acker, H.H.; Versteven, M.; Lichtenegger, F.S.; Roex, G.; Campillo-Davo, D.; Lion, E.; Subklewe, M.; Van Tendeloo, V.F.; Berneman, Z.N.; Anguille, S. Dendritic Cell-Based Immunotherapy of Acute Myeloid Leukemia. *J. Clin. Med.* **2019**, *8*, 579. [CrossRef]
46. Rackl, E.; Li, L.; Klauer, L.K.; Ugur, S.; Pepeldjiyska, E.; Seidel, C.L.; Gunsilius, C.; Weinmann, M.; Doraneh-Gard, F.; Reiter, N.; et al. Dendritic Cell-Triggered Immune Activation Goes along with Provision of (Leukemia-Specific) Integrin Beta 7-Expressing Immune Cells and Improved Antileukemic Processes. *Int. J. Mol. Sci.* **2022**, *24*, 463. [CrossRef] [PubMed]
47. Platt, A.M.; Randolph, G.J. Dendritic cell migration through the lymphatic vasculature to lymph nodes. *Adv. Immunol.* **2013**, *120*, 51–68. [CrossRef] [PubMed]
48. Pepeldjiyska, E.; Li, L.; Gao, J.; Seidel, C.L.; Blasi, C.; Ozkaya, E.; Schmohl, J.; Kraemer, D.; Schmid, C.; Rank, A.; et al. Leukemia derived dendritic cell (DCleu) mediated immune response goes along with reduced (leukemia-specific) regulatory T-cells. *Immunobiology* **2022**, *227*, 152237. [CrossRef]
49. Grabrucker, C.; Liepert, A.; Dreyig, J.; Kremser, A.; Kroell, T.; Freudenreich, M.; Schmid, C.; Schweiger, C.; Tischer, J.; Kolb, H.J.; et al. The quality and quantity of leukemia-derived dendritic cells from patients with acute myeloid leukemia and myelodysplastic syndrome are a predictive factor for the lytic potential of dendritic cells-primed leukemia-specific T cells. *J. Immunother.* **2010**, *33*, 523–537. [CrossRef]
50. Logan, C.; Koura, D.; Taplitz, R. Updates in infection risk and management in acute leukemia. *Hematology Am. Soc. Hematol. Educ. Program.* **2020**, *2020*, 135–139. [CrossRef]
51. Hobo, W.; Hutten, T.J.A.; Schaap, N.P.M.; Dolstra, H. Immune checkpoint molecules in acute myeloid leukaemia: Managing the double-edged sword. *Br. J. Haematol.* **2018**, *181*, 38–53. [CrossRef] [PubMed]
52. Rowshanravan, B.; Halliday, N.; Sansom, D.M. CTLA-4: A moving target in immunotherapy. *Blood* **2018**, *131*, 58–67. [CrossRef]
53. Boeck, C.L.; Amberger, D.C.; Doraneh-Gard, F.; Sutanto, W.; Guenther, T.; Schmohl, J.; Schuster, F.; Salih, H.; Babor, F.; Borkhardt, A.; et al. Significance of Frequencies, Compositions, and/or Antileukemic Activity of (DC-stimulated) Invariant NKT, NK and CIK Cells on the Outcome of Patients With AML, ALL and CLL. *J. Immunother.* **2017**, *40*, 224–248. [CrossRef]
54. Yu, Z.; Liu, W.; He, Y.; Sun, M.; Yu, J.; Jiao, X.; Han, Q.; Tang, H.; Zhang, B.; Xian, Y.; et al. HLA-A2.1-restricted ECM1-derived epitope LA through DC cross-activation priming CD8(+) T and NK cells: A novel therapeutic tumour vaccine. *J. Hematol. Oncol.* **2021**, *14*, 71. [CrossRef] [PubMed]
55. Ugur, S.; Schmetzer, H.M. *'Kit'-Mediated Blastmodulation to Leukemia-Derived DC Significantly Improves Antileukemic Activities in Whole Blood Independent of AML-Patients' Subtypes*; Department of Medicine III, University Hospital of Munich: Munich, Germany, 2023; *in preparation*.
56. Baudrexler, T.; Boeselt, T.; Li, L.; Bohlscheid, S.; Boas, U.; Schmid, C.; Rank, A.; Schmohl, J.; Koczulla, R.; Schmetzer, H.M. Volatile Phases Derived from Serum, DC, or MLC Culture Supernatants to Deduce a VOC-Based Diagnostic Profiling Strategy for Leukemic Diseases. *Biomolecules* **2023**, *13*, 989. [CrossRef]
57. Shenghui, Z.; Yixiang, H.; Jianbo, W.; Kang, Y.; Laixi, B.; Yan, Z.; Xi, X. Elevated frequencies of CD4(+) CD25(+) CD127lo regulatory T cells is associated to poor prognosis in patients with acute myeloid leukemia. *Int. J. Cancer* **2011**, *129*, 1373–1381. [CrossRef]
58. Hassin, D.; Garber, O.G.; Meiraz, A.; Schiffenbauer, Y.S.; Berke, G. Cytotoxic T lymphocyte perforin and Fas ligand working in concert even when Fas ligand lytic action is still not detectable. *Immunology* **2011**, *133*, 190–196. [CrossRef] [PubMed]
59. Doucette, K.; Karp, J.; Lai, C. Advances in therapeutic options for newly diagnosed, high-risk AML patients. *Ther. Adv. Hematol.* **2021**, *12*, 20406207211001138. [CrossRef] [PubMed]
60. Gulati, S.; Bennett, C.; Phillips, J.; Van-Poznak, C. GM-CSF as an adjunct to autologous bone marrow transplantation. *Stem Cells* **1993**, *11*, 20–25. [CrossRef]
61. Negrin, R.S.; Greenberg, P.L. The use of colony stimulating factors in clinical bone marrow transplantation. *Curr. Opin. Immunol.* **1992**, *4*, 567–570. [CrossRef]
62. McIntosh, B.; Kaushansky, K. Transcriptional regulation of bone marrow thrombopoietin by platelet proteins. *Exp. Hematol.* **2008**, *36*, 799–806. [CrossRef]
63. Ugolini, A.; Nuti, M. CD137(+) T-Cells: Protagonists of the Immunotherapy Revolution. *Cancers* **2021**, *13*, 456. [CrossRef] [PubMed]
64. Aktas, E.; Kucuksezer, U.C.; Bilgic, S.; Erten, G.; Deniz, G. Relationship between CD107a expression and cytotoxic activity. *Cell Immunol.* **2009**, *254*, 149–154. [CrossRef] [PubMed]
65. Morath, A.; Schamel, W.W. alphabeta and gammadelta T cell receptors: Similar but different. *J. Leukoc. Biol.* **2020**, *107*, 1045–1055. [CrossRef]

6. Publication II

biomolecules

MDPI

Article

Volatile Phases Derived from Serum, DC, or MLC Culture Supernatants to Deduce a VOC-Based Diagnostic Profiling Strategy for Leukemic Diseases

Tobias Baudrexler [1,†], Tobias Boeselt [2,†], Lin Li [1], Sophia Bohlscheid [1], Ursel Boas [2], Christoph Schmid [3], Andreas Rank [3], Jörg Schmohl [4], Rembert Koczulla [2] and Helga Maria Schmetzer [1,*]

[1] Medical Department III, Hospital Großhadern, Ludwig-Maximilians-University, 81377 Munich, Germany
[2] Department of Pulmonary Rehabilitation, German Center for Lung Research (DZL), Phillipps-University of Marburg, 35043 Marburg, Germany
[3] Department of Hematology and Oncology, University Hospital of Augsburg, 86156 Augsburg, Germany
[4] Department of Hematology and Oncology, Diaconia Hospital Stuttgart, 70176 Stuttgart, Germany
* Correspondence: helga.schmetzer@med.uni-muenchen.de; Tel./Fax: +49-(0)89-4400-73137
† These authors contributed equally to this work.

Abstract: Volatile organic compounds (VOCs) reflect the metabolism in healthy and pathological conditions, and can be collected easily in a noninvasive manner. They are directly measured using electronical nose (eNose), and may qualify as a systemic tool to monitor biomarkers related to disease. Myeloid leukemic blasts can be transformed into leukemia-derived dendritic cells (DC_{leu}) able to improve (anti-leukemic) immune responses. To profile immunological changes in healthy and acute myeloid leukemic (AML) patients' ex vivo cell cultures, we correlated the cell biological data with the profiles of cell culture supernatant-derived VOCs. DC/DC_{leu} from leukemic or healthy whole blood (WB) were generated without (Control) or with immunomodulatory Kit M (Granulocyte macrophage-colony-stimulating-factor (GM-CSF) + prostaglandin E_1 (PGE_1)) in dendritic cell cultures (DC culture). Kit-pretreated/not pretreated WB was used to stimulate T cell-enriched immunoreactive cells in mixed lymphocyte cultures (MLC culture). Leukemia-specific adaptive and innate immune cells were detected with a degranulation assay (Deg) and an intracellular cytokine assay (InCyt). Anti-leukemic cytotoxicity was explored with a cytotoxicity fluorolysis assay (CTX). VOCs collected from serum or DC- and MLC culture supernatants (with vs. without Kit M pretreatment and before vs. after culture) were measured using eNose. Compared to the Control (without treatment), Kit M-pretreated leukemic and healthy WB gave rise to higher frequencies of mature (leukemia-derived) DC subtypes of activated and (memory) T cells after MLC. Moreover, antigen (leukemia)-specific cells of several lines (innate and adaptive immunity cells) were induced, giving rise to blast-lysing cells. The eNose could significantly distinguish between healthy and leukemic patients' serum, DC and MLC culture supernatant-derived volatile phases and could significantly separate several supernatant (with vs. without Kit M treatment, cultured vs. uncultured)-derived VOCs within subgroups (healthy DC or leukemic DC, or healthy MLC or leukemic MLC supernatants). Interestingly, the eNose could indicate a Kit M- and culture-associated effect. The eNose may be a prospective option for the deduction of a VOC-based profiling strategy using serum or cell culture supernatants and could be a useful diagnostic tool to recognize or qualify AML disease.

Keywords: leukemia-derived DC; acute myeloid leukemia; anti-leukemia functionality; leukemia-specific cells; volatile phases above serum and cell culture supernatants; immune monitoring

Citation: Baudrexler, T.; Boeselt, T.; Li, L.; Bohlscheid, S.; Boas, U.; Schmid, C.; Rank, A.; Schmohl, J.; Koczulla, R.; Schmetzer, H.M. Volatile Phases Derived from Serum, DC, or MLC Culture Supernatants to Deduce a VOC-Based Diagnostic Profiling Strategy for Leukemic Diseases. *Biomolecules* **2023**, *13*, 989. https://doi.org/10.3390/biom13060989

Academic Editors: Javier Leon and Robert J. Kreitman

Received: 18 December 2022
Revised: 29 May 2023
Accepted: 31 May 2023
Published: 14 June 2023

1. Introduction

1.1. Acute Myeloid Leukemia (AML)

AML is a clonal stem cell disorder of the hematopoiesis, which comes with uncontrolled proliferation of myeloid progenitor cells (blasts) [1]. Cytochemistry, immunophe-

notyping, cytogenetics and molecular biological investigations are usually conducted to confirm diagnosis and to allocate patients to prognostic risk groups [2,3]. The standard treatment of AML leads to high rates of remission; however, there are high rates of relapses in up to 80% of cases in the following two years [4–6]. Currently, new treatment strategies based on new chemotherapies or (targeted) passive or active immunotherapies are being developed (e.g., hypomethylating agents, venetoclax) [6,7].

1.2. DC-Based Immunotherapy

DCs are professional antigen-presenting cells (APCs). They are activated and maturate after danger-signaling adhesions (e.g., nucleic acids, infectious particles), resulting in upregulated chemokine receptors (e.g., CCR7), MHC-antigens and other costimulatory factors [8–11]. Ex vivo DCs can be generated from CD14+ monocytes (and loaded with tumor antigens) or from myeloid blasts (DC_{leu}, leukemia-derived DC; without induction of blast proliferation) from AML patients' WB in the presence of different combinations of response modifiers (Kits) [9,12,13]; the resulting DCs express costimulatory molecules together with individual patients' leukemic antigens, and gain the capacity to activate the cells of the immune system against blasts. Ex vivo-generated (and manipulated) DCs or DC_{leu} could be used for an adoptive transfer; applying Kits directly to AML patients could induce DC_{leu} from blasts, leading to an antileukemic immunoreaction in vivo [9]. Immunomodulatory Kit M, composed of granulocyte macrophage colony-stimulating factor (GM-CSF) and prostaglandin E1 (PGE_1), has proved to be one of the best combinations of immune response modifiers to generate DC/DC_{leu} from leukemic WB [9,13]; therefore, it was used in this ex vivo study.

1.3. Immune System

The key players of the innate immune system are APCs (e.g., monocytes, macrophages, DC), cytokine-induced killer (CIK), invariant natural killer T cells (iNKT cells) and natural killer (NK) cells; they mediate the earliest interactions with pathogens/tumors [12–14]. Antigen-specific response and generation of immunologic memory are the central tasks of the adaptive immune system [12,13]. After activation, naive T cells (T_{naive}, CD3+CD45RO−) are probably converted to non-naive T cells ($T_{non\text{-}naive}$, CD3+CD45RO+), which mediate various immune responses or develop into long-living central memory cells (T_{cm}, CD3+CD45RO+CD197+) or effector memory cells ($T_{em/eff}$, CD3+CD45RO+CD197−) to facilitate a faster reactivation of the immune system against recurring antigens [8,15]. These immunoreactive cells can be detected using flow cytometry (abbreviations are given in Table 1).

Table 1. Cells and cell subsets as evaluated by flow cytometry.

		Name of Subgroups	Abbreviation of Subgroups	Surface Marker	Referred to	Abbreviation	Reference
	Blast cells	Blasts	BLA	BLA, e.g., CD34+, CD117+	WB (whole blood)	BLA/WB	[16]
		Proliferating blasts	$BLA_{prol-CD71}$	BLA+DC-CD71+	BLA	$BLA_{prol-CD71}$/BLA	[17]
		Proliferating blasts	$BLA_{prol-IPO38}$	BLA+DC-IPO38+	BLA	$BLA_{prol-IPO38}$/BLA	[6]
	Monocytoid cells	CD14+ monocytes	Mon	CD14+	WB	Mon/WB	[18]
		Proliferating CD14+ monocytes	$Mon_{prol-CD71}$	CD14+DC-CD71+	CD14+	$Mon_{prol-CD71}$/Mon	[9]
		Proliferating CD14+ monocytes	$Mon_{prol-IPO38}$	CD14+DC-IPO38+	CD14+	$Mon_{prol-IPO38}$/Mon	[9]
	Dendritic cells	Dendritic cells	DC	DC+, e.g., CD80+, CD206+	WB	DC/WB	[16]
		Leukemia-derived DC	DC_{leu}	DC+BLA+	WB or DC or BLA	DC_{leu}/WB DC_{leu}/BLA	[16]
		Mature migratory DC	DC_{mat}	DC+CD197+	WB or DC	DC_{mat}/WB DC_{mat}/DC	[18]
		Mature migratory DC_{leu}	$DC_{leu-mat}$	DC+BLA+CD197+	WB or DC or DC_{leu} oder DC_{mat} or BLA	$DC_{leu-mat}$/WB $DC_{leu-mat}$/DC $DC_{leu-mat}$/BLA	[18]
	B lymphocytes	CD19+ B cells	Bcell	CD19+	lymphocytes	Bcell/cells	[19]
	T lymphocytes	CD3+ pan T cells	CD3+	CD3+	lymphocytes	CD3+/cells	[8]
		CD4+ coexpressing T cells	T_{CD4+}	CD3+CD4+	CD3+	T_{CD4+}/CD3+	[8]
		CD8+ coexpressing T cells	T_{CD4-}	CD3+CD4−	CD3+	T_{CD4-}/CD3+	[8]
		Naive T cells	T_{naive} $T_{naiveCD4+}$ $T_{naiveCD4-}$	CD3+CD45RO− CD3+CD45RO-CD4+ CD3+CD45RO-CD4−	CD3+ or T_{CD4+} or T_{CD4-}	T_{naive}/CD3+ $T_{naiveCD4+}$/T_{CD4+} $T_{naiveCD4-}$/T_{CD4-}	[12]
Adaptive immune system		Non-naive T cells	$T_{non-naive}$ $T_{non-naiveCD4+}$ $T_{non-naiveCD4-}$	CD3+CD45RO+ CD3+CD45RO+CD4+ CD3+CD45RO+CD4−	CD3+ or T_{CD4+} or T_{CD4-}	$T_{non-naive}$/CD3+ $T_{non-naiveCD4+}$/T_{CD4+} $T_{non-naiveCD4-}$/T_{CD4-}	[12]
		Central memory T cells	T_{cm} T_{cmCD4+} T_{cmCD4-}	CD3+CD45RO+CD197+ CD3+CD45RO+CD197+CD4+ CD3+CD45RO+CD197+CD4−	CD3+ or T_{CD4+} or T_{CD4-}	T_{cm}/CD3+ T_{cmCD4+}/T_{CD4+} T_{cmCD4-}/T_{CD4-}	[12]
		Effector memory T cells	$T_{em/eff}$ $Tem/effCD4+$ $Tem/effCD4-$	CD3+CD45RO+CD197− CD3+CD45RO+CD197-CD4+ CD3+CD45RO+CD197-CD4−	CD3+ or T_{CD4+} or T_{CD4-}	$T_{em/eff}$/CD3+ $T_{em/effCD4+}$/T_{CD4+} $T_{em/effCD4-}$/T_{CD4-}	[12]
		Proliferating T cells, early	$T_{prol-early}$	CD3+CD69+	CD3+	$T_{prol-early}$/CD3+	[12]
		Proliferating T cells, late	$T_{prol-late}$	CD3+CD71+	CD3+	$T_{prol-late}$/CD3+	[12]

Table 1. *Cont.*

		Name of Subgroups	Abbreviation of Subgroups	Surface Marker	Referred to	Abbreviation	Reference
Leukemia-specific cells							
	B lymphocyte cells	CD19+ B $cells_{leu}$	$Bcell_{107a+}$	CD19+CD107a+	Bcell	$Bcell_{107a+}$/Bcell	
	T lymphocyte cells	CD3+ pan T $cells_{leu}$	CD3+107a+ CD3+INFy+ CD3+TNFa+ CD3+INFy+TNFa+	CD3+CD107a+ CD3+INFy+ CD3+TNFa+ CD3+INFy+TNFa+	CD3+ CD3+ CD3+ CD3+	$CD3+_{107a+}$/CD3+ $CD3+_{INFy+}$/CD3+ $CD3+_{TNFa+}$/CD3+ $CD3+_{INFy+TNFa+}$/CD3+	[20] [12]
		CD4+ coexpressing T $cells_{leu}$	$T_{CD4+107a+}$ $T_{CD4+INFy+}$ $T_{CD4+TNFa+}$ $T_{CD4+INFy+TNFa+}$	CD3+CD4+CD107a+ CD3+CD4+INFy+ CD3+CD4+TNFa+ CD3+CD4+INFy+TNFa+	T_{CD4+} T_{CD4+} T_{CD4+} T_{CD4+}	$T_{CD4+107a+}/T_{CD4+}$ $T_{CD4+INFy+}/T_{CD4+}$ $T_{CD4+TNFa+}/T_{CD4+}$ $T_{CD4+INFy+TNFa+}/T_{CD4+}$	[20] [12]
Adaptive immune system		CD8+ coexpressing T $cells_{leu}$	$T_{CD4107a+}$ $T_{CD4-INFy+}$ $T_{CD4-TNFa+}$ $T_{CD4-INFy+TNFa+}$	CD3+CD4−CD107a+ CD3+CD4−INFy+ CD3+CD4−TNFa+ CD3+CD4−INFy+TNFa+	T_{CD4-} T_{CD4-} T_{CD4-} T_{CD4-}	$T_{CD4-107a+}/T_{CD4-}$ $T_{CD4-INFy+}/T_{CD4-}$ $T_{CD4-TNFa+}/T_{CD4-}$ $T_{CD4-INFy+TNFa+}/T_{CD4-}$	[20] [12]
		Naive T $cells_{leu}$	$T_{naive107a+}$ $T_{naive\ INFy+}$	CD3+CD45RO-CD107a+ CD3+CD45-INFy+	T_{naive} T_{naive}	$T_{naive107a+}/T_{naive}$ $T_{naive\ INFy+}/T_{naive}$	[20] [12]
		Non-naive T $cells_{leu}$	$T_{non-naive107a+}$ $T_{non-naive\ INFy+}$	CD3+CD45RO+CD107a+ CD3+CD45RO+INFy+	$T_{non-naïve}$ $T_{non-naive}$	$T_{non-naive107a+}/T_{non-naive}$ $T_{non-naïve\ INFy+}/T_{non-naive}$	[20] [12]
		Central memory T $cells_{leu}$	$T_{cm107a+}$ $T_{cm\ INFy+}$	CD3+CD45RO+CD197+CD107a+ CD3+CD45RO+CD197+INFy+	T_{cm} T_{cm}	$T_{cm107a+}/T_{cm}$ $T_{cm\ INFy+}/T_{cm}$	[20] [12]
		Effector memory T $cells_{leu}$	$T_{em/eff107a+}$ $T_{em/eff\ INFy+}$	CD3+CD45RO+CD197- CD107a+ CD3+CD45Ro+CD197+INFy+	$T_{em/eff}$ $T_{em/eff}$	$T_{em/eff107a+}/T_{em/eff}$ $T_{em/eff\ INFy+}/T_{em/eff}$	[20] [12]
Innate	Cytokine-induced killer cells	CD3+CD56+ CIK $cells_{leu}$	$CIKcell_{107a+}$ $CIKcell_{INFy+}$ $CIKcell_{TNFa+}$ $CIKcell_{INFy+TNFa+}$	CD3+CD56+CD107a+ CD3+CD56+INFy+ CD3+CD56+TNFa+ CD3+CD56+INFy+TNFa+	CIKcell CIKcell CIKcell CIKcell	$CIKcell_{107a+}$/CIKcell $CIKcell_{INFy+}$/CIKcell $CIKcell_{TNFa+}$/CIKcell $CIKcell_{INFy+TNFa+}$/CIKcell	[20] [12]
Immune system	Natural killer cells	CD3-CD56+ NK $cells_{leu}$	$NKcell_{107a+}$ $NKcell_{INFy+}$ $NKcell_{TNFa+}$ $NKcell_{INFy+TNFa+}$	CD3-CD56+CD107a+ CD3-CD56+INFy+ CD3-CD56+TNFa+ CD3-CD56+INFy+TNFa+	NKcell NKcell NKcell NKcell	$NKcell_{107a+}$/NKcell $NKcell_{INFy+}$/NKcell $NKcell_{TNFa+}$/NKcell $NKcell_{INFy+TNFa+}$/NKcell	[20] [12]
	Invariant natural killer T cells	6B11+ iNKT $cells_{leu}$	$iNKTcell_{107+}$	6B11+CD107a+	NKcell	$iNKTcell_{107a+}$/NKcell	[20]
		CD3+ coexpressing 6B11+ iNKT $cells_{leu}$	$iNKTcell_{CD3+107a+}$	6B11+CD3+CD107a+	NKcell	$iNKTcell_{CD3+107a+}$ /NKcell	[20]
		CD56+ coexpressing 6B11+ iNKT $cells_{leu}$	$iNKTcell_{CD56+107a+}$	6B11+CD56+CD107a+	NKcell	$iNKTcell_{CD56+107a+}$/NKcell	[20]

1.4. Leukemia-Specific Cells and Antileukemic Process

The degranulation assay (Deg) allows the detection and quantification of lysosomal-associated membrane glycoproteins (LAMPs), such as LAMP-1 (CD107a), which are involved in granzyme/perforin-associated degranulation granules. The intracellular cytokine assay (InCyt) allows the intracellular (antigen specific) quantification of cytokines (interferon gamma (INFy) and tumor necrosis factor alpha (TNFa) on a single-cell level, representing triggers of immune responses and mediators of cell apoptosis [12,15,21]. Cytotoxicity assays (CTX) evaluate the antileukemic potential of stimulated and unstimulated effector cells [12]. The Deg assay in combination with the InCyt assay and the CTX provides a refined and complex analysis of the functionality of cells, especially with respect to immune cells' (leukemia-specific) activity and cytotoxicity [12].

1.5. Methodological Tools to Monitor AML Disease or Antileukemically Related Processes

Analyses of different (activating or inhibitory) cellular/humoral, soluble factors, or even the smallest molecules could contribute to our understanding of leukemia-related as well as antileukemic processes [8,15,21–24]. In recent years, the role of physical factors (e.g., physiological hypoxia [25] or circulating vesicles (e.g., extracellular vesicles (EVs) [26,27]) has been tested with respect to a refined monitoring of immunological or tumor-associated processes.

1.6. VOC Analysis as a New Option to Characterize and Monitor (Malignant) Diseases

Every creature (human, plants, animals) emits organic compounds into the environment. Since exhaled molecules reflect the metabolism in healthy and pathological conditions, exhaled air may qualify as a systemic tool to monitor biomarkers related to disease [28]. VOCs are organic chemicals containing hydrocarbon compounds. Exhaled volatile organic compounds (VOC) can be collected easily, in a noninvasive matter (either by collecting exhaled breath directly into an electronical nose (eNose) or by analyzing collected VOCs bound to carriers (fleeze or earloop masks)), and afterwards analyzed using an eNose. Proof that VOC analyses can contribute to detecting disease-associated endogenic metabolic or cell-derived molecular VOC markers, e.g., in Parkinson's, Alzheimer's, lung cancer or AML, has been presented [29–32].

Although applications of VOC-detecting technologies are still diverse, promising results in the profiling of breath-derived VOC patterns have contributed to differentiating breath from patients with vs. without lung cancer, and from (COPD) patients with vs. without an alpha-1 deficiency. It is even possible to detect COVID-19 infection vs. no infection using VOC analyses of patients' urine samples [31,33–35], and to identify patients with vs. without major depression [36]. Moreover, specific VOC analyses have been shown to be a promising tool for detecting bladder tumors, using measurements of urine-derived VOCs [37]. Moreover, VOCs collected above cell culture supernatants have been shown to correlate with subtypes of the underlying disease [38].

The aims of this trial were as follows:

1. Generation and quantification of DC/DC_{leu} (subpopulations) using Kit M-treated (vs. untreated) WB from AML patients and healthy volunteers;
2. Characterization of (activated) immune cells before (uncultured MLC) and after MLC (with Kit M-pretreated vs. untreated WB);
3. Detection and quantification of antileukemic/leukemia-specific innate and adaptive immune cells using Deg and InCyt assays, or CTX after MLC;
4. VOC analyses above collected serum and cell culture supernatants (DC, MLC, with/without Kit M treatment) using eNose;
5. Correlation of cell biology with the VOC results, and potentially the deduction of a VOC-based profiling strategy using serum or cell culture supernatants

2. Material and Methods

2.1. Cell Biological Experiments

2.1.1. Sample Collection

The sample acquisition for this work was conducted between 2019 and 2021 through the University Hospitals of Munich, Oldenburg, Augsburg, the Rotkreuzklinikum in Munich, and the Diakonieklinikum in Stuttgart. After patients' and donors' written agreement to experimental use of their blood donation, WB samples were collected in syringes containing standardized concentrations of heparin (7.5 mL, Sarstedt, Nuembrecht, Germany) from patients in acute phases of AML, and from healthy volunteers. This was in consensus with the Declaration of Helsinki and the local ethics committee of LMU in Munich (Pettenkoferstr. 8a, 80336 München, Ludwig-Maximilian University Hospital, Munich; vote no. 339-05). The patients' diagnostics of clinical findings were provided by the cooperating hospitals.

2.1.2. Patients' Characterization

WB samples were collected from AML patients (n = 17) and healthy volunteers (n = 14). On average, AML patients were 61 (range 29–98), and healthy volunteers were 30 years old (range 22–58). The female-to-male ratio in AML patients was 1:0.55, and in healthy volunteers was 1:1. AML patients' samples were characterized using the French American British (FAB) classification (as far as possible and available), and assigned to primary (pAML) or secondary AML (sAML). AML patients were sub-grouped into stages of the disease (first diagnosis, persisting disease, relapse after stem cell transplantation (SCT)) and risk groups (EuropeanLeukemiaNet (ELN) risk stratification) [38]. Moreover, blast phenotypes and blood parameters (white blood cells, platelets, hemoglobin in PB) were collected on the day of sampling. Nine patients presented at first diagnosis, five patients with persisting disease and three patients with relapse after SCT. An overview is presented in Table 2.

The cellular composition of blood samples from AML patients was 32.18% blasts (range 11–79), 14.38% T cells (range 1.85–56.00), 3.25% NK cells (range 0.9–6.3), and 1.3% CIK cells (range 0.56–4.60). The cellular composition of blood samples from healthy volunteers was 8.49% monocytes (range 4.55–14.64), 16.91% T cells (range 10.45–44.80), 6.5% NK cells (range 4.34–9.30), and 1.5% CIK cells (range 0.32–3.21). In cases of aberrant expression of lineage markers on blasts, these markers were not included.

Table 2. Characteristics of acute myeloid leukemia (AML) patients and healthy volunteers are presented.

FAB/WHO Classification *	Stage	Patient	Age at Diagn.	Sex	ELN Risk Stratification	Blasts Phenotype (CD)	Blast in PB (%) **	WBC in PB (/nl) *	PLT in PB (/nl) *	Hemoglobin in PB (g/dl) *	Conducted Cell Biological Experiments	Sources for VOC Analyses (Supernatant-Derived VOCs)
pAML	First diagnosis	P1567	98	f	very unfavourable	**34**,**117**,15,65	16	7.96	12	8.3	DC, MLC, CTX, Deg, InCyt	Serum, DCD0 M/0, DCDE M, DCDE 0
pAML/M5		P1572	63	f	very unfavourable	**34**,**117**,65,33,13	12	1.87	77	9.4	DC, MLC, CTX, Deg, InCyt	Serum, DCD0 M/0, DCDE M/0, MLCD0 M/0, MLCDE M/0
pAML/M6		P1573	61	m	unfavourable	**34**,**117**,65,13,71	13	3.8	19	7.7	DC, MLC, CTX, Deg, InCyt	Serum, DCD0 M/0, DCDE M/0, MLCD0 M/0, MLCDE M/0
pAML/M4		P1581	56	m	unfavourable	**34**,**117**,33,13,15	58	31.4	21	8.3	DC, MLC, CTX, Deg, InCyt	Serum, DCD0 M/0, DCDE M/0, MLCD0 M/0, MLCDE M/0
pAML/M3		P1602	67	m	favourable	**117**,**34**,33,13,56	16	3.4	162	9.1	DC, MLC, CTX	Serum, DCD0 M/0, DCDE M/0, MLCD0 M/0, MLCDE M/0
sAML		P1604	60	f	intermediate	**117**,**34**,13,33,65,7	16	0.21	16	6	DC, MLC, CTX, Deg, InCyt	Serum, DCD0 M/0, DCDE M/0, MLCD0 M/0, MLCDE M/0
pAML/M4		P1630	29	m	favourable	**34**,**117**,13,33,15,64	16	24.56	117	14.5	DC, MLC, CTX, Deg, InCyt	Serum, DCD0 M/0, DCDE M/0, MLCD0 M/0, MLCDE M/0
pAML/M2		P1635	51	m	intermediate	**34**,117,**15**,33	25	0.6	53	7.6	DC, MLC, Deg, InCyt	Serum, DCD0 M/0
pAML		P1638	68	m	unfavourable	**34**,**117**,33,13,56,4,71	60	9.8	20	7.9	DC, MLC, CTX, Deg, InCyt	Serum, DCD0 M/0, DCDE M/0, MLCD0 M/0, MLCDE M/0
pAML/M4	Persisting	P1594	70	f	favourable	**34**,**117**,65,33,13	11	1.32	232	11.9	DC, MLC, CTX, Deg, InCyt	Serum, DCD0 M/0, DCDE M/0, MLCD0 M/0
pAML	disease	P1595	50	f	intermediate	**34**,**117**,65,13,33,56	15	3	43	7.4	DC, MLC, CTX	Serum, DCD0 M/0, DCDE M/0, MLCD0 M/0, MLCDE M/0
sAML		P1597	83	f	intermediate	**117**,56,**34**,15,65,33	54	88.6	41	11.3	DC, MLC, CTX, Deg, InCyt	Serum, DCD0 M, DCDE M/0
pAML		P1603	32	f	unfavourable	**34**,**117**,15,33	50	0.71	25	6	DC, MLC, CTX, Deg, InCyt	Serum, DCD0 M/0, DCDE M/0, MLCD0 M/0, MLCDE M/0
pAML		P1616	69	f	intermediate	**34**,**117**,33	16	1.01	86	9.1	-	Serum, DCD0 M/0, DCDE M/0, MLCD0 M/0, MLCDE M/0
sAML	Relapse after	P1598	61	f		**117**,**34**,33,13	25	19.6	15	8.3	DC, MLC, CTX, Deg, InCyt	Serum, MLCD0 M/0, MLCDE M/0
pAML/M4	stem cell	P1599	71	f		**34**,**117**,33,7,13	79	54.8	180	9.2	DC, MLC, CTX, Deg	Serum, DCD0 M/0, DCDE M/0, MLCD0 M/0, MLCDE M/0
pAML	transplantation	P1632	56	f		**34**,13,65,33,56,**117**	65	21.73	40	14.1	DC, MLC, CTX, Deg, InCyt	Serum, DCD0 M/0, DCDE M/0, MLCD0 M/0, MLCDE M/0
Healthy		P1566	54	f							DC, MLC, Deg, InCyt	Serum, DCD0 M/0, DCDE M/0, MLCD0 M/0, MLCDE M/0
		P1579	30	m							DC, MLC, Deg, InCyt	Serum, DCD0 M/0, DCDE M/0, MLCD0 M/0, MLCDE M/0
		P1580	24	f							DC, MLC, Deg, InCyt	Serum, DCD0 M/0, DCDE M/0, MLCD0 M/0, MLCDE M/0
		P1582	27	m							DC, MLC, Deg, InCyt	Serum, DCD0 M/0, DCDE M/0, MLCD0 M/0, MLCDE M/0
		P1583	28	m							DC, MLC, Deg, InCyt	Serum, DCD0 M/0, DCDE M/0, MLCD0 M/0, MLCDE M/0

Table 2. *Cont.*

FAB/WHO Classification *	Stage	Patient	Age at Diagn.	Sex	ELN Risk Stratification	Blasts Phenotype (CD)	Blast in PB (%) **	WBC in PB (/nl) *	PLT in PB (/nl) *	Hemoglobin in PB (g/dl) *	Conducted Cell Biological Experiments	Sources for VOC Analyses (Supernatant-Derived VOCs)
		P1585	29	m							DC, MLC, Deg, InCyt	Serum, DCD0 M/0, DCDE M/0, MLCD0 M/0, MLCDE M/0
		P1586	29	m							DC, MLC	Serum, DCDE M/0, MLCD0 M/0, MLCDE M/0
		P1590	23	f							DC, MLC	Serum, DCD0 M/0, DCDE M/0, MLCD0 M/0, MLCDE M/0
		P1592	58	f							DC, MLC, Deg, InCyt	Serum, DCD0 M/0, DCDE M/0, MLCD0 M/0, MLCDE M/0
		P1596	26	m							DC, MLC	Serum, DCD0 M/0, DCDE M/0, MLCD0 M/0, MLCDE M/0
		P1611	27	f							DC, MLC, Deg, InCyt	Serum, DCD0 M/0, DCDE M/0, MLCD0 M/0, MLCDE M/0
		P1613	24	f							DC, MLC, Deg, InCyt	Serum, DCD0 M/0, DCDE M/0, MLCD0 M/0, MLCDE M/0
		P1636	22	m							DC, MLC, Deg, InCyt	Serum, DCD0 M/0, DCDE M/0, MLCD0 M/0, MLCDE M/0
		P1637	22	f							DC, MLC, Deg, InCyt	Serum, DCD0 M/0, DCDE M/0, MLCD0 M/0, MLCDE M/0

FAB classification, French American British classification of acute myeloid leukemia; WHO classification, World Health Organization classification of AML; ELN, EuropeanLeukemiaNet; VOC, volatile organic compounds; WBC, white blood cells; PLT, platelets/thrombocytes; f, female; m, male; DC, dendritic cell culture measurements; MLC, mixed lymphocyte culture measurement; CTX, cytotoxicity measurements; Deg, degranulation assay; InCyt, intracellular cytokine assay; bold text indicates the blast markers used for DC_{leu} evaluation; * indicates the FAB types of patients, given where available. If they were not available (or not performed) only 'pAML/sAML' is given; ** indicates a clinical parameter on the day of sampling.

2.1.3. Cell Characterization by Flow Cytometry

To evaluate and quantify phenotypes of DC/DC_{leu}, leukemic blasts, monocytes and immune reactive cell subsets of the adaptive and innate immunity analyses were conducted via flow cytometry, using a fluorescence-activating cell-sorting flow cytometer (FACSCalibur^{TM}). Using a refined gating technique and the analysis software CellQuest-Pro (Becton Dickinson, Heidelberg, Germany), the functionalities of cells (proliferation, cytokine production, degranulation and cytotoxicity) could be investigated [12,15]. Panels with various monoclonal antibodies (moAbs) labelled with fluorescein isothiocyanate (FITC), phycoerythrin (PE), phycoerythrin cyanin 7 (PCy7) or allophycocyanin (APC) were used, provided by Becton Dickinson, Heidelberg, Germany[a], Beckman Coulter, Krefeld, Germany[b], Santa Cruz Biotechnology, Heidelberg, Germany[c], and Bio Legend, San Diego, CA, USA[d]. Clone numbers are given in brackets. For the detection of CD3[a] (HIT3a 55339), CD4[a] (SK3 345768 BD), CD14[b] (RMO52 B36297), CD15[b] (80H5 B36298), CD19[b] (REA675 5200608927), CD34[b] (581 IM1870), CD45RO[b] (UCHL1 IM1247U), CD71[b] (YDJ1.2.2 IM0483), CD117[d] (104D2 313232), CD197[d] (REA546 130-099-174), CD107a[d] (H4A3 328606), and IPO38[c] (E2108), FITC moAbs were used. PE-conjugated moAbs were used for the discovery of CD3[b] (UCHT1 A07747), CD4[a] (RPA-T4 555347), CD80[b] (MAB104 IM1976U), CD206[b] (3.29B1.10 IM2741), and INFy[d] (RUO XMG1.2). PCy7-labelled moAbs against CD3[b] (UCHT1 737657), CD4[b] (SFCI12T4D11 737660), CD14[a] (M5E2 557742), CD20[b] (B9E9 IM3629), CD34[b] (581 A21691), CD56[b] (N901 A21692), CD117[b] (104D2D1 B49221), CD197[a] (3D12 557648 BD), and TNFa[d] (Mab11 502930), and moAbs labelled with APC against CD3[b] (UCHT1 IM2467), 6B11[d] (6B11 342908), CD14[b] (RMO52 IM2580), CD15[a] (HI98 551376), CD19[b] (J3-119 IM2470), CD20[b] (B9E9 A21693), CD34[b] (581 IM2472), CD45RO[d] (UCHL1 304210), CD56[b] (N901 IM2474), CD69[a] (FN50 555533), CD80[d] (2D10 305220), CD117[b] (104D2D1 B36300), and CD206[a] (19.2 550889 BD) were utilized for detection. Isotype controls were included according to the manufacturer's instructions [39]. 7AAD[a] (RUO 559925 BD) was used to distinguish between non-viable and viable cells.

2.1.4. Staining and Measurement

Before or after culture, cells were stained using fluorochrome-labeled monoclonal antibodies, and were quantified as described [12,21]. Additionally, for intracellular staining (e.g., IPO38, INFy, TNFa) cell fixation and cell permeabilization were performed with Medium A (FIX&PERM®, Thermo Fisher Scientific, Waltham, MA, USA) and Medium B (FIX&PERM®, Thermo Fisher Scientific, Waltham, MA, USA). Generated DC/DC_{leu} were stained with patient-specific blast markers (e.g., CD15, CD34, CD56, CD65, CD117), and with antibodies against DC typical markers (e.g., CD80, CD206), using DC markers not expressed on 'uncultured' blasts [12,15]. The expression of CD197 (CCR7) determined mature DCs (DC_{mat}). Moreover, proliferating blasts and monocytes were defined by the co-expression of blast markers (or monocyte-specific surface markers in healthy samples), together with CD71 or IPO38 (proliferation markers) without co-expression of DC markers [8]. Abbreviations are given in Table 1.

2.1.5. Preparation of Cells

AML or healthy WB was either directly used for experiments (the workup of all blood samples was routinely carried out under a hood), and mononuclear cells (MNC) and T cells were isolated and frozen for later use. The MNCs isolated from the WB (according to standard preparations [12]) were used for the isolation of T cells via MACS microbead technology, based on a CD3 magnetic cell selection (CD3 Microbeads, Milteney Biotech, Bergisch Gladbach, Germany), as described in the manufacturer's instructions [40]. T cell purity, verified by flow cytometry, was on average 91% $\pm$ 8.2% in healthy WB and 84% $\pm$ 9.3% in AML samples. Isolated T cells were further quantified with trypan blue (Biochrom, Berlin, Germany), counted (Neubauer counting chambers), and resuspended in 1 mL RPMI/PS (Penicillin/Streptomycin) (for use with T cells in MLC) or in 1 mL

cytotoxicity medium containing 85% RPMI/PS and 15% human serum (CTX medium, for use as a target MNC in the CTX assay) [8,12].

2.1.6. Dendritic Cell Culture (DC Culture)

DC and DC_{leu} were cultured as described [8]. For stimulation of the blasts' differentiation into DC_{leu}, response modifiers ('Kit M') were added before and during culture, as a restimulation, on day 2/3 [12]: Kit M contained 800 U/mL granulocyte macrophage colony-stimulating factor (GM-CSF, Sanofi-Aventis, Frankfurt, Germany), and 1 µg/mL prostaglandin E1 (PGE1, Santa Cruz Biotechnology, Dallas, TX, USA) [22]. WB not treated with response modifiers served as a Control. WB cultures were incubated for 7–8 days under physiological conditions (37 °C, 5% CO_2, 21% O_2 and 95% humidity) [12].

2.1.7. Mixed Lymphocyte Culture (MLC Culture)

DC cultures were harvested on day 7–8, and MLC cultures were set up as described [12]. For stimulating the immune reactive cells, 5 µL of 50 U/mL interleukin 2 (IL-2, PeproTech, Berlin, Germany) was added on day 0 of MLC cultures. On day 2/3 and 5/6, restimulations with IL-2 were conducted for every single well. Cell analyses before culture served as the Control ('uncultured MLC'). Under physiological conditions (37 °C, 5% CO_2, 21% O_2 and 95% humidity), the MLC was incubated for 7 days. After culture, measurements were carried out with Kit M ($MLC^{WB\text{-}DC(Kit\text{-}M)}$) and Control ($MLC^{WB\text{-}DC(Control)}$), and cells were used for the Deg-, the InCyt- and the CTX-assays [8]. Different immune cell subtypes after MLC were quantified using flow cytometry. Abbreviations are given in Table 1.

2.1.8. Degranulation Assay (Deg) and Intracellular Assay (InCyt)

Deg and InCyt cultures were set up as described [12] to detect leukemia-specific cells, as given in Table 1. AML samples were stimulated (or not stimulated) in parallel with two leukemia-associated antigens (LAA): 2 µg/mL Wilms tumor 1 protein (WT-1, PepTivator®, Miltenyi Botech, Bergisch Gladbach, Germany) and 2 µg/mL PRAME ('Melanoma antigen preferentially expressed in tumors', UniProt ID: P78395, PepTivator®, Miltenyi biotech, Bergisch Gladbach, Germany). Healthy cells were stimulated/not stimulated with 10 µg/mL staphylococcal enterotoxin B (SEB, Sigma-Aldrich, St. Louis, MO, USA). Cultures without antigen stimulation served as a negative Control ('Unstimulated') [12].

2.1.9. Degranulation Assay (Deg)

A FITC-conjugated antibody against CD107a (Bio Legend, San Diego, CA, USA) was used to detect cell degranulation as a marker of cell cytotoxicity [20]. After one hour of incubation, 2 µg/mL Monensin solution (Bio Legend, San Diego, CA, USA) was added to the culture according to the manufacturer's instructions to avoid loss or weakening of FITC-CD107a antibodies' fluorescence due to endosomal or lysosomal reinternalization [41]. Afterwards, the culture was incubated under physiological conditions (37 °C, 5% CO_2, 21% O_2 and 95% humidity) for an additional 15 h. After incubation, cells were harvested, centrifuged, resuspended in PBS/FCS (phosphate-buffered saline/fetal calf serum), and stained with antibodies [12,15].

2.1.10. Intracellular Assay (InCyt)

Production of tumor necrosis factor alpha (TNFa) [42] and interferon gamma (INFy) [12] was used to analyze intracellular cytokine production. The cells were stained with PCy7-conjugated TNFa antibodies (Bio Legend, San Diego, CA, USA) and PE-conjugated INFy antibodies (Bio Legend, San Diego, CA, USA). Cellular cytokine production was stopped after one hour of incubation with 5 µg/mL Brefeldin A solution (Bio Legend, San Diego, CA, USA), according to the manufacturer's instructions. Afterwards, the culture was incubated for 15 h, and cells were harvested, centrifuged, resuspended in PBS/FCS, and stained with antibodies [12,15].

2.1.11. Cytotoxicity Fluorolysis Assay (CTX)

To investigate the ability of effector cells (T cell-enriched cells stimulated with or without Kit M- treated WB after MLC) to lyse target cells (thawed viable patients' MNCs stained with two different blast markers), a cytotoxicity fluorolysis assay was conducted as described [12]. For each test, equal amounts of effector cells and target cells were mixed. Afterwards, these tubes were incubated for 0, 3 and 24 h in standard physiological conditions (37 °C, 5% CO_2, 21% O_2 and 95% humidity). For the control group, effector and target cells were separately incubated and mixed shortly before measurement. By adding 7AAD (Becton Dickinson, Heidelberg, Germany) and fluorosphere beads (Beckman Coulter, Krefeld, Germany), the cytotoxic activity of effector cells could be evaluated through quantification of viable target cells. The lytic activity of effector cells was calculated and defined as the percentage of viable target cells in the culture with co-cultured effector and target cells (for 3 h and 24 h), as compared to Control [8].

An overview of the cell biological experiments is given in the following Scheme 1.

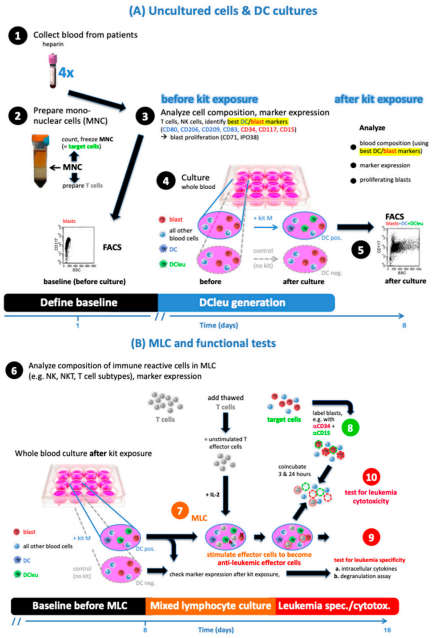

Scheme 1. Set up of cell biological experiments. 1. Heparinized blood samples from healthy and leukemia probands were used for cell biological experiments; 2. MNC (mononuclear cells) and T cells were gained from WB and later used for MLC ('T cell-enriched' mixed lymphocyte culture) and CTX; 3./4./5. DC cultures were set up with leukemic and healthy WB and measured using flowcytometry before and after culture with (vs. without) Kit M; 6./7./8. MLC cultures were set up with harvested DC culture + T cells, stimulated with IL-2, and measured using flowcytometry before and after culture; 9./10. Several immune assays were performed after MLC: DEG + InCyt, as well as a CTX assay after the mixture of MNC and MLC.

2.2. VOC Experiments

2.2.1. Collection of Serum and Cell Culture Supernatant

As a source for VOC analyses, we collected serum as well as cell culture supernatants from healthy and AML sample donors. Cell culture supernatants were taken from DC cultures and MLC cultures (see above); these were the supernatants of DC cultures before culture with and without the addition of Kit M (DCD0 M/DCD0 ø), or after culture (DCDE M/DCDE ø), and the supernatants of MLC cultures before culture with or without WB pretreated with Kit M (MLCD0 M/MLCD0 ø), or after culture (MLCDE M/MLCDE ø). An overview of the collected supernatants of each proband is given in Table 2. For the preparation of cell culture supernatants, 1 mL of DC/MLC cell suspension was centrifuged at 480× *g* and 4 °C for 5 min, and the supernatants were again centrifuged at 2000× *g* and 4 °C for 10 min. Afterwards, supernatants were collected and stored in 300–500 µL aliquots in 1.5 mL safe-lock tubes (Eppendorf Tubes®, Hamburg, Germany), frozen, and stored at −80 °C.

For preparation of serum supernatants, 4 mL serum was collected (S-Monovette®, Sarstedt, Nuembrecht, Germany) and centrifuged at 1200× *g* for 10 min at 4 °C; afterwards, supernatants were centrifuged again at 1800× *g* for 10 min at 4 °C. Aliquots of 300–500 µL were filled in 1.5 mL safe-lock tubes (Eppendorf Tubes®, Hamburg, Germany), frozen, and stored at −80 °C [43].

Collected serum and culture supernatants were sent on dry ice to the analytical laboratory of the Marburg University Hospital, where the VOC analyses were conducted.

2.2.2. Experimental Set-Up of the Cyranose 320

Serum and cell culture supernatants were thawed in Marburg, and afterwards, VOCs were collected from the surface above every single supernatant (healthy, leukemia, serum, DC- or MLC-samples) and measured in a sealed room using the Cyranose 320 electronic nose (eNose) [43,44]. The Cyranose 320® belongs to the group of polymers sensors and consists of 32 thin-film carbon polymer chemiresistors (NoseChip). The sensor response is based on binding volatile organic components (VOCs) depending on structure, size, polarity and proton affinity. The sensors convert chemical signals to electronical signals [45]. Exposure to gases causes the polymer layer to swell while the analyte is absorbed. Each sensor responds differently to an analyte; conversely, no sensor usually responds to only a single analyte. The magnitude of a sensor's response depends on the doping of the sensor and the physicochemical character of the analyte. For single substances or for a mixture, respectively, characteristic pattern smellprints are produced; these are composed of 32 individual signals. The measurement is based on the change in the resistance of each sensor when exposed to volatile organic gases. In this process, the medical air did not have any effect on the VOCs to be measured. In this context, it rather stood for a standard to not allow any contamination by the ambient air. To ensure that the sensors were working correctly in each study, defined olfactory substances were used to check their functions. Only when all 32 sensors of the eNose indicated correct reference ranges could the study begin. Before each measurement series, the sensors were trained with the so-called training set. The sensors were calibrated once a month with a test battery of odors. Every single measurement was performed in three steps. A reference value was determined using medicinal air (Aer medicinalis, Linde Gas Therapeutics GmbH, Unterschleißheim, Germany) (1). After 60 s of step 1, the VOCs on the volatile surface of the cell supernatants were measured (2), followed by a cleaning step of the sensors of the eNose with exposed ambient air within another 60 s (3) [31]. All samples were measured in triplicate, and arithmetic mean values were used for principal component analysis. Afterwards, linear discriminant analyses (LD) were performed, and the LD results were used for further analyses, particularly contingency table analyses. The Mahalanobis distance between groups was then determined [43,44]. An overview of the VOC sampling, measurement and analysis is given in the following Scheme 2.

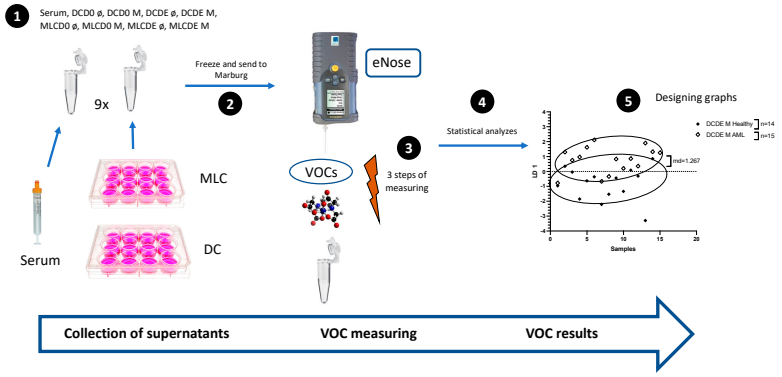

Scheme 2. Overview of the VOC experiments. 1. Collection of supernatants of serum, DC- and MLC cultures; 2. Freezing, transportation to Marburg and thawing of the tubes; 3. Measurement of VOCs above supernatants using the eNose; 4./5. Statistical analyses of VOC data and presentation of VOC differentiations in graphs.

2.3. Statistical Methods

All cell biological measurements were conducted using flow cytometry (FACSCalibur^{TM}, Becton Dickinson, Heidelberg, Germany) and the software BD CellQuestPro (Becton Dickinson, Heidelberg, Germany). Statistical analyses were conducted with Excel (Microsoft® Excel, version 16.52, Redmond, WA, USA) and Prism 9 (GraphPad Software, version 9.1.1, San Diego, CA, USA). Data are presented as mean ± standard deviation. Statistical comparisons of two groups were performed using multiple two-tailed *t*-tests.

Statistical investigations of VOC data calculated via linear discriminant analyses were conducted with Prism 9 (GraphPad Software, version 9.1.1, San Diego, CA, USA). Data are presented as sensitivity, specificity, a positive predictive value (PPV) and a negative predictive value (NPV). Statistical comparisons for contingency table analyses were conducted with Fisher's exact test. Moreover, differences were considered highly significant with p values ≤ 0.005, significant with p values ≤ 0.05, and borderline significant with p values 0.05 to 0.10.

3. Results

3.1. Cell Biological Results

DC/DC_{leu} were generated by treating blasts (monocytes) in leukemic and healthy WB with (vs. without) blast-modulating Kit M. DCs and their subtypes (DC_{leu}, DC_{mat}, $DC_{leu\text{-}mat}$) were quantified after culture with ($DC^{WB(Kit\ M)}$) or without Kit M ($DC^{WB(Control)}$). Afterwards, DC/DC_{leu}-containing samples were used to stimulate T cell-enriched immune cells in MLC. The composition of the immune reactive cells was analyzed before (uncultured MLC) and after MLC ($MLC^{WB\text{-}DC(Control)}$ or $MLC^{WB\text{-}DC(Kit\ M)}$). Additionally, specific antileukemic effects were studied via Deg and InCyt. The cytotoxic impact of T cell-enriched MLC (with and without pretreatment with Kit M) was evaluated via CTX in AML samples. Abbreviations for cell populations are given in Table 1. An overview of the experiments is given in Scheme 1.

Successful generation of DC/DC_{leu} from healthy and AML WB

Significantly higher frequencies of (mature) DC and their subtypes were generated with (vs. without) Kit M-pretreated healthy WB compared to Control

Using healthy samples, we could generate significantly higher frequencies of DC and DC_{mat} within WB when using $DC^{WB(Kit\ M)}$ rather than $DC^{WB(Control)}$ (%DC/WB: Kit M:

22 ± 5.47; Control: 13 ± 3; p = 0.0001, and %DC_{mat}/WB: Kit M: 13 ± 5.73; Control: 7 ± 3; p = 0.003 or %DC_{mat}/DC: Control: 28 ± 10; Kit M: 65 ± 19; p = 0.034). Proliferation of monocytes (as detected by co-expression of CD71 or IPO-38) from healthy WB was not induced under the influence of Kit M (Figure 1 'healthy').

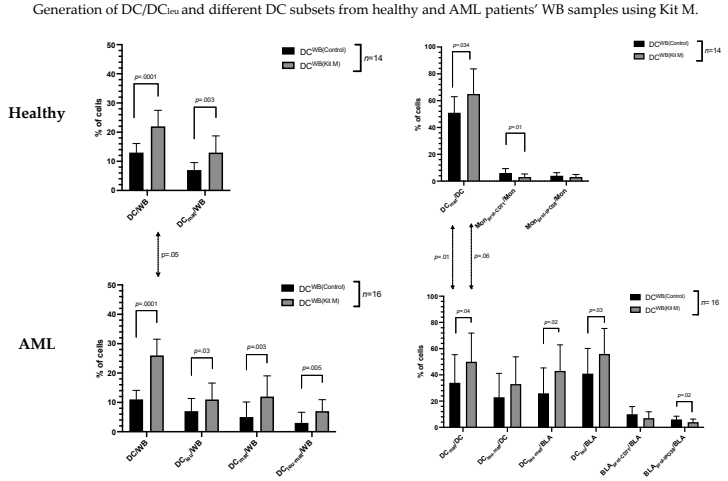

Figure 1. DC/DC_{leu} generation from AML and healthy WB: '**left side**' shows the average frequencies ± standard deviation of generated DC (subtypes) in healthy and leukemic WB fractions (with and without Kit M-pretreated WB ($DC^{WB(Control)}$; $DC^{WB(Kit\ M)}$)). '**right side**' shows the average frequencies ± standard deviation of generated DC subtypes, proliferating blasts and monocytes for AML or healthy samples in different cell subtype fractions (with and without Kit M-pretreated WB ($DC^{WB(Control)}$; $DC^{WB(Kit\ M)}$)). Statistical tests were performed using multiple t-tests. Differences were considered as highly significant with p values ≤ 0.005, significant with p values ≤ 0.05, and borderline significant with p values between 0.05 and 0.10. Abbreviations of cell types are given in Table 1.

In leukemic samples, we found significantly higher frequencies of mature and leukemia-derived DC (subsets) in $DC^{WB(Kit\ M)}$, compared to $DC^{WB(Control)}$ (e.g., %DC/WB: Kit M: 26± 5.55; Control: 16 ± 3; p = 0.0001, and %DC_{leu}/WB: Kit M: 11 ± 5.58; Control: 7 ± 4; p = 0.03% or DC_{mat}/WB: Kit M: 12 ± 7.06; Control: 5 ± 5; p = 0.003). We found significantly increased frequencies of DC subsets in $DC^{WB(Kit\ M)}$ compared to $DC^{WB(Control)}$ (e.g., %DC_{mat}/DC: Kit M: 50 ± 22; Control: 34 ± 21; p = 0.04, and %$DC_{leu\text{-}mat}$/BLA: Kit M: 43 ± 20; Control: 26 ± 19; p = 0.02 and %DC_{leu}/BLA: Kit M: 56 ± 19; Control: 41 ± 19; p = 0.03). Proliferation of blasts (as detected in the co-expression of CD71 or IPO-38) from leukemic WB was not induced by Kit M treatment (Figure 1 'AML').

Significantly higher frequencies of DC (subtypes) were found in healthy vs. AML WB samples after Kit M treatment

We found significantly higher frequencies of DC (subtypes) in leukemic compared to healthy WB samples under the influence of Kit M (e.g., %DC/WB: healthy: 22 ± 5; leukemia: 26 ± 6; p = 0.05). Significantly higher frequencies of DC_{mat}/DC were found in healthy (vs. leukemic) $DC^{WB(Control)}$ (%DC_{mat}/DC: healthy: 51 ± 12; leukemia: 34 ± 21; p = 0.01).

In summary, we found higher frequencies of DCs and their subtypes in Kit-treated healthy and leukemic WB when compared to Control, while we could not detect an

induction of blast or monocyte proliferation after Kit M treatment. Moreover, we conclude that Kit M-pretreated healthy WB gave rise to higher frequencies of DCmat compared to Kit M-pretreated AML samples.

Stimulation of immune cells was successful after healthy and leukemic MLC culture compared to uncultured MLC

After MLC culture (vs. uncultured MLC) with healthy or leukemic samples, we found significantly higher frequencies of proliferating, activated T cells ($T_{prol\text{-}early}/CD3+$, $T_{prol\text{-}late}/CD3+$, $T_{non\text{-}naive}/CD3+$, $T_{non\text{-}naiveCD4+}/T_{CD4+}$, $T_{non\text{-}naiveCD4-}/T_{CD4-}$), and memory T cells ($T_{em/eff}/CD3+$, $T_{em/effCD4+}/T_{CD4+}$, $T_{em/effCD4-}/T_{CD4-}$) ($T_{cm}/CD3+$, T_{cmCD4+}/T_{CD4+}, T_{cmCD4-}/T_{CD4-}) (Figure 2).

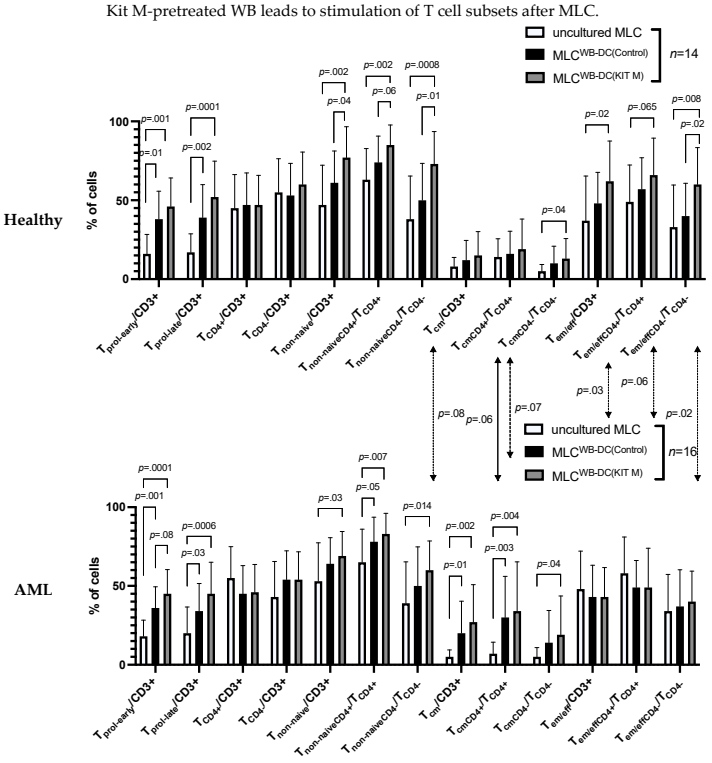

Figure 2. Stimulatory effect of DC/DC_{leu} generated with (vs. without) Kit M from healthy or AML WB on the composition of immunoreactive cells in mixed lymphocyte culture (MLC). The average frequencies ± standard deviation of T cell subsets after stimulation of T cell-enriched immunoreactive cells containing Kit M-pretreated WB ($MLC^{WB\text{-}DC(Kit\ M)}$) from leukemic or healthy WB compared to WB not pretreated with Kit M ($MLC^{WB\text{-}DC(Control)}$) and uncultured cells (uncultured MLC) are given. Statistical tests were performed using multiple *t*-tests. Differences were considered highly significant with p values ≤ 0.005, significant with p values ≤ 0.05, and borderline significant with p values between 0.05 and 0.10. Abbreviations of cell types are given in Table 1.

Significantly higher frequencies of T cell subsets were found in $MLC^{WB\text{-}DC(Kit\ M)}$ compared to $MLC^{WB\text{-}DC(Control)}$ in healthy and AML samples

In healthy samples, we found significantly higher frequencies of non-naïve T cell subsets and of $T_{em/effCD4-}/T_{CD4-}$ in $MLC^{WB\text{-}DC(Kit\ M)}$ compared to $MLC^{WB\text{-}DC(Control)}$ ($\%T_{non\text{-}naïve}/CD3+$: Kit M: 77 ± 20; Control: 61 ± 20; $p = 0.04$ and $\%T_{non\text{-}naiveCD4-}/T_{CD4-}$: Kit M: 73 ± 21; Control: 50 ± 23; $p = 0.01$ and $\%T_{em/effCD4-}/T_{CD4-}$: Kit M: 60 ± 23; Control: 40 ± 21; $p = 0.02$). In leukemic samples, we found borderline significantly higher frequencies of $T_{prol\text{-}early}/CD3+$ in $MLC^{WB\text{-}DC(Kit\ M)}$ compared to $MLC^{WB\text{-}DC(Control)}$ ($\%T_{prol\text{-}early}/CD3+$: Kit M: 45 ± 15; Control: 36 ± 13; $p = 0.08$), and (non-significantly) increased frequencies of $T_{cm}/CD3+$ (Figure 2).

Significant differences were found between healthy and AML patients' T cell subsets

In healthy samples (compared to AML patients' samples), we found significantly higher frequencies of $T_{em/eff}/CD3+$ and $T_{em/effCD4-}/T_{CD4-}$ after $MLC^{WB\text{-}DC(Kit\ M)}$ ($\%T_{em/eff}/CD3+$: healthy: 62 ± 26; leukemia: 43 ± 19; $p = 0.03$ and $\%T_{em/effCD4-}/T_{CD4-}$: healthy: 60 ± 23; leukemia: 40 ± 19; $p = 0.02$) (Figure 2).

We summarize that IL-2 had a significant effect on the provision, proliferation and activation of T cells after culture compared to uncultured T cells. Moreover, Kit M-treated WB had a (significant) impact on the proliferation and activation of healthy and AML T cells. Additionally, we found significantly higher frequencies of memory T cell subsets in healthy samples compared to AML patients' samples.

Degranulation and intracellular assay results

The degranulation activity of immune reactive cells was evaluated with a Deg assay in WB (uncultured WB) and after MLC ($MLC^{WB\text{-}DC(Control)}$ and $MLC^{WB\text{-}DC(Kit\ M)}$); the intracellular TNFa and INFy production was analyzed with an InCyt assay. Deg and InCyt assays were both conducted with/without stimulation with leukemia- associated antigens (LAA) (WT-1 and PRAME) for leukemic samples, or with/without stimulation with SEB for healthy samples ('Stimulated'/'Unstimulated') (Figures 3 and 4).

Stimulation of (leukemia/antigen) specific immune cells was successful after healthy and leukemic MLC culture compared to uncultured WB

In healthy and leukemic WB without SEB/LAA stimulation after MLC (vs. uncultured WB) (significantly), we found higher frequencies of antigen-specific degranulating and INFy-producing T cells (e.g., $\%CD3+_{107a+/INFy+}/CD3+$: Kit M: 32 ± 23; uncultured WB: 24 ± 15; $p = 0.001$ and $\%CD3+_{107a+/INFy+}/CD3+$: Control: 24 ± 15; uncultured WB: 6 ± 9; $p = 0.01$), degranulating non-naive T cells ($T_{non\text{-}naive107a+/INFy+}/T_{non\text{-}naive}$), effector memory and central memory T cell subsets ($T_{em/eff107a+/INFy+}/T_{em/eff}$) ($T_{cm107a+/INFy+}/T_{cm}$), degranulating B cells ($Bcell_{107a+}/Bcell$) (Figure 3A,B), and several subtypes of degranulating innate immunity cells ($CIKcell_{107a+/INFy+}/CIKcell$, $NKcell_{107a+/INFy+}/NKcell$, $iNKTcell_{107a+}/iNKTcell$) (Figure 4A,B).

(Data with vs. without SEB/LAA stimulation after MLC were similar (data not shown).

In summary, we conclude that IL-2 had a significant effect on the (antigen-specific) activation and differentiation of degranulating and INFy-producing innate and adaptive immunity cells after MLC compared to uncultured WB.

Significantly higher frequencies of leukemia/antigen-specific, adaptive immune cells were found in $MLC^{WB\text{-}DC(Kit\ M)}$ compared to $MLC^{WB\text{-}DC(Control)}$ in healthy and AML samples

In healthy samples without SEB stimulation, we found significantly higher frequencies of $Bcell_{107a+}/Bcell$ ($\%Bcell_{107a+}/Bcell$: Kit M: 32 ± 11; Control: 13 ± 4; $p = 0.017$) (Figure 3A 'Healthy'), and (borderline) significantly higher frequencies of $CD3+_{INFy+}/CD3+$, $T_{CD4+INFy+}/T_{CD4+}$, $T_{CD4-INFy+}/T_{CD4-}$, $T_{non\text{-}naive\ INFY+}/T_{non\text{-}naive}$ in $MLC^{WB\text{-}DC(Kit\ M)}$ compared to $MLC^{WB\text{-}DC(Control)}$ (e.g., $\%CD3+_{INFy+}/CD3+$: Kit M: 45 ± 19; Control: 24 ± 16; $p = 0.025$) (Figure 3B, 'Healthy').

In leukemia samples without LAA stimulation, we found borderline significantly higher frequencies of $T_{non\text{-}naive107a+}/T_{non\text{-}naive}$ in $MLC^{WB\text{-}DC(Kit\ M)}$ compared to $MLC^{WB\text{-}DC(Control)}$ ($\%T_{non\text{-}naive107a+}/T_{non\text{-}naive}$: Kit M: 48 ± 28; Control: 28 ± 17; $p = 0.09$) (Figure 3A 'AML'). Significantly higher production of intracellular INFy in $MLC^{WB\text{-}DC(Kit\ M)}$ compared to $MLC^{WB\text{-}DC(Control)}$ was found in, e.g., $CD3+_{INFy+}$, $T_{CD4-INFy+}$, ($\%CD3+_{INFy+}/CD3+$: Kit M: 32 ± 15; Control: 14 ± 10; $p = 0.006$ and $\%T_{CD4+INFy+}/T_{CD4+}$: Kit M: 50 ± 26; Control: 24 ± 17; $p = 0.016$ (Figure 3B 'AML').

We conclude that Kit M treatment (vs. no treatment) led to an increased degranulation activity and an increased production of intracellular INFy and TNFa in leukemic and healthy samples' adaptive immune cells.

Kit M-pretreated WB without LAA leads to incresed degranulation activity and intracellular INFy production of (leukemia-specific) immunoreactive T and B cells

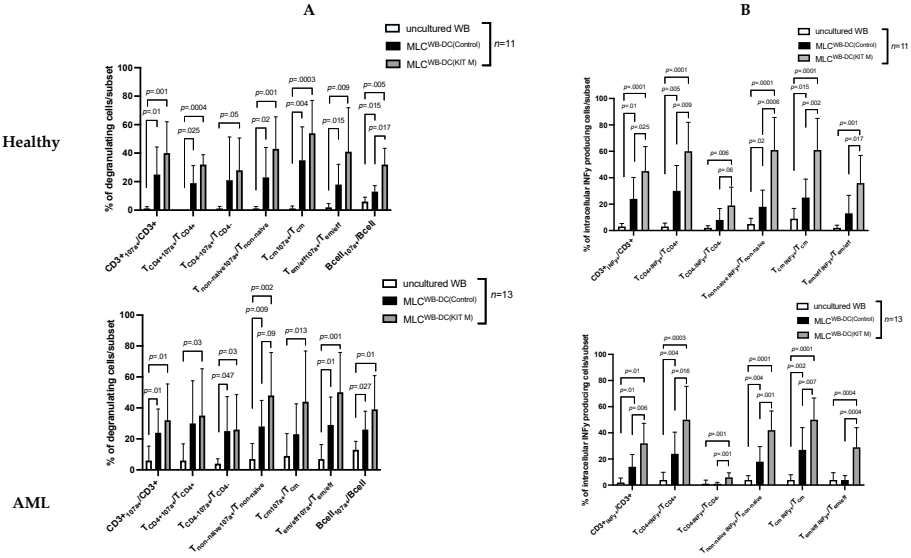

Figure 3. Stimulatory effect of Kit M-pretreated WB on (leukemia-specific) immunoreactive T cell subsets and B cells. Presented herein are the degranulation activities (**A**) and intracellular INFy production of adaptive immune cells (**B**) of leukemic or healthy WB (uncultured WB), before and after culture of leukemic and healthy MLC pretreated with ($MLC^{WB\text{-}DC(KIT\ M)}$) or without Kit M ($MLC^{WB\text{-}DC(Control)}$), without LAA stimulation. Also given are the average frequencies ± standard deviation of CD107a expressing T cell subsets and B cells, and of intracellular INFy producing T cell subsets. Statistical tests were performed using multiple *t*-tests. Differences were considered highly significant with p values ≤ 0.005, and significant with p values ≤ 0.05. Abbreviations of subtypes are given in Table 1.

Kit M-pretreated WB without LAA leads to increased degranulation activity and intracellular INFy production of (leukemia-specific) NK, CIK and iNKT cells.

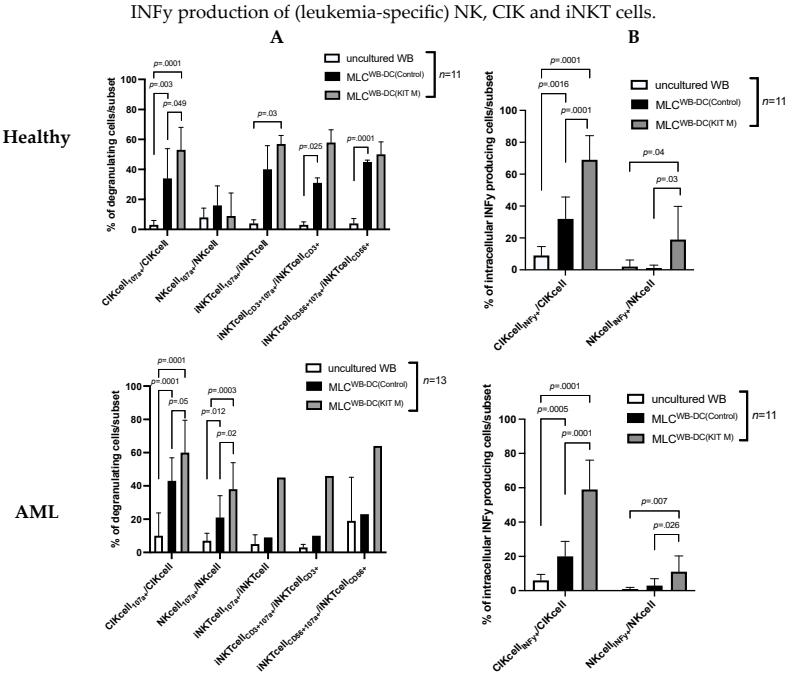

Figure 4. Stimulatory effect of Kit M-pretreated WB on (leukemia-specific) immunoreactive T cell subsets and B cells. Given are the degranulation activities (**A**) and intracellular INFy production of innate immune cells (**B**) of leukemic or healthy WB (uncultured WB), before and after culture of leukemic and healthy MLC pretreated with ($MLC^{WB\text{-}DC(KIT\ M)}$) or without Kit M ($MLC^{WB\text{-}DC(Control)}$), without LAA stimulation. Given are the average frequencies ± standard deviation of CD107a expressing NK, CIK and iNKT cell subsets, and of intracellular INFy producing NK and CIK cell subsets. Statistical tests were performed using multiple *t*-tests. Differences were considered highly significant with *p* values ≤ 0.005, and significant with *p* values ≤ 0.05. Abbreviations of subtypes are given in Table 1.

Significantly higher frequencies of leukemia/antigen-specific innate immune cells were found in $MLC^{WB\text{-}DC(Kit\ M)}$ compared to $MLC^{WB\text{-}DC(Control)}$ in healthy and AML samples

In healthy samples, significantly higher frequencies of $CIKcell_{107+}$/CIKcell (%$CIKcell_{107a+}$/CIKcell: Kit M: 53 ± 15; Control: 34 ± 20; p = 0.049) (Figure 4A 'Healthy') and of $CIKcell_{INFy+}$/CIKcell and $NKcell_{INFy+}$/Nkcell were found after $MLC^{WB\text{-}DC(Kit\ M)}$ compared to $MLC^{WB\text{-}DC(Control)}$ (%$CIKcell_{INFy+}$/CIKcell: Kit M: 69 ± 15; Control: 32 ± 14; p = 0.0001 and %$Nkcell_{INFy+}$/Nkcell: Kit M: 19 ± 21; Control: 1 ± 2; p = 0.03) (Figure 4B 'Healthy').

In leukemic samples, we found significantly higher frequencies of degranulating CIK and NK cells (%$CIKcell_{107a+}$/CIKcell: Kit M: 60 ± 19; Control: 43 ± 14; p = 0.05 and %$NKcell_{107a+}$/NKcell: Kit M: 38 ± 16; Control: 21 ± 13; p = 0.02) (Figure 4A 'AML') and of $CIKcell_{INFy+}$/CIKcell and $NKcell_{INFy+}$/NKcell in $MLC^{WB\text{-}DC(Kit\ M)}$ compared to $MLC^{WB\text{-}DC(Control)}$ (%$CIKcell_{INFy+}$/CIKcell: Kit M: 59 ± 17; Control: 20 ± 9; p = 0.0001 and %$NKcell_{INFy+}$/NKcell: Kit M: 11 ± 9; Control: 3 ± 4; p = 0.026) (Figure 4B 'AML').

We can conclude that Kit M-pretreated (vs. untreated) WB led to an increased degranulation activity and a higher production of intracellular INFy and TNFa of innate immune cells.

The antileukemic activity of T cell-enriched MLC is improved with Kit M-pretreated stimulated cells

After co-culture of 'effector cells' (T cell-enriched MLC with Kit M-pretreated (vs. not pretreated) WB) with 'target cells' (thawed blast-containing MNC), we compared blast lysis of MLCWB-DC(Control) ('Control') vs. MLCWB-DC(Kit M) ('Kit M') using a cytotoxicity fluorolysis assay. Analyses were conducted after 3 or 24 h of incubation of the target with effector cells, and finally the better antileukemic effectivity after either 3 or 24 h was selected as the 'best' achieved lysis value. The lytic activity was calculated and defined as the frequencies of (un)viable target cells compared to a control [8,12].

After 3 h, blast lysis was found in 86.67% of cases (13/15) after MLCWB-DC(Kit M) vs. 73.33% of cases (11/15) in the Control (MLCWB-DC(Control)). After 24 h, blast lysis was found in 100% of cases (15/15) after MLCWB-DC(Kit M) vs. 73.33% of cases (11/15) in Control (MLCWB-DC(Control)). After 3 h, the frequencies of lysed blasts after MLCWB-DC(Kit M) were significantly lower compared to MLCWB-DC(Control) (%lysed blasts: Kit M: -32.36 ± 29.34; Control: -10.62 ± 20.83; $p = 0.03$). After 24 h, we found significantly lower frequencies of lysed blasts after MLCWB-DC(Kit M) compared to MLCWC-DC(Control) (%lysed blasts: Kit M: -46.57 ± 23.32; Control: -22.19 ± 29.40; $p = 0.02$) (Figure 5A).

After 3 and 24 h of incubation, 100% (15/15) of cases showed improved lysis after MLCWB-DC(Kit M) compared to MLCWB-DC(Control). The proportions of cases with improved lysis after 3 h were -24.59 ± 22.93, and after 24 h were -29.62 ± 24.33 (Figure 5B).

After selecting the 'best' achieved lysis value after 3 h and 24 h of incubation time, we found more cases with lysis after MLCWB-DC(Kit M) vs. MLCWB-DC(Control) (MLCWB-DC(Kit M): 100% vs. MLCWB-DC(Control): 66.67% cases of lysis). The frequencies of lysed blasts were significantly lower after MLCWB-DC(Kit M) compared to MLCWB-DC(Control) (%lysed blasts: Kit M: -48.07 ± 23.86; Control: -13.04 ± 25.02; $p = 0.0005$) (Figure 5A). We found improved blast lysis in 15/15 cases (100%) after MLCWB-DC(Kit M) compared to MLCWB-DC(Control), which only led to improved lysis of -41.82 ± 23.77% (Figure 5B).

In summary, Kit M pretreatment significantly improved blast lysis after MLC.

We can conclude that Kit M-pretreated (vs. untreated) leukemia and healthy WB gave rise to higher frequencies of mature (leukemia-derived) DC subtypes and (after MLC) of (leukemia) specific cells of several lines (innate and adaptive immunity cells, including memory cells), finally giving rise to blast-lysing cells.

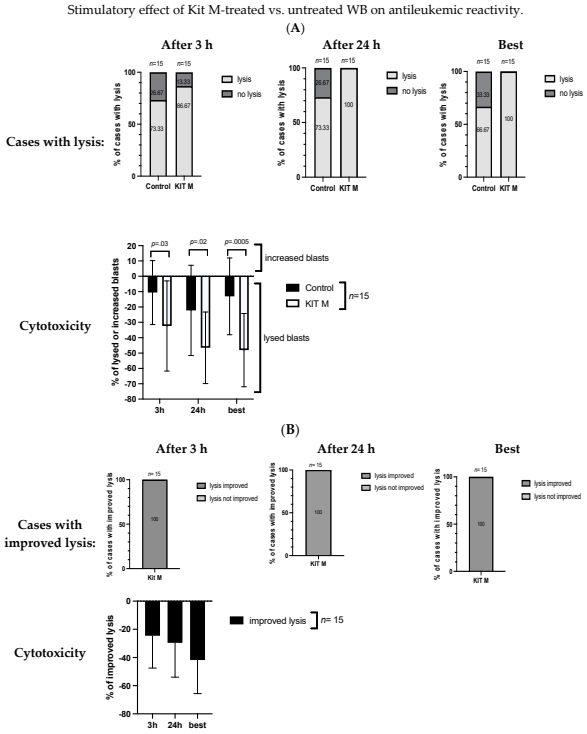

Figure 5. (**A**) Kit M-treated leukemic WB (compared to untreated WB) leads to stimulation of blast lytic activity. (**B**) Improved blast lysis with Kit M-pretreated WB compared to Control. Stimulatory effect of Kit M-pretreated (vs. untreated) WB on the cytotoxic activity after 3 h and 24 h of co-culture of immunoreactive cells ('effector cells') and blasts ('target cells'). Given are the proportions of cases with blast lysis and the frequencies ± standard deviation of increased or lysed blasts after $MLC^{WB\text{-}DC(Kit\ M)}$ (Kit M), compared to $MLC^{WB\text{-}DC(Control)}$ (Control), after 3 h and 24 h, and the 'best' achieved blast lysis after 3 h or 24 h (**A**) and the proportions of cases with an improvement in blast lysis (or without an improvement in blast lysis), the frequencies ± standard deviation of improved (or not improved) lysed blasts after $MLC^{WB\text{-}DC(Kit\ M)}$ in relation to $MLC^{WB\text{-}DC(Control)}$ after 3 h and 24 h, and the 'best' achieved improvement in blast lysis (or without improvement in blast lysis) after 3 h or 24 h (**B**). Statistical tests were performed using a paired *t*-test. Differences were considered highly significant with p values ≤ 0.005, and significant with p values ≤ 0.05.

3.2. Volatile Organic Compounds (VOC) Results

Serum supernatants and cell culture supernatants were obtained from healthy and AML samples' serum, DC, and MLC cultures. As a source for VOC analyses conducted using eNose, we used volatile phases above healthy and leukemic serum supernatants ('Serum'), DCD0 ø/MLCD0 ø, DCDE ø/MLCDE ø (DC/MLC culture without Kit M treatment), DCD0 M/MLCD0 M, and DCDE M/MLCDE M (DC/MLC culture pretreated with Kit M), as described in the section *DC culture* or *MLC culture*. An overview of the collected supernatants of every proband is given in Table 2, and of the VOC experiments in Scheme 2. After measuring, various comparisons were calculated using linear discriminant

analyses (LD), and the smellprints are graphically shown in two-dimensional principal component analysis (PCA) plots (Figures 6–8). The sensitivity, specificity, Mahalanobis distance (md), negative and positive predictive values, and the *p*-value calculated by Fishers' exact test gave information about the significant discrimination.

The VOC profiles of the healthy and AML serum-derived volatile phases are significantly different

Using 14 healthy and 17 AML patients' serum supernatants, the eNose showed a significant differentiation (%sensitivity: 79; %specificity: 82; $p = 0.0011$). Detailed information about the serum results obtained with the eNose are given in Figure 6A.

The volatile phases above healthy and leukemic serum, DC and MLC supernatants are significantly different.

(A) The VOC profiles of healthy and AML serum-derived volatile phases are significantly different.

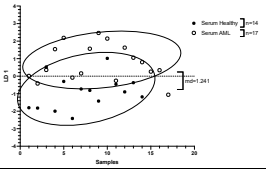

	Serum Healthy	Serum AML			
	Correct/False (%[1])	Correct/False (%[2])	PPV[3] (%)	NPV[4] (%)	P[5]
eNose results	11/3 (79)	14/3 (82)	79	82	.0011

(B) The VOC profiles of healthy and leukemic DC culture supernatant-derived volatile phases are significantly different.

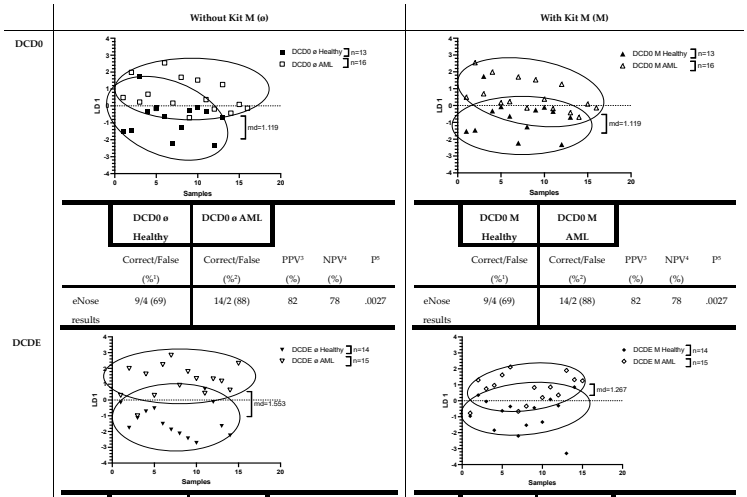

	DCD0 ø Healthy	DCD0 ø AML			
	Correct/False (%[1])	Correct/False (%[2])	PPV[3] (%)	NPV[4] (%)	P[5]
eNose results	9/4 (69)	14/2 (88)	82	78	.0027

	DCD0 M Healthy	DCD0 M AML			
	Correct/False (%[1])	Correct/False (%[2])	PPV[3] (%)	NPV[4] (%)	P[5]
eNose results	9/4 (69)	14/2 (88)	82	78	.0027

	DCDE ø Healthy	DCDE ø AML			
	Correct/False (%[1])	Correct/False (%[2])	PPV[3] (%)	NPV[4] (%)	P[5]
eNose results	12/2 (86)	14/1 (93)	92	88	.0001

	DCDE M Healthy	DCDE M AML			
	Correct/False (%[1])	Correct/False (%[2])	PPV[3] (%)	NPV[4] (%)	P[5]
eNose results	11/3 (79)	12/3 (80)	79	80	.0028

Figure 6. *Cont*.

(C) The VOC profiles of healthy and leukemic MLC culture supernatant-derived volatile phases are significantly different.

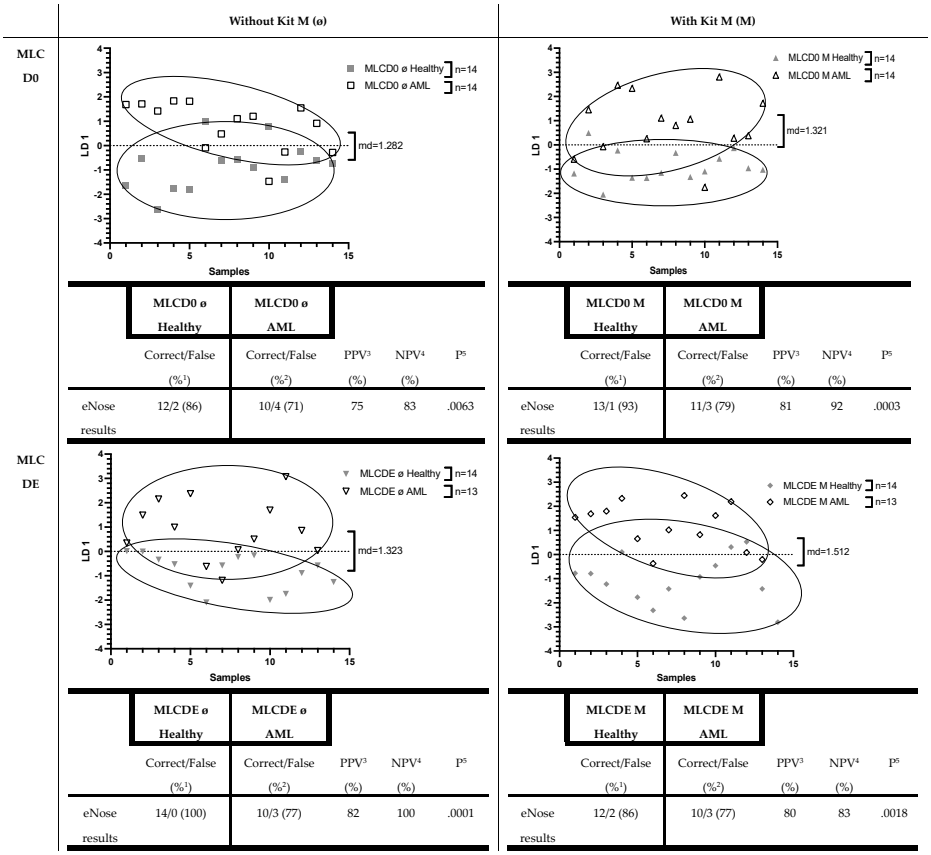

	MLCD0 ø Healthy	MLCD0 ø AML			
	Correct/False (%[1])	Correct/False (%[2])	PPV[3] (%)	NPV[4] (%)	P[5]
eNose results	12/2 (86)	10/4 (71)	75	83	.0063

	MLCD0 M Healthy	MLCD0 M AML			
	Correct/False (%[1])	Correct/False (%[2])	PPV[3] (%)	NPV[4] (%)	P[5]
eNose results	13/1 (93)	11/3 (79)	81	92	.0003

	MLCDE ø Healthy	MLCDE ø AML			
	Correct/False (%[1])	Correct/False (%[2])	PPV[3] (%)	NPV[4] (%)	P[5]
eNose results	14/0 (100)	10/3 (77)	82	100	.0001

	MLCDE M Healthy	MLCDE M AML			
	Correct/False (%[1])	Correct/False (%[2])	PPV[3] (%)	NPV[4] (%)	P[5]
eNose results	12/2 (86)	10/3 (77)	80	83	.0018

[1] Sensitivity. [2] Specificity. [3] Positive predictive value. [4] Negative predictive value. [5] *p* values calculated with Fisher's exact test.

Figure 6. Significantly different eNose results between serum, DC culture, or MLC culture supernatant-derived VOCs using healthy or AML patients' samples. Given are the absolute and graphically represented differences of volatile phases derived from healthy serum, DC culture supernatants (DCD0 ø, DCD0 M, DCDE ø, DCDE M), and MLC culture supernatants (MLCD0 ø, MLCD0 M, MLCDE ø, MLCDE M) compared to the corresponding leukemic volatile phases. Given underneath are the dimensionless LD 1 values and tables, presenting an overview of the sensitivity, specificity, negative and positive predictive values. Statistical tests were performed using Fisher's exact test: Differences were considered significant with p values ≤ 0.05. Abbreviations of analyzed samples are given in Table 2.

3.3. The VOC Profiles of Uncultured and Cultured Healthy and Leukemic DC Culture Supernatants (with/without Kit M Pretreatment) of Derived Volatile Phases Are Significantly Different

We differentiated VOCs in supernatants from healthy vs. leukemic cultures. In healthy DC culture supernatant-derived volatile phases, we found significantly different VOC results compared to leukemic DC culture supernatants. Healthy donors' DCD0 ø and DCD0 M achieved a sensitivity of 69%, and AML patients' DCD0 ø and DCD0 M a specificity of 88% (healthy vs. leukemic DCD0 ø and healthy vs. leukemic DCD0 M: $p = 0.0027$). A less significant difference was found in healthy and leukemic DCDE M (%sensitivity: 79; %specificity: 80; $p = 0.0028$). A more significant difference was found in healthy and AML patients' DCDE ø (%sensitivity: 86; %specificity: 93; $p = 0.0001$). Graphs and more details are shown in Figure 6B).

3.4. The VOC Profiles of Uncultured and Cultured Healthy and Leukemic MLC Culture Supernatants (with/without Kit M Pretreatment) of Derived Volatile Phases Are Significantly Different

eNose analyses of healthy and AML samples' MLC culture supernatants achieved significantly different results. With a sensitivity of 86% and a specificity of 71%, the eNose could separate healthy MLCD0 ø from leukemic MLCD0 ø ($p = 0.0063$). Compared to AML patients' supernatant, we found significant differences in healthy MLCD0 M (%sensitivity: 93; %specificity: 79; $p = 0.0003$), in healthy MLCDE ø (%sensitivity: 100; %specificity: 77; $p = 0.0001$), and in healthy MLCDE M (%sensitivity: 86; %specificity: 77; $p = 0.0018$) (Figure 6C)).

In summary, we conclude that the eNose, by using LD analyses, could significantly differentiate volatile phases above both healthy and leukemic serum supernatants, and healthy and leukemic DC and MLC culture supernatants (both cultured and uncultured DC/MLC) in a direct comparison. Furthermore, we conclude that the eNose yielded significantly different results between healthy and leukemic DC and MLC supernatants, whether pretreated or not with Kit M.

3.5. The Volatile Phases above Healthy DC Supernatants Are Significantly Different

We differentiated VOCs from culture supernatants before vs. after culture and with vs. without Kit M pretreatment in healthy or in AML VOC samples. We found significantly different volatile phases in several healthy DC supernatants (DCD0 ø vs. DCD0 M vs. DCDE ø vs. DCDE M). Healthy DCD0 ø compared to healthy DCDE ø showed a significant difference in VOC analyses (%sensitivity: 77; %specificity: 77; $p = 0.017$). Moreover, healthy DCD0 M compared to healthy DCDE M could be distinguished most significantly (%sensitivity: 85; %specificity: 100; $p = 0.0001$). The eNose achieved a sensitivity of 77% and a specificity of 92% in healthy DCD0 ø compared to DCD0 M ($p = 0.001$). Furthermore, analyses of healthy DCDE ø and healthy DCDE M yielded a significant difference (%sensitivity: 69; %specificity: 77; $p = 0.047$). Healthy DCD0 ø supernatants compared to DCDE M supernatants were identified by eNose, with a sensitivity of 85% and a specificity of 85% ($p = 0.0012$) (Figure 7A).

Significant differences between volatile phases of healthy or leukemic DC/MLC culture supernatants before vs. after culture and with vs. without Kit M pretreatment.

(A) The volatile phases above healthy DC supernatants are significantly different.

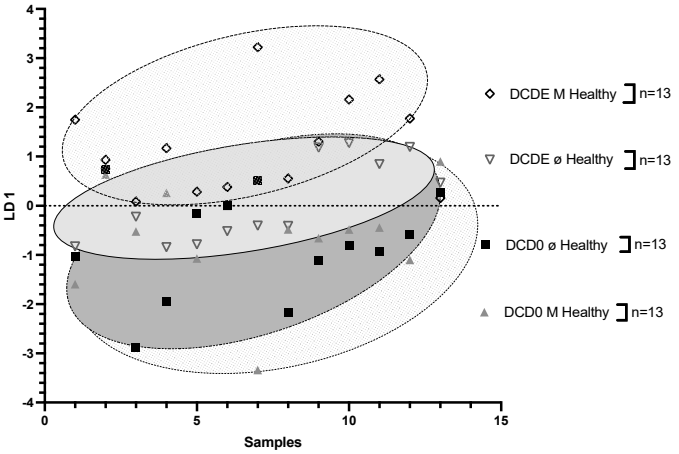

	DCD0 ø Healthy	DCDE ø Healthy			
	Correct/False (%[1])	Correct/False (%[2])	PPV[3] (%)	NPV[4] (%)	P[5]
eNose results	10/3 (77)	10/3 (77)	77	77	.017

	DCD0 M Healthy	DCDE M Healthy			
	Correct/False (%[1])	Correct/False (%[2])	PPV[3] (%)	NPV[4] (%)	P[5]
eNose results	11/2 (85)	13/0 (100)	100	87	.0001

	DCD0 ø Healthy	DCD0 M Healthy			
	Correct/False (%[1])	Correct/False (%[2])	PPV[3] (%)	NPV[4] (%)	P[5]
eNose results	10/3 (77)	12/1 (92)	91	80	.001

	DCDE ø Healthy	DCDE M Healthy			
	Correct/False (%[1])	Correct/False (%[2])	PPV[3] (%)	NPV[4] (%)	P[5]
eNose results	9/4 (69)	10/3 (77)	75	71	.047

	DCD0 ø Healthy	DCDE M Healthy			
	Correct/False (%[1])	Correct/False (%[2])	PPV[3] (%)	NPV[4] (%)	P[5]
eNose results	11/2 (85)	11/2 (85)	85	85	.0012

[1] Sensitivity. [2] Specificity. [3] Positive predictive value. [4] Negative predictive value. [5] *p* values calculated with Fisher's exact test.

Figure 7. *Cont*.

(B) The volatile phases above healthy MLC supernatants are significantly different.

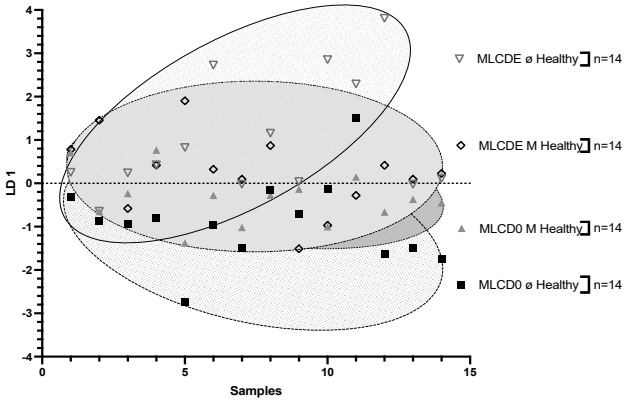

	MLCD0 ø Healthy	**MLCDE ø Healthy**			
	Correct/False (%[1])	Correct/False (%[2])	PPV[3] (%)	NPV[4] (%)	P[5]
eNose results	11/3 (79)	11/3 (79)	79	79	.007

	MLCD0 M Healthy	**MLCDE M Healthy**			
	Correct/False (%[1])	Correct/False (%[2])	PPV[3] (%)	NPV[4] (%)	P[5]
eNose results	11/3 (79)	11/3 (79)	79	79	.007

	MLCD0 ø Healthy	**MLCD0 M Healthy**			
	Correct/False (%[1])	Correct/False (%[2])	PPV[3] (%)	NPV[4] (%)	P[5]
eNose results	10/4 (71)	13/1 (93)	91	76	.0013

	MLCDE ø Healthy	**MLCDE M Healthy**			
	Correct/False (%[1])	Correct/False (%[2])	PPV[3] (%)	NPV[4] (%)	P[5]
eNose results	11/3 (79)	12/2 (86)	85	80	.0018

	MLCD0 ø Healthy	**MLCDE M Healthy**			
	Correct/False (%[1])	Correct/False (%[2])	PPV[3] (%)	NPV[4] (%)	P[5]
eNose results	10/4 (71)	11/3 (79)	77	73	.0213

[1] Sensitivity. [2] Specificity. [3] Positive predictive value. [4] Negative predictive value. [5] *p* values calculated with Fisher's exact test.

Figure 7. *Cont*.

(C) The volatile phases above leukemic DC supernatants are significantly different.

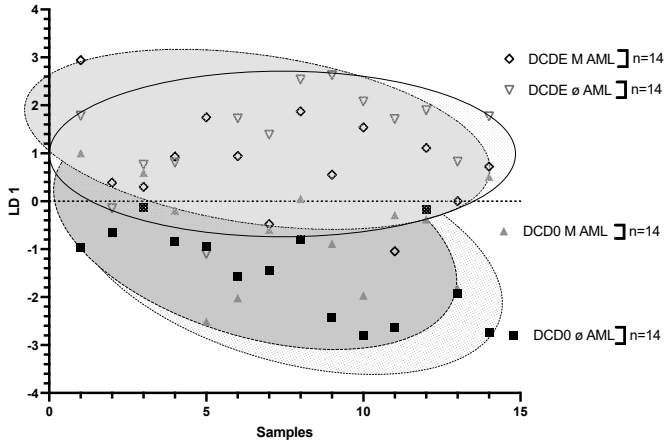

	DCD0 ø AML	**DCDE ø AML**			
	Correct/False (%[1])	Correct/False (%[2])	PPV[3] (%)	NPV[4] (%)	P[5]
eNose results	14/0 (100)	12/2 (86)	88	100	.0001

	DCD0 M AML	**DCDE M AML**			
	Correct/False (%[1])	Correct/False (%[2])	PPV[3] (%)	NPV[4] (%)	P[5]
eNose results	13/1 (93)	13/1 (93)	93	93	.0001

	DCD0 ø AML	**DCD0 M AML**			
	Correct/False (%[1])	Correct/False (%[2])	PPV[3] (%)	NPV[4] (%)	P[5]
eNose results	11/3 (79)	11/3 (79)	79	79	.007

	DCDE ø AML	**DCDE M AML**			
	Correct/False (%[1])	Correct/False (%[2])	PPV[3] (%)	NPV[4] (%)	P[5]
eNose results	12/2 (86)	10/4 (71)	75	83	.0063

	DCD0 ø AML	**DCDE M AML**			
	Correct/False (%[1])	Correct/False (%[2])	PPV[3] (%)	NPV[4] (%)	P[5]
eNose results	13/1 (93)	13/1 (93)	93	93	.0001

[1] Sensitivity. [2] Specificity. [3] Positive predictive value. [4] Negative predictive value. [5] *p* values calculated with Fisher's exact test.

Figure 7. *Cont*.

(D) The volatile phases above healthy MLC supernatants are significantly different.

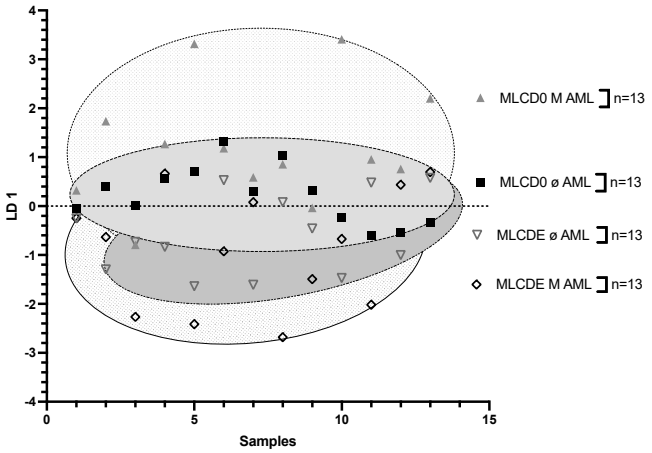

	MLCD0 ø AML	MLCDE ø AML			
	Correct/False (%[1])	Correct/False (%[2])	PPV[3] (%)	NPV[4] (%)	P[5]
eNose results	12/1 (92)	12/1 (92)	92	92	.0001

	MLCD0 M AML	MLCDE M AML			
	Correct/False (%[1])	Correct/False (%[2])	PPV[3] (%)	NPV[4] (%)	P[5]
eNose results	11/2 (85)	10/3 (77)	83	83	.0048

	MLCD0 ø AML	MLCD0 M AML			
	Correct/False (%[1])	Correct/False (%[2])	PPV[3] (%)	NPV[4] (%)	P[5]
eNose results	10/3 (77)	10/3 (77)	77	77	.017

	MLCDE ø AML	MLCDE M AML			
	Correct/False (%[1])	Correct/False (%[2])	PPV[3] (%)	NPV[4] (%)	P[5]
eNose results	11/2 (85)	11/2 (85)	85	85	.0012

	MLCD0 ø AML	MLCDE M AML			
	Correct/False (%[1])	Correct/False (%[2])	PPV[3] (%)	NPV[4] (%)	P[5]
eNose results	10/3 (77)	10/3 (77)	77	77	.017

[1] Sensitivity. [2] Specificity. [3] Positive predictive value. [4] Negative predictive value. [5] p values calculated with Fisher's exact test.

Figure 7. Shown are the graphically represented differences of volatile phases derived from either healthy and leukemic DC culture supernatants (DCD0 ø, DCD0 M, DCDE ø, DCDE M) or healthy and leukemic MLC culture supernatants, comparing before vs. after culture and with vs. without Kit M pretreatment. Given underneath are the dimensionless LD 1 values and tables, presenting an overview of the sensitivity, specificity, negative and positive predictive values. Statistical tests were performed using the Fisher's exact test. Differences were considered significant with p values ≤ 0.05. Abbreviations of analyzed samples are given in Table 2.

3.6. The Volatile Phases above Healthy MLC Supernatants Are Significantly Different

The eNose could significantly differentiate between the volatile phases of healthy MLC culture supernatants, both before vs. after culture and with vs. without Kit M pretreatment (MLCD0 ø vs. MLCD0 M vs. MLCDE ø vs. MLCDE M). We found a significant difference between healthy MLCD0 ø and healthy MLCDE ø (%sensitivity: 79; %specificity: 79; $p = 0.007$). With the same results, we could separate healthy MLCD0 M from healthy MLCDE M (%sensitivity: 79; %specificity: 79; $p = 0.007$).

The eNose could also significantly distinguish healthy MLCD0 ø from healthy MLCD0 M (%sensitivity: 71; %specificity: 93; $p = 0.0013$). Moreover, we found significantly different VOC results in healthy MLCDE ø compared to healthy MLCDE M (%sensitivity: 79; %specificity: 86; $p = 0.0018$). A less significant difference was achieved in a VOC analysis with healthy MLCD0 ø and healthy MLCDE M (%sensitivity: 71; %specificity: 79; $p = 0.0213$) (Figure 7B).

3.7. The Volatile Phases above Leukemic DC Culture Supernatants Are Significantly Different

For analyzing the eNose's ability to distinguish several AML patients' DC culture supernatants (before vs. after culture and with vs. without Kit M pretreatment), we used 14 AML supernatants. We found significantly different VOC results in leukemic DCD0 ø compared to leukemic DCDE ø (%sensitivity: 100; %specificity: 86; $p = 0.0001$). We investigated the difference between leukemic DCD0 M and leukemic DCDE M, as well as the difference between leukemic DCD0 ø and leukemic DCDE M. In both, we found similar significantly different results (%sensitivity: 93; %specificity: 93; $p = 0.0001$). Furthermore, the eNose could significantly distinguish leukemic DCD0 ø from leukemic DCD0 M (%sensitivity: 79; %specificity: 79; $p = 0.007$). In addition, we investigated the LD analysis of leukemic DCDE ø and leukemic DCDE M. The eNose could correctly identify the leukemic DCDE ø with a sensitivity of 86%, and the leukemic DCDE M with a specificity of 71% ($p = 0.0063$) (Figure 7C).

3.8. The Volatile Phases above Leukemic MLC Culture Supernatants Are Significantly Different

The eNose could significantly differentiate between the volatile phases of leukemic MLC culture supernatants before vs. after culture and with vs. without Kit M pretreatment. We found significantly different volatile phases in 13 several leukemic MLC supernatants (MLCD0 ø vs. MLCD0 M vs. MLCDE ø vs. MLCDE M). Leukemic MLCD0 ø showed significantly different VOC results compared to leukemic MLCDE ø (%sensitivity: 92; %specificity: 92; $p = 0.0001$). The comparison of AML patients' MLCD0 M and MLCDE M yielded a sensitivity of 85% and a specificity of 77%, which led to a significant difference in their VOC results ($p = 0.0048$). In addition, the eNose significantly distinguished leukemic MLCD0 ø from leukemic MLCD0 M (%sensitivity: 77; %specificity: 77; $p = 0.017$). With the same effectiveness, the eNose could separate leukemic MLCD0 ø from leukemic MLCDE M (%sensitivity: 77; %specificity: 77; $p = 0.017$). More significant results could be achieved in a comparison of leukemic MLCDE ø with leukemic MLCDE M (%sensitivity: 85; %specificity: 85; $p = 0.0012$) (Figure 7D).

Using LD analyses, we conclude that the eNose could significantly distinguish volatile phases above healthy DC (DCD0 ø vs. DCD0 M or DCDE ø vs. DCDE M) and healthy MLC (MLCD0 ø vs. MLCD0 M or MLCDE ø vs. MLCDE M) culture supernatants, and above several AML patients' DC (DCD0 ø or DCD0 M vs. DCDE ø vs. DCDE M) and leukemic MLC (MLCD0 ø vs. MLCD0 M or MLCDE ø vs. MLCDE M) culture supernatants.

Summary of differences in culture and Kit M-associated effects on healthy or leukemic supernatant-derived VOCs

Figure 8 gives an overview of healthy and leukemic (with or without Kit M-pretreated) cultures (DC/MLC)-derived VOCs, and the influence of culture or Kit M-associated effects. In healthy DC culture supernatant-derived VOCs, we found a Kit M-associated effect ($\Delta p = -0.0169$) and a high culture-associated effect ($\Delta p = 0.046$) (Figure 8; upper

left). In healthy MLC culture supernatant-derived VOCs, we found no Kit M effect ($\Delta p = 0$) and a small culture effect ($\Delta p = 0.0005$) (Figure 8; upper right). In AML patients' DC culture supernatant-derived VOCs, we found (in contrast to healthy samples) no Kit M effect ($\Delta p = 0$) and a small culture effect ($\Delta p = -0.0007$) (Figure 8; lower left). Moreover, (compared to healthy samples) we found significant Kit M-mediated differences in leukemic MLC culture supernatant-derived VOCs ($\Delta p = 0.0047$) alongside high culture effects ($\Delta p = -0.0158$) (Figure 8; lower right).

Summary of differences in culture or Kit M-associated effects in healthy and leukemic supernatant-derived VOCs.

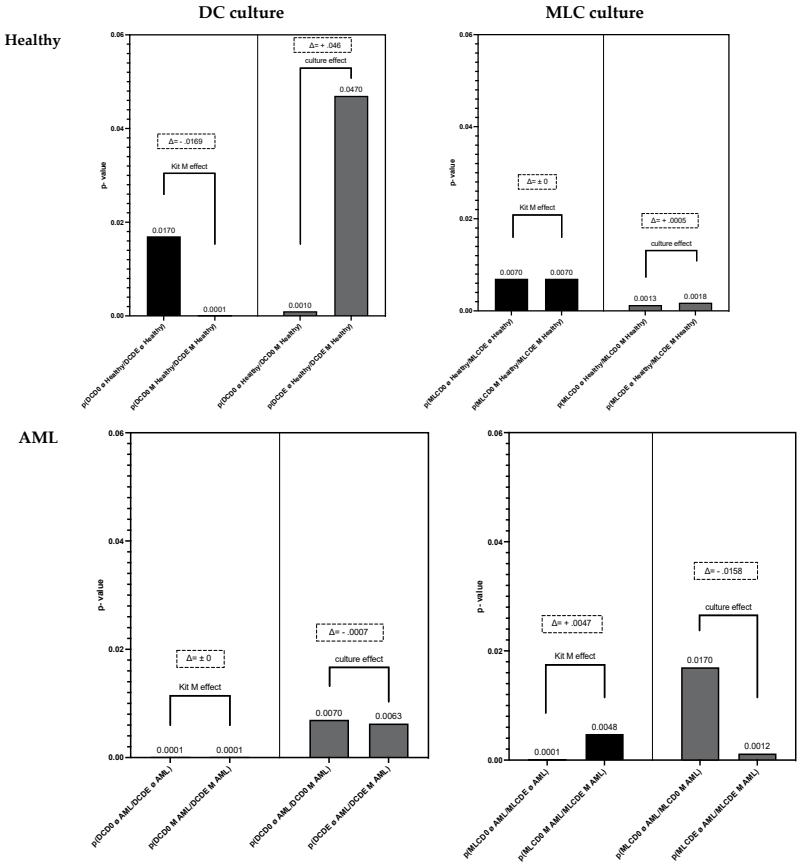

Figure 8. Given are the summarized VOC results, focusing on culture- or Kit M-mediated effects on the identification with eNose of VOC profiles derived from healthy or leukemic DC or MLC culture supernatants. The X-axis shows p values from comparisons from Figure 7A–D. Statistical tests were performed using Fisher's exact test. Differences were considered significant with p values ≤ 0.05. Differences between p values are shown with Δ. Differences were considered significant with $\Delta \geq$ I0.001I. Abbreviations of analyzed samples are given in Table 2.

Following our results, we can summarize that the eNose could significantly distinguish between healthy and leukemia patients' serum, DC (DCD0 ø, DCD0 M, DCDE ø, DCDE M) and MLC (MLCD0 ø, MLCD0 M, MLCDE ø, MLCDE M) culture supernatant-derived volatile phases. Moreover, the eNose could significantly separate several supernatant (with vs. without Kit M treatment, cultured vs. uncultured)-derived VOCs within subgroups (healthy DC or leukemic DC or healthy MLC or leukemic MLC supernatants). Furthermore, the eNose could indicate a clear Kit M-associated effect in healthy cultures (but not in AML-DC cultures), and clear Kit M-mediated effects in leukemic MLC cultures.

4. Discussion

4.1. DC Based Immunotherapy

We can confirm with preliminary data that DC/DC_{leu} can be generated in Kit M-pretreated (vs. not pretreated) healthy patients' WB samples without inducing blast/monocyte proliferation [8,12,22,46,47]. Tendentially, more (mature) DC could be generated from healthy samples' WB, probably due to partly impaired DC generation from patients' WB due to the inherent immune suppressive effect of leukemia [15]. Moreover, we could confirm the immune cell activation of Kit M-pretreated WB after MLC; cells of the adaptive as well as of the innate immune system were activated and had increased frequencies vs. Control. Increased frequencies of immune cells after MLC compared to uncultured MLC are due to the influence of IL-2, as already previously stated [12,15,48]. We confirm with preliminary data that Kit M-treated (vs. untreated) WB leads to (antigen-specific) activation of immune cells and increased antileukemic activity (or 'cytotoxicity') in cases with AML after MLC [12]. This antileukemic effect can be ascribed to the different killing mechanisms of Kit M-mediated immunoreactive cells, i.e., the faster perforin/granzyme pathways and the slower Fas/FasL pathway [12,49].

4.2. VOC Based AML Monitoring

To monitor AML patients' disease or antileukemic immunoreactions, analyses of different cellular, humoral, and soluble factors are important [12,15,22,24–26]. VOCs released by leukemic or immune cells' processes and measured directly by the eNose might be an important tool to monitor biomarkers related to the disease, as previously shown in VOC studies with other diseases [31,36]. Moreover, quantitative and qualitative evaluations of VOCs (collected above cell culture supernatants) were shown to be technically possible, and could show correlations with subtypes of the underlying disease [38].

4.3. Strengths and Limitations of VOC Analyses

An electronic nose such as the one used here utilizes a standardized approach. An important requirement is that its sensors work correctly, and the 32 sensors of the eNose indicate correct reference ranges. Moreover, sensors must be trained with a training set before the start of measurements and must be regularly calibrated. In contrast to other methods, such as ion mobility spectrometry or mass spectrometry, identification of the individual component in a mixture is usually not possible here or is only possible under very restricted conditions [50]. Consequently, this method has the disadvantage that identification of individual analytes in a complex mixture, such as exhaled air, is usually not possible. Conversely, it provides an overall picture of all volatile compounds present in the breath, including those that were not originally the focus of interest but could be a previously unrecognized indicator of (systemic) disease. The principle of the evaluation is based on pattern recognition, so the identification of individual substances is not necessary for classification applications. One of the big advantages of this method is its mobility, and its fast measurement process, which takes only 30 s. In previous studies, it was shown that samples of exhaled air as well as liquid samples could be used as a medium, whereas solid, non-organic materials could not. The Cyranose 320® polymer sensor enables investigations in the ppm range [mL/m^3]. Its 32 sensors have a variation of coefficient of 2–10%. The addition of all 32 signals and the determination of the precision of the

total signal finally resulted in a mean coefficient of variation of 4.64%. Digitally sensed VOCs using an electronic nose have the potential to become a rapid, immediate, and non-invasive diagnostic tool. With the advent of inexpensive, environmentally friendly, and biocompatible sensor systems, health monitoring using VOCs may transform laborious or invasive procedures that currently can only be used in facilities specialized for this purpose into a technology that can be used anywhere and anytime by individuals.

4.4. VOC Differentiation of Healthy vs. Leukemic Serum, DC- and MLC-Cultures as a New Refined, Clinical Monitoring Tool

Analyses of different cellular/humoral, soluble factors [8,15,21–24] or circulating vesicles (e.g., extracellular vesicles (EVs) [26,27]) were tested with respect to a refined monitoring of immunological or tumor-associated processes. VOC differentiation of healthy and leukemic serum or culture samples might be a new strategy for screening recurrence and quantifying the tumor load of diseased patients. Our study demonstrates that an eNose could significantly distinguish healthy VOCs from leukemic VOCs derived from serum, DC- and MLC-culture supernatants. This was true for both healthy and leukemic Kit M-pretreated and non-pretreated cell culture supernatants analyzed using the eNose (Figure 6). Differences in VOCs could have cell biological/immunological causes; AML blasts produce (in contrast to healthy samples) specific mediators and factors (e.g., IL-1-b, IL-6 and angioregulatory factors) to stimulate their proliferation [50,51]. Moreover, the differing frequencies of cell compositions in healthy and leukemic cultures secreting variant factors into the supernatant might lead to different VOCs (Figures 1 and 2); for example, DC_{mat} secrete different exosomes compared to immature DCs (there are higher frequencies of DC_{mat} subsets in healthy vs. leukemic samples). Exosomes from mature DCs (compared to immature DCs) can be enriched with MHC class II, B7.2, and ICAM-1, and depleted in MFG-E8 [52].

4.5. IL-2-Associated Effects on Differences between Uncultured and Cultured MLC-VOCs

A culture effect could be detected by the eNose in leukemic MLC culture supernatant-derived VOCs. VOCs collected before culture were significantly different compared to after culture (leukemic MLC: $\Delta p = -0.0158$) (Figure 8). These VOC results can probably be explained by the IL-2 effect. Following our cell biological results, IL-2 had a stimulatory effect on the immune cells and a significant effect on the provision and activation of (antigen-specific) immune cells (compared to uncultured cells). However, this effect could only be measured in leukemic MLC culture supernatant-derived VOCs.

4.6. Kit M-Associated Effects on DC- and MLC-VOCs

We could deduce the following culture and Kit M-related effects detectable by VOC profiles in healthy and AML cultures:

1. With respect to culture effects, we found significant differences in the VOC profiles of healthy DC culture supernatants (independent of the addition of Kit M), whereas the culture effects of AML samples in the same settings were not different. These findings might be explained by the different compositions of DC culture supernatants in healthy vs. AML DC culture supernatants; healthy samples contain higher frequencies of 'healthy cells', and AML samples contain high frequencies of blasts. After culture, different releases of VOCs in the different settings might explain the good differentiation of healthy DC supernatant VOCs, but not AML DC culture supernatant VOCs.
2. With respect to Kit M-mediated effects, we found significant differences in the VOC profiles of healthy DC culture supernatants when comparing Kit M-pretreated vs. non-pretreated samples, whereas the culture effects of AML samples in the same settings were not different. These findings might be explained by different DC compositions in healthy vs. AML DC culture supernatants; healthy samples yield higher frequencies of mature monocyte-derived DCs, and AML samples yield (in addition) leukemia-

derived DCs and blasts, which may proliferate/differentiate and produce leukemia-associated VOCs.
3. Moreover, AML patients' DC supernatants might contain traces of drug (derivates) after chemotherapy and antibiotic/antimycotic therapy, which could be responsible for alternated VOC profiles compared to healthy DC culture supernatant-derived VOCs.
4. With respect to culture effects, we found no significant differences in the VOC profiles of healthy MLC supernatants (independent of Kit M addition), whereas the culture effects of AML samples in the same settings were significantly different. These findings might be explained by different MLC-related supernatants in healthy vs. AML MLC supernatants (e.g., higher frequencies of 'healthy immune cells' in healthy samples, and high frequencies of blasts in AML samples).
5. With respect to Kit M-mediated effects, we did not find significant differences in the VOC profiles of healthy MLC supernatants when comparing Kit M-pretreated vs. non-pretreated samples, whereas the culture effects of AML samples in the same settings were significantly different. These findings might be explained by the different compositions of immune cells in AML vs. healthy cells; the activation of leukemia-specific immune reactive cells in AML cases might yield significantly different VOCs under the influence of Kit M vs. Control.

This means that culture alone gives rise to other changes in healthy and AML VOC profiles; the presence of Kit M changes the setting and produces different results in AML and healthy VOC samples.

5. Conclusions

We have shown that the role and metabolic influences of drugs of different cellular compositions with respect to qualitative/quantitative differences in VOC release profiles are complex, although our chosen technology yielded differences in different settings. Other strategies or more standardized settings might contribute to more refined VOC-based monitoring strategies in the future. According to our results, eNose analyses might then yield a prospective option for deriving a VOC-based disease profiling strategy using serum or cell culture supernatants from patients with leukemia.

Due to rapid sample collection and analysis, the present study shows good reproducibility of data. It could therefore be recommended to include VOC analyses as an additional component to monitor the course of disease, and potentially to guide therapy-related decisions.

Author Contributions: Conceptualization: T.B. (Tobias Boeselt), R.K., C.S. and H.M.S.; Data acquisition: T.B. (Tobias Baudrexler), T.B. (Tobias Boeselt), A.R., C.S., J.S., L.L., S.B. and U.B.; Formal analyses: T.B. (Tobias Baudrexler) and S.B.; Investigations: T.B. (Tobias Baudrexler); Methodology: H.M.S., T.B. (Tobias Boeselt) and C.S.; Project administration: T.B. (Tobias Baudrexler), R.K. and H.M.S.; Resources: intramural fundings of the groups of R.K., T.B. (Tobias Boeselt) and H.M.S.; Software: T.B. (Tobias Boeselt); Supervision: H.M.S.; Validation: T.B. (Tobias Baudrexler), T.B. (Tobias Boeselt) and A.R.; Graphically design: T.B. (Tobias Baudrexler); Drafting: T.B. (Tobias Baudrexler) and H.M.S.; Reviewing: T.B. (Tobias Boeselt) and H.M.S. All authors have read and agreed to the published version of the manuscript.

Funding: This research received no external funding.

Institutional Review Board Statement: Sample collection was conducted after obtaining written informed consent from the blood donor, and in accordance with the World Medical Association Declaration of Helsinki and the ethics committee of the Ludwig-Maximilian University, Munich (vote no. 339-05; 22 February 2019).

Informed Consent Statement: Informed consent was obtained from all subjects involved in the study.

Data Availability Statement: The data presented in this study are available in this article.

Acknowledgments: The authors thank the patients, nurses, physicians, and technicians (special thanks to Boas U.) for their support with sample materials and diagnostic reports. The results presented in this manuscript are part of the doctoral thesis of Tobias Baudrexler at the University Hospital of Ludwig-Maximilian-Universität Munich.

Conflicts of Interest: Modiblast Pharma GmbH (Oberhaching, Germany) holds the European Patent 15 801 987.7-1118 and US Patent 15-517627: 'Use of immunomodulatory effective compositions for the immunotherapeutic treatment of patients suffering from myeloid leukemias', with which Schmetzer H. is involved.

References

1. Appelbaum, F.R.; Gundacker, H.; Head, D.R.; Slovak, M.L.; Willman, C.L.; Godwin, J.E.; Anderson, J.E.; Petersdorf, S.H. Age and acute myeloid leukemia. *Blood* **2006**, *107*, 3481–3485. [CrossRef] [PubMed]
2. Marcucci, G.; Haferlach, T.; Döhner, H. Molecular Genetics of Adult Acute Myeloid Leukemia: Prognostic and Therapeutic Implications. *J. Clin. Oncol.* **2011**, *29*, 475–486. [CrossRef] [PubMed]
3. Malcovati, L.; Nimer, S.D. Myelodysplastic syndromes: Diagnosis and staging. *Cancer Control.* **2008**, *15*, 4–13. [CrossRef] [PubMed]
4. Röllig, C. Diagnostik und Therapie der akuten myeloischen Leukämie. *Best Pract. Onkol.* **2019**, *14*, 386–397. [CrossRef]
5. Gardin, C.; Dombret, H. Hypomethylating Agents as a Therapy for AML. *Curr. Hematol. Malig. Rep.* **2017**, *12*, 1–10. [CrossRef]
6. Ansprenger, C.; Amberger, D.C.; Schmetzer, H.M. Potential of immunotherapies in the mediation of antileukemic responses for patients with acute myeloid leukemia (AML) and myelodysplastic syndrome (MDS)—With a focus on Dendritic cells of leukemic origin (DCleu). *Clin. Immunol.* **2020**, *217*, 108467. [CrossRef]
7. Jonas, B.A.; Pollyea, D.A. How we use venetoclax with hypomethylating agents for the treatment of newly diagnosed patients with acute myeloid leukemia. *Leukemia* **2019**, *33*, 2795–2804. [CrossRef]
8. Amberger, D.C.; Doraneh-Gard, F.; Gunsilius, C.; Weinmann, M.; Möbius, S.; Kugler, C.; Rogers, N.; Böck, C.; Ködel, U.; Werner, J.-O.; et al. PGE1-Containing Protocols Generate Mature (Leukemia-Derived) Dendritic Cells Directly from Leukemic Whole Blood. *Int. J. Mol. Sci.* **2019**, *20*, 4590. [CrossRef]
9. Amberger, D.C.; Schmetzer, H.M. Dendritic Cells of Leukemic Origin: Specialized Antigen-Presenting Cells as Potential Treatment Tools for Patients with Myeloid Leukemia. *Transfus. Med. Hemotherapy* **2020**, *47*, 432–443. [CrossRef]
10. Sabado, R.L.; Balan, S.; Bhardwaj, N. Dendritic cell-based immunotherapy. *Cell Res.* **2017**, *27*, 74–95. [CrossRef]
11. Sallusto, F.; Lanzavecchia, A. Understanding dendritic cell and T-lymphocyte traffic through the analysis of chemokine receptor expression. *Immunol. Rev.* **2000**, *177*, 134–140. [CrossRef] [PubMed]
12. Klauer, L.K.; Schutti, O.; Ugur, S.; Doraneh-Gard, F.; Amberger, D.C.; Rogers, N.; Krämer, D.; Rank, A.; Schmid, C.; Eiz-Vesper, B.; et al. Interferon Gamma Secretion of Adaptive and Innate Immune Cells as a Parameter to Describe Leukaemia-Derived Dendritic-Cell-Mediated Immune Responses in Acute Myeloid Leukaemia in vitro. *Transfus. Med. Hemotherapy* **2021**, *49*, 44–61. [CrossRef] [PubMed]
13. Schwepcke, C.; Klauer, L.K.; Deen, D.; Amberger, D.C.; Fischer, Z.; Doraneh-Gard, F.; Gunsilius, C.; Hirn-Lopez, A.; Kroell, T.; Tischer, J.; et al. Generation of Leukaemia-Derived Dendritic Cells (DCleu) to Improve Anti-Leukaemic Activity in AML: Selection of the Most Efficient Response Modifier Combinations. *Int. J. Mol. Sci.* **2022**, *23*, 8333. [CrossRef] [PubMed]
14. Robertson, F.C.; Berzofsky, J.A.; Terabe, M. NKT Cell Networks in the Regulation of Tumor Immunity. *Front. Immunol.* **2014**, *5*, 543. [CrossRef] [PubMed]
15. Rackl, E.; Li, L.; Klauer, L.K.; Ugur, S.; Pepeldjiyska, E.; Seidel, C.L.; Gunsilius, C.; Weinmann, M.; Doraneh-Gard, F.; Reiter, N. Dendritic Cell-Triggered Immune Activation Goes along with Provision of (Leukemia-Specific) Integrin Beta 7-Expressing Immune Cells and Improved Antileukemic Processes. *Int. J. Mol. Sci.* **2023**, *24*, 463. [CrossRef]
16. Schmetzer, H.M.; Kremser, A.; Loibl, J.; Kroell, T.; Kolb, H.J. Quantification of ex vivo generated dendritic cells (DC) and leukemia-derived DC contributes to estimate the quality of DC, to detect optimal DC-generating methods or to optimize DC-mediated T-cell-activation-procedures ex vivo or in vivo. *Leukemia* **2007**, *21*, 1338–1341. [CrossRef]
17. Plett, C.; Amberger, D.; Rabe, A.; Deen, D.; Stankova, Z.; Hirn Lopez, A.; Vokac, Y.; Werner, J.; Krämer, D.; Rank, A. Kits do not induce AML-blasts' proliferation ex vivo. IPO-38 is an appropriate and reliable marker to detect and quantify proliferating blasts. *J. Immunother. Cancer* **2017**, *52*, S398.
18. Grabrucker, C.; Liepert, A.; Dreyig, J.; Kremser, A.; Kroell, T.; Freudenreich, M.; Schmid, C.; Schweiger, C.; Tischer, J.; Kolb, H.-J.; et al. The Quality and Quantity of Leukemia-derived Dendritic Cells From Patients With Acute Myeloid Leukemia and Myelodysplastic Syndrome Are a Predictive Factor for the Lytic Potential of Dendritic Cells-primed Leukemia-Specific T Cells. *J. Immunother.* **2010**, *33*, 523–537. [CrossRef]
19. Hansen, N.; Önder, D.; Schwing, K.; Widman, G.; Leelaarporn, P.; Prusseit, I.; Surges, R.; Becker, A.J.; Witt, J.-A.; Helmstaedter, C.; et al. CD19+ B-cells in autoantibody-negative limbic encephalitis. *Epilepsy Behav.* **2020**, *106*, 107016. [CrossRef]
20. Aktas, E.; Kucuksezer, U.C.; Bilgic, S.; Erten, G.; Deniz, G. Relationship between CD107a expression and cytotoxic activity. *Cell. Immunol.* **2009**, *254*, 149–154. [CrossRef]

21. Pepeldjiyska, E.; Li, L.; Gao, J.; Seidel, C.L.; Blasi, C.; Özkaya, E.; Schmohl, J.; Kraemer, D.; Schmid, C.; Rank, A. Leukemia derived dendritic cell (DCleu) mediated immune response goes along with reduced (leukemia-specific) regulatory T-cells. *Immunobiology* **2022**, *227*, 152237. [CrossRef] [PubMed]
22. Boeck, C.L.; Amberger, D.C.; Doraneh-Gard, F.; Sutanto, W.; Guenther, T.; Schmohl, J.; Schuster, F.; Salih, H.; Babor, F.; Borkhardt, A.; et al. Significance of Frequencies, Compositions, and/or Antileukemic Activity of (DC-stimulated) Invariant NKT, NK and CIK Cells on the Outcome of Patients With AML, ALL and CLL. *J. Immunother.* **2017**, *40*, 224–248. [CrossRef] [PubMed]
23. Vogt, V.; Schick, J.; Ansprenger, C.; Braeu, M.; Kroell, T.; Kraemer, D.; Köhne, C.-H.; Hausmann, A.; Buhmann, R.; Tischer, J.; et al. Profiles of Activation, Differentiation–Markers, or β-Integrins on T Cells Contribute to Predict T Cells' Antileukemic Responses After Stimulation With Leukemia-derived Dendritic Cells. *J. Immunother.* **2014**, *37*, 331–347. [CrossRef] [PubMed]
24. Merle, M.; Fischbacher, D.; Liepert, A.; Grabrucker, C.; Kroell, T.; Kremser, A.; Dreyssig, J.; Freudenreich, M.; Schuster, F.; Borkhardt, A.; et al. Conversion of AML-blasts to leukemia-derived dendritic cells (DCleu) in 'DC-culture-media' shifts correlations of released chemokines with antileukemic T-cell reactions. *Immunobiology* **2021**, *226*, 152088. [CrossRef] [PubMed]
25. Doraneh gard, F.; Amberger, D.; Weinmann, M.; Boeck, C.; Gunsilius, C.; Kugler, C.; Werner, J.; Kraemer, D.; Rank, A.; Schmid, C.; et al. Standard normoxic versus physiological hypoxic culture of AML patients' (pts) whole blood (WB) samples with immune modulatory kits yields comparable proportions of dendritic cells and functional results. *Eur. J. Cancer* **2018**, *92*, S10–S11. [CrossRef]
26. Tkach, M.; Kowal, J.; Zucchetti, A.E.; Enserink, L.; Jouve, M.; Lankar, D.; Saitakis, M.; Martin-Jaular, L.; Théry, C. Qualitative differences in T-cell activation by dendritic cell-derived extracellular vesicle subtypes. *EMBO J.* **2017**, *36*, 3012–3028. [CrossRef]
27. Li, L.; Görgens, A.; Mussack, V.; Pepeldjiyska, E.; Hartz, A.S.; Rank, A.; Schmohl, J.; Krämer, D.; Andaloussi, S.E.; Pfaffl, M.W.; et al. Description and optimization of a multiplex bead-based flow cytometry method (MBFCM) to characterize extracellular vesicles in serum samples from patients with hematological malignancies. *Cancer Gene Ther.* **2022**, *29*, 1600–1615. [CrossRef]
28. Mazzatenta, A.; Pokorski, M.; Sartucci, F.; Domenici, L.; Di Giulio, C. Volatile organic compounds (VOCs) fingerprint of Alzheimer's disease. *Respir. Physiol. Neurobiol.* **2015**, *209*, 81–84. [CrossRef]
29. Bach, J.-P.; Gold, M.; Mengel, D.; Hattesohl, A.; Lubbe, D.; Schmid, S.; Tackenberg, B.; Rieke, J.; Maddula, S.; Baumbach, J.I.; et al. Measuring Compounds in Exhaled Air to Detect Alzheimer's Disease and Parkinson's Disease. *PLoS ONE* **2015**, *10*, e0132227. [CrossRef]
30. Dragonieri, S.; Annema, J.T.; Schot, R.; van der Schee, M.P.C.; Spanevello, A.; Carratú, P.; Resta, O.; Rabe, K.F.; Sterk, P.J. An electronic nose in the discrimination of patients with non-small cell lung cancer and COPD. *Lung Cancer* **2009**, *64*, 166–170. [CrossRef]
31. Biehl, W.; Hattesohl, A.; Jorres, R.A.; Duell, T.; Althohn, U.; Koczulla, A.R.; Schmetzer, H. VOC pattern recognition of lung cancer: A comparative evaluation of different dog- and eNose-based strategies using different sampling materials. *Acta Oncol.* **2019**, *58*, 1216–1224. [CrossRef] [PubMed]
32. Dutta, D.; Chong, N.S.; Lim, S.H. Endogenous volatile organic compounds in acute myeloid leukemia: Origins and potential clinical applications. *J. Breath Res.* **2018**, *12*, 034002. [CrossRef]
33. Gaida, A.; Holz, O.; Nell, C.; Schuchardt, S.; Lavae-Mokhtari, B.; Kruse, L.; Boas, U.; Langejuergen, J.; Allers, M.; Zimmermann, S. A dual center study to compare breath volatile organic compounds from smokers and non-smokers with and without COPD. *J. Breath Res.* **2016**, *10*, 026006. [CrossRef] [PubMed]
34. Boeselt, T.; Terhorst, P.; Kroenig, J.; Nell, C.; Spielmanns, M.; Heers, H.; Boas, U.; Veith, M.; Vogelmeier, C.; Greulich, T. Pilot Study On Non-Invasive Diagnostics Of Volatile Organic Compounds Over Urine From COVID-19 Patients. *Arch. Clin. Biomed. Res.* **2022**, *6*, 65–73. [CrossRef]
35. Hattesohl, A.D.; Jörres, R.A.; Dressel, H.; Schmid, S.; Vogelmeier, C.; Greulich, T.; Noeske, S.; Bals, R.; Koczulla, A.R. Discrimination between COPD patients with and without alpha 1-antitrypsin deficiency using an electronic nose. *Respirology* **2011**, *16*, 1258–1264. [CrossRef]
36. Lueno, M.; Dobrowolny, H.; Gescher, D.; Gbaoui, L.; Meyer-Lotz, G.; Hoeschen, C.; Frodl, T. Volatile Organic Compounds From Breath Differ Between Patients With Major Depression and Healthy Controls. *Front. Psychiatry* **2023**, *13*, 819607. [CrossRef] [PubMed]
37. Heers, H.; Gut, J.M.; Hegele, A.; Hofmann, R.; Boeselt, T.; Hattesohl, A.; Koczulla, A.R. Non-invasive Detection of Bladder Tumors Through Volatile Organic Compounds: A Pilot Study with an Electronic Nose. *Anticancer Res.* **2018**, *38*, 833–837.
38. Accardo-Palumbo, A.; Ferrante, A.; Cadelo, M.; Ciccia, F.; Parrinello, G.; Lipari, L.; Giardina, A.; Riili, M.; Giardina, E.; Dieli, F. The level of soluble granzyme A is elevated in the plasma and in the Vg9/Vd2 T cell culture supernatants of patients with active Behcet's disease. *Clin. Exp. Rheumatol.* **2004**, *22*, S45–S49.
39. Döhner, H.; Estey, E.H.; Amadori, S.; Appelbaum, F.R.; Büchner, T.; Burnett, A.K.; Dombret, H.; Fenaux, P.; Grimwade, D.; Larson, R.A.; et al. Diagnosis and management of acute myeloid leukemia in adults: Recommendations from an international expert panel, on behalf of the European LeukemiaNet. *Blood* **2010**, *115*, 453–474. [CrossRef]
40. Kufner, S.; Zitzelsberger, H.; Kroell, T.; Pelka-Fleischer, R.; Salem, A.; De Valle, F.; Schweiger, C.; Nuessler, V.; Schmid, C.; Kolb, H.J.; et al. Leukemia-Derived Dendritic Cells can be Generated from Blood or Bone Marrow Cells from Patients with Acute Myeloid Leukaemia: A Methodological Approach under Serum-Free Culture Conditions. *Scand. J. Immunol.* **2005**, *62*, 86–98. [CrossRef]

41. Willasch, A.; Eing, S.; Weber, G.; Kuçi, S.; Schneider, G.; Soerensen, J.; Jarisch, A.; Rettinger, E.; Koehl, U.; Klingebiel, T.; et al. Enrichment of cell subpopulations applying automated MACS technique: Purity, recovery and applicability for PCR-based chimerism analysis. *Bone Marrow Transplant.* **2010**, *45*, 181–189. [CrossRef] [PubMed]
42. Betts, M.R.; Koup, R.A. Detection of T-Cell Degranulation: CD107a and b. In *Methods in Cell Biology*; Academic Press: Cambridge, MA, USA, 2004; Volume 75, pp. 497–512.
43. Lobb, R.J.; Becker, M.; Wen Wen, S.; Wong, C.S.F.; Wiegmans, A.P.; Leimgruber, A.; Möller, A. Optimized exosome isolation protocol for cell culture supernatant and human plasma. *J. Extracell. Vesicles* **2015**, *4*, 27031. [CrossRef]
44. Koczulla, A.R.; Hattesohl, A.; Biller, H.; Hofbauer, J.; Hohlfeld, J.; Oeser, C.; Gessner, C.; Vogelmeier, C.; Baumbach, J.I.; Wirtz, H.; et al. Krankheiten erriechen? Eine kurze Übersicht über elektronische Nasen. *Pneumologie* **2011**, *65*, 401–405. [CrossRef] [PubMed]
45. Greulich, T.; Hattesohl, A.; Grabisch, A.; Koepke, J.; Schmid, S.; Noeske, S.; Nell, C.; Wencker, M.; Jörres, R.A.; Vogelmeier, C.F.; et al. Detection of obstructive sleep apnoea by an electronic nose. *Eur. Respir. J.* **2013**, *42*, 145–155. [CrossRef] [PubMed]
46. Lewis, N.S. Comparisons between mammalian and artificial olfaction based on arrays of carbon black− polymer composite vapor detectors. *Acc. Chem. Res.* **2004**, *37*, 663–672. [CrossRef] [PubMed]
47. Hirn Lopez, A.; Deen, D.; Fischer, Z.; Rabe, A.; Ansprenger, C.; Stein, K.; Vogt, V.; Schick, J.; Kroell, T.; Kraemer, D.; et al. Role of Interferon (IFN)a in ´Cocktails´ for the Generation of (Leukemia-derived) Dendritic Cells (DCleu) From Blasts in Blood From Patients (pts) With Acute Myeloid Leukemia (AML) and the Induction of Antileukemic Reactions. *J. Immunother.* **2019**, *42*, 143–161. [CrossRef]
48. Plett, C.; Klauer, L.K.; Amberger, D.C.; Ugur, S.; Rabe, A.; Fischer, Z.; Deen, D.; Hirn-Lopez, A.; Gunsilius, C.; Werner, J.-O.; et al. Immunomodulatory kits generating leukaemia derived dendritic cells do not induce blast proliferation ex vivo: IPO-38 as a novel marker to quantify proliferating blasts in acute myeloid leukaemia. *Clin. Immunol.* **2022**, *242*, 109083. [CrossRef]
49. Martínez-Lostao, L.; Anel, A.; Pardo, J. How Do Cytotoxic Lymphocytes Kill Cancer Cells? *Clin. Cancer Res.* **2015**, *21*, 5047–5056. [CrossRef]
50. Koczulla, R.; Hattesohl, A.; Biller, H.; Hofbauer, J.; Hohlfeld, J.; Oeser, C.; Wirtz, H.; Jörres, R. Vergleich von vier baugleichen elektronischen Nasen und drei Messaufbauten. *Pneumologie* **2011**, *65*, 465–470. [CrossRef]
51. Oster, W.; Cicco, N.A.; Klein, H.; Hirano, T.; Kishimoto, T.; Lindemann, A.; Mertelsmann, R.H.; Herrmann, F. Participation of the cytokines interleukin 6, tumor necrosis factor-alpha, and interleukin 1-beta secreted by acute myelogenous leukemia blasts in autocrine and paracrine leukemia growth control. *J. Clin. Investig.* **1989**, *84*, 451–457. [CrossRef]
52. Segura, E.; Amigorena, S.; Théry, C. Mature dendritic cells secrete exosomes with strong ability to induce antigen-specific effector immune responses. *Blood Cells Mol. Dis.* **2005**, *35*, 89–93. [CrossRef] [PubMed]

7. **Literaturverzeichnis** *References*

ACCARDO-PALUMBO, A., FERRANTE, A., CADELO, M., CICCIA, F., PARRINELLO, G., LIPARI, L., GIARDINA, A., RIILI, M., GIARDINA, E. & DIELI, F. 2004. The level of soluble granzyme A is elevated in the plasma and in the Vg9/Vd2 T cell culture supernatants of patients with active Behcet's disease. *Clin Exp Rheumatol,* 22**,** S45-S49.

AL-DACCAK, R., MOONEY, N. & CHARRON, D. 2004. MHC class II signaling in antigen-presenting cells. *Current Opinion in Immunology,* 16**,** 108-113.

AMBERGER, D. C., DORANEH-GARD, F., GUNSILIUS, C., WEINMANN, M., MÖBIUS, S., KUGLER, C., ROGERS, N., BÖCK, C., KÖDEL, U., WERNER, J.-O., KRÄMER, D., EIZ-VESPER, B., RANK, A., SCHMID, C. & SCHMETZER, H. M. 2019. PGE1-Containing Protocols Generate Mature (Leukemia-Derived) Dendritic Cells Directly from Leukemic Whole Blood. *International Journal of Molecular Sciences,* 20**,** 4590.

AMBERGER, D. C. & SCHMETZER, H. M. 2020. Dendritic Cells of Leukemic Origin: Specialized Antigen-Presenting Cells as Potential Treatment Tools for Patients with Myeloid Leukemia. *Transfusion Medicine and Hemotherapy,* 47**,** 432-443.

ANSPRENGER, C., AMBERGER, D. C. & SCHMETZER, H. M. 2020. Potential of immunotherapies in the mediation of antileukemic responses for patients with acute myeloid leukemia (AML) and myelodysplastic syndrome (MDS) - With a focus on Dendritic cells of leukemic origin (DCleu). *Clinical Immunology,* 217**,** 108467.

APPELBAUM, F. R., GUNDACKER, H., HEAD, D. R., SLOVAK, M. L., WILLMAN, C. L., GODWIN, J. E., ANDERSON, J. E. & PETERSDORF, S. H. 2006. Age and acute myeloid leukemia. *Blood,* 107**,** 3481-3485.

BACH, J.-P., GOLD, M., MENGEL, D., HATTESOHL, A., LUBBE, D., SCHMID, S., TACKENBERG, B., RIEKE, J., MADDULA, S., BAUMBACH, J. I., NELL, C., BOESELT, T., MICHELIS, J., ALFERINK, J., HENEKA, M., OERTEL, W., JESSEN, F., JANCIAUSKIENE, S., VOGELMEIER, C., DODEL, R. & KOCZULLA, A. R. 2015. Measuring Compounds in Exhaled Air to Detect Alzheimer's Disease and Parkinson's Disease. *PLOS ONE,* 10**,** e0132227.

BAUDREXLER, T., BOESELT, T., LI, L., BOHLSCHEID, S., BOAS, U., SCHMID, C., RANK, A., SCHMOHL, J., KOCZULLA, R. & SCHMETZER, H. M. 2023. Volatile Phases Derived from Serum, DC, or MLC Culture Supernatants to Deduce a VOC-Based Diagnostic Profiling Strategy for Leukemic Diseases. *Biomolecules,* 13**,** 989.

BAUDREXLER, T., BOESELT T., ATZLER M., HARTZ A., BOAS U., SCHMID C., RANK A., SCHMOHL J., KOCZULLA R., SCHMETZER H. M. 2024. Volatile Profiling using an eNose - Exploiting Breath Volatile Organic Compounds for Disease Monitoring in Refractory Acute Myeloid Leukemia Patients. *Annual Case Report,* 9**,** 1836.

BIEHL, W., HATTESOHL, A., JORRES, R. A., DUELL, T., ALTHOHN, U., KOCZULLA, A. R. & SCHMETZER, H. 2019. VOC pattern recognition of lung cancer: a comparative evaluation of different dog- and eNose-based strategies using different sampling materials. *Acta Oncologica,* 58**,** 1216-1224.

BOECK, C. L., AMBERGER, D. C., DORANEH-GARD, F., SUTANTO, W., GUENTHER, T., SCHMOHL, J., SCHUSTER, F., SALIH, H., BABOR, F., BORKHARDT, A. & SCHMETZER, H. 2017. Significance of Frequencies, Compositions, and/or Antileukemic Activity of (DC-stimulated) Invariant NKT, NK and CIK Cells on the Outcome of Patients With AML, ALL and CLL. *Journal of Immunotherapy,* 40**,** 224-248.

BOESELT, T., TERHORST, P., KROENIG, J., NELL, C., SPIELMANNS, M., HEERS, H., BOAS, U., VEITH, M., VOGELMEIER, C. & GREULICH, T. 2022. Pilot Study On Non-Invasive Diagnostics Of Volatile Organic Compounds Over Urine From COVID-19 Patients. *Archives of Clinical and Biomedical Research,* 6**,** 65-73.

BONILLA, F. A. & OETTGEN, H. C. 2010. Adaptive immunity. *Journal of Allergy and Clinical Immunology,* 125**,** S33-S40.

CAMPANA, D. & BEHM, F. G. 2000. Immunophenotyping of leukemia. *Journal of Immunological Methods,* 243**,** 59-75.

DÖHNER, H., WEI, A. H., APPELBAUM, F. R., CRADDOCK, C., DINARDO, C. D., DOMBRET, H., EBERT, B. L., FENAUX, P., GODLEY, L. A. & HASSERJIAN, R. P. 2022. Diagnosis and management of AML in adults: 2022 recommendations from an international expert panel on behalf of the ELN. *Blood, The Journal of the American Society of Hematology,* 140**,** 1345-1377.

DORANEH GARD, F., AMBERGER, D., AMEND, C., WEINMANN, M., SCHWEPCKE, C., KLAUER, L., SCHUTTI, O., HOSSEINI, H., KRÄMER, D., RANK, A., SCHMID, C. & SCHMETZER, H. 2024. Anti-Leukemic Effects Induced by Dendritic Cells of Leukemic Origin from Leukemic Blood Samples Are Comparable under Hypoxic vs. Normoxic Conditions. *Cancers,* 16**,** 2383.

DRAGONIERI, S., ANNEMA, J. T., SCHOT, R., VAN DER SCHEE, M. P. C., SPANEVELLO, A., CARRATÚ, P., RESTA, O., RABE, K. F. & STERK, P. J. 2009. An electronic nose in the discrimination of patients with non-small cell lung cancer and COPD. *Lung Cancer,* 64**,** 166-170.

GARDIN, C. & DOMBRET, H. 2017. Hypomethylating Agents as a Therapy for AML. *Current Hematologic Malignancy Reports,* 12**,** 1-10.

GREULICH, T., HATTESOHL, A., GRABISCH, A., KOEPKE, J., SCHMID, S., NOESKE, S., NELL, C., WENCKER, M., JÖRRES, R. A., VOGELMEIER, C. F., KÖHLER, U. & KOCZULLA, A. R. 2013. Detection of obstructive sleep apnoea by an electronic nose. *European Respiratory Journal,* 42**,** 145-155.

HARADA, Y., NAGATA, Y., KIHARA, R., ISHIKAWA, Y., ASOU, N., OHTAKE, S., MIYAWAKI, S., SAKURA, T., OZAWA, Y., USUI, N., KANAMORI, H., ITO, Y., IMAI, K., SUEHIRO, Y., KOBAYASHI, S., KITAMURA, K., SAKAIDA, E., ONIZUKA, M., TAKESHITA, A., ISHIDA, F., SUZUSHIMA, H., ISHIZAWA, K., NAOE, T., MATSUMURA, I., MIYAZAKI, Y., OGAWA, S. & KIYOI, H. 2018. Prognostic analysis according to the 2017 ELN risk stratification by genetics in adult acute myeloid leukemia patients treated in the Japan Adult Leukemia Study Group (JALSG) AML201 study. *Leukemia Research,* 66**,** 20-27.

HEERS, H., GUT, J. M., HEGELE, A., HOFMANN, R., BOESELT, T., HATTESOHL, A. & KOCZULLA, A. R. 2018. Non-invasive Detection of Bladder Tumors Through Volatile Organic Compounds: A Pilot Study with an Electronic Nose. *Anticancer Research,* 38**,** 833-837.

HOU, G.-L., HUANG, J.-S. & TSAI, C.-C. 1997. Analysis of oral manifestations of leukemia: a retrospective study. *Oral Diseases,* 3**,** 31-38.

KEEFE, D., SHI, L., FESKE, S., MASSOL, R., NAVARRO, F., KIRCHHAUSEN, T. & LIEBERMAN, J. 2005. Perforin Triggers a Plasma Membrane-Repair Response that Facilitates CTL Induction of Apoptosis. *Immunity,* 23**,** 249-262.

KLAUER, L. K., SCHUTTI, O., UGUR, S., DORANEH-GARD, F., AMBERGER, D. C., ROGERS, N., KRÄMER, D., RANK, A., SCHMID, C., EIZ-VESPER, B. & SCHMETZER, H. M. 2021. Interferon Gamma Secretion of Adaptive and Innate Immune Cells as a Parameter to Describe Leukaemia-Derived Dendritic-Cell-Mediated Immune Responses in Acute Myeloid Leukaemia in vitro. *Transfusion Medicine and Hemotherapy*.

KOCZULLA, A. R., HATTESOHL, A., BILLER, H., HOFBAUER, J., HOHLFELD, J., OESER, C., GESSNER, C., VOGELMEIER, C., BAUMBACH, J. I., WIRTZ, H. & JÖRRES, R. A. 2011. Krankheiten erriechen? Eine kurze Übersicht über elektronische Nasen. *Pneumologie,* 65**,** 401-405.

LAUMONT, C. M., BANVILLE, A. C., GILARDI, M., HOLLERN, D. P. & NELSON, B. H. 2022. Tumour-infiltrating B cells: immunological mechanisms, clinical impact and therapeutic opportunities. *Nature Reviews Cancer,* 22**,** 414-430.

LETSCH, A. & SCHEIBENBOGEN, C. 2003. Quantification and characterization of specific T-cells by antigen-specific cytokine production using ELISPOT assay or intracellular cytokine staining. *Methods,* 31**,** 143-149.

LEWIS, N. S. 2004. Comparisons between mammalian and artificial olfaction based on arrays of carbon black− polymer composite vapor detectors. *Accounts of chemical research,* 37**,** 663-672.

LI, L., MUSSACK, V., PEPELDJIYSKA, E., HARTZ, A., RANK, A., SCHMID, C., ÖZKAYA, E., UGUR, S., PFAFFL, M. & SCHMETZER, H. 2020. P01.11 Role of exosomes as promotors or biomarkers to study activation of leukemia-derived dendritic cells (DCleu)-mediated antileukemic activation of adaptive and innate immune-reactive cells against AML-blasts. *Journal for ImmunoTherapy of Cancer,* 8**,** A13-A14.

LIU, Q., SUN, Z. & CHEN, L. 2020. Memory T cells: strategies for optimizing tumor immunotherapy. *Protein & cell,* 11**,** 549-564.

LOWENBERG, B., DOWNING, J. R. & BURNETT, A. 1999. Acute Myeloid Leukemia. *New England Journal of Medicine,* 341**,** 1051-1062.

MALCOVATI, L. & NIMER, S. D. 2008. Myelodysplastic syndromes: diagnosis and staging. *Cancer Control,* 15 Suppl**,** 4-13.

MARCUCCI, G., HAFERLACH, T. & DÖHNER, H. 2011. Molecular Genetics of Adult Acute Myeloid Leukemia: Prognostic and Therapeutic Implications. *Journal of Clinical Oncology,* 29**,** 475-486.

MAZZATENTA, A., POKORSKI, M., SARTUCCI, F., DOMENICI, L. & DI GIULIO, C. 2015. Volatile organic compounds (VOCs) fingerprint of Alzheimer's disease. *Respiratory Physiology & Neurobiology,* 209**,** 81-84.

PARKIN, J. & COHEN, B. 2001. An overview of the immune system. *The Lancet,* 357**,** 1777-1789.

PAULOSE, P. J. & FATHIMA, J. L. 2023. Classification of Acute Leukaemia based on Blast Morphology, Cytochemistry and Flow Cytometry. *JOURNAL OF CLINICAL AND DIAGNOSTIC RESEARCH,* 17**,** EC01-EC05.

PEPELDJIYSKA, E., LI, L., GAO, J., SEIDEL, C. L., BLASI, C., ÖZKAYA, E., SCHMOHL, J., KRAEMER, D., SCHMID, C. & RANK, A. 2022. Leukemia derived dendritic cell (DCleu) mediated immune response goes along with reduced (leukemia-specific) regulatory T-cells. *Immunobiology,* 227**,** 152237.

PISTRITTO, G., TRISCIUOGLIO, D., CECI, C., GARUFI, A. & D'ORAZI, G. 2016. Apoptosis as anticancer mechanism: function and dysfunction of its modulators and targeted therapeutic strategies. *Aging,* 8**,** 603-619.

PLETT, C., KLAUER, L. K., AMBERGER, D. C., UGUR, S., RABE, A., FISCHER, Z., DEEN, D., HIRN-LOPEZ, A., GUNSILIUS, C., WERNER, J.-O., SCHMOHL, J., KRÄMER, D., RANK, A., SCHMID, C. & SCHMETZER, H. M. 2022. Immunomodulatory kits generating leukaemia derived dendritic cells do not induce blast proliferation ex vivo: IPO-38 as a novel marker to quantify proliferating blasts in acute myeloid leukaemia. *Clinical Immunology,* 242**,** 109083.

ROBERTSON, F. C., BERZOFSKY, J. A. & TERABE, M. 2014. NKT Cell Networks in the Regulation of Tumor Immunity. *Frontiers in Immunology,* 5.

RÖLLIG, C. 2019. Diagnostik und Therapie der akuten myeloischen Leukämie. *best practice onkologie,* 14**,** 386-397.

SABADO, R. L., BALAN, S. & BHARDWAJ, N. 2017. Dendritic cell-based immunotherapy. *Cell Research,* 27**,** 74-95.

SCHOCH, C. & HAFERLACH, T. 2002. Cytogenetics in acute myeloid leukemia. *Current Oncology Reports,* 4**,** 390-397.

SCHUTTI, O., KLAUER, L., BAUDREXLER, T., BURKERT, F., SCHMOHL, J., HENTRICH, M., BOJKO, P., KRAEMER, D., RANK, A., SCHMID, C. & SCHMETZER, H. 2024. Effective and Successful Quantification of Leukemia-Specific Immune Cells in AML Patients' Blood or Culture, Focusing on Intracellular Cytokine and Degranulation Assays. *International Journal of Molecular Sciences,* 25**,** 6983.

SCHWEPCKE, C., KLAUER, L. K., DEEN, D., AMBERGER, D. C., FISCHER, Z., DORANEH-GARD, F., GUNSILIUS, C., HIRN-LOPEZ, A., KROELL, T., TISCHER, J., WEINMANN, M., WERNER, J.-O., RANK, A., SCHMID, C. & SCHMETZER, H. M. 2022. Generation of Leukaemia-Derived Dendritic Cells (DCleu) to Improve Anti-Leukaemic Activity in AML:

Selection of the Most Efficient Response Modifier Combinations. *International Journal of Molecular Sciences,* 23**,** 8333.

SHIMIZU, K., IYODA, T., YAMASAKI, S., KADOWAKI, N., TOJO, A. & FUJII, S.-I. 2020. NK and NKT cell-mediated immune surveillance against hematological malignancies. *Cancers,* 12**,** 817.

SMYTH, M. J. & TRAPANI, J. A. 1995. Granzymes: exogenous porteinases that induce target cell apoptosis. *Immunology Today,* 16**,** 202-206.

TKACH, M., KOWAL, J., ZUCCHETTI, A. E., ENSERINK, L., JOUVE, M., LANKAR, D., SAITAKIS, M., MARTIN-JAULAR, L. & THÉRY, C. 2017. Qualitative differences in T-cell activation by dendritic cell-derived extracellular vesicle subtypes. *The EMBO Journal,* 36**,** 3012-3028.

UNTERFRAUNER, M., ASLAN, H., HARTZ, A., BOHLSCHEID, S., RACKL, E., BAUDREXLER, T., FENG, X., LI, L., VELAZQUEZ, G. F. & RANK, A. IMPACT OF (LEUKAEMIA-DERIVED) DENDRITIC CELLS GENERATED FROM AML-PATIENTS'WHOLE BLOOD-VERSUS WHOLE BONE MARROW CELLS ON THE MEDIATION OF ANTILEUKAEMIC PROCESSES AFTER MIXED LYMPHOCYTE CULTURE. BONE MARROW TRANSPLANTATION, 2023. SPRINGERNATURE CAMPUS, 4 CRINAN ST, LONDON, N1 9XW, ENGLAND, 500-500.

VOGT, V., SCHICK, J., ANSPRENGER, C., BRAEU, M., KROELL, T., KRAEMER, D., KÖHNE, C.-H., HAUSMANN, A., BUHMANN, R., TISCHER, J. & SCHMETZER, H. 2014. Profiles of Activation, Differentiation–Markers, or β-Integrins on T Cells Contribute to Predict T Cells' Antileukemic Responses After Stimulation With Leukemia-derived Dendritic Cells. *Journal of Immunotherapy,* 37**,** 331-347.

WONGKAJORNSILP, A., HTWE, K. S. S., SAWATPIBOON, N., DUANGSA-ARD, S. & KASETSINSOMBAT, K. 2019. The induction of iNKT cells and CIK cells toward anti-tumor phenotypes. *Cancer Research,* 79**,** 4141-4141.

Anhang: Publication III *Appendix*

Annals of Case Reports
Baudrexler T., et al. Ann Case Rep: 9: 101836
www.doi.org/10.29011/2574-7754.101836
www.gavinpublishers.com

OPEN ACCESS

Research Article

GAVIN PUBLISHERS

Volatile Profiling using an eNose - Exploiting Breath Volatile Organic Compounds for Disease Monitoring in Refractory Acute Myeloid Leukemia Patients

Baudrexler Tobias[1,5*], Boeselt Tobias[2,5], Atzler Michael[1,5], Hartz Anne[1,5], Boas Ursel[2], Schmid Christoph[3,5], Rank Andreas[3,5], Schmohl Jörg[4], Koczulla Rembert[2], Schmetzer Helga Maria[1,5]

[1]Medical Department III, University Hospital Großhadern, Ludwig-Maximilians-University, 81377 Munich, Germany

[2]Department of Pulmonary Rehabilitation, Phillipps-University of Marburg, German Center for Lung Research (DZL), 35043 Marburg, Germany

[3]Department of Hematology and Oncology, University Hospital of Augsburg, 86156 Augsburg, Germany [4]Department of Hematology and Oncology, Diakonia Hospital Stuttgart, 70176 Stuttgart, Germany.

[5]Bavarian Cancer Research Center (BZKF), Germany.

[*]**Corresponding author:** Baudrexler Tobias and Helga Maria Schmetzer, Medical Department III, University Hospital Großhadern, Ludwig-Maximilians-University, 81377 Munich, Germany.

Citation: Baudrexler T. et al. (2024) Volatile Profiling using an eNose - Exploiting Breath Volatile Organic Compounds for Disease Monitoring in Refractory Acute Myeloid Leukemia Patients. Ann Case Report 9: 1836. DOI: 10.29011/2574-7754.101836

Received: 03 June 2024; **Accepted:** 07 June 2024; **Published:** 10 June 2024

Abstract

Introduction: The demand for systemic tools to monitor disease-related biomarkers is ever more pressing. Volatile organic compound (VOC) analysis, capable of detecting individual molecules in human metabolism offers a non-invasive and easily collectible avenue for measurement via electronic nose (eNose) and might qualify as a systemic tool for disease monitoring. We analyzed VOC results from breath samples of AML patients (throughout the course of their disease, with/without treatment) with breath samples from healthy individuals. **Methods**: Clinical and immunological monitoring encompassed the observation of three refractory AML patients undergoing different therapies. Patient P1511 received chemotherapy, while patients P1482 and P1601 were treated with Kit M (GM-CSF and PGE_1).

Myeloid leukemic blasts can be transformed into dendritic cells of leukemic origin (DC_{leu}) ex vivo and in vivo, with the potential to stimulate and activate the immune system specifically against leukemia. These patients underwent repeated clinical and hematological/immunological assessments. Blood samples were periodically collected to monitor (leukemia-specific) immune cells using flow cytometry, cytokine secretion assay (CSA), and intracellular cytokine assay (InCyt). VOC monitoring involved the collection of VOCs in earloop masks containing exhaled air from AML patients and healthy volunteers measured using an

Citation: Baudrexler T. et al. (2024) Volatile Profiling using an eNose - Exploiting Breath Volatile Organic Compounds for Disease Monitoring in Refractory Acute Myeloid Leukemia Patients. Ann Case Report 9: 1836. DOI: 10.29011/2574-7754.101836

eNose. All samples were measured in triplicate, and the mean values were used for principal component analysis. Subsequently, linear discriminant analyses (LD) were performed. **Results**: The findings underscore Kit M as a safe clinical drug that fosters the generation of DC/DC_{leu} and augments the frequencies of leukemia-specific/antileukemic cells within the adaptive and innate immune systems, both ex vivo and in vivo, in AML patients. VOC profiles exhibited significant differences between healthy and AML breath donors, as well as between profiles during chemotherapy and Kit M therapy. Moreover, the eNose can detect differences in VOC profiles between breath samples taken with and without chemo-/immunotherapy. **Conclusion**: We posit that breath profiling with an eNose, capturing disease-related VOCs, could serve as a diagnostic or monitoring tool for leukemia patients. This approach entails the collection of VOCs using breath masks, eliminating the need for direct VOC measurement via an eNose during the course of the disease.

Keywords: Leukemia Derived DC; Acute Myeloid Leukemia; Anti-Leukemia Functionality; Leukemia-Specific Cells; VOCs of Exhaled Breath; Immune Monitoring in the Course of The Disease

Introduction

Acute Myeloid Leukemia (AML)

Up to now prognosis of AML patients is unfavorable due to high relapse rates of about 70-80% after induction therapy. For therapy intolerable or refractory patients' prognosis is even worse [1, 2]. High-dose induction chemotherapy with cytarabine ± anthracycline followed by allogeneic hematopoietic stem cell transplantation (HSCT) is the only potential curative treatment and is the standard therapy, especially for young AML patients with fewer comorbidities [3]. For patients with less tolerance for the induction therapy low-dose cytarabine or hypomethylating agents are potential therapy strategies [4, 5]. New immune therapeutic strategies address the dysfunctional reactivity of the immune system against leukemic blasts [6, 7].

DC-Based Immunotherapy

DC cells play a central role in connecting the innate and the adaptive immune system [8, 9]. DCs can be generated directly from leukemic blasts, rendering the complicated antigen loading process on (monocyte derived) DCs unnecessary [10]. Those DC_{leu} are characterized by the expression of individual patients' whole leukemic antigen repertoire including known as well as unknown leukemic antigens [11, 12]. These DCs have to be re-administrated to patients as a 'vaccine'. Alternatively, DC_{leu} could be induced in patients in vivo after application of 'DC_{leu}- inducing kits' (combinations of Granulocyte–Macrophage-Colony Stimulating Factor (GM-CSF) and a second response modifier (e.g., Picibanil, Prostaglandin E1 or E2), which triggers DC/DC_{leu} differentiation and maturation) [11, 13, 14].

Due to their immunomodulatory properties (in combination with GM-CSF) PGE1 and PGE2 have been shown to be highly efficient ex vivo DC-generating factors by providing a danger signaling, enhancing DCs' maturation and migratory capacity [13-16].

The Immune System

The immune system comprises both the innate and adaptive branches. The innate immune system is composed of antigen-presenting cells (APCs) like monocytes and dendritic cells (DCs), as well as specialized cell types like cytokine-induced killer (CIK) cells, invariant natural killer T (iNKT) cells, and natural killer (NK) cells. These components play a crucial role in the initial defence against pathogens and tumour cells [14, 17-19]. The adaptive immune system involves B cells (CD19+) and T cells (CD3+) and their various subtypes. After activation they provide (cytotoxic) effector as well as cytotoxic cells of different lines. Additionally, they develop memory cells enabling a quicker reactivation of the immune system upon encountering recurring antigens [13, 18, 20]. Abbreviations are summarized in Table 1, supplement.

Citation: Baudrexler T. et al. (2024) Volatile Profiling using an eNose - Exploiting Breath Volatile Organic Compounds for Disease Monitoring in Refractory Acute Myeloid Leukemia Patients. Ann Case Report 9: 1836. DOI: 10.29011/2574-7754.101836

		Name of Subgroups	Abbreviation of Subgroups	Surface Marker	Referred to	Abbreviation	Reference
Adaptive immune system	Blast cells	Blasts	Bla	Bla e.g. CD34+, CD117+	WB	Bla/WB	[51]
		Proliferating blasts	Bla_{prol71}	Bla+DC-CD71+	Bla	Bla_{prol71}/Bla	[52]
		Proliferating blasts	$Bla_{prolIPO38}$	Bla+DC-IPO38+	Bla	$Bla_{prolIPO38}$/Bla	[6]
	Dendritic cells	Dendritic cells	DC	DC+ e.g. CD80+, CD206+	WB	DC/WB	[51]
		Leukaemia derived DC	DC_{leu}	DC+Bla+	WB	DC_{leu}/WB	[51]
		Mature migratory DC	DC_{mat}	DC+CD197+	WB	DC_{mat}/WB	[53]
		Mature migratory DC_{leu}	$DC_{leu-mat}$	DC+Bla+CD197+	WB	$DC_{leu-mat}$/WB	[53]
	B lymphocytes	CD19+ B $cells_{memory}$	$Bcell_{meomory}$	CD19+CD27+IgD-	CD19+	$Bcell_{memory}$/ CD19+	[54]
	T lymphocytes	CD3+ pan T cells	CD3+	CD3+	lymphocytes	CD3+/cells	[13]
		CD4+ T cells	T_{CD4+}	CD3+CD4+	CD3+	TCD4+/CD3+	[13]
		CD4- T cells	T_{CD4-}	CD3+CD4-	CD3+	TCD4-/CD3+	[13]
		T helper cells 1	TH_1+	CCR4-CXCR3+CCR5+CCR6-	CD4+	TH1+/CD4+	[55]
		Naive T cells	T_{naive}	CD3+CD45RO-	CD3+	Tnaive/CD3+	[17]
		Non-naive T cells	$T_{non-naive}$	CD3+CD45RO+	CD3+	$T_{non-naive}$/CD3+	[17]
			$T_{non-naïve\ CD4+}$	CD3+CD45RO+CD4+	T_{CD4+}	$T_{non-naive\ CD4+}$/ T_{CD4+}	
			$T_{non-naïve\ CD4-}$	CD3+CD45RO+CD4-	T_{CD4-}	$T_{non-naive\ CD4-}$/ T_{CD4-}	
		Central (memory) T cells	T_{cm}	CD3+CD45RO+CD197+	CD3+	T_{cm}/CD3+	[17]
			T_{cmCD4+}	CD3+CD45RO+CD197+CD4+	T_{CD4+}	$T_{cm\ CD4+}/T_{CD4+}$	
			T_{cmCD4-}	CD3+CD45RO+CD197+CD4-	T_{CD4-}	$T_{cm\ CD4-}/T_{CD4-}$	
		Effector (memory) T cells	T_{em}	CD3+CD45RO+CD197-	CD3+	T_{em}/CD3+	[17]
			$T_{em\ CD4+}$	CD3+CD45RO+CD197-CD4+	TCD4+	$T_{em\ CD4+}/T_{CD4+}$	
			$T_{em\ CD4-}$	CD3+CD45RO+CD197+CD4-	TCD4-	$T_{em\ CD4}$-/T_{CD4-}	
		Proliferating T cells - early	$T_{prolCD69+}$	CD3+CD69+	CD3+	$T_{prolCD69+}$/CD3+	[17]
			$T_{prolCD4-CD69+}$	CD3+CD4-CD69+	TCD4-	$T_{prolCD4-CD69+}$/ T_{CD4-}	
		Proliferating T cells - late	$T_{prolCD71+}$	CD3+CD71+	CD3+	$T_{prolCD71+}$/CD3+	[17]

Citation: Baudrexler T. et al. (2024) Volatile Profiling using an eNose - Exploiting Breath Volatile Organic Compounds for Disease Monitoring in Refractory Acute Myeloid Leukemia Patients. Ann Case Report 9: 1836. DOI: 10.29011/2574-7754.101836

Innate immune system	Cytokine induced killer cells	CD3+CD56+ CIK cells	CIKcell	CD3+CD56+	lymphocytes	CIKcell/cells	[13]
	Natural killer cells	CD3-CD56+ NK cells	NKcell	CD3-CD56+	lymphocytes	NKcell/cells	[13]
	Invariant natural killer T cells	6B11+ iNKT cells	iNKTcell	6B11+	lymphocytes	iNKTcell/cells	[22]
Leukemia specific cells	T lymphocytes *	CD4+ coexpressing T $cells_{leu}$	$T_{CD4+leu}$	CD3+CD4+INFy+	$T_{CD4+leu}$	$T_{CD4+leu}/T_{CD4+}$	[17]
Adaptive immune system		CD8+ coexpressing T $cells_{leu}$	$T_{CD4-leu}$	CD3+CD4-INFy+	$T_{CD4-leu}$	$T_{CD4-leu}/T_{CD4-}$	[17]
Innate immune system	Cytokine induced killer cells **	CD3+CD56+ CIK $cells_{leu}$	$CIKcell_{leu}$	CD3+CD56+INFy+	CIKcell	$CIKcell_{leu}$/ CIKcell	[17]
	Natural killer cells **	CD3-CD56+ NK $cells_{leu}$	$NKcell_{leu}$	CD3-CD56+INFy+	NKcell	$NKcell_{leu}$/ NKcell	[17]

Table S1: Cell subsets and their abbreviations.

Leukemia-Specific Cells and Anti-Leukemic Processes

The cytokine secretion assay (CSA) and the intracellular cytokine assay (InCyt) enable the intracellular quantification of cytokines (e.g., interferon-gamma (IFN-γ)) on a single-cell level. These cytokines are key factors in immune responses and mediators of cell apoptosis [17, 18, 21] and provide a comprehensive analysis of cell functionality, particularly in terms of the activity and cytotoxicity of immune cells specific to leukemia [17].

Methodological Tools for Monitoring AML and Anti-Leukemic Processes

Understanding both leukemia-related and anti-leukemic processes requires the analysis of various cellular and humoral factors, whether activating or inhibitory, as well as soluble factors and even small molecules [13, 18, 21-25]. In recent years, the role of physical factors, such as physiological hypoxia [26] and circulating vesicles (e.g., extracellular vesicles (EVs)) [27, 28], has been investigated for their potential in refined monitoring immunological or tumor-associated processes.

VOC Analysis as a Novel Approach for Characterizing and Monitoring (Malignant) Diseases

Every living organism, whether human, plant, or animal, emits organic compounds into the environment. Exhaled molecules reflect metabolic changes in both healthy and pathological conditions, making exhaled air a potential tool for monitoring disease-related biomarkers [29]. Volatile organic compounds (VOCs) are organic chemicals containing hydrocarbon compounds. Exhaled VOCs can be easily collected noninvasively, either by directly capturing exhaled breath using an electronic nose (eNose) or by analyzing VOCs collected on carriers such as fleece or earloop masks. Subsequent analysis is conducted using an eNose. Proof of concept has demonstrated that VOC analysis can aid in the detection of disease-associated markers, such as AML (characterized by cell-molecular anomalies and metabolic changes resulting in different endogenous VOCs), Parkinson's disease, Alzheimer's disease, COVID-19 infection and lung cancer [30-35].

Objectives of this study

The aims of the studies presented here were to explore VOC profiles during in vivo treatment of refractory AML patients with DC_{leu}-inducing Kits compared to chemotherapy and compared to healthy breath donors' VOC profiles using an eNose. In addition, clinical parameters of refractory AML patients during the course of the disease under chemotherapy and/or Kit M treatment as well as (leukemia specific) immune cell compositions were collected.

Finally, a VOC-based breath profiling strategy was discussed for its further use to augment hematological and immunological profiling strategies.

Material, Methods and Patients

Sample Collection

The blood and breath sample collection for this study was carried out in collaboration with the University Hospitals of Augsburg (P1511, P1482) and the Diakonieklinikum in Stuttgart (P1601).

Citation: Baudrexler T. et al. (2024) Volatile Profiling using an eNose - Exploiting Breath Volatile Organic Compounds for Disease Monitoring in Refractory Acute Myeloid Leukemia Patients. Ann Case Report 9: 1836. DOI: 10.29011/2574-7754.101836

In accordance with ethical guidelines and the Declaration of Helsinki, patients provided written consent for the experimental use of their blood/breath donations. Whole blood (WB) samples were obtained from patients in refractory phases of Acute Myeloid Leukemia (AML). Ethical approval for this research was obtained from the local Ethics Committee of LMU in Munich (Pettenkoferstr. 8a, 80336 Munich, Ludwig-Maximilian-University Hospital in Munich; Protocol Number 339-05).

Characterization of Healthy Volunteers and Patients

Patient 1511, a 79-year-old Caucasian male diagnosed with AML in December 2015 at the age of 76, demonstrated refractoriness to several lines of therapy. Following his initial AML diagnosis, he underwent 22 cycles of decitabine treatment, subsequently followed by cytarabine and midostaurin therapies. In September 2018, a relapse of the disease was observed, characterized by more than 50% blasts in peripheral blood (PB). This patient was subjected to chemotherapy treatment (without the use of Kit M) and served as a control in this study. Over the entire course of the chemotherapy phase, the patient underwent comprehensive clinical, hematological, and immunological monitoring. Furthermore, periodic blood samples were collected to monitor the population of leukemia-specific immune cells using flow cytometry and cytokine secretion assays (CSA). Clinical and hematological data are given in Figure 1.

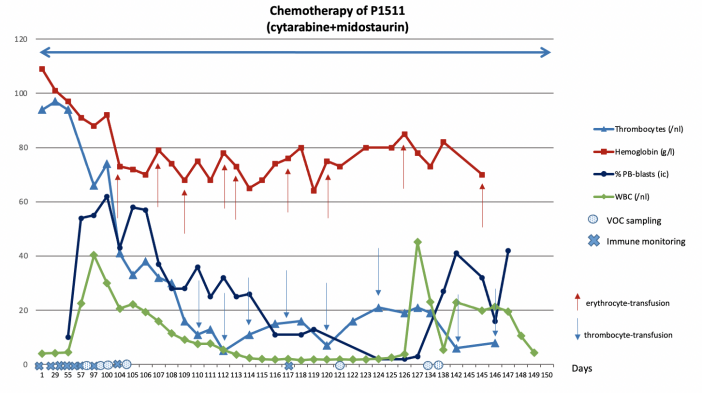

Figure 1: Clinical course of P1511 during chemotherapy treatment (without Kit M). Chemotherapy (cytarabine, midostaurin) was given from the start until the end of observation. Blood cells (thrombocytes, hemoglobin, blasts) in peripheral blood (PB) and leukocytes/white blood cells (WBC) are given. ↑ Timepoints of erythrocyte-transfusion, ↓ timepoints of thrombocyte-transfusion.

Kit M treated patients: P1482 and P1601 presented with pancytopenia and were deemed clinically unfit for further intensive therapy. In the absence of established treatment options, we offered them an individualized salvage treatment involving the systemic administration of blast modulatory drugs. These patients received daily intravenous doses of GM-CSF (Granulocyte-Macrophage Colony-Stimulating Factor) and PGE1 (Prostaglandin E1), referred to as Kit M. The decision to pursue this treatment was made based on recommendations from medical specialists. Before start of treatment both patients had been elaboratorately informed by experienced hematologists on several occasions about the experimental nature as well as possible side effects of the treatment and had given written informed consent into the treatment as well as examinations on blood samples drawn in addition to routine monitoring. Treatment plans were adapted to individual conditions (Table 2, supplement).

Citation: Baudrexler T. et al. (2024) Volatile Profiling using an eNose - Exploiting Breath Volatile Organic Compounds for Disease Monitoring in Refractory Acute Myeloid Leukemia Patients. Ann Case Report 9: 1836. DOI: 10.29011/2574-7754.101836

Day	Drug	Dosage (iv)	Schedule
11	GM-CSF	50 mg/m²/4 hours	8-12 am
	PGE_1	20 mg (in total)	1-3 pm
12	PGE_1	20 mg (in total)	8-10 am
	GM-CSF	50 mg/m²/4 hours	11 am-3 pm
	PGE_1	20 mg (in total)	8-10 pm
13	PGE_1	20 mg (in total)	8-10 am
	GM-CSF	50 mg/m²/4 hours	11 am-3 pm
	PGE_1	20 mg (in total)	8-10 pm
14	PGE_1	20 mg (in total)	8-10 am
	GM-CSF	75 mg/m²/4 hours	11 am-3 pm
	PGE_1	40 mg (in total)	8-10 pm
15	PGE_1	40 mg (in total)	8-10 am
	GM-CSF	75 mg/m²/4 hours	11 am-3 pm
	PGE_1	40 mg (in total)	8-10 pm
16-38		Percede as day 15	

a) P1482

Day	Drugs	Dosage (iv)	Schedule
9	GM-CSF	50 mg/m²/4 hours	8-12 am
		(77.5 mg in total)	
	PGE_1	20 mg (in total)	1-3 pm
10	PGE_1	20 mg (in total)	8-10 am
	GM-CSF	50 mg/m²/4 hours	11 am- 3 pm
		(77.5 ug in total)	
	PGE_1	20 mg (in total)	6-8 pm
11	PGE_1	20 mg (in total)	8-10 am
	GM-CSF	50 ug/m²/4 hours	11 am- 3 pm
		(77.5 mg in total)	
	PGE_1	20 mg (in total)	6-8 pm
12	PGE_1	20 mg (in total)	8-10 am
	GM-CSF	75 mg/m²/4 hours	11 am- 3 pm
		(116 mg in total)	
	PGE_1	40 mg (in total)	6-8 pm
13	PGE_1	40mg (in total)	8-10 am
	GM-CSF	75 mg/m²/4 hours	11 am- 3pm
	PGE_1	40 mg (in total)	6-8 pm
14	PGE_1	40 mg (in total)	8-10 am
	GM-CSF	75 mg/m2/4 hours	10 am- 12 pm
	PGE_1	40 mg (in total)	12- 1 pm
15-26		Percede as day 14	

b) P1601

Table S2: Treatment regime for P1482 and P1601 using Kit M (leukine (GM-CSF) and Prostavasin (PGE1). Courses of the disease are given in Figures 2 and 3.

Patient 1482 a 72-year-old Caucasian male, was initially diagnosed with AML in April 2015. After achieving complete remission through induction chemotherapy, a relapse occurred in May 2017. Clinical assessments, including morphological and cytological evaluations, revealed leukocytosis with 90% peripheral blood (PB) blasts and 70% bone marrow (BM) blasts. To address this relapse, the patient underwent treatment with two cycles of decitabine at a dosage of 20 mg/m2 for 11 days, followed by hydroxyurea and cytarabine (100 mg/m²). Although this treatment led to a reduction in blast counts, complete remission was not achieved. Subsequently, the patient received GM-CSF at an initial dose of 50 µg/m², administered intravenously over 4 hours for three days, starting on day 11 of treatment. The GM-CSF dosage was gradually increased to 75 µg/m² from day 14 to day 38. Additionally, the patient received intravenous doses of PGE1 (Alprostadil, Prostavasin®) ranging from 20 to 80 µg daily. PGE1 was administered over a duration of 2 hours, once or twice daily (Table 2, supplement).

The patient underwent comprehensive clinical, haematological, and immunological monitoring throughout the entire treatment phase. Additionally, blood samples were collected at various intervals during the observation period to assess the population of immune cells specific to leukemia, employing techniques such as flow cytometry and cytokine secretion assays (CSA).

Citation: Baudrexler T. et al. (2024) Volatile Profiling using an eNose - Exploiting Breath Volatile Organic Compounds for Disease Monitoring in Refractory Acute Myeloid Leukemia Patients. Ann Case Report 9: 1836. DOI: 10.29011/2574-7754.101836

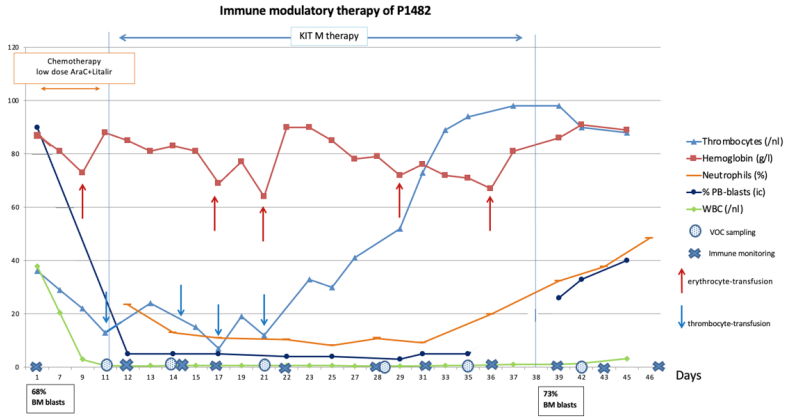

Figure 2: Clinical course of P1482 during chemotherapy or Kit M treatment. Chemotherapy (hydroxycarbamide, cytarabine) was given from the start of observation till day 11. Kit M treatment between day 11 and 38, no treatment from day 38 till the end of observation. Blood cells (thrombocytes, hemoglobin, neutrophils, blasts) in peripheral blood (PB), frequencies of BM blasts and leukocytes/white blood cells (WBC) are given. ↑ Timepoints of erythrocyte-transfusion, ↓ timepoints of thrombocyte-transfusion.

Patient 1601: Patient 1601, a 74-year-old Caucasian female, received an AML diagnosis in January 2020. She underwent treatment with azacytidine (75 mg/m^2 day 1-7) for four cycles and, additionally, Venetoclax (initial dose 400 mg/day) for one cycle. Due to developing pancytopenia, treatment with both medications was discontinued after five cycles. The patient demonstrated refractoriness to this therapy, evidenced by 90% blasts in peripheral blood (PB) and a concurrent bout of pneumonia, aggravated by a history of heavy smoking.

P1601 received GM-CSF at an initial dose of 50 µg/m^2, administered intravenously over 4 hours for three days, commencing on day 9 and concluding on day 11. This GM-CSF dosage was escalated to 75 µg/m² from day 12 to day 26. Additionally, the patient received intravenous infusions of PGE1 (Alprostadil, Prostavasin®) ranging from 20 to 80 µg daily, administered over 2 hours, either once or twice daily (refer to Table 2 for details). Between day 19 and day 26, the patient underwent additional chemotherapy, receiving 500 mg of hydroxycarbamide twice a day. Following the cessation of Kit M treatment, hydroxycarbamide was continued until day 29.

Throughout the entire treatment phase, the patient underwent comprehensive clinical, haematological, and immunological monitoring. Periodic blood samples were collected during the observation period to assess leukemia-specific immune cells, employing techniques such as flow cytometry and intracellular cytokine assays (InCyt).

Citation: Baudrexler T. et al. (2024) Volatile Profiling using an eNose - Exploiting Breath Volatile Organic Compounds for Disease Monitoring in Refractory Acute Myeloid Leukemia Patients. Ann Case Report 9: 1836. DOI: 10.29011/2574-7754.101836

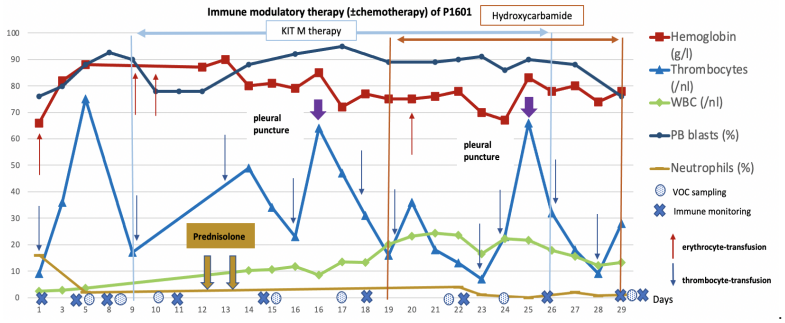

Figure 3: Clinical course of P1601 during Kit M treatment ± chemotherapy. No treatment was given between day 1 and 9, Kit M treatment from day 9-26, chemotherapeutical treatment (hydroxycarbamide) from day 19-29. Patients' pneumonia was additionally daily treated by prednisolone on day 12-14. Blood cells (thrombocytes, hemoglobin, neutrophils, blasts) in peripheral blood (PB) and leukocytes/white blood cells (WBC) are given. ↑ Timepoints of erythrocyte-transfusion, ↓ timepoints of thrombocyte-transfusion, pleural punctions.

Status	Stage	Patient	Age at first diagn	Sex	ELN-risk-stratification at first diagnosis	Clinical treatment	Blast phenotype (CD)	Blasts in PB/BM (%)*	Conducted cell biological experiments	Sourses for VOC-measurements in the course of disease
AML	Persisting Relapse	P1511	76	m	Intermediate	chemotherapy (cytarabine+ midostaurin)	34,117, 13,33	54/40	DC, MLC, CTX, CSA	7x masks
AML	Persisting Relapse	P1482	72	m	Unfavourable	chemotherapy (hydroxycarbamid+ cytarabine) and immune therapy (Kit M)	117,34,15, 13, 33,64	90/68	DC, MLC, CTX, CSA	6x masks
AML	Persisting Relapse	P1601	74	f	Unfavourable	chemotherapy (hydroxycarbamide) and immune therapy (Kit M)	34,117, 33,13	76/43	DC, MLC, CTX, InCyt	8x masks
Healthy Stuttgart		HS1	35	f						1x mask
		HS2	31	f						1x mask
		HS3	53	f						1x mask
		HS4	39	m						1x mask
		HS5	35	m						1x mask

Citation: Baudrexler T. et al. (2024) Volatile Profiling using an eNose - Exploiting Breath Volatile Organic Compounds for Disease Monitoring in Refractory Acute Myeloid Leukemia Patients. Ann Case Report 9: 1836. DOI: 10.29011/2574-7754.101836

Augsburg		HA1	46	m						1x mask
		HA2	33	f						1x mask
		HA3	39	f						1x mask
		HA4	20	m						1x mask
		HA5	32	m						1x mask
		HA6	28	f						1x mask
		HA7	40	f						1x mask
		HA8	23	m						1x mask
		HA9	37	f						1x mask
		HA10	21	f						1x mask
		ELN risk stratification risk evaluation based on assessments of EuropeanLeukemiaNet; PB peripheral blood; BM bone marrow; m male; f female; bold: blast markers used for DCleu evaluation; DC dendritic cell culture; MLC mixed lymphocyte culture; CTX cytotoxicity assay; CSA cytokine secretion assay; InCyt intracellular cytokine assay; Details of clinical treatments and hematological values are given in Figure 1,2 and 3; last value before start of chemotherapy (P1511) or Kit M treatment (P1482, P1601).								

Table 3: Characteristics of acute myeloid leukemia (AML) patients and healthy controls.

Cell Characterization by Flow Cytometry

To assess and quantify the phenotypes of DC/DC_{leu}, leukemic blasts, monocytes, and various subsets of immune-reactive cells within the adaptive and innate immune systems (as given in table 1, supplement), flow cytometry analyses were conducted using the FACSCalibur™ fluorescence-activated cell sorting flow cytometer. Employing a refined gating technique and CellQuestPro analysis software (Becton Dickinson, Heidelberg, Germany), the functionalities of cells, including proliferation, cytokine production, and cytotoxicity, were investigated [17, 18].

Preparation of Cells

AML whole blood (WB) samples were either used directly for experiments or subjected to mononuclear cell (MNC) isolation and frozen for future use (all blood sample processing was routinely performed under a hood). MNCs were isolated from WB following standard procedures [17] and used for the isolation of T cells via MACS-microbeads as shown before [36].

Dendritic Cell Culture (DC Culture)

DC/DC_{leu} were cultured following established protocols using 'Kit M' (800 U/ml granulocyte macrophage colony-stimulating factor (GM-CSF, Sanofi-Aventis, Frankfurt, Germany) and 1 µg/ml prostaglandin E1 (PGE1, Santa Cruz Biotechnology, Dallas, Texas, USA)) vs control without added Kit M, as shown before and analyzed by flow cytometry [7,11,22 ,17].

Mixed Lymphocyte Culture (MLC)

After 7-8 days DC cultures containing approximately $2.5x10^5$ DCs and MLC were started adding patients' previously frozen Tcells ($1x10^6$) and 5 µl of 50 U/ml interleukin 2 in RPMI medium as shown before [17]. After culture, measurements were conducted with Kit M ($MLC^{WB\text{-}DC(Kit\text{-}M)}$) and Control ($MLC^{WB\text{-}DC(Control)}$), and cells were utilized for the CSA, the InCyt, and the CTX assays [13]. Flow cytometry was employed to quantify different immune cell subtypes after MLC. For a reference to abbreviations, please refer to Table 1, supplement.

Cytokine Secretion Assay (CSA) and Intracellular Assay (InCyt) to detect antigen specific

CSA and InCyt assays were used to quantify intracellularly producing or secreting IFNγ, with or without simultaneously stimulated with two leukemia-associated antigens (LAA): 2 µg/ml Wilms tumour 1 protein (WT-1) and an additional 2 µg/ml PRAME ("preferentially expressed antigen in melanoma," as previously described [17]. CSA and InCyt were carried out to quantify potentially leukemia specific cells after MLC ex vivo or in patients' PB the course of the disease. Subtypes are given in table 1, supplement [17].

Cytotoxicity Fluorolysis Assay (CTX)

To assess the ability of effector cells (T cell-enriched cells, stimulated with or without Kit M-treated whole blood after MLC) to lyse target cells (thawed viable patients' mononuclear cells [MNCs] stained with two different blast markers), the cytotoxicity fluorolysis assay was conducted, as previously described [17]. For each test, equal amounts of effector cells and target cells were combined within a medium. The lytic activity of effector cells was calculated as the percentage of viable target cells in the culture with co-cultured effector and target cells (for 3 hours and 24 hours) compared to the control [13]. A flowchart summarizing the cell biological experiments is provided in Baudrexler et al. [30] and is given in the supplement (Flow chart 1).

Citation: Baudrexler T. et al. (2024) Volatile Profiling using an eNose - Exploiting Breath Volatile Organic Compounds for Disease Monitoring in Refractory Acute Myeloid Leukemia Patients. Ann Case Report 9: 1836. DOI: 10.29011/2574-7754.101836

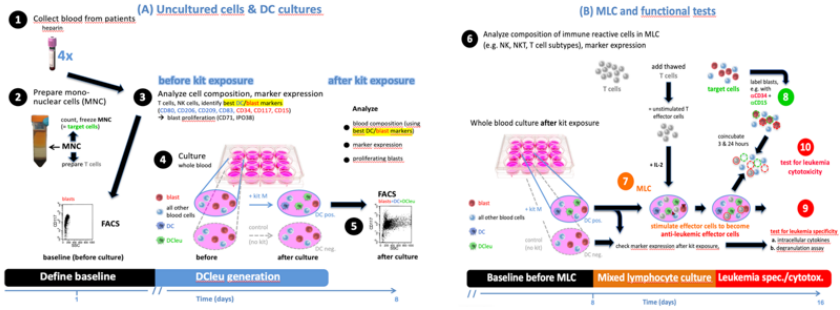

Flow Chart S1: 1. Heparinized blood samples from AML patients were used for cell biological experiments; 2. MNC (mononuclear cells) and T cells were gained from WB and later on used for MLC ('T cell enriched' mixed lymphocyte culture) and CTX; 3./4./5. DC cultures were set up with leukemic WB and measured by flowcytometry before and after culture with (vs. without) Kit M; 6./7./8. MLC culture were set up with harvested DC culture + T cells, stimulated with IL-2 and measured by flowcytometry before and after culture; 9./10. Several immune assays were performed after MLC: CSA + InCyt as well as CTX after mixture of MNCs and MLC.

Collection of AML Patients' and Healthy Donors' Breath Masks

To obtain samples for volatile organic compound (VOC) analysis, we collected earloop masks containing exhaled air from both AML patients and healthy individuals (Table 3). This breath sampling took place in rooms within the hospitals of Stuttgart and Augsburg to ensure consistent background air quality. We used fleece earloop masks (Henry Schein Medical GmbH, Hamburg, Germany) as a medium for transmission, which were stored in plastic cups. Participants were instructed not to brush their teeth or use any cosmetics, such as perfume or lipstick, within the two hours preceding sampling. During the sampling process, individuals wore unpowdered latex gloves (Meditrade) while breathing through the masks for a duration of five minutes. The collected masks were then placed in plastic cups with lids, stored in zipper bags, and kept in a dark environment at 10°C until they were ready for measurement. All breath samples collected were sent to the University Hospital Marburg, where VOC analyses were conducted [32].

Healthy Donors

We collected one earloop mask from each of the 15 healthy Caucasian volunteers (labelled as 'Healthy': n=15). Specifically, we collected 5 masks from healthy donors in Stuttgart ('Healthy Stuttgart': n=5) and 10 masks from healthy donors in Augsburg ('Healthy Augsburg': n=10). On average, the healthy donors from Stuttgart were 39 years old (with a range of 31-53), and those from Augsburg were 32 years old (with a range of 20-46). The female-to-male ratio was 1:0.6 in both hospitals. The masks from healthy individuals served as a control group. Characteristics of the healthy donors are summarized in Table 3.

AML-patients' samples

A total of 7 earloop masks were collected from P1511 during the course of treatment under chemotherapy (n=7). Specific sampling dates are provided in Figure 1.

We collected 6 earloop masks during the course of treatment from P1482 under both chemotherapy and Kit M therapy. This included 1 mask before Kit M therapy and 1 mask after Kit M therapy. Additionally, we collected 4 masks during Kit M treatment. Sampling dates are detailed in Figure 2.

In total, we collected 8 earloop masks during the course of disease management from P1601, including Kit M therapy, Kit M therapy with simultaneous chemotherapy, and phases without any treatment. Among these, 3 masks were sampled before and after Kit M/chemotherapy treatment (referred to as 'without therapy'). Furthermore, 3 masks were collected during Kit M therapy, and 2 masks during Kit M therapy with simultaneous chemotherapy. Sampling dates are provided in Figure 3.

Experimental Set-up of the eNose

Earloop masks containing breath samples were transported to Marburg for measurement and analysed in a sealed room using the Cyranose 320® electronic nose (eNose) [37, 38]. The Cyranose

Citation: Baudrexler T. et al. (2024) Volatile Profiling using an eNose - Exploiting Breath Volatile Organic Compounds for Disease Monitoring in Refractory Acute Myeloid Leukemia Patients. Ann Case Report 9: 1836. DOI: 10.29011/2574-7754.101836

320® is categorized as a polymer sensor-based eNose, featuring 32 thin-film carbon polymer chemiresistors (NoseChip). These sensors operate by detecting volatile organic components (VOCs) based on their structure, size, polarity, and proton affinity. Upon exposure to gases, the polymer layer swells as it absorbs analytes. Each sensor responds differently to various analytes, and no single sensor typically responds to only one analyte. The sensors generate a pattern of signals, referred to as smell-prints, composed of 32 individual signals for single substances or mixtures. The measurements are based on changes in resistance experienced by each sensor when exposed to VOCs. The eNose technology used in this study followed a standardized approach, ensuring that medical air did not affect the measured VOCs. This approach maintained a standard to prevent contamination by ambient air. Before initiating the study, the sensors were tested with defined olfactory substances to ensure their proper functioning. Only when all 32 sensors indicated correct reference ranges could the study proceed. The sensors were also calibrated once a month using a test battery of odours, including liquorice, menthol, and aromatics, among others. Each measurement consisted of three steps: establishing a reference value using medicinal air (Aer medicinalis), measuring the VOCs in the volatile surface of cell supernatants, and cleaning the eNose sensors with ambient air. All samples were measured in triplicate, and the mean values were used for principal component analysis. Subsequently, linear discriminant analyses (LD) were performed, and the LD results were employed for further analyses, especially contingency table analyses. The Mahalanobis distance between groups was determined as well [37, 38]. An overview of the VOC sampling, measurement, and analysis process is provided in Flow Chart 2.

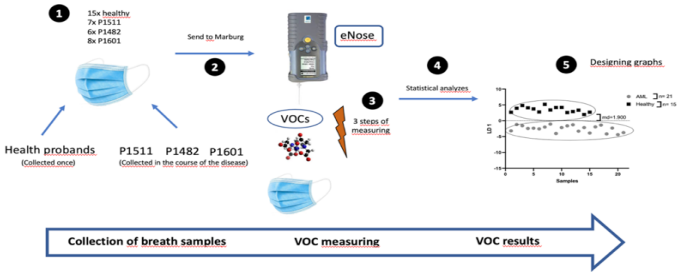

Flow chart 2: Overview about the VOC experiments

1. Collection of breath masks in the course of the disease of AML patients and healthy probands; 2. Transportation to Marburg; 3. Measurement of VOCs above breath masks by eNose; 4./5. Statistical analyzes of VOC data and presentation of VOC differentiations in graphs.

Statistical Methods

All cell biological measurements were performed using flow cytometry (FACSCalibur™, Becton Dickinson, Heidelberg, Germany) with BD CellQuestPro software. Statistical analyses were conducted using Microsoft Excel (version 16.52, Redmond, USA) and Prism 9 (GraphPad Software, version 9.1.1, San Diego, USA). Data are presented as mean ± standard deviation [11]. Statistical investigations of VOC data, calculated by linear discriminant analyses, were conducted using Prism 9 (GraphPad Software, version 9.1.1, San Diego, USA). Principal component analysis (PCA) and linear differential analysis (LDA) were conducted for data modeling and statistical analysis for the VOC results. PCA is an unsupervised multi-variable statistical analysis method for linear data compression, decreasing the data dimension, and feature extraction. This method is used for presenting the response of an olfactory machine to offer qualitative information about emitted organic compounds for pattern recognition [39]. LDA is a supervised classification approach, to find a linear combination of features that characterizes or separates two or more classes of objects [39]. Data from VOC analyses are presented as sensitivity, specificity, positive predictive value (PPV), and negative predictive value (NPV). Fisher's exact test was used for statistical comparisons in contingency table analyses. The Mahalanobis distance (md) between groups was used as a distance measure for multidimensional data. An MD value greater than 1.96 was considered significant, as it corresponds to a p-value of < 0.05. A MD value greater than 2.58 indicated a p-value of < 0.01 [40]. Significance was considered at p values ≤ 0.05, and borderline significance was

Citation: Baudrexler T. et al. (2024) Volatile Profiling using an eNose - Exploiting Breath Volatile Organic Compounds for Disease Monitoring in Refractory Acute Myeloid Leukemia Patients. Ann Case Report 9: 1836. DOI: 10.29011/2574-7754.101836

considered at p values between 0.05 and 0.10.

Results

Ex vivo generation of DC- and T cell subtypes with (vs. without) Kit M pretreated WB of AML patients' blood samples and increased antileukemic activity

Treating blasts containing leukemic WB with (vs. without) blast modulating Kit M we found higher frequencies of mature leukemia derived DC ($DC_{leu-mat}$) in $DC^{WB(Kit\ M)}$ compared to $DC^{WB(Control)}$ in all three patients without induction of blasts' proliferation (Figure S4A, supplement). Moreover, we stimulated T cell enriched immunoreactive cells with Kit M pretreated (DC/DC_{leu} containing) WB. Immune reactive cells before (uncultured MLC) and after MLC ($MLC^{WB\text{-}DC(Control)}$ or $MLC^{WB\text{-}DC(Kit\ M))}$ showed that T cells were activated and particularly induced to proliferate and to create memory cells in Kit M pretreated settings (Figure S4B, supplement). Abbreviations for cell populations are given in Table 1.

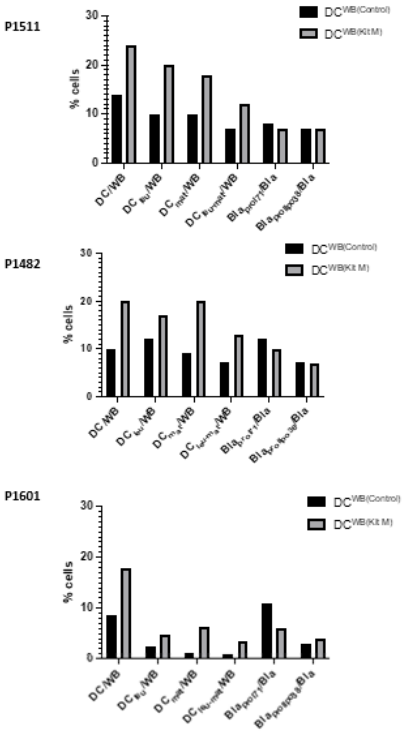

S4A: Increased frequencies of DC/DC_{leu} subtypes could be generated from (blast containing) AML patients' WB pretreated with Kit M (DCWB(Kit M)) compared to Control (DCWB(Control)) without induction of blasts' proliferation.

Citation: Baudrexler T. et al. (2024) Volatile Profiling using an eNose - Exploiting Breath Volatile Organic Compounds for Disease Monitoring in Refractory Acute Myeloid Leukemia Patients. Ann Case Report 9: 1836. DOI: 10.29011/2574-7754.101836

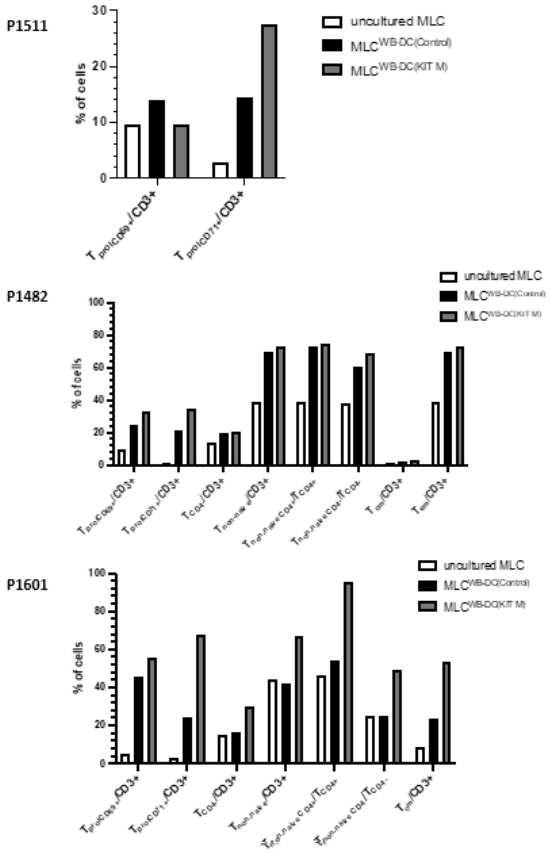

S4B: Stimulation of immunoreactive T cell subtypes could be achieved from patients' WB pretreated with Kit M ($MLC^{WB\text{-}DC(Kit\ M))}$ compared to Control ($MLC^{WB\text{-}DC(Control))}$ after MLC.

Citation: Baudrexler T. et al. (2024) Volatile Profiling using an eNose - Exploiting Breath Volatile Organic Compounds for Disease Monitoring in Refractory Acute Myeloid Leukemia Patients. Ann Case Report 9: 1836. DOI: 10.29011/2574-7754.101836

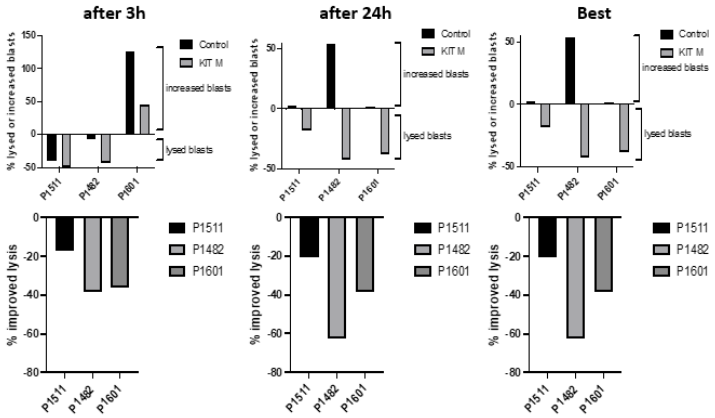

S4C: Stimulatory effect of Kit M treated (vs. untreated) WB on antileukemic reactivity after MLC.

Figure 4: Figure 4A shows the frequencies of generated DC/DC_{leu} (subtypes) after ex vivo treatment of WB with Kit M (DCWB(Kit M)) compared to Control (without Kit treatment, DCWB(Control)) for P1511, P1482 and P1601. Figure 4B shows the frequencies of T cell subsets after stimulation of T cell enriched immunoreactive cells with Kit M pretreated WB (MLCWB-DC(Kit M)) compared to not pretreated WB (MLCWB-DC(Control)) and uncultured cells (uncultured MLC). Figure 4C demonstrates the improved antileukemic blast lytic activity (using a non-radioactive fluorolysis assay) for Kit M pretreated (vs. untreated) patients' WB samples after T cell enriched MLC. Frequencies of lysed or increased blasts as detected after 3 or 24 hours of effector-target cells incubation (and the best achieved antileukemic reactions) are given in the upper part. Proportion of improved lysis is given in the lower part. Abbreviations are given in Table 1.

The cytotoxic impact of T cell enriched MLC (with and without pretreatment with Kit M) showed in all 3 cases an improved blast lysis (especially after 24 hours of target-effector cell incubation) after $MLC^{WB\text{-}DC(Kit\ M)}$ compared to $MLC^{WB\text{-}DC(Control)}$, as evaluated via CTX and (Figure S4C, supplement).

We show that Kit M gives rise to antileukemic immune cells ex vivo without induction of blasts' proliferation. We conclude that Kit M application to patients probably is safe and could give rise to antileukemic processes in vivo.

In Vivo Kit M Improved Clinical Courses Of AML Patients Compared To Control-Patient

P1511 (Patient without immunomodulatory treatment): The clinical course of P1511 was observed over a period of 4 months, while he was being treated with chemotherapy (without Kit M). During this time, the evaluated laboratory parameters (thrombocytes, hemoglobin, white blood cells) were continuously reduced, and 9 erythrocyte and 8 platelet transfusions were given. In addition, the patient was consistently suffering from high frequencies of PB blasts (in general: >3%; mostly >20%) (Figure 1).

Immune monitoring: During chemotherapy we found a decrease of DCs, of proliferating T cells and $T_{non\text{-}naive\ CD4-}/T_{CD4-}$. Other adaptive immune cell subtypes (like TH_{1+}/CD4+ as well as $T_{cm\ CD4}+/T_{CD4+}$, $T_{em\ CD4+}/T_{CD4+}$ and $Bcell_{memory}$/CD19+) decreased under chemotherapy. Regarding cells of the innate immune system, frequencies of NK cells decreased, whereas frequencies of CIK cells and iNKT cells, stable over 100 or 60 days, decreased in the further course of observation. Antigen specific cells were monitored after LAA stimulation by CSA: In general, decreasing frequencies of leukemia specific cells of the adaptive and innate lines were found (Figure 5A and 5B lower part, for details see supplement).

Citation: Baudrexler T. et al. (2024) Volatile Profiling using an eNose - Exploiting Breath Volatile Organic Compounds for Disease Monitoring in Refractory Acute Myeloid Leukemia Patients. Ann Case Report 9: 1836. DOI: 10.29011/2574-7754.101836

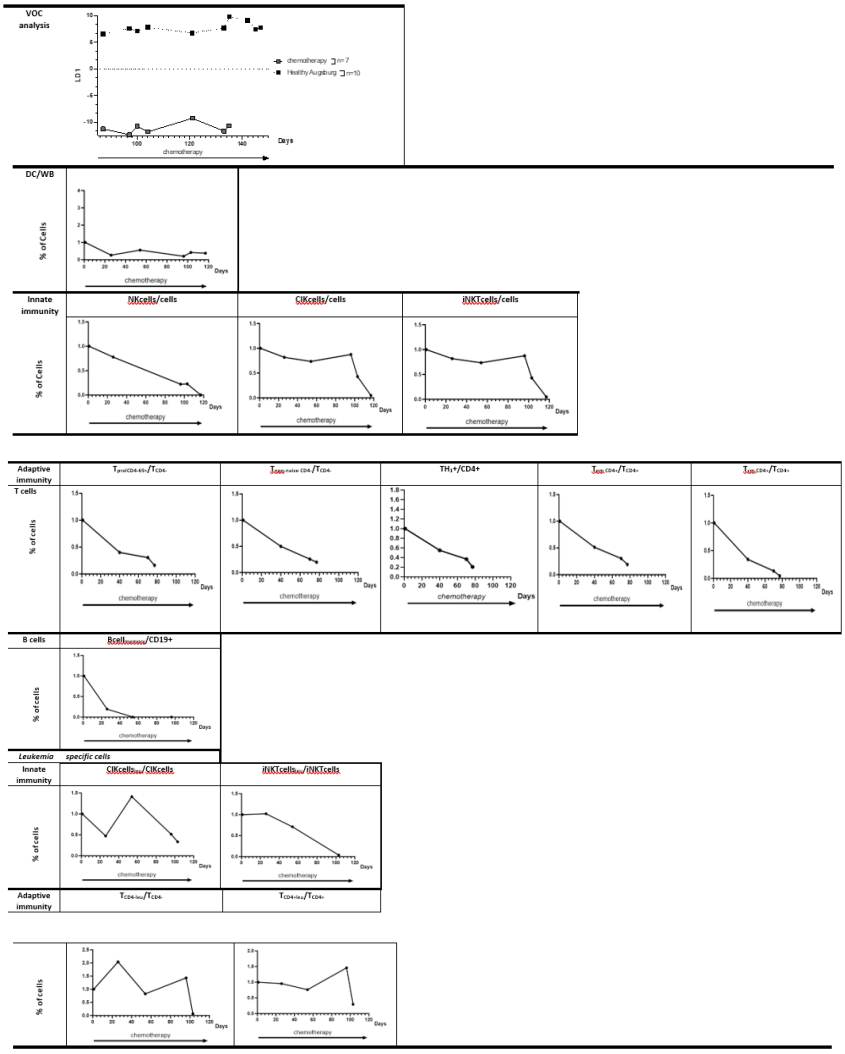

Citation: Baudrexler T. et al. (2024) Volatile Profiling using an eNose - Exploiting Breath Volatile Organic Compounds for Disease Monitoring in Refractory Acute Myeloid Leukemia Patients. Ann Case Report 9: 1836. DOI: 10.29011/2574-7754.101836

S5A: Profiles obtained from samples from P1511 under chemotherapy vs. healthy controls: healthy and P1511 VOC samples could be clearly differentiated. Decreased frequencies of (leukemia specific) immunoreactive cell subtypes could be detected in the course of disease.

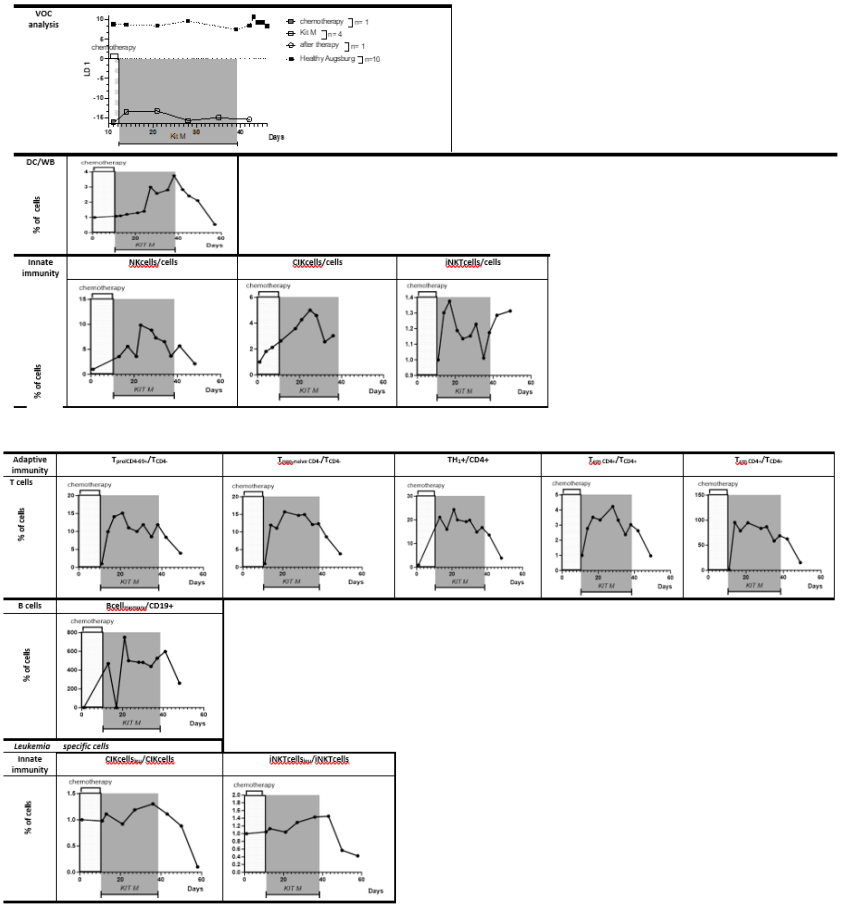

Citation: Baudrexler T. et al. (2024) Volatile Profiling using an eNose - Exploiting Breath Volatile Organic Compounds for Disease Monitoring in Refractory Acute Myeloid Leukemia Patients. Ann Case Report 9: 1836. DOI: 10.29011/2574-7754.101836

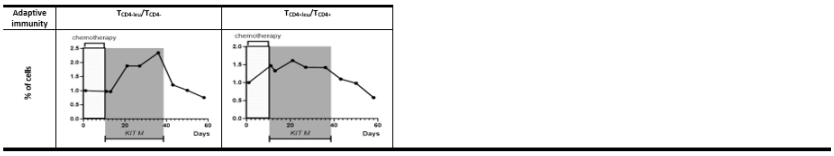

S5B: Profiles obtained from samples from P1482 under treatment with Kit M vs. healthy controls: healthy and P1482 VOC samples could be clearly differentiated and increased frequencies of (leukemia specific) immunoreactive cell subtypes could be detected in the course of disease under Kit M treatment.

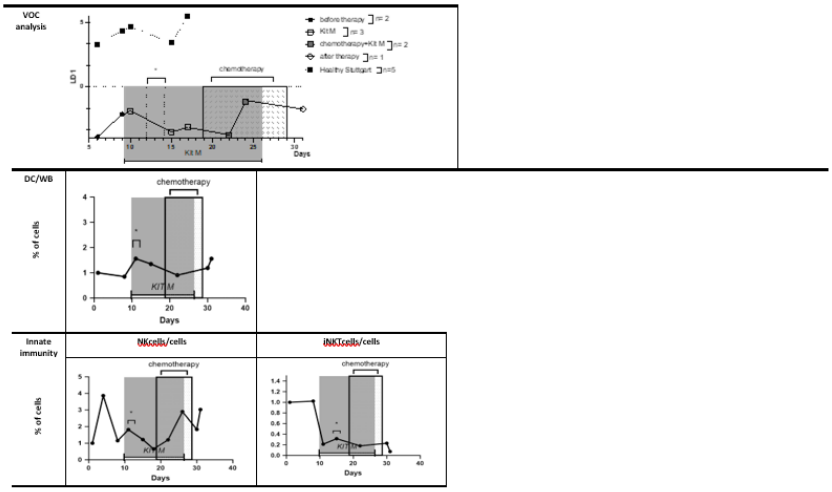

Citation: Baudrexler T. et al. (2024) Volatile Profiling using an eNose - Exploiting Breath Volatile Organic Compounds for Disease Monitoring in Refractory Acute Myeloid Leukemia Patients. Ann Case Report 9: 1836. DOI: 10.29011/2574-7754.101836

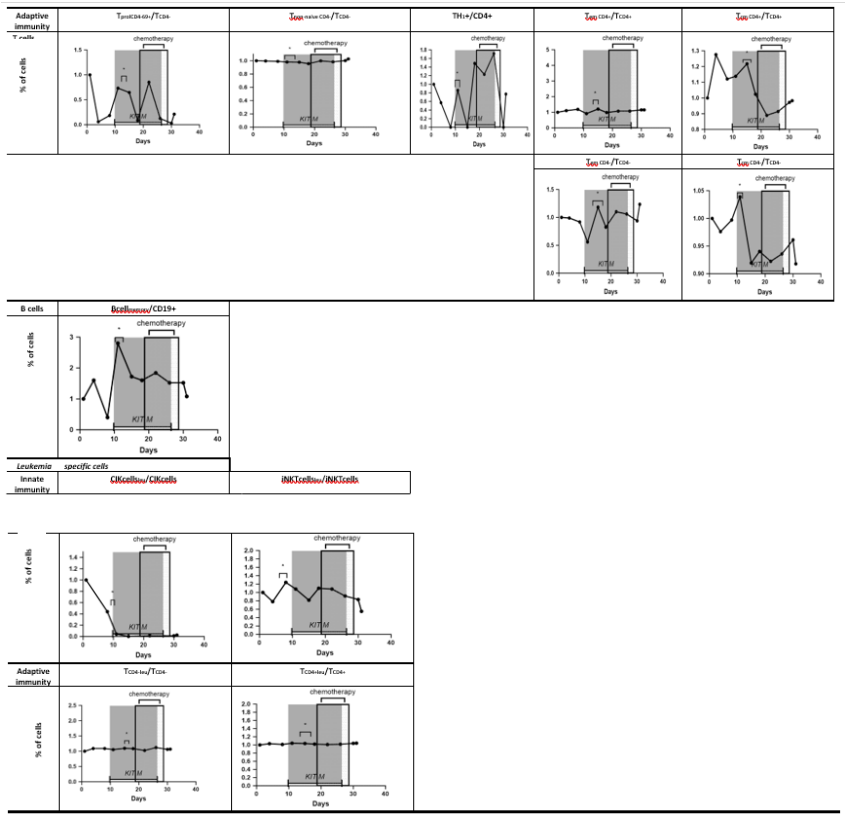

S5C: Profiles obtained from samples from P1601 under treatment with Kit M vs. healthy controls: healthy and P1601 VOC samples could be clearly differentiated and slightly increased frequencies of (leukemia specific) immunoreactive cell subtypes could be detected in the course of disease under Kit M treatment (±prednisolone('*')/chemotherapy).

Figure S5: Influences of patients' treatment with chemotherapy and/or Kit M on the provision of (leukemia specific) immunoreactive cells in the course of disease of therapy refractory patients (P1511, P1482, P1601) are given. All values in the course of disease are given as 'fold change' values referred to the value at the beginning of observation. VOC breath samples were collected with earloop masks. Phases under chemotherapy are given in hatched grey, under Kit M therapy in grey and single prednisolone applications as '*'. Details of the clinical courses including treatment phases of all patients are given in Figure 1,2 and 3. Abbreviations of cell subtypes are given in Table 1.

Citation: Baudrexler T. et al. (2024) Volatile Profiling using an eNose - Exploiting Breath Volatile Organic Compounds for Disease Monitoring in Refractory Acute Myeloid Leukemia Patients. Ann Case Report 9: 1836. DOI: 10.29011/2574-7754.101836

VOC Monitoring: During observation, we compared breath samples collected from healthy probands from Augsburg and from P1511 in the course of the disease. We found clearly differentiated healthy and leukemic VOC results during the whole observation time with stable distances between healthy and leukemic LD values. Nevertheless, we found an approximation of leukemic to healthy VOCs around day 10, 100 and 120 (Figure 5A, upper part).

P1482: 11 days before start of Kit M therapy the patient was treated, as a rescue medication, with 2 cycles of decitabine (20 mg/m^2), followed by hydroxyurea and cytarabine (100 mg/m^2). During pancytopenia he was offered an individual therapy option with Kit M. During observation time the patient was in need for 5 erythrocyte and 4 platelet transfusions. Routine clinical and laboratory parameters showed that Kit M treatment was well tolerated, and the patient improved clinically: Neutrophils in white blood cells (WBC) increased from 10% to 50%, thrombocytes reached 100/nl after 24 days going along with no need for new platelet transfusions, whereas WBC and hemoglobin values (need for new erythrocyte transfusions) stayed low. After 4 weeks of Kit M treatment, the patient was discharged in good clinical conditions. 8 days later, progression of AML was seen with high blast counts in PB (40%) and BM (73%). The patient suffered with severe sepsis and died few days later (Figure 2).

Immune monitoring: In the course of Kit M treatment a continuous increase of DC, $Tpro_{lCD4\text{-}69+}/T_{CD4+}$, $T_{non\text{-}naive\ CD4-}/T_{CD4-}$ as well as $T_{em\ CD4+}/T_{CD4+}$ and $T_{cm\ CD4+}/T_{CD4+}$ could be shown. $TH_{1+/-}CD4+$ and $Bcell_{memory}$/CD19+ increased during the 4-week treatment. Moreover, we found increased frequencies of NK-, CIK- and iNKT cells. Antigen specific cells analyzed after LAA stimulation by CSA showed increasing frequencies of innate and adaptive immune cells during Kit M therapy. We found rising frequencies of $T_{CD4\text{-}leu}/T_{CD4}$-, $T_{CD4+leu}/T_{CD4+}$, $CIKcells_{leu}$/CIKcells and $iNKTcells_{leu}$/iNKTcells suggesting an in vivo production of (potentially leukemia-specific) cells.

Immune stimulatory effects decreased after discontinuation of Kit M treatment, although not to the base line before start of therapy (Figure S5B, lower part)

VOC monitoring: During observation, we compared breath samples collected from healthy probands from Augsburg and from P1482 in the course of the disease. We found clearly differentiated healthy and leukemic VOC results during the whole observation time. Nevertheless, we found an approximation of leukemic to healthy VOCs in the beginning of Kit M treatment (day 11-28) (Figure 5B, upper part).

P1601: 8 weeks after treatment with azacytidine and venetoclax a therapy refractory status of the disease (90% blasts in PB) was confirmed, and the patient was offered a treatment with Kit M. During the observation time 4 erythrocytes and 10 platelet-transfusions were necessary. On day 12-14 the patient was treated with (50 g/day) prednisolone and had to undergo two times a pleural puncture (going along with platelet transfusion before puncture at day 16 and 25). Kit M was first applied as continuous infusion on day 9. On day 19 the patient received a simultaneous chemotherapy with 1 g/day hydroxycarbamide to reduce the tumor-load.

Clinically the Kit M treatment was well tolerated without adverse events: Neutrophils in WBC (<4%), hemoglobin and thrombocytes remained low during Kit M and chemotherapy. PB blast counts were constantly high (>75%) but decreased in the course of Kit M treatment between day 9-10 (from 90% to 78%) and between day 17-19 (from 95% to 89%). Interestingly, the blast counts increased by application of prednisolone (day 12-14; from 78% to 88%) and were not further reduced under hydroxycarbamide therapy between day 19-29. On day 29 the patient decided to stop all treatments and died with refractory disease on day 31 (Figure 3).

Immune monitoring: In the course of Kit M treatment, we found a slight increase of DCs, proliferating T cells ($T_{prolCD4\text{-}69+/T_{CD4-}}$) and stable $T_{non\text{-}naive\ CD4-}/T_{CD4-}$. Additionally, $TH_{1+/-}CD4+$ and $Bcell_{memory}$/CD19+ increased during Kit M therapy. Whereas T_{cm} subtypes decreased, and T_{em} subtypes stayed on a stable line. Regarding cells of the innate immunity, stable frequencies of NK cells and decreased frequencies of iNKT cells were seen during Kit M therapy. Leukemia specific cells, detected by intracellular production of INFy after LAA stimulation using the InCyt showed stable frequencies of $T_{CD4\text{-}leu}/T_{CD4-}$ and $T_{CD4+leu}/TCD4+$ and decreased frequencies of CIK cells. Frequencies of iNKT cells, proliferating T cells and B-memory-cells slightly increased during Kit M therapy but decreased under chemotherapy. Interestingly, prednisolone had an immunosuppressive effect on frequencies of DCs, NK cells, proliferating T, TH1+, central memory T cell subtypes, B memory cells as well as INFy producing iNKT and CIK cells (day 12-14) (Figure S5C, lower part).

VOC Monitoring: During observation, we compared breath samples collected from healthy probands from Stuttgart and from P1601 in the course of the disease. We found clearly differentiated healthy and leukemic VOC results during the whole observation time. Nevertheless, we found an approximation of leukemic to healthy VOCs in the beginning of Kit M treatment (around day 10) that flattened out by application of prednisolone (day 12-14). Leukemic VOCs showed an approximation to healthy VOCs in the beginning of supportive chemotherapy (day 22-24) (Figure 5C, upper part).

VOC comparisons

As a source for VOC analyzes conducted by eNose, we used healthy and leukemic breath samples collected by earloop masks. An overview about the collected breath samples of every proband is given in Figure 6. Various comparisons were analyzed by linear

Citation: Baudrexler T. et al. (2024) Volatile Profiling using an eNose - Exploiting Breath Volatile Organic Compounds for Disease Monitoring in Refractory Acute Myeloid Leukemia Patients. Ann Case Report 9: 1836. DOI: 10.29011/2574-7754.101836

discriminant analyses (LD) and the smell-prints were graphically shown in two-dimensional principal component analysis (PCA) plots. Sensitivity, specificity, Mahalanobis distance (md), negative and positive predictive values as well as the p-value calculated by Fishers' exact test are given.

Significant differences between healthy and AML patients' breath samples

The eNose showed a significant differentiation between 21 leukemic- collected from 3 AML patients in the course of the disease- and 15 healthy breath samples (%sensitivity: 100; %specificity: 100; p=.0001). To compare AML patients' breath samples with healthy probands' under comparable hospital conditions (e.g., comparable background smell) we analyzed these samples in the course of the disease of P1511 (patient from Augsburg) with 10 healthy probands' breath samples from Augsburg. We found significantly different VOC results (%sensitivity: 100; %specificity: 100; p=.0001). Comparing 10 healthy breath samples from Augsburg with breath samples from P1482 (patient from Augsburg) the eNose showed significant differences (%sensitivity: 100; %specificity: 100; p=.0001). Comparable results could be found in healthy (n=5) and leukemic (P1601 in the course of the disease) breath samples from Stuttgart (%sensitivity: 100; %specificity: 100; p=.0008). Detailed information about VOC results and a graphical overview are given in Figure 6.

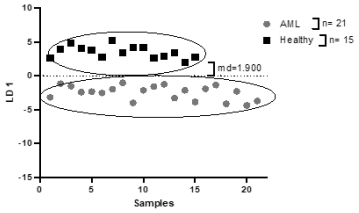

	AML P1511, P1482, P1601	Healthy Augsburg, Stuttgart			
	Correct/false (%[1])	Correct/false (%[2])	PPV[3] (%)	NPV[4] (%)	P[5]
eNose results	21/0 (100)	15/0 (100)	100	100	.0001

6.1 VOC profiles of healthy and AML patients' masks were significantly different

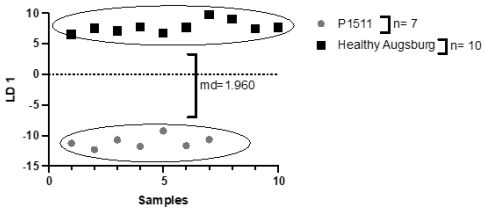

	AML P1511	Healthy Augsburg			
	Correct/false (%[1])	Correct/false (%[2])	PPV[3] (%)	NPV[4] (%)	P[5]
eNose results	7/0 (100)	10/0 (100)	100	100	.0001

6.1 VOC profiles of healthy and AML patients' masks were significantly different

Citation: Baudrexler T. et al. (2024) Volatile Profiling using an eNose - Exploiting Breath Volatile Organic Compounds for Disease Monitoring in Refractory Acute Myeloid Leukemia Patients. Ann Case Report 9: 1836. DOI: 10.29011/2574-7754.101836

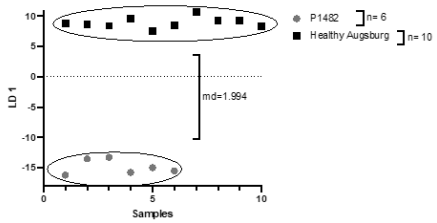

	AML P1482	Healthy Augsburg			
	Correct/false (%[1])	Correct/false (%[2])	PPV[3] (%)	NPV[4] (%)	p[5]
eNose results	6/0 (100)	10/0 (100)	100	100	.0001

6.3 VOC profiles of P1482 and healthy probands in Augsburg were significantly different

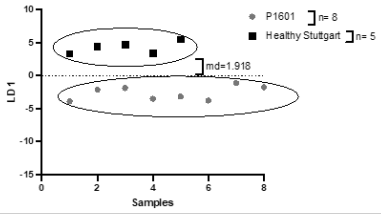

	AML P1601	Healthy Stuttgart			
	Correct/false (%[1])	Correct/false (%[2])	PPV[3] (%)	NPV[4] (%)	p[5]
eNose results	8/0 (100)	5/0 (100)	100	100	.0008

6.4 VOC profiles of P1601 and healthy probands in Stuttgart were significantly different

1 Sensitivity.

2 Specificity.

3 positive predictive value.

4 negative predictive value.

5 p values calculated with Fisher's exact test.

6 md, Mahalanobis distance

Figure 6: Breath samples were collected from healthy donors (n=10 from Augsburg, n=5 from Stuttgart) and from 3 AML patients (P1511 and P1482 from Augsburg, P1601 from Stuttgart) in the course of disease (irrespective of applied therapies) using earloop masks collecting exhaled breath for 5 minutes. VOC analyses were conducted using an eNose. Differences in VOC profiles were calculated by linear discriminant (LD-) analyses (dimensionless LD 1 values). Differences in VOC profiles between AML patients and their respective healthy donors' sample are given. Tables underneath giving an overview about the sensitivity, specificity, negative and positive predictive value. Statistical tests were performed using Fisher's exact test. Differences are considered as borderline significant with p values ≤.1 and significant with p values ≤.05.

Citation: Baudrexler T. et al. (2024) Volatile Profiling using an eNose - Exploiting Breath Volatile Organic Compounds for Disease Monitoring in Refractory Acute Myeloid Leukemia Patients. Ann Case Report 9: 1836. DOI: 10.29011/2574-7754.101836

Influence of Kit M ± chemotherapy on VOC profiles in P1601

To understand the influence of Kit M with or without simultaneous chemotherapy we compared VOCs of P1601s' breath samples. The eNose could (not significantly) differentiate breath samples before and after therapy (=no therapy; n=3) from breath samples taken during chemotherapy and simultaneous Kit M treatment (n=2) (%sensitivity: 100; %specificity: 50; p=.4). Moreover, the eNose could (not significantly) differentiate breath samples under no therapy from samples collected during Kit M treatment (%sensitivity: 66.7; %specificity: 66.7; p=.99). An overview about VOC results and treatment periods are given in Figure 7 and 3.

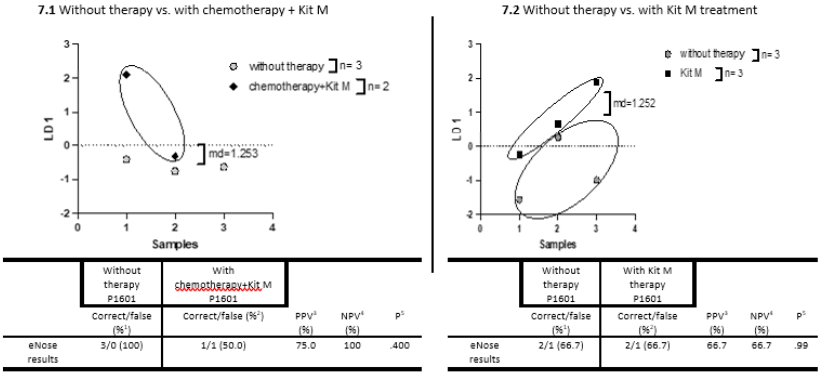

	Without therapy P1601	With chemotherapy+Kit M P1601			
	Correct/false (%[1])	Correct/false (%[2])	PPV[3] (%)	NPV[4] (%)	P[5]
eNose results	3/0 (100)	1/1 (50.0)	75.0	100	.400

	Without therapy P1601	With Kit M therapy P1601			
	Correct/false (%[1])	Correct/false (%[2])	PPV[3] (%)	NPV[4] (%)	P[5]
eNose results	2/1 (66.7)	2/1 (66.7)	66.7	66.7	.99

1 Sensitivity.

2 Specificity.

3 positive predictive value.

4 negative predictive value.

5 p values calculated with Fisher's exact test.

6 md, Mahalanobis distance.

Figure 7: Breath samples were collected from P1601 in course of disease using earloop masks collecting exhaled breath for 5 minutes. VOC analyses were conducted using an eNose. Differences in VOC profiles were calculated by linear discriminant (LD-) analyses (dimensionless LD 1 values). Differences in VOC profiles collected under chemotherapy ± Kit M therapy or without therapy were evaluated. Tables underneath giving an overview about the sensitivity, specificity, negative and positive predictive value. Statistical tests were performed using Fisher's exact test. Differences are considered as borderline significant with p values ≤.1 and significant with p values ≤.05.

Significantly different VOC results during chemotherapy compared to Kit M treatment

Using breath samples from P1511 under chemotherapy and from P1482 and P1601 under Kit M treatment, we could significantly distinguish these two therapy options by an eNose using VOC profiles (%sensitivity: 100; %specificity: 100; p=.0006). Detailed information is given in Figure 8A.

Citation: Baudrexler T. et al. (2024) Volatile Profiling using an eNose - Exploiting Breath Volatile Organic Compounds for Disease Monitoring in Refractory Acute Myeloid Leukemia Patients. Ann Case Report 9: 1836. DOI: 10.29011/2574-7754.101836

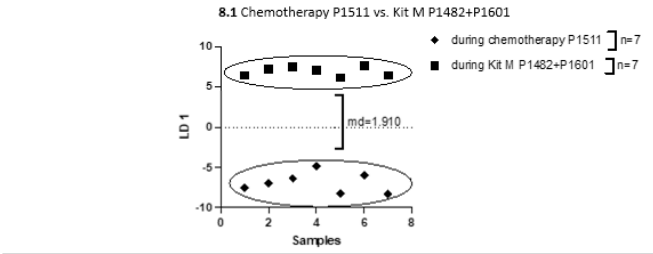

	During chemotherapy P1511	During Kit M therapy P1482, P1601			
	Correct/false (%[1])	Correct/false (%[2])	PPV[3] (%)	NPV[4] (%)	P[5]
eNose results	7/0 (100)	7/0 (100)	100	100	.0006

Figure 8A: Breath samples from 3 AML patients collected under chemotherapy and under Kit M therapy were significantly different.

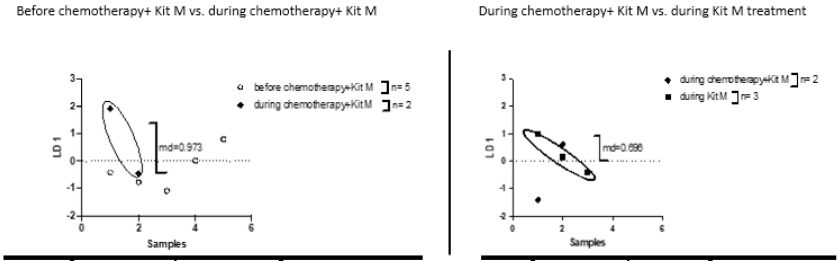

	Before chemotherapy+ Kit M P1601	During chemotherapy+ Kit M P1601			
	Correct/false (%[1])	Correct/false (%[2])	PPV[3] (%)	NPV[4] (%)	P[5]
eNose results	5/0 (100)	1/1 (50.0)	83.0	100	.286

	During chemotherapy+ Kit M P1601	During Kit M therapy P1601			
	Correct/false (%[1])	Correct/false (%[2])	PPV[3] (%)	NPV[4] (%)	P[5]
eNose results	1/1 (50.0)	3/0 (100)	100	75.0	.400

Figure 8B: Breath samples from P1601 collected before simultaneous therapy, under chemotherapy+ Kit M therapy and under Kit M therapy were different.

1 Sensitivity.

2 Specificity.

3 positve predictive value.

4 negative predictive value.

5 p values calculated with Fisher's exact test.

6 md, Mahalanobis distance

Citation: Baudrexler T. et al. (2024) Volatile Profiling using an eNose - Exploiting Breath Volatile Organic Compounds for Disease Monitoring in Refractory Acute Myeloid Leukemia Patients. Ann Case Report 9: 1836. DOI: 10.29011/2574-7754.101836

Figure 8: Breath samples were collected from 3 AML patients (P1511 and P1482 from Augsburg, P1601 from Stuttgart) in the course of disease (respective of applied therapies) using earloop masks collecting exhaled breath for 5 minutes. VOC analyses were conducted using an eNose. Differences in VOC profiles were calculated by linear discriminant (LD-) analyses (dimensionless LD 1 values). Figure 8A shows significant differences in VOC profiles collected under chemotherapy from P1511 compared to under Kit M therapy from P1482 and P1601. Figure 8B shows differences in VOC profiles collected from P1601 before simultaneous therapy compared to under chemotherapy+ Kit M therapy and shows differences in VOC profiles collected from P1601 under chemotherapy+ Kit M therapy compared to under Kit M therapy. Tables underneath giving an overview about the sensitivity, specificity, negative and positive predictive value. Statistical tests were performed using Fisher's exact test. Differences are considered as borderline significant with p values ≤.1 and significant with p values ≤.05.

Different breath samples from P1601 collected before therapy, under combined (chemo- and Kit M) therapy and under Kit M therapy

We found different VOC profiles in breath samples from P1601 before simultaneous therapy (Kit M and chemotherapy) compared to during chemotherapy and simultaneous Kit M therapy (%sensitivity: 100; %specificity: 50; p=.286). Furthermore, we found different VOC profiles in breath samples during chemotherapy and simultaneous Kit M treatment compared to under Kit M therapy (%sensitivity: 50; %specificity: 100; p=.4). Graphs and more details are shown in Figure 8B and 3.

In summary, these findings suggest that the eNose can effectively differentiate between healthy individuals and AML patients based on their breath samples. Additionally, it indicates that the eNose can detect differences in VOC profiles between breath samples taken with and without therapy (Kit M/chemotherapy). Furthermore, it demonstrates the eNoses' ability to distinguish between breath samples collected during chemotherapy and those collected under Kit M therapy.

Discussion

After induction therapy the relapse rate of AML patients is about 70-80% [6, 41, 42]. Therefore, there is a great need for new (non) immunotherapeutic options [43]).

DC/DC_{leu} Based Immunotherapy

DC/DC_{leu} can be generated ex vivo from monocytes (loaded with LAA) or leukemic blasts and have the advantage of already containing the patients' specific leukemic antigens needed for an appropriate immunological answer and therefore bypassing the need of antigen-loading [13]. We and others could prove that DC/DC_{leu} can be generated ex vivo from patients' blast containing WB independent of patients' sex, age, MHC, leukemic subtype, or risk profile [12, 13, 17, 30, 44]. DC vaccinations were shown to induce leukemia specific immune responses and to improve the outcome of patients [7, 11, 45].

Ex vivo generation of DC/DC_{leu} with Kit M pretreated patients' WB resulting in increased antileukemic activity

We can confirm preliminary data [13, 14, 17, 18, 30, 44], that DC/DC_{leu} could be generated ex vivo in Kit M pretreated (compared to not pretreated) AML patients' WB (P1511, P1482, P1601) without inducing blast proliferation. In addition, blast-lytic activity was shown to be regularly improved using Kit M pretreated WB samples as 'stimulator cells' in MLC [13, 14, 17, 18, 22, 30, 46] (Figure 4A-C). These findings prompted us to deduce a Kit M-based treatment protocol for P1482 and P1601: Our data show, that treatment of (therapy refractory) patients (P1482, P1601) with Kit M stabilized or even reduced blast counts in PB, increased thrombocyte counts (P1482), compared to a patient without Kit M treatment (P1511) (Figure 1-3). Even more we could show a (leukemia-specific) activation of cells of the innate and adaptive immune system in P1482 and in part in P1601, but not in P1511 (Figure 5A-C). These data could point to antileukemic effects after Kit M treatment (induced by blast-conversion to $DC_{leu,}$ leading to leukemia specific immune effects as shown before ex vivo [6, 13, 14, 17]. These effects were abrogated by infusion of (immune suppressive) prednisolone (to treat pneumonia) in P1601. Under that influence of prednisolone these effects were diminished. This could point to an effect of cortisone on the exhalation of VOCs (Figure 5A-C). In vivo immunostimulant effects might be more efficient in cases with low blast counts/in remission and might contribute to stabilize disease or maintain remissions, as discussed by us before [13, 17].

VOC Profiling to Differentiate Healthy and AML Patients' Breath

It is well known that age, gender as well as smoking behavior, infections (e.g: pneumonia) or in the presence of impaired/damaged tissue (e.g: COPD) does not disturb the differentiation of malignant vs. non-malignant breath profiles/breath donors [32, 34, 47]. Our data show, that earloop masks qualify as carriers to be used for VOC profiling, as already shown before in patients with

Citation: Baudrexler T. et al. (2024) Volatile Profiling using an eNose - Exploiting Breath Volatile Organic Compounds for Disease Monitoring in Refractory Acute Myeloid Leukemia Patients. Ann Case Report 9: 1836. DOI: 10.29011/2574-7754.101836

lung cancer, COPD vs. healthy donors [32]. There is no need to breath directly in an eNose. We have already demonstrated that a VOC profiling can differentiate between malignant (lung cancer) and nonmalignant breath donors [32, 34]. It has already been investigated that volatile samples above urine samples (to detect bladder tumor [48]) or above serum supernatants from diseased patients (to detect AML [30]) can be clearly separated from healthy samples. Moreover, we can add, that breath samples from healthy breath donors could not only be clearly differentiated from breath samples from lung cancer, COPD [34] or Alzheimer's and Parkinson's disease [29, 40], but also from breath samples from AML patients (independent of disease, stage and treatment), as we could show here (Figure 6).

A clear differentiation of AML patients (treated by chemotherapy or Kit M or chemotherapy combined with Kit M or without any treatment) from healthy breath samples was possible- thereby pointing to volatile profiles (differentiating AML and healthy breath) being in general independent from applied therapies. This differentiation between healthy and AML samples was significantly different and independent of different institutions, where the healthy and AML breath samples were collected (Figure 6.2 and 6.3 in Hospital in Augsburg, Figure 6.4 in Hospital in Stuttgart). An interesting finding was, that differences between healthy and leukemic breath were lower soon after application of Kit M. This was true for P1482 (Figure S5B) and P1601 (Figure S5C). This might point to a positive influence of immune modulation on disease activity-shifting AML patients' breath closer to healthy breath patterns.

We moreover found clear (although due to low sample numbers not significant) differences between breath samples from AML patients without any therapy vs. with chemotherapy combined with Kit M or vs. Kit M alone (Figure 7). The same was true for samples taken before vs. during applied chemotherapy combined with Kit M (Figure 8B). The most impressive and highly significant differences were seen comparing breath samples during chemotherapy vs. during Kit M treatment (Figure 8A).

This means, that breath profiling in AML patients not only allows a clear differentiation between healthy and leukemic breath samples but can also differentiate between breath obtained under chemotherapy vs. during immune modulating therapy.

For the future use of eNose-based breath profiling, it should be examined whether breath samples from AML patients in different phases of remission (e.g. early remission, long-term remission, remission shortly before relapse) may allow conclusions to be drawn about a change of VOC profiles to monitor the quality or the stability of a remission. These results could contribute to detect imminent relapses early.

Colombo et al. examined cytokines in condensed exhaled breath and could correlate immune reactions with exhaled air profiles in these patients [49]. Moreover, our group could show, that an eNose can differentiate VOCs in healthy vs. leukemic DC- and Mixed lymphocyte culture supernatants [30].

Here we confirm, that immune- and VOC-profiling in the course of patients' diseases is possible and allows the detection of quantitative changes of immune cells as well as of volatile markers-independent of smoking behavior and AML subtype. For the future we therefore recommend correlating immune with VOC profiles to contribute to a refined monitoring to estimate the quality of remissions.

We conclude, that systemic effects in healthy vs. AML PB might be not only monitored on the cellular side (by monitoring cell subsets [50]), on the soluble side (by monitoring chemokines/cytokines/extracellular vesicles (EVs) [24]30,52), but also on the volatile side (ex vivo) [30] Table or directly using breath samples collected with earloop masks from patients. Dysregulated release of pro- and anti-inflammatory cytokines/EVs in AML might influence anti- or pro-leukemic mechanism of the immune system [51]. In addition, EVs released by immune or tumor cells- detectable in serum from patients with leukemia- might contribute to a refined monitoring [28, 52]. These EVs might lead to increased release of cytokines and going along with different VOCs in exhaled air [53, 54].

Conclusion

VOCs can be collected on earloop masks and allow a differentiation of healthy and leukemic breath donors. Moreover, breath samples in different phases of the disease or under (chemo- or immune modulatory) therapy can be differentiated. These findings could contribute to deduce a refined VOC based monitoring strategy (optional in conjunction with immune monitoring), that allows a monitoring of the efficacy of applied therapies, of the quality of achieved responses/remissions to (immune)therapies or might contribute to detect imminent relapses on a volatile basis.

Acknowledgment: The authors thank patients, nurses, physicians, and technicians (special thanks to Boas U.) for their support with sample materials and diagnostic reports. The results presented in this manuscript are part of the doctoral thesis of Baudrexler Tobias at the University Hospital of Ludwig-Maximilian-University Munich.

Ethics: Sample collection was conducted after obtaining written informed consent of the blood donor and in accordance with the World Medical Association Declaration of Helsinki and the ethic committee of the Ludwig-Maximilian-University Munich (vote no. 339-05).

Citation: Baudrexler T. et al. (2024) Volatile Profiling using an eNose - Exploiting Breath Volatile Organic Compounds for Disease Monitoring in Refractory Acute Myeloid Leukemia Patients. Ann Case Report 9: 1836. DOI: 10.29011/2574-7754.101836

Conflict of Interests: Modiblast Pharma GmbH (Oberhaching, Germany) holds the European Patent 15 801 987.7-1118 and US Patent 15-517627 'Use of immunomodulatory effective compositions for the immunotherapeutic treatment of patients suffering from myeloid leukemias', with whom Schmetzer H. is involved with.

Author Contributions: Conceptualization, Tobias Baudrexler, Tobias Boeselt, Christioph Schmid, Rembert Koczulla and Helga Schmetzer; Data curation, Tobias Baudrexler, Tobias Boeselt, Michael Atzler, Anne Hartz, Ursula Boas, Andreas Rank and Joerg Schmohl; Formal analysis, Tobias Baudrexler; Funding acquisition, Christioph Schmid, Rembert Koczulla and Helga Schmetzer; Investigation, Tobias Baudrexler, Michael Atzler, Anne Hartz, Ursula Boas and Andreas Rank; Methodology, Tobias Boeselt, Christioph Schmid, Rembert Koczulla and Helga Schmetzer; Project administration, Christioph Schmid, Rembert Koczulla and Helga Schmetzer; Software, Tobias Baudrexler and Tobias Boeselt; Supervision, Christioph Schmid, Rembert Koczulla and Helga Schmetzer; Validation, Tobias Baudrexler, Tobias Boeselt, Michael Atzler, Anne Hartz, Andreas Rank and Joerg Schmohl; Visualization, Tobias Baudrexler; Writing – original draft, Tobias Baudrexler; Writing – review & editing, Tobias Baudrexler, Tobias Boeselt and Helga Schmetzer.All authors have read and agreed to the published version of the manuscript.

Informed Consent Statement: Informed consent was obtained from all subjects involved in the study.

Data Availability Statement: The data presented in this study are available in this article.

Fundings: This research received no external funding.

References

1. Tamamyan G, Tervonen H, Mendoza L, Batmunkh T, Yap ML, et al., (2018) Future of Global Cancer From the Perspective of Young Oncology Leaders. Journal of Global Oncology 4: 74s-74s.
2. Yanada M, Naoe T. (2012) Acute myeloid leukemia in older adults. International Journal of Hematology 96: 186-193.
3. Döhner H, Wei AH, Appelbaum FR, Craddock C, DiNardo CD, et al. (2022) Diagnosis and management of AML in adults: 2022 recommendations from an international expert panel on behalf of the ELN. Blood, The Journal of the American Society of Hematology 140: 1345-1377.
4. Gil-Perez A, Montalban-Bravo G (2019) Management of myelodysplastic syndromes after failure of response to hypomethylating agents. Therapeutic advances in hematology 10: 2040620719847059.
5. Burnett AK. (2018) Treatment of older patients with newly diagnosed AML unfit for traditional therapy. Clinical Lymphoma Myeloma and Leukemia 18: 553-557.
6. Ansprenger C, Amberger DC, Schmetzer HM. (2020) Potential of immunotherapies in the mediation of antileukemic responses for patients with acute myeloid leukemia (AML) and myelodysplastic syndrome (MDS) - With a focus on Dendritic cells of leukemic origin (DCleu). Clinical Immunology 217: 108467.
7. Lichtenegger FS, Krupka C, Haubner S, Köhnke T, Subklewe M. (2017) Recent developments in immunotherapy of acute myeloid leukemia. Journal of Hematology & Oncology 10: 142.
8. Wan H, Dupasquier M (2005) Dendritic cells in vivo and in vitro. Cellular & Molecular Immunology 2: 28-35.
9. Palucka K, Banchereau J. (1999) Dendritic Cells: A Link Between Innate and Adaptive Immunity. Journal of Clinical Immunology 19: 12-25.
10. Van Acker HH, Versteven M, Lichtenegger FS, Roex G, Campillo-Davo D, et al. (2019) Dendritic Cell-Based Immunotherapy of Acute Myeloid Leukemia. Journal of Clinical Medicine 8: 579.
11. Amberger DC, Schmetzer HM, (2020) Dendritic Cells of Leukemic Origin: Specialized Antigen-Presenting Cells as Potential Treatment Tools for Patients with Myeloid Leukemia. Transfusion Medicine and Hemotherapy 47: 432-443.
12. Kremser A, Dressig J, Grabrucker C, Liepert A, Kroell T, et al. (2010) Dendritic Cells (DCs) Can Be Successfully Generated From Leukemic Blasts in Individual Patients With AML or MDS: An Evaluation of Different Methods. Journal of Immunotherapy 33: 185-199.
13. Amberger DC, Doraneh-Gard F, Gunsilius C, Weinmann M, Möbius S, et al. (2019) PGE1-Containing Protocols Generate Mature (Leukemia-Derived) Dendritic Cells Directly from Leukemic Whole Blood. International Journal of Molecular Sciences 20: 4590.
14. Schwepcke C, Klauer LK, Deen D, Amberger DC, Fischer Z, et al. (2022) Generation of Leukaemia-Derived Dendritic Cells (DCleu) to Improve Anti-Leukaemic Activity in AML: Selection of the Most Efficient Response Modifier Combinations. International Journal of Molecular Sciences 23: 8333.
15. Okamoto M, Sato T, (2003) Toll-like receptor signaling in anti-cancer immunity. Journal of Medical Investigation 50: 9-24.
16. Conejo-Garcia JR, Rutkowski MR, Cubillos-Ruiz JR, (2016) State-of-the-art of regulatory dendritic cells in cancer. Pharmacology & Therapeutics 164: 97-104.
17. Klauer LK, Schutti O, Ugur S, Doraneh-Gard F, Amberger DC, et al. (2021) Interferon Gamma Secretion of Adaptive and Innate Immune Cells as a Parameter to Describe Leukaemia-Derived Dendritic-Cell-Mediated Immune Responses in Acute Myeloid Leukaemia in vitro. Transfusion Medicine and Hemotherapy 49: 44-61.
18. Rackl E, Li L, Klauer LK, Ugur S, Pepeldjiyska E, et al. (2023) Dendritic Cell-Triggered Immune Activation Goes along with Provision of (Leukemia-Specific) Integrin Beta 7-Expressing Immune Cells and Improved Antileukemic Processes. International Journal of Molecular Sciences 24: 463.
19. Robertson FC, Berzofsky JA, Terabe M. (2014) NKT Cell Networks in the Regulation of Tumor Immunity. Frontiers in Immunology 5(543).
20. Bonilla FA, Oettgen HC. (2010) Adaptive immunity. Journal of Allergy and Clinical Immunology 125: S33-S40.
21. Pepeldjiyska E, Li L, Gao J, Seidel CL, Blasi C, et al. (2022) Leukemia derived dendritic cell (DCleu) mediated immune response goes along with reduced (leukemia-specific) regulatory T-cells. Immunobiology 227: 152237.
22. Boeck CL, Amberger SC, Doraneh-Gard F, Sutanto W, Guenther T, et al. (2017) Significance of Frequencies, Compositions, and/or Antileukemic Activity of (DC-stimulated) Invariant NKT, NK and CIK Cells on the Outcome of Patients With AML, ALL and CLL. Journal of Immunotherapy 40: 224-248.

Citation: Baudrexler T. et al. (2024) Volatile Profiling using an eNose - Exploiting Breath Volatile Organic Compounds for Disease Monitoring in Refractory Acute Myeloid Leukemia Patients. Ann Case Report 9: 1836. DOI: 10.29011/2574-7754.101836

23. Vogt V, Schick J, Ansprenger C, Braeu M, Kroell T, et al. (2014) Profiles of Activation, Differentiation–Markers, or β-Integrins on T Cells Contribute to Predict T Cells' Antileukemic Responses After Stimulation With Leukemia-derived Dendritic Cells. Journal of Immunotherapy 37: 331-347.

24. Merle M, Fischbacher D, Liepert A, Grabrucker C, Kroell T, et al. (2021) Conversion of AML-blasts to leukemia-derived dendritic cells (DCleu) in 'DC-culture-media' shifts correlations of released chemokines with antileukemic T-cell reactions. Immunobiology 226: 152088.

25. Li L, Mussack V, Görgens A, Pepeldjiyska E, Hartz AS, et al. (2022) P07.01 The potential role of extracellular vesicle-derived small RNAS in AML research as non-invasive biomarker. Journal for ImmunoTherapy of Cancer 10: A24.

26. Doraneh gard F, Amberger D, Weinmann M, Seidel CL.(2018) Standard normoxic versus physiological hypoxic culture of AML patients' (pts) whole blood (WB) samples with immune modulatory kits yields comparable proportions of dendritic c s and functional results. European Journal of Cancer 92: S10-S11.

27. Tkach M, Kowal J, Zucchetti AE, Enserink L, Jouve M, et al. (2017) Qualitative differences in T-cell activation by dendritic cell-derived extracellular vesicle subtypes. The EMBO Journal 36: 3012-3028.

28. Li L, Görgens A, Mussack V, Pepeldjiyska E, Hartz AS, et al. (2022) Description and optimization of a multiplex bead-based flow cytometry method (MBFCM) to characterize extracellular vesicles in serum samples from patients with hematological malignancies. Cancer Gene Therapy 29: 1600-1615.

29. Mazzatenta A, Pokorski M, Sartucci F, Domenici L, Di Giulio C, et al. (2015) Volatile organic compounds (VOCs) fingerprint of Alzheimer's disease. Respiratory PhysioloAgy & Neurobiology 209: 81-84.

30. Baudrexler T, Boeselt T, Li L, Bohlscheid S, Boas U, et al. (2023) Volatile Phases Derived from Serum, DC, or MLC Culture Supernatants to Deduce a VOC-Based Diagnostic Profiling Strategy for Leukemic Diseases. Biomolecules 13:989.

31. Bach JP, Gold M, Mengel D, Hattesohl A, Lubbe D, et al. (2015) Measuring Compounds in Exhaled Air to Detect Alzheimer's Disease and Parkinson's Disease. PLOS ONE 10: e0132227.

32. Biehl W, Hattesohl A, Jörres RA, Duell T, Althöhn U, et al, (2019) VOC pattern recognition of lung cancer: a comparative evaluation of different dog- and eNose-based strategies using different sampling materials. Acta Oncologica 58: 1216-1224.

33. Boeselt T, Terhorst P, Kroenig J, Nell1 C, Spielmanns M, et al. (2022) Pilot Study on Non-Invasive Diagnostics of Volatile Organic Compounds over Urine from COVID-19 Patients. Archives of Clinical and Biomedical Research 6: 65-73.

34. Dragonieri S, Annema JT, Schot R, van der Schee MPC, Spanevello A, et al. (2009) An electronic nose in the discrimination of patients with non-small cell lung cancer and COPD. Lung Cancer 64: 166-170.

35. Dutta D, Chong NS, Lim SH. (2018) Endogenous volatile organic compounds in acute myeloid leukemia: origins and potential clinical applications. Journal of Breath Research 12: 034002.

36. Willasch A, Eing S, Weber G, Kuçi S, Schneider G, et al. (2010) Enrichment of cell subpopulations applying automated MACS technique: purity, recovery and applicability for PCR-based chimerism analysis. Bone Marrow Transplantation, 45: 181-189.

37. Greulich T, Hattesohl A, Grabisch A, Koepke J, Schmid S, et al. (2013) Detection of obstructive sleep apnoea by an electronic nose. European Respiratory Journal 42: 145-155.

38. Koczulla AR, Hattesohl A, Biller H, Hofbauer J, et al. (2011) Krankheiten erriechen? Eine kurze Übersicht über elektronische Nasen. Pneumologie 65: 401-405.

39. Aghili NS, Rasekh M, Karami H, Edriss O, Wilson AD, et al. (2023) Aromatic fingerprints: VOC analysis with E-nose and GC-MS for rapid detection of adulteration in sesame oil. Sensors 23: 6294.

40. Bach JP, Gold M, Mengel D, Hattesohl A, Lubbe D, et al. (2015) Measuring compounds in exhaled air to detect Alzheimer's disease and Parkinson's disease. PloS one 10: e0132227.

41. Röllig C. (2019) Diagnostik und Therapie der akuten myeloischen Leukämie. best practice onkologie 14: 386-397.

42. Gardin C, Dombret H (2017) Hypomethylating Agents as a Therapy for AML. Current Hematologic Malignancy Reports 12: 1-10.

43. Przespolewski A, Szeles A, Wang ES. (2018) Advances in immunotherapy for acute myeloid leukemia. Future Oncology 14: 963-978.

44. Plett C, Lara Kristina K, Daniel Christophet A, Selda U, Alexander R, et al. (2022) Immunomodulatory kits generating leukaemia derived dendritic cells do not induce blast proliferation ex vivo: IPO-38 as a novel marker to quantify proliferating blasts in acute myeloid leukaemia. Clinical Immunologyb242: 109083.

45. Rosenblatt J, Stone RM, Uhl L, Neuberg D, Joyce R, et al, (2016) Individualized vaccination of AML patients in remission is associated with induction of antileukemia immunity and prolonged remissions. Science Translational Medicine 8: 368ra171-368ra171.

46. Hirn Lopez A, Deen D, Fischer Z, Rabe A, Ansprenger C, et al. (2019) Role of Interferon (IFN)a in ´Cocktails´ for the Generation of (Leukemia-derived) Dendritic Cells (DCleu) From Blasts in Blood From Patients (pts) With Acute Myeloid Leukemia (AML) and the Induction of Antileukemic Reactions. Journal of Immunotherapy 42:143-161.

47. Dragonieri S, Quaranta VC, Carratu P, Ranieri T, Resta O, et al. (2016) Influence of age and gender on the profile of exhaled volatile organic compounds analyzed by an electronic nose. J Bras Pneumol 42: 143-5.

48. Heers H, Gut JM, Hegele A, Hofmann R, Boesel T, et al. (2018) Non-invasive Detection of Bladder Tumors Through Volatile Organic Compounds: A Pilot Study with an Electronic Nose. Anticancer Research 38: 833-837.

49. Colombo C, Faelli N, Tirelli AS, Fortunato F, Biffi A, et al. (2011) Analysis of Inflammatory and Immune Response Biomarkers in Sputum and Exhaled Breath Condensate by a Multi-Parametric Biochip Array in Cystic Fibrosis. International Journal of Immunopathology and Pharmacology 24: 423-432.

50. Wang W, Li H, Zhang L, Jiang W, Shen L, et al., (2021) Clinical applications of monitoring immune status with 90 immune cell subsets in human whole blood by 10□color flow cytometry. International Journal of Laboratory Hematology 43: 1132-1144.

51. Binder S, Luciano M, Horejs-Hoeck J. (2018) The cytokine network in acute myeloid leukemia (AML): A focus on pro- and anti-inflammatory mediators. Cytokine & Growth Factor Reviews 43: 8-15.

52. Li L, Mussack V, Pepeldjiyska E, Hartz A, Rank A, et al., (2020) P01.11 Role of exosomes as promotors or biomarkers to study activation of leukemia-derived dendritic cells (DCleu)-mediated antileukemic activation of adaptive and innate immune-reactive cells against AML-blasts. Journal for ImmunoTherapy of Cancer 8: A13-A14.

53. Ma X, Yan W, Zheng H, Du Q, Zhang L, et al. (2015) Regulation of IL-10 and IL-12 production and function in macrophages and dendritic cells. F1000Research 4: p. F1000 Faculty Rev-1465.

54. Segura E, Amigorena S, Théry C. (2005) Mature dendritic cells secrete exosomes with strong ability to induce antigen-specific effector immune responses. Blood Cells Mol Dis 3: 89-93.

Danksagung *Acknowledgements*

Hiermit möchte ich mich bei allen beteiligten Personen bedanken, die mich während meiner wissenschaftlichen (Labor)arbeit und der Anfertigung meiner Dissertation unterstützt haben.

Gesondert möchte ich Frau Prof. Dr. Helga Schmetzer, meiner Doktormutter, für die Möglichkeit danken, mein Promotionsvorhaben als Teil Ihrer Forschungsgruppe zu verwirklichen. Ich verdanke Ihr eine durchgehend hervorragende Betreuung und eine wertvolle Unterstützung in der Ausarbeitung der Manuskripte.

Es war mir eine große Freude, gemeinsam mit Prof. Dr. Helga Schmetzer, Prof. Dr. med. Rembert Koczulla und Dr. med. Dr. phil. Tobias Boeselt ein neues Forschungsfeld in der Diagnostik und dem Monitoring von AML-Patienten zu bearbeiten und wir gemeinsam die Ergebnisse in herausragender Zusammenarbeit zu veröffentlichen.

Ebenfalls möchte ich den Koautor*innen und Laborkolleg*innen für die gute Kooperation danken.

Ein großer Dank gilt zudem allen Patient*innen und Proband*innen für die Bereitstellung von Blut- und Atemmaskenproben sowie den behandelnden Ärzt*innen für die Bereitstellung von Arztbriefen und Patientenverlaufsdaten.

Zuletzt möchte ich mich bei meiner Familie, Nahestehenden sowie meinen Freunden bedanken, welche mich während des Studiums und der Zeit meiner Promotion immer unterstützt haben.

Lebenslauf *Curriculum vitae*

Persönliche Daten:

VORNAME / NACHNAME	Baudrexler, Tobias Georg
STAATSANGEHÖRIGKEIT	Deutsch
GEBURTSDATUM	12.02.1999
GESCHLECHT	Männlich

Ausbildung

DATEN	Juni 2017
QUALIFIKATIONEN	Abschluss der allgemeinen Hochschulreife, Abitur
INSTITUTION	Ruperti-Gymnasium Mühldorf am Inn
DATEN	Oktober 2017 - August 2019
INSTITUTION	Vorklinik an der LMU München
QUALIFIKATION	Erste ärztliche Prüfung, Physikum am 10.9.2019
DATEN	Seit Dezember 2020
INSTITUTION	Doktorandenstelle, MED III, Klinikum Großhadern
DATEN	September 2019 - Oktober 2022
INSTITUTION	Klinik an der LMU München
QUALIFIKATION	Zweite ärztliche Prüfung am 13.20.2022
DATEN	November 2022 – November 2023
INSTITUTION	Praktisches Jahr an der LMU München
QUALIFIKATION	Dritte ärztliche Prüfung am 09.11.2023
DATUM	November 2023
QUALIFIKATION	Approbation als Arzt